Modulation of the tumour immune microenvironment by cancer-associated fibroblasts

Liam S. Jenkins

A thesis submitted for the degree of Doctor of Philosophy

Breast Cancer Now Research Centre
The Institute of Cancer Research
237 Fulham Road
London

This thesis was completed under the supervision of Professor Clare M. Isacke and Dr James Harper. The work described here was carried out in the Breast Cancer Now Research Centre, The Institute of Cancer Research, 237 Fulham Road, London SW3 6JB and MedImmune (AstraZeneca), Sir Aaron Klug Building, Granta Park, Cambridge, CB21 6GH.

I, Liam S. Jenkins confirm that the work presented in this thesis is my own. Where information has been derived from other sources, I confirm that this has been indicated in the thesis.

Date: October 1st, 2019

……..

Abstract

The breast tumour microenvironment (TME) consists of a variety of non-cancerous cell types that can promote or inhibit cancer progression. Cancer-associated fibroblasts (CAFs) represent a major component of the breast TME and are generally considered to have pro-tumourigenic activity through their ability to promote proliferation, invasion, and metastasis of cancer cells. Similarly, immune cells residing within the TME have profound effects upon cancer development, and an appreciation for their role has led to the development of immunotherapies that have revolutionised the treatment of certain cancer types through promotion of anti-tumour immune responses. However, breast cancers remain largely refractory to immunotherapy. One hypothesis for this insensitivity is that the TME protects cancer cells by adopting a highly immunosuppressive state.

The overall aim of my PhD project was to better characterise the role of CAFs in modulating the immune microenvironment of breast cancer, with a focus on assessing whether CAFs contribute to immune checkpoint blockade insensitivity. Immune profiling of paired syngeneic mouse mammary carcinoma models, which differ in their CAF content, has revealed how an abundance of CAFs is associated with an immunologically 'cold' immune microenvironment. Characterisation of isolated CAF populations demonstrated an immunomodulatory role for CAFs both *in vitro* and *in vivo*. Furthermore, CAF-rich models are insensitive to immune checkpoint blockade, and transcriptomic and histopathological analysis identified a link between stromal activation and an immune excluded tumour phenotype. Finally, alteration of CAFs, either through genetic deletion of CAF-restricted receptors, or epigenetic modulation, has provided new insights into CAF-induced immunosuppression and identified possible novel CAF-associated approaches to enhancing the sensitivity of breast cancer to immune checkpoint blockade.

Acknowledgements

First and foremost I would like to thank my academic supervisor Professor Clare Isacke for giving me the opportunity to carry out my PhD in her laboratory. I am extremely grateful for her insight, support, and guidance throughout the duration of this project.

Secondly, I would like to thank my industrial supervisor Dr James Harper for his expertise, unwavering encouragement and insightful advice, which have been invaluable on both an academic and personal level.

Thank you also to all members of the Isacke Lab and the Oncology team at MedImmune (AZ), both past and present, not only for their valuable input and helpful discussions, but also for making the lab a fantastic environment to work in. In particular I want to thank Ute for generating cell lines used in this thesis, Marjan for her endless wisdom and technical advice, and Suzanne for her immunology expertise.

I am grateful to the Biotechnology and Biological Sciences Research Council (BBSRC) for funding my PhD project, as well as Breast Cancer Now, the Institute of Cancer Research and MedImmune (AZ) for funding equipment and core facilities.

Thank you also to the staff of the Breast Cancer Now Histopathology facility for sample processing, the Biological Services Unit for their assistance with *in vivo* experiments and the Breast Cancer Now Bioinformatics facility for help with data analysis.

Finally, thank you to all my friends and family who have supported and encouraged me during this PhD and throughout my education. Special thank you to my partner, Claire, for her persistent encouragement, love and unshakable belief in me.

I would like to dedicate this thesis to my late grandfather, Gomer Royston Jenkins.

Table of contents

List of figures

List of tables

List of abbreviations

ADCC	Antibody dependent cell-mediated cytotoxicity
AF	Alexa Fluor
AI	Aromatase inhibitor
ANOVA	Analysis of variance
APC	Antigen-presenting cell
ArC	Amine reactive compensation
ATP	Adenosine triphosphate
AZ	AstraZeneca
BBSRC	Biotechnology and Biological Sciences Research Council
BCN	Breast Cancer Now
BET	Bromodomain and extraterminal
BiTE	Bi-specific T cell engager
BRCA1	Breast cancer type 1 susceptibility protein
BRCA2	Breast cancer type 2 susceptibility protein
BSA	Bovine serum albumin
BSU	Biological Service Unit
BWA	Burrows-Wheeler Aligner
CAF	Cancer-associated fibroblast
CAR	Chimeric antigen receptor
CAV1	Caveolin 1
CCL	Chemokine ligand
CD	Cluster of differentiation
CFSE	Carboxyfluorescein succinimidyl ester
Chi3L1	Chitinase 3-like 1
CK	Cytokeratin
CM	Conditioned medium
CNV	Copy-number variation
COMBO	Anti-CTLA-4 plus anti-PD-L1 treatment

CSF1	Colony-stimulating factor 1
CSF1R	Colony-stimulating factor 1 receptor
CTL	Cytotoxic T lymphocyte
CTLA-4	Cytotoxic T lymphocyte-associated protein 4
CXCL	Chemokine (C-X-C motif) ligand
CXCR	CXC-chemokine receptor
CyTOF	Mass cytometry
DAMP	Damage-associated molecular pattern
DAPI	4', 6-diamidino-2-phenylindole
DC	Dendritic cell
DCIS	Ductal carcinoma *in situ*
DMEM	Dulbecco's modified Eagle's medium
DMSO	Dimethyl sulphoxide
DNA	Deoxyribonucleic acid
DR	Death receptor
DSB	Double strand break
dTMP	Deoxythymidine monophosphate
dUMP	Deoxyuridine monophosphate
$E180^{KO}$	Endo180-deficient
ECM	Extracellular matrix
EDTA	Ethylenediaminetetraacetic acid
EGF	Epidermal growth factor
EMT	Epithelial to mesenchymal transition
EN^{KO}	Endosialin-deficient
ER	Oestrogen receptor
Fab	Fragment antigen-binding
FAC	5-Fluorouracil, Adriamycin and cyclophosphamide
FAC/T	5-Fluorouracil, Adriamycin and cyclophosphamide and Taxol
FACS	Fluorescence-activated cell sorting

FAP	Fibroblast activation protein-alpha
FBS	Foetal bovine serum
Fc	Fragment crystallisable
FDA	Food and Drug Administration
FEC	5-Fluorouracil, epirubicin and cyclophosphamide
FEC/T	5-Fluorouracil, epirubicin and cyclophosphamide and Taxotere
FFPE	Formalin-fixed paraffin-embedded
FITC	Fluorescein isothiocyanate
FMO	Fluorescence minus one
FN	Fibronectin
FOV	Field of view
FoxP3	Forkhead box P3
FRC	Fibroblast reticular cell
FSC	Forward scatter
FSP1	Fibroblast specific protein 1
GATK	Genome Analysis Toolkit
GFP	Green fluorescent protein
GM-CSF	Granulocyte-macrophage colony-stimulating factor
gMDSC	Granulocytic myeloid-derived suppressor cell
gMFI	Geometric mean fluorescence intensity
GZMA	Granzyme A
GZMB	Granzyme B
H&E	Haematoxylin and eosin
HEPES	4-(2-hydroxyethyl)-1-piperazineethanesulphonic acid
HER2	Human epidermal growth factor receptor 2/ERBB2
HGF	Hepatocyte growth factor
HPV	Human papillomavirus
HRP	Horseradish peroxidase
iCAFS	Inflammatory CAFs

ICB	Immune checkpoint blockade
ICOS	Inducible T cell costimulators
ICR	Institute of Cancer Research
ID4	Inhibitor of DNA binding 4
IDO	Indoleamine 2,3-dioxygenase
IFF	Immunofluorescence buffer
IFITM1	Interferon-induced transmembrane protein 1
IFNγ	Interferon gamma
IgG	Immunoglobulin G
IHC	Immunohistochemistry
IL	Interleukin
ILC	Innate lymphoid cell
IP	Intraperitoneal
IPA	Ingenuity Pathway Analysis
irRC	Immune-related response criteria
ISO	Isotype control antibodies
IVC	Individually vented cages
JAM2	Junctional adhesion molecule 2
KO	Knockout
LAG-3	Lymphocyte-activation gene 3
LOX	Lysyl oxidase
LPS	Lipopolysaccharide
LSS	Laboratory Support Services
MAPK	Mitogen-activated protein kinase
Mb	Megabase
MCP1	Monocyte chemoattractant protein-1
MDSC	Myeloid-derived suppressor cells
METABRIC	Molecular Taxonomy of Breast Cancer International Consortium
MHC	Major histocompatibility complex

MHCI	MHC class I
MHCII	MHC class II
mMDSC	Monocytic myeloid-derived suppressor cell
MMP	Matrix metalloproteinase
myCAFs	Myofibroblastic CAFs
NG2	Neural/glial antigen 2
NHS	National Health Service
NK	Natural killer
NM	Normal complete medium
NMF	Normal mammary fibroblast
NS	Not significant
NSG	NOD-scid gamma
OPN	Osteopontin
P/S	Penicillin/streptomycin
PAM50	Prediction Analysis of Microarray 50
PAMP	Pathogen-associated molecular pattern
Pan-F-TBRS	Pan-fibroblast TGFβ response signature
PAP	Prostatic acid phosphatase
PAR1	Protease-activated receptor-1
PARP	Poly-ADP ribose polymerase
PBS	Phosphate-buffered saline
PD-1	Programmed cell death protein 1
PD-L1	Programmed death ligand-1
PD-L2	Programmed death ligand-2
PDAC	Pancreatic ductal adenocarcinoma
PDGF	Platelet-derived growth factor
PDGFRα	Platelet-derived growth factor receptor alpha
PDGFRβ	Platelet-derived growth factor receptor beta
PDPN	Podoplanin

PGE2	Prostaglandin E2
PI3K	Phosphoinositide 3-kinase
PR	Progesterone receptor
PRR	Pattern recognition receptors
PVR	Poliovirus receptor
RBC	Red blood cell
RECIST	Response evaluation criteria in solid tumours
RNA	Ribonucleic acid
S100A8	S100 calcium-binding protein A8
S100A9	S100 calcium-binding protein A9
SDF1	Stromal cell-derived factor 1
SEM	Standard error of the mean
SERD	Selective ER down-regulator
SERM	Selective ER modulator
SHP2	Src homology region 2 domain-containing phosphatase-2
SNP	Single-nucleotide polymorphism
SSC	Side scatter
SSP	Single sample predictor
STAT	Signal transducer and activator of transcription
T-bet	T-box transcription factor TBX21
TAM	Tumour-associated macrophage
TCGA	The Cancer Genome Atlas
TCR	T cell receptor
T_{FH}	Follicular helper T cell
TGFβ	Transforming growth factor beta
T_H	T helper cell
TIL	Tumour-infiltrating lymphocyte
TIM-3	T cell immunoglobulin and mucin-domain containing-3
TLR	Toll-like receptor

TLS	Tertiary lymphoid structure
TME	Tumour microenvironment
TNBC	Triple-negative breast cancer
TNC	Tenascin C
TNF	Tumour necrosis factor
TNFα	Tumour necrosis factor alpha
TNM	Tumour, lymph node, metastasis
TPU	Tumour Profiling Unit
TRAIL	Tumour necrosis factor-related apoptosis-inducing ligand
T_{reg}	Regulatory T cell
TSP	Thrombospondin
UF	Ultra-filtered
UV	Ultraviolet
V(D)J	Variable, (Diversity), Joining
VEGF	Vascular endothelial growth factor
w/v	Weight/volume
WES	Whole exome sequencing
Wnt11	Wnt family member 11
Wnt7A	Wnt family member 7A
WT	Wild-type
αSMA	Alpha smooth muscle actin

Chapter 1: Introduction

1.1 General introduction

Cancer is the name given to a group of related diseases involving abnormal cell growth, each with their own sub-classification, diagnosis and standards of care. In the United Kingdom alone, there are annually around 363,000 new cancer cases and cancers are responsible for close to 164,000 deaths (Cancer Research UK statistics, 2014-2016). Worldwide, cancer results in about 8 million deaths each year, making it one of the leading causes of mortality, second only to ischaemic heart disease.

Cancer begins when genetic and epigenetic changes within healthy cells result in them acquiring the ability to escape normal restraints on cell growth. The mutated genes are usually either gain of function mutations in oncogenes, which promote cell growth, or loss of function mutations in tumour suppressor genes, that ordinarily inhibit cell division and survival. Generally, multiple genetic changes are required in normal cells before they acquire the defining characteristics of cancer cells.

In a seminal paper published in 2000, Hanahan and Weinberg outlined the necessary alterations enabling a normal cell to become fully transformed (Hanahan and Weinberg, 2000). Known as the original 'hallmarks of cancer', the six functional capabilities they proposed were: self-sufficiency in growth signals, insensitivity to anti-growth signals, evasion of apoptosis, limitless replicative potential, angiogenesis induction and activation of invasion and metastasis. More recently, this was deemed a reductionist view of cancer formation that fails to acknowledge the role of the host system in influencing the acquisition of these hallmarks. Thus, these hallmarks were updated in 2011 to include two emerging hallmarks - the deregulation of cellular energetics and the avoidance of immune destruction - and two enabling characteristics - tumour-promoting inflammation and genome instability (Hanahan and Weinberg, 2011).

It is now widely accepted that whilst cell autonomous mechanisms are required for cancer initiation, non-malignant cells of the tumour microenvironment (TME) can be active participants in modulating disease progression. The TME consists of non-cellular components such as the extracellular matrix (ECM), and a cellular component including endothelial cells, immune cells and fibroblasts (Kalluri and Zeisberg, 2006). The composition of the TME varies considerably between different cancer types and individual patients, and much research is focused on understanding cellular interactions between different cell types within the TME in the hope of identifying stromal therapeutic targets (Chen and Song, 2018). Accumulating evidence suggests that the TME plays a significant role in driving the progression of breast cancer, both by promoting primary tumour growth and through facilitating invasion and metastasis (Mao et al., 2013). Cancer-associated fibroblasts (CAFs), which are abundant in most breast cancers (Aboussekhra, 2011), have been heavily implicated in these processes, but also in inhibiting responses to treatment (Mao et al., 2013). This thesis sets out to elucidate how CAFs influence the responsiveness of breast cancer to immunotherapy through modulation of the tumour immune microenvironment.

1.2 Breast cancer biology, diagnosis and treatment

1.2.1 Breast cancer biology

The normal breast is a highly ordered network of cell types that interact to ensure its normal development and physiological function (Figure 1.1A). Mammary ducts in the breast consist of a luminal epithelial layer, responsible for producing milk in the lactating gland, surrounded by a contractile outer myoepithelial layer, which synthesises the duct-enveloping basement membrane. This basement membrane forms a physical barrier between the breast epithelium and the surrounding microenvironment, which is composed of ECM components produced by fibroblasts, vascular cells and immune cells.

Analogously to the adenoma-carcinoma sequence described for other solid cancers, breast cancer originates from a transforming event in a normal breast

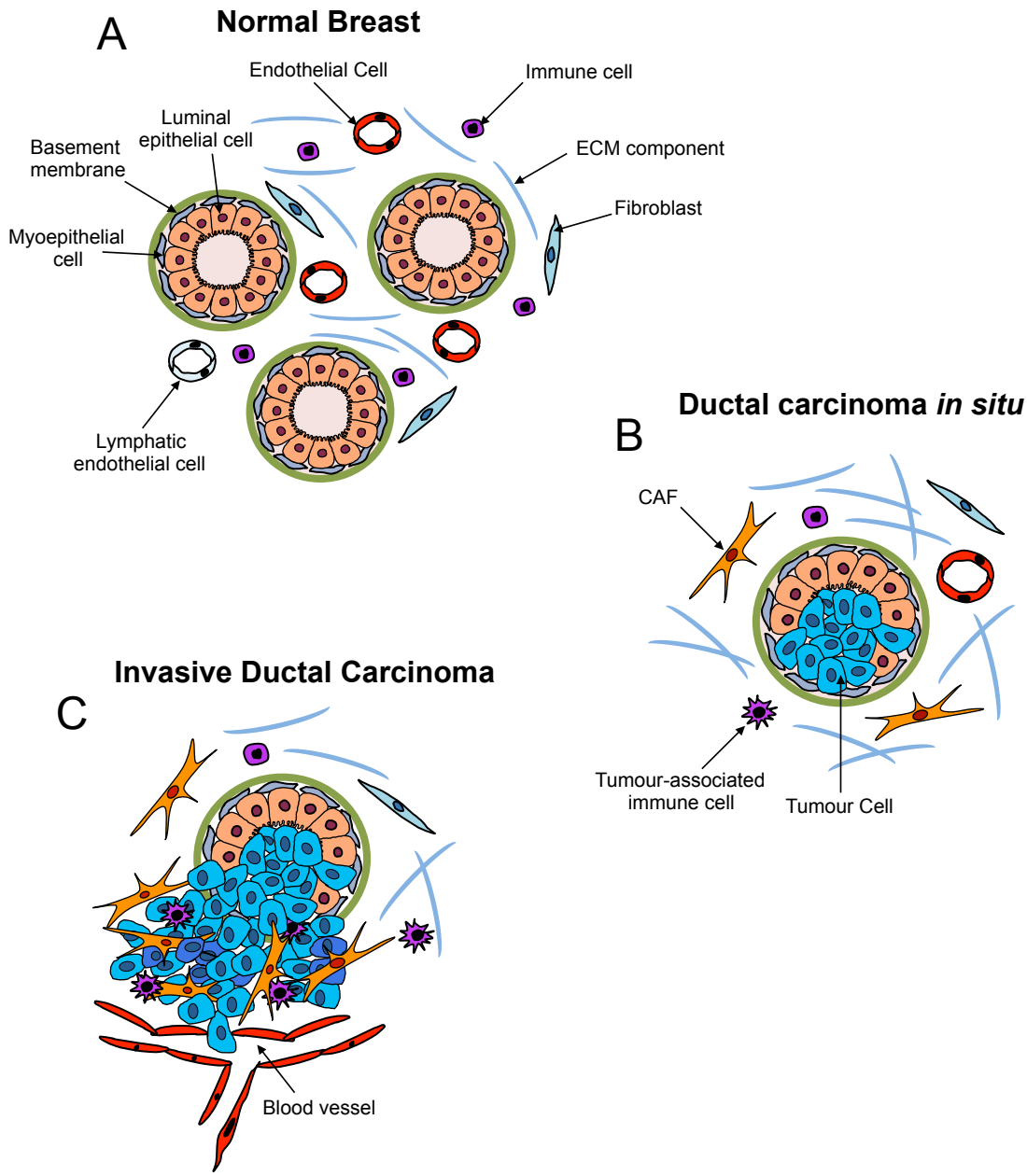

Figure 1.1: Breast cancer initiation. A. The normal breast tissue is an ordered structure containing mammary ducts embedded in extracellular matrix (ECM), containing non-epithelial stromal cells. The mammary duct consists of a luminal epithelial layer and an underlying basal epithelial layer, encased within the basement membrane. **B.** Ductal carcinoma *in situ* (DCIS) describes when hyper-proliferative cells of the mammary epithelium have filled the mammary duct, but have not breached the basement membrane. The surrounding stroma can be altered in structure and composition, including the activation of cancer-associated fibroblasts (CAFs). DCIS may or may not progress to become invasive breast cancer. **C.** Invasive ductal carcinoma describes when the tumour cells of the mammary epithelium have broken through the encapsulating basement membrane and have invaded the surrounding stroma. The stroma becomes infiltrated by different subsets of immune cells and activated stromal cells including fibroblasts and vascular cells.

epithelial cell, likely a stem or progenitor cell, which accumulates additional genetic and epigenetic alterations that initiate tumourigenesis (Stingl and Caldas, 2007). This leads

to what is known as ductal hyperplasia, which can be followed by other premalignant states such as ductal carcinoma *in situ* (DCIS) (Figure 1.1B), where the lumen of the mammary duct contains proliferating epithelial cells that are encapsulated by the basement membrane and myoepithelial layer. Other premalignant lesions that precede the onset of invasive carcinoma include columnar cell lesions, hyperplasia of the usual type, atypical ductal hyperplasia and lobular carcinoma *in situ.* Pre-malignant lesions such as these can progress to invasive carcinoma when the cells of the luminal epithelium escape the basement membrane and invade into the surrounding breast stroma (Burstein et al., 2004) (Figure 1.1C). However, the molecular changes underlying this progression are yet to be fully understood, and often, premalignant lesions such as DCIS do not progress to fully invasive disease.

In contrast to premalignant lesions, invasive breast carcinomas have breached the basement membrane where they make direct contact with breast stromal tissue. From here, breast cancer is capable of spreading to distant organs around the body. This process is known as metastasis, and is responsible for the majority of deaths in patients with solid tumours. The metastatic process is often simplified into five distinct steps known as the metastatic cascade (Chambers et al., 2002). These steps are: local invasion into the breast stroma, intravasation into the vasculature and/or lymphatics, survival in the circulation, extravasation from the vasculature at the distal tissue and extravasation and colonisation at secondary sites. Cells such as fibroblasts, vascular cells and immune cells within the breast stromal tissue play key roles in modulating breast cancer progression, and some of these interactions will be discussed in Sections 1.3 and 1.4.

During metastatic tumour cell transformation, reduced cell-cell adhesions often occur as a result of loss of expression of the transmembrane glycoprotein E-cadherin, either through mutation, promoter hypermethylation or degradation (Jeanes et al., 2008). Adhesion of tumour cells is also altered by changes in the expression of integrins, proteins that play a key role in cell adhesion to the ECM. Subsequent invasion of breast tumour cells through the laminin-rich basement membrane and the

collagen-rich stroma involves a coordinated set of molecular events (Wolf and Friedl, 2011). This includes tumour cell polarisation and protrusion of an actin-rich pseudopodium that adheres to the ECM through integrin-based contacts. These focal adhesions generate an adhesive force, before localised proteolysis of impeding ECM collagen fibres and actomyosin-based contraction pulls the cell forward. These events all require remodelling of the actin cytoskeleton that provides a structural framework for cell migration.

In order to metastasise, tumour cells must first enter the vasculature in a process known as intravasation (Figure 1.1C). This is facilitated by angiogenesis, whereby new blood vessels are formed that supply the growing tumour mass with nutrients and oxygen. Tumour cells can break through the vascular basement membrane surrounding blood vessels, disrupting endothelial cell junctions in order to access the lumen of the vessel. Factors such as matrix metalloproteinases (MMPs), vascular endothelial growth factor (VEGF) and transforming growth factor beta (TGFβ) are implicated in this process (Reymond et al., 2013), but discovering exact mechanisms is complicated by distinguishing between factors that promote general tumour cell invasion as opposed to intravasation.

Once tumour cells have reached the vasculature, they encounter a range of cellular stresses that must be overcome to ensure their survival. Tumour cell membranes can be damaged by the hydrodynamic shearing forces of flowing blood, possibly resulting in cell death through physical disruption alone. Furthermore, once tumour cells are in the bloodstream, the absence of anchorage to an ECM can induce a programme of cell death known as anoikis, which prevents the survival of un-anchored cells (Paoli et al., 2013). Finally, the bloodstream contains a large number of circulating innate and adaptive immune cells, some of which can destroy tumour cells through their cytotoxic activity. Tumour cells must evade immune destruction both in the bloodstream, and at primary and secondary sites. The mechanisms they use to evade immune control are described in greater depth in Section 1.3.

The final steps of the metastatic cascade, extravasation and colonisation, involve cellular processes at distant metastatic sites. Extravasation is similar to intravasation in that tumour cells must pass between endothelial cell junctions and through the vascular basement membrane. However, during extravasation, tumour cells first encounter the endothelial cell layer rather than the basement membrane, and utilise cell surface adhesion molecules such as CD44 for this purpose (Strilic and Offermanns, 2017). Interestingly, where in the body tumour cells extravasate and colonise is largely determined by their origin, with breast cancer cells predominantly metastasising to the bones and lungs, and to a lesser degree to the liver and brain. This specificity can be explained by the 'seed and soil' theory first proposed by the surgeon Stephen Paget in 1889, who hypothesised that tumour cells can only grow in a microenvironment (soil) permissive for that particular tumour cell (seed) (Paget, 1889). Other theories postulate an alternative mechanism for tumour-type dependent metastatic organ specificity based on the circulatory patterns of the body. However, it has also been established that different subtypes of breast cancer have different metastatic profiles (Kennecke et al., 2010). Since the primary site is the same regardless of the subtype of breast cancer, this observation cannot be explained by circulatory patterns and instead suggests the existence of active tissue tropism that is likely influenced by crosstalk between tumour cells and stromal cells at metastatic sites. The ability of tumour cells to signal to stromal cells at these sites and create a 'metastatic niche' is crucial in supporting tumour cell survival and eventual formation of secondary metastatic tumours (Kaplan et al., 2006).

1.2.2 Diagnosis, receptor status and molecular subtyping

It is estimated that around 1 in 7 UK females will develop breast cancer in their lifetime (Cancer Research UK statistics, 2014-2016), and tumours are normally identified either through routine mammographic imaging or self-palpation. In the UK, the National Health Service (NHS) offers a screening programme for women aged between 50 and 70 year old that receive mammograms every 3 years during this period. Risk factors

pre-disposing women to breast cancer include reproductive factors (such as age at first menstruation, age at first full-term pregnancy, number of children and duration of breastfeeding), genetic familial risk factors (such as *BRCA1/2* mutation) and environmental factors (such as alcohol consumption, smoking status and obesity) (Rudolph et al., 2016).

Following diagnosis, breast cancer is classified according to TNM system, which evaluates tumour size (T), lymph node involvement (N) and metastatic status (M). Good public awareness of breast cancer, coupled with the effectiveness of screening programmes, means that most breast cancers are identified early on in disease progression. Patients whose breast cancer is diagnosed between TNM stages I-II have a 5-year relative survival rate of > 95%, however, those not diagnosed until TNM stages III and IV have rates of < 50% and < 15%, respectively (Cancer Research UK statistics, 2002-2006).

Tumour tissue from biopsies can be examined histopathologically, providing an additional means of classifying breast cancer. Features such as nuclei pleomorphism, tumour cell differentiation and mitotic count are assessed when grading tumours (Elston and Ellis, 1991). Breast cancers can also be assessed for expression of three hormone receptors via immunohistochemistry (IHC). IHC staining for oestrogen receptor (ER), progesterone receptor (PR) and the receptor tyrosine-kinase ErbB2 (HER2) defines the receptor status of the breast cancer. The three main receptor statuses are outlined in Figure 1.2. Around 70-80% are positive for ER and/or PR expression but negative for HER2 expression, and are classified as ER-positive (ER^+) tumours. HER2-positive ($HER2^+$) tumours are divided into two more subtypes: ER^+ (with or without PR expression) or ER and PR negative. Tumours negative for expression of all three receptors are known as triple-negative breast cancers (TNBC) and have the worst clinical prognosis. However, as discussed further in Section 1.3.2.5, compared to patients with other subtypes of breast cancer, TNBC patients often have a more robust tumour immune infiltrate, and appear to be more sensitive to immunotherapy (Disis and Stanton, 2015).

	ER+	HER2+		TNBC
Prevalence (%)	~70	~20		~10
ER expression	+	+	-	-
PR expression	+	+	-	-
HER2 amplification	-	+	+	-
Pathological grade	Low	High	High	High
Ki67 Positivity	Low	High	High	High
Standard of care	Endocrine therapy± chemotherapy	Trastuzumab ± endocrine therapy± chemotherapy		Chemotherapy
Prognosis	Good	Good	Poor	Poor
Risk of relapse	Low	Low	High	High

Figure 1.2: Pathology, treatment and prognosis of breast cancer subtypes. Summary of breast cancer subtypes based on receptor status. ER, oestrogen receptor; PR, progesterone receptor; HER2, Human epidermal growth factor receptor 2/ERBB2; TNBC, triple-negative breast cancer.

Recent developments in gene expression profiling have helped enabled more in-depth subtyping of breast cancers, referred to as intrinsic or molecular subtyping. These subtypes have different prognoses and often have different responses to specific therapies. Five molecular subtypes of breast cancer have been identified: luminal-A, luminal-B, HER2-enriched, basal-like and normal-like (Perou et al., 2000). Luminal-A and luminal-B subtypes encompass around 67% of ER^+ tumours, and this luminal subdivision is attributed to the increased proliferation of luminal-B tumours. Luminal-B tumours tend to have worse prognosis than luminal-A tumours, and also typically have reduced expression of ER (Cheang et al., 2009). Most tumours classified as $HER2^+$ via IHC are also defined as HER2-enriched following molecular subtyping. Basal-like tumours, expressing the cytokeratins (CK) 5, 14 and 17 that are exclusively expressed in the basal epithelium, are primarily TNBC tumours. Whilst luminal tumours are most responsive to endocrine therapy, basal-like tumours are more sensitive to chemotherapy.

More recently, a further five potential subtypes of breast cancer have been revealed in studies using data obtained from The Cancer Genome Atlas (TCGA) (Hoadley et al., 2018) and the Molecular Taxonomy of Breast Cancer International Consortium (METABRIC) (Curtis et al., 2012), though these are yet to be fully validated in the clinic. These re-classifications, based on the genetic fingerprint of breast cancers, could eventually offer insight into unknown breast cancer biology, allowing a prediction as to whether breast cancers will respond to particular treatments or whether they will relapse following treatment. Already, molecular subtyping in this way has been proven to hold clinical prognostic value, including responses to treatment, using single sample predictors (SSPs) such as the Prediction Analysis of Microarray 50 (PAM50) classifier, which makes calls based on a 50 gene centroid correlation distance to luminal-A, luminal-B, basal-like, HER2-enriched and normal-like centroids (Raj-Kumar et al., 2019).

Similar gene expression profiling studies have been performed to investigate the relative proportions of immune cell subsets in breast cancer and whether their abundance correlates to disease relapse or response to chemotherapy. In tumours lacking ER expression, the presence of $CD8^+$ cytotoxic T cells, also known as cytotoxic T lymphocytes (CTLs), is associated with a reduction in the risk of relapse following neoadjuvant chemotherapy treatment, whilst in ER^+ tumours; the presence of macrophages is associated with poor prognosis (Ali et al., 2016). Efforts to further classify breast cancers based on their immune infiltrate has the potential to enhance clinical prediction and identify patients who may respond to immunotherapy. The role of the immune system in shaping cancer progression will be discussed in greater depth in Section 1.3.2.

The variety of approaches to sub-classifying breast cancers discussed emphasises the heterogeneous nature of the disease. However, despite advances in the subtyping of breast cancers, diagnosis and subsequent treatment regimens are still based largely on the TNM and receptor status of tumours (Reis-Filho and Pusztai, 2011).

1.2.3 Breast cancer treatment

1.2.3.1 Surgery

Compared to other solid tumour cancer types, breast cancer has a relatively low mortality rate compared to incidence, with a ~78% 10-year survival rate from diagnosis, compared to < 1% for pancreatic cancer (Cancer Research UK statistics, 2011). In part, this can be attributed to both increased public awareness and the screening programme in the UK, which facilitates early diagnosis. This high survival rate is also likely a result of the ease of surgical intervention for breast cancer compared to other solid tumours. Despite advances in both radiotherapy and systemic therapy, surgery remains the most effective treatment for breast cancer and is often curative if the disease has not yet spread.

Two main types of surgery exist for breast cancer, local resection (sometimes called lumpectomy), where small tumours are removed together with defined margins of stromal tissue preserving the majority of the breast tissue, or mastectomy, where larger tumours likely to spread are removed together with all of the breast tissue. Surgery is usually used to remove the primary tumour and local lymph nodes. Commonly, a sentinel lymph node biopsy is performed, which aids in cancer staging and achieves the same survival and regional control as removing a greater number of axillary lymph nodes, but with fewer side effects. Removal of metastatic lesions in secondary sites requires more invasive surgery that can have a negative impact on a patient's survival. Thus, this type of surgery is usually reserved for palliative care when symptoms are very severe, as can be the case with liver metastases.

Metastasis poses a much greater mortality risk than the primary tumour itself, and patients with metastatic disease have lower overall survival rates. The 5-year survival rate for patients with stage III breast cancer is 60%, but this reduces to 15% for patients with stage IV cancer (Cancer Research UK statistics, 2011). Patients presenting with existing metastatic disease have already missed the point at which surgery has any beneficial effects, and it is not clear whether surgically removing the

primary tumour at this stage has any positive effect on prognosis (Badwe et al., 2015; Soran et al., 2018). Often, primary tumours are removed in these cases as a form of palliative treatment. However, preclinical studies using models of metastasis have revealed how the presence of primary tumours can in fact prevent the growth of secondary growth implants (Chiarella et al., 2012), presumably a result of promoting anti-tumour immune surveillance, a topic discussed in greater depth in Section 1.3.2.

Overall 80% of patients who are diagnosed with breast cancer in the UK have received surgery as part of their treatment (The Second All Breast Cancer Report, 2011). This figure includes both patients who had surgery alone, without other therapeutic interventions, and also patients who received adjuvant or neoadjuvant treatments. Neoadjuvant treatments are those administered before removal of the primary tumour, and can include radiotherapy, chemotherapy or endocrine therapy. These treatments aim to reduce the size of the primary tumour in the breast, facilitate tumour removal and improve the chances of achieving clear margins following surgery. In addition, neoadjuvant treatment provides important information as to the response of the tumour cells to therapy. Adjuvant treatments are those given following tumour removal and include the same treatments as above, but also targeted agents and immunomodulatory drugs, and are used to prevent local recurrence.

1.2.3.2 Radiotherapy

Radiotherapy uses X-irradiation that induces DNA damage and results in tumour cell death. The short wavelength of X-rays gives good penetrance through tissues, and their high energy induces DNA double strand breaks, which are toxic to cells (Jackson and Bartek, 2009).

In external beam radiotherapy, radiation is delivered from outside the patient's body, whilst brachytherapy involves implanting hollow tubes into the breast during surgery into which radioactive emitting metal isotopes are placed. Another experimental form of radiotherapy, known as intraoperative or intrabeam radiotherapy,

involves positioning a radiation emitter within the breast cavity following tumour removal, and is currently being trialled in UK hospitals.

Radiotherapy is routinely used for treating breast cancer, often following surgery in order to minimise the chance of local disease recurrence. However, since it induces DNA damage without specificity there is always a risk of damaging non-malignant cells, which can cause side effects. One side effect is fibrosis, which is characterised by increased collagen deposition in the ECM and myofibroblast activity. Tissue fibrosis changes the structure and stiffness of the tissue which can be uncomfortable for the patient, and deleterious to long term outcome as it reduces tissue function.

1.2.3.3 Endocrine therapies

As previously discussed in Section 1.2.2, breast cancer can be divided into subtypes based on both their receptor expression and intrinsic molecular subtype, and these are used to determine therapeutic approaches (Figure 1.2). Early stage breast cancers are primarily treated with surgery, so these classifications are more useful in determining the choice of systemic therapy for the metastatic disease.

Both oestrogen and progesterone are hormones that regulate the reproductive cycle and development of breast tissue, pregnancy and lactation. Epithelial cells in mammary ducts express receptors for these hormones, allowing their proliferation to be controlled. The majority of breast cancers continue to express these receptors and rely on their transcriptional activity to proliferate. In menopausal women, oestrogen is no longer produced by the ovaries, so instead is generated by conversion of androgens (like testosterone) by an enzyme called aromatase.

Endocrine therapies manipulate the endocrine system and block proliferation of tumour cells dependent on oestrogen (Jackson and Bartek, 2009). There are three classes of endocrine therapy that have different mechanisms of action, indications and side effects. Selective ER modulators (SERMs) such as tamoxifen are small molecule competitive inhibitors that antagonise oestrogen binding to the ER; selective ER down-

regulators (SERDs) bind to the ER and induce proteolytic degradation by the cell; and aromatase inhibitors (AIs), which are given only to postmenopausal women, block oestrogen production in peripheral tissues to reduce ER signalling.

Tamoxifen, which acts as a partial ER agonist, has both oestrogenic and antioestrogenic activity depending on in which tissue it acts upon. In the uterus and liver, tamoxifen primarily has oestrogenic effects, but in breast tissue it acts as an ER antagonist, inhibiting the transcription of oestrogen-responsive genes (Katzenellenbogen and Katzenellenbogen, 2000). Although tamoxifen and other SERMS are highly effective, their usefulness is often limited by the development of intrinsic and acquired resistance (Osborne and Schiff, 2011). Multiple mechanisms have been proposed for driving this resistance, including deregulation of components of the ER pathway, alterations in cell cycle and cell survival signalling molecules, and activation of alternative proliferation and survival pathways, and many of these resistance mechanisms are now themselves targets for novel treatments.

1.2.3.4 Targeted agents for breast cancer

Targeted agents for breast cancer refers to drugs which block the growth of cancer by interfering with the function of specific molecules responsible for tumour cell proliferation and survival (Masoud and Pagès, 2017). Types of targeted therapy include monoclonal antibodies, which block specific targets on the surface of cancer cells, and small-molecules drugs, that typically target intracellular proteins. A well-known target in breast cancer is the receptor tyrosine kinase HER2.

HER2 is a member of the epidermal growth factor (EGF) receptor family that drives intracellular mitotic signalling, and expression of HER2 is often upregulated in breast cancer due to gene amplification. Herceptin (trastuzumab) is a humanised anti-HER2 monoclonal antibody, which is approved in the UK for treating $HER2^+$ breast cancer. By binding to the extracellular domain of HER2, Herceptin prevents its homo-dimerisation with another HER2 molecule, which in turn prevents transactivation and blocks downstream intracellular signalling pathways. Furthermore, Herceptin has also

been shown to induce antibody dependent cell-mediated cytotoxicity (ADCC), which contributes to the destruction of breast cancer cells and is discussed further in Section 1.3.2.

BRCA1/2 mutations are the highest heritable risk locus for breast cancer, and cause defects to the cell's DNA repair pathways. Poly-ADP ribose polymerase (PARP) is an enzyme that is also required for DNA repair, especially in *BRCA1/2* deficient cells. PARP inhibitors (such as olaparib) have been shown to be highly effective in inducing cell death in breast cancer cells that harbour *BRCA1/2* mutations. This synthetic lethal mechanism of action ensures specificity for the cancer cells over normal tissue, since only tumour cells which have defective DNA repair pathways will be sensitive to the drug (Griguolo et al., 2018).

Like endocrine therapy before, a major challenge in using targeted therapies is resistance. Often, resistance occurs soon after targeted therapies have been approved for use, and sometimes mechanisms driving resistance are identified before the drugs are routinely used in the clinic (Lord and Ashworth, 2013). This rapid evolution of the tumour means that treatments of this kind have limited long-term therapeutic effects, and often, the only remaining option for treating advanced metastatic disease is chemotherapy.

1.2.3.5 Chemotherapy

Despite advancements in targeted cancer therapies, chemotherapy, which was first used in the 1940s, remains widely used in breast cancer. Most commonly, chemotherapy is given following surgery (adjuvant setting) to treat local or systemic metastatic disease. However, increasingly, patients will receive a course of treatment before surgery (neoadjuvant setting) in order to shrink the tumour before resection. Around 40% of ER^+ and 80% ER^- patients will receive chemotherapy, and for patients with TNBC, it remains the mainstay treatment.

Administering chemotherapy treatment as a combination of multiple drugs with different mechanisms of action is standard practice for treating breast cancer. FAC or

FEC are the combinations of 5-fluorouracil with either Adriamycin (doxorubicin) or Pharmorubicin (epirubicin) together with cyclophosphamide. Taxane based drugs such as Taxol (paclitaxel) and Taxotere (docetaxel) are often included in these combinations, and are normally given in subsequent treatment cycles; these combination therapies are referred to as FAC/T or FEC/T. The rationale behind combination chemotherapy is to reduce the emergence of resistance, minimise side effects and maximise therapeutic response.

Chemotherapeutic agents are either DNA repair/replication inhibitors or nucleotide mimetics, though most work by inducing some form of DNA damage (Malhotra and Perry, 2003). Examples of DNA targeting agents are doxorubicin, and cyclophosphamide and 5-fluorourcil. Doxorubicin is a member of the anthracycline family of chemotherapeutics; there are several mechanisms of action, and it is not fully known which contributes the most to its cytotoxicity. Doxorubicin is a topoisomerase II inhibitor that prevents proper resolution of stalled replication forks, resulting in DNA double strand breaks (DSBs). Cyclophosphamide is an alkylating agent that forms DNA adducts by binding to guanine residues, leading to DSBs during DNA replication. 5-Fluorouracil is a nucleotide mimetic drug which closely resembles the nucleotide uridine; it irreversibly inhibits the enzyme require to catalyse the conversion of deoxyuridine monophosphate (dUMP) to deoxythymidine monophosphate (dTMP) which is required for DNA synthesis, thus inhibiting DNA replication.

Docetaxel is a member of the taxane family of drugs, whose mechanism of action is mostly distinct from the DNA targeting agents described above. They are amongst the most widely used agents across all cancers, and especially breast cancer. Taxanes work as microtubule poisons, binding to β-tubulin subunits, and stabilising the polymer. The effect of this stabilisation inhibits the de-polymerisation of the tubules, which affects vesicle trafficking and chromosomal segregation. Their mechanism of action strongly inhibits cell division but does not necessarily rely on DNA damage or DSBs for its efficacy (Poruchynsky et al., 2015).

Chemotherapy is proposed to induce apoptosis in cancer cells more than normal cells due to their increased rate of proliferation. However, this assumption has been challenged, and it has been postulated that cancer cells are 'primed for death' as a result of their genomic and signalling abnormalities (Ni Chonghaile et al., 2011). Nevertheless, damage to normal cells by chemotherapy results in side effects including nausea, skin irritation and hair loss. Certain chemotherapy regimens are also known to result in systemic immune suppression, which in theory could blunt the effectiveness of newer therapies designed to enhance anti-tumour immune activity. However, it is becoming clear that successful responses to chemotherapy in fact depend on the host immune system, and that tumour cell death induced by chemotherapeutic agents can augment the efficacy of immunotherapeutic agents when used in combination (Antonia et al., 2017). Immunotherapy is only recently gaining traction as a viable option for breast cancer treatment, and will be discussed in more detail in Section 1.3.2.5.

1.3 The immune system and cancer

Tumours consist not just of cancer cells, but also a variety of non-malignant cell types including lymphatic and vascular endothelial cells, fibroblasts, pericytes and cells of the innate and adaptive immune systems. These cells, together with the ECM, are collectively known as the tumour stroma or tumour microenvironment (TME). Traditionally, the TME was viewed as an inert bystander in cancer, and drug discovery has predominantly focused on developing therapies that target cancer cells. However, it is now widely appreciated that the TME plays an important role in cancer progression and drug resistance across multiple cancer types, and approaches to treating cancer have advanced accordingly (Hanahan and Weinberg, 2011).

The immune system shapes cancer progression through multiple, opposing mechanisms, and it is increasingly apparent that the number, type and activation status of immune cells in the TME has a considerable influence on cancer prognosis (Gajewski et al., 2013). Whilst certain immune cells can recognise and destroy developing cancer cells, others can promote immunosuppression, tumour cell

proliferation and metastasis. As a result, much effort has been directed towards designing anti-cancer therapies that either directly enhance anti-tumour immunity, or block the tumour-promoting or immunosuppressive properties of others. As discussed in Section 1.3.2.2, such therapies have revolutionised the field of oncology, and in some cancer types, have replaced conventional treatments. A summary of the components of a fully functional immune system is presented in the following sections, followed by a description of its role in carcinogenesis.

1.3.1 The immune system

The immune system is a complex and evolutionary advanced host defence system consisting of a variety of biological structures and processes. Through a series of well-defined steps known as the immune response, the immune system protects against infection and disease by recognising and neutralising pathogens such as viruses and bacteria. Crucially, in physiological conditions, certain parts of the immune system are able to distinguish pathogens from the host's own cells, thus limiting damage to healthy tissues.

In most mammalian organisms, the immune response consists of innate and adaptive immunity. Though both use a combination of humoral immunity (mediated by proteins in extracellular fluids) and cell-mediated immunity, their functions differ considerably. Whilst the evolutionary older innate immune system is responsible for non-cell type specific responses, the adaptive immune system is a highly specialised system responsible for targeted non-self specific responses and the development of immunological memory. The cells responsible for orchestrating innate and adaptive immune responses are known as immune cells (leukocytes), and are derived from multipotent cells in the bone marrow known as haematopoietic stem cells (Figure 1.3). Immune cells can be categorized as either lymphoid or myeloid, depending on from which cells they are derived. Myeloid cells, including monocytes, macrophages and neutrophils, are derived from common myeloid progenitors and make up the majority of cells of the innate immune system (Charles A Janeway et al., 2001). Lymphoid cells,

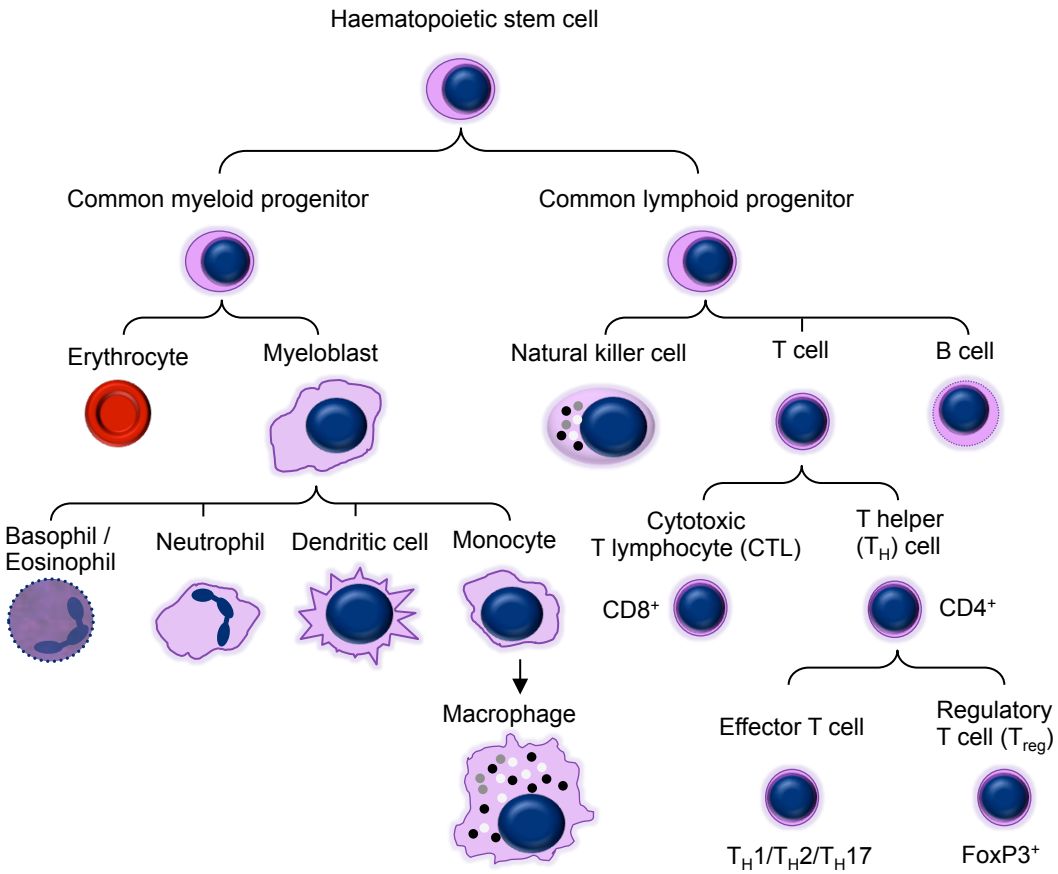

Figure 1.3: Cell lineages making up the innate and adaptive immune systems. All immune cells are derived from multipotent haematopoietic stem cells in the bone marrow. The innate immune system comprises cells derived primarily from the myeloid lineage, whilst the adaptive immune system comprises cells derived from the lymphoid lineage. Although natural killer cells are of lymphoid origin, their function is more similar to that of the innate immune system, and so their classification is controversial. The cell lineage of dendritic cells also remains not fully elucidated.

including T cells and B cells, are derived from common lymphoid progenitors and constitute the majority of the adaptive immune system. Though natural killer (NK) cells also belong to the lymphoid lineage, they lack the antigen specificity of T and B cells and instead have an important role in innate immune responses (Charles A Janeway et al., 2001). Dendritic cells (DCs) are professional antigen-presenting cells (APCs) whose exact origin is controversial, yet they are known to be important in coupling innate to adaptive immune responses (van Vliet et al., 2008).

1.3.1.1 The innate immune system

Infectious agents such as bacteria are prevented from entering the body by physical, chemical and biological barriers. The skin and other epithelial surfaces provide an initial physical barrier that protects against microbial insults. However, those microorganisms that do manage to penetrate the epithelial surfaces of the body are immediately met by a variety of cells and molecules that constitute the innate immune response. Inflammation, stimulated by damaged cells, represents one of the first responses to infection and is initiated by tissue resident cells such as macrophages and dendritic cells. These cells are able to distinguish self from non-self through recognition of pathogen-associated molecular patterns (PAMPs), which are small molecular motifs common to many pathogens but are not found in the host. PAMPs, including bacterial lipopolysaccharides (LPS) and endotoxins found on gram-negative bacteria, are recognised by innate immune cells through toll-like receptors (TLRs) and other pattern recognition receptors (PRRs). Recognition results in activation of associated cells that release inflammatory mediators, further stimulating the inflammatory response. Chemical factors produced during inflammation attract phagocytic cells that themselves release factors attracting other immune cells.

The phagocytic cells of the immune system include macrophages, dendritic cells and neutrophils. These cells engulf invading pathogens and cellular debris, destroying them in intracellular vesicles in a process known as phagocytosis (Rosales and Uribe-Querol, 2017). Macrophages are large cells found in strategic points in tissues and organs throughout the body where they await microbial invasion or accumulation of foreign particles. In addition to their phagocytic role, they also act as an important link between the innate and adaptive immune systems due to their ability to recruit lymphocytes and present antigens. Macrophages are also able to modulate inflammation through the release of cytokines: small proteins that regulate the differentiation, proliferation and activity of other immune cell populations. Macrophages activated by LPS, interferon gamma (IFNγ) and tumour necrosis factor (TNF) acquire a pro-inflammatory role and are known as M1 macrophages. In contrast, an alternative subset of macrophages, known as M2 macrophages, is activated by interleukin 4 (IL4)

and has anti-inflammatory properties (Mantovani et al., 2002). Though this classification has come under criticism for being over simplistic (Martinez and Gordon, 2014), particularly in light of recent single cell RNA sequencing experiments demonstrating the plasticity of myeloid cells (Song et al., 2019), it is still commonly used for broadly assessing the phenotype of tumour-associated macrophages (TAMs).

Much like macrophages, dendritic cells are tissue-resident cells that act as messengers between the innate and adaptive immune systems. Unlike macrophages, their main function is not primarily to destroy pathogens, but to present antigens to T cells of the adaptive immune system. Immature dendritic cells continually take up extracellular material, including bacteria and viruses, and upon activation migrate to nearby lymph nodes. Activation also results in maturation of dendritic cells into highly effective APCs capable of presenting fragments of engulfed, degraded proteins at their cell surface using major histocompatibility complex (MHC) molecules. These MHC molecules bind to receptors on T cells, and in the presence of co-stimulatory signals, result in T cell stimulation and the initiation of a targeted adaptive immune response. Activation of T cells without co-stimulation results in T cell anergy, a mechanism of immune tolerance in which T cells become intrinsically functionally inactivated (Schwartz, 2003).

The third phagocytic cell type of the immune system, neutrophils, are the most abundant type of immune cell in most mammals and are one of the first to migrate towards sites of inflammation. Neutrophils have three methods for destroying microorganisms: phagocytosis, degranulation and through generation of neutrophil extracellular traps. Furthermore, neutrophils release several cytokines, augmenting inflammatory responses by other immune cells. It was once though that neutrophils were a homogenous population of cells with a unique function. However, more recently, the concept of neutrophil phenotypic and functional heterogeneity is widely accepted (Rosales, 2018).

The existence of cells with the characteristics of lymphoid cells, but which lack specific antigen receptors, has been recognised for decades. These cells are known as

innate lymphoid cells (ILCs), and as the name suggests, are a part of the innate immune response unlike other lymphoid cells that play a role in adaptive immunity. The best-known ILCs are NK cells, which are larger than T and B cells, and possess cytoplasmic granules containing cytotoxic proteins such as perforin and granzymes. Release of perforins onto the surface of a target cell results in the formation of pores in the cell membranes through which granzymes can enter, inducing programmed cell death (apoptosis). Another pathway used by NK cells to kill target cells is through the interaction of tumour necrosis factor-related apoptosis-inducing ligand (TRAIL), expressed on the surface of NK cells, with the death receptors DR4 and DR5, expressed on many cell types. Stimulation of DR4 and DR5 upon NK cell recognition of target cells results in their apoptosis via a caspase 8-dependent mechanism (Zamai et al., 1998). Finally, NK cells, as a result of their expression of fragment crystallisable (Fc) receptors, mostly CD16, can also induce ADCC which as mentioned in Section 1.2.3.4, is a recognised mechanism of action for HER2-targeted antibodies used in breast cancer treatment (Muntasell et al., 2017). During typical ADCC, Fc receptors on the surface of NK cells engage with the Fc portion of immunoglobulins bound to the surface of target cells. This interaction activates NK cells, triggering the recruitment of adaptive immune cells through secretion of IFNγ and the direct lysis of target cells through release of perforin and granzymes (Wang et al., 2015).

To protect against pathogens such as viruses, NK cells must recognise healthy cells from infected cells. To do this, NK cells utilise a variety of activating and inhibitory receptors, the balance of which determines the NK cell response and whether target cells are destroyed. Activating receptors recognise cellular stress ligands induced by cellular events such as DNA damage, metabolic stress, infection or transformation (Pegram et al., 2011). Stimulation of activating receptors increases the likelihood of NK-cell induced death of the target cells, however, whether this occurs or not is also controlled by inhibitory receptors. Inhibitory receptors on NK cells primarily recognise MHC class I molecules that are expressed on nearly all cells of the body, and this interaction prevents NK cells from killing normal host cells. However, this inhibitory

signal is lost when target cells do not express MHC class I, such as in infected or transformed cells, resulting in NK cell activation, release of granule contents and apoptosis of target cells (Bubenik, 2003).

1.3.1.2 The adaptive immune system

Whilst innate immune responses are only able to defend against pathogens that have certain molecular patterns, in order to defend against a wider variety of pathogens, lymphocytes of the adaptive immune system have evolved to recognise virtually any foreign antigen. Two major types of lymphocytes exist: B cells, which can differentiate into antibody secreting plasma cells and play a key role in humoral immunity; and T cells, of which there are two main classes that are involved in cell-mediated responses. Both B and T cells are derived from common lymphoid progenitor cells (Figure 1.3) and together constitute 20-40% of all immune cells. Together, these highly specialised cells work together to eliminate specific pathogens or prevent their growth, also resulting in creation of an immunological memory that enhances responses to specific pathogens upon subsequent encounters. This long-lasting protection forms the basis of vaccination and contributes to the efficacy of cancer immunotherapy (Tsung and Norton, 2016).

An antigen is any molecule or part of a molecule that is specifically recognised by specialised proteins on the surface of lymphocytes. In B cells, these proteins are the immunoglobulins, known as B cell receptors when membrane-bound and as antibodies when secreted. In T cells, antigen recognition is achieved through T cell receptors (TCRs) that instead of directly binding to antigens like the immunoglobulins are only able to recognise antigens when they are processed and presented by MHC molecules. These antigen-specific receptors are acquired during the lifetime of an organism, whereas in innate immunity, pathogen-specific receptors are inherited in the germline. To generate the TCR repertoire required to recognise virtually any antigen, a mechanism known as V(D)J recombination is utilised, which diversifies the number of TCRs generated (Alcover et al., 2018). Different TCRs are uniquely expressed on

individual lymphocytes and are inherited by all progeny, contributing to long-lasting specific immunity.

In mammals, B cells mature in the bone marrow. Upon activation in secondary lymphoid organs such as the spleen and lymph nodes, B cells secrete antibodies that circulate in the bloodstream and other bodily fluids where they bind specifically to the antigen that stimulated their production. Antibodies use their fragment antigen-binding (Fab) variable region for this purpose, and this interaction either neutralises the target directly or acts as a tag on infected cells or microbes, marking them for destruction by other immune cells. Cells that recognise tagged pathogens express Fc receptors, which interact with the Fc region of antibodies, triggering effector mechanisms such as phagocytosis by macrophages, degranulation by neutrophils and the release of cytotoxic molecules by NK cells (Ravetch and Bolland, 2001). Importantly, Fc receptor expression varies depending on the antibody isotype, allowing the system to invoke appropriate immune mechanisms for distinct pathogens. Additionally, B cells can act as professional APCs, and this function also plays a role in their initial activation. Upon binding a T cell-dependent antigen, B cells will take it up through receptor-mediated endocytosis, degrade it and present it to T cells on MHC class II molecules. T cells known as follicular helper T (T_{FH}) cells activated by the same antigen will recognise the MHC class II-peptide complex on the B cell surface and express proteins such as CD40L that, through engagement with B cell-expressed CD40, results in B cell survival and differentiation into plasma cells and memory B cells.

T cells mature in the thymus and can be grouped into various subsets based on their function. They express TCRs, which are similar to immunoglobulins, but are adapted to detect antigens within host cells. Those T cells that have not yet encountered their specific antigen are known as naïve T cells, whereas those that have differentiate in effector T cells which assist in combating infection. It is in lymph nodes that circulating naïve T cells are exposed to antigens that are brought there from the periphery by APCs such as dendritic cells and macrophages (Chen and Mellman, 2013).

T helper (T_H) cells, sometimes known as $CD4^+$ cells because of their expression of the surface protein CD4, play an important role in adaptive immunity. By releasing cytokines, T_H cells modulate the activity of other immune cells and are also essential to antibody class switching in B cells, enhancing the bactericidal activity of macrophages and enhancing the activation and growth of CTLs. T_H cells, upon activation by an APC, can differentiate into T_H1 or T_H2 effector helper cells (Figure 1.3), which can be identified based on the cytokines they produce. T_H1 cells secrete IL2, IFNγ and tumour necrosis factor alpha (TNFα), and activate macrophages and CTLs, defending against intracellular pathogens by promoting cell-mediated responses. Key transcription factors for driving T_H1 polarisation are signal transducer and activator of transcription 4 (STAT4) and T-bet (Dorfman et al., 2005). In contrast, T_H2 cells secrete IL4, IL5, IL10 and IL13 and promote a humoral immune response against extracellular parasites such as helminths. T_H2 cells enhance antibody production, eosinophil activation and inhibit many macrophage functions (Romagnani, 1999). Key T_H2 transcription factors include STAT6 and GATA3. These two T_H subsets have opposing roles in cancer, T_H1 cells being associated with anti-tumour immunity and T_H2 cells with tumour growth.

Another subset of T_H cells, known as T_H17 cells because of their production of pro-inflammatory IL17, are distinct from T_H1 and T_H2 subsets and are normally induced in response to extracellular bacteria and fungi. IL17 has powerful effects on stromal cells, promoting production of other inflammatory cytokine and also aids in recruitment of other immune cells, such as neutrophils (Tesmer et al., 2008). Recently, evidence suggests that T_H17 cells are key mediators of some autoimmune and inflammatory diseases, and research into their biology has since intensified.

Regulatory T cells (T_{regs}) play a critical role in modulating the immune system. Like T_H cells, T_{regs} also express CD4, but in addition express the master transcriptional regulator, forkhead box P3 (FoxP3) (Figure 1.3). They are immunosuppressive cells that maintain tolerance to self-antigens and prevent autoimmune disease, primarily through inhibition of effector T cells. Although the mechanisms through which T_{regs} exert their immunosuppressive functions have not been fully elucidated, *in vitro*

experiments have demonstrated that they can produce a number of inhibitory cytokines such as TGFβ and IL10 (Corthay, 2009). Furthermore, T_{regs} have also been shown to suppress effector T cell function through metabolic disruption, by inducing their cytolysis using granzyme B and by indirectly blocking the maturation or antigen presentation of dendritic cells. Regarding the modulation of dendritic cells, T_{regs}, through expression of cytotoxic T lymphocyte-associated protein 4 (CTLA-4) can down-regulate dendritic cell expression of the co-stimulatory proteins CD80 (B7-1) and CD86 (B7-2) that ordinarily promote T cell activation by binding to CD28 (Sakaguchi et al., 2019).

T cell activation occurs only following engagement of the TCR with peptide-MHC complexes. CD4 expressing T_H cells recognise antigens presented by MHC class II molecules on the surface of APCs eventually leading to their activation. In contrast, CD8 expressing CTLs recognise antigens bound to MHC class I molecules that are expressed on the majority of cells in the body. The most direct action of T cells is cytotoxicity, which CTLs use to kill virus-infected and transformed cells. MHC class I molecules take antigens derived from intracellular viral particles to the surface of infected cells. Here, the MHC molecule interacts with the CD8 co-receptor: this represents the first CTL activation signal. The second signal involves the binding of the costimulators CD80 (B7-1) and CD86 (B7-2) with the cell surface protein CD28 on the surface of naïve CTLs. Only following both signals are CTLs activated. CTL effector function, which involves release of the cytotoxins perforin, granzymes and granulysin that eventually lead to apoptosis of target cells, is co-stimulation independent.

To mount responses against most tumours and viruses that do not readily infect APCs, a mechanism known as cross-presentation is utilised. Cross-priming, the result of this process, describes the activation of CTLs by APCs that have taken up, processed and presented extracellular antigens with MHC class I molecules. Certain APCs are able to utilise the MHC class I pathway in this way but remain uninfected (Heath and Carbone, 2001). Cross-presentation is particularly important in generating cytotoxic responses to tumour antigens (Schnurr et al., 2005).

1.3.2 The immune system's role in carcinogenesis

Cancers are defined by genetic alterations causing mutations that contribute to their ability to grow and metastasise. These mutations often result in the creation of tumour neoantigens: newly formed antigens encoded by tumour-specific mutated genes (Lu and Robbins, 2016). Fragments of tumour neoantigens can be presented on the surface of cancer cells by MHC class I molecules, differentiating them from normal cells (Thorsson et al., 2018). Thus, an attractive way of treating cancer would be to generate immune responses against specific tumour neoantigens in the same way that vaccination provides immunity against specific pathogens. Recent successes in treating cancer with drugs that augment anti-tumour immune responses by targeting inhibitory immune checkpoints have ignited interest in this therapeutic strategy (Pardoll, 2012).

Interactions between cancer cells and immune cells occur throughout progression: in the primary tumour, at local lymph nodes and in the circulation during dissemination and at secondary, metastatic sites. The notion that immune cells are capable of detecting and destroying cancer cells was first described by Burnet in the 1950s. Burnet hypothesised that developing cancer cells acquire new antigenic properties, inducing an immune response resulting in tumour regression before any evidence of cancer becomes clinically apparent (Burnet, 1957). Evidence to support this theory has since been demonstrated in both mouse models and in patients (Buell et al., 2005; Shankaran et al., 2001); and evasion of immune control has more recently been described as a key hallmark of cancer (Hanahan and Weinberg, 2011).

It is now clear that the interaction between cancer and the host immune system is highly complex, but is well summarised by the 'three Es' of cancer immunoediting (Dunn et al., 2004). In the first stage, known as elimination, effector immune cells such as CTLs and NK cells are activated by cytokines produced by the neoplastic lesion and recognise developing neoplastic cells either through their expression of stress ligands or tumour neoantigens. These cells are then destroyed by the activity of effector cells,

either through granule exocytosis or the death ligand/death receptor system that trigger intracellular events leading to apoptotic cell death (Martinez-Lostao et al., 2015). Neoplastic cells not killed during this stage enter into the next stage known as equilibrium, where immunological pressure selects for cancer cells with a non-immunogenic phenotype. During this phase, the developing tumour does not grow, and this may take place over a number of years. Finally, in the escape phase, the tumour gains dominance over the immune system and, through multiple mechanisms, can evade immune control and grow into clinically detectable disease (Vinay et al., 2015).

1.3.2.1 The cancer-immunity cycle

For anti-tumour immune responses to lead to killing of tumour cells, a series of stepwise events must occur. These events are referred to as the cancer-immunity cycle (Chen and Mellman, 2013), and are summarised in Figure 1.4. In Step 1, tumour neoantigens are released and captured by dendritic cells for processing and presentation. To generate an effective anti-tumour T cell response, this step must be accompanied by stimulatory immunological signals to avoid generation of peripheral tolerance (Lutz and Schuler, 2002). These signals include proinflammatory cytokines such as IL1 and TNFα, immune cell factors such as CD40L/CD40 interactions, endogenous adjuvants released from dying cancer cells such as adenosine triphosphate (ATP) and gut microbiome products such TLR ligands. In Step 2, dendritic cells then present the neoantigens to T cells using MHC molecules, resulting in the priming and activation of tumour neoantigens-specific T cell responses (Step 3). This interaction occurs in lymph nodes and the nature of the immune response generated is modulated at this stage by immune checkpoints such as CTLA-4 that initiates inhibitory signals in T cells, dampening T cell development and proliferation (Pardoll, 2012). In Step 4, activated effector T cells, including CTLs, migrate to tumours in response to chemokines such as CXCL9 and CXCL10, before infiltrating into the tumour bed (Step 5). Once in the tumour, CTLs are able to recognise (Step 6), and kill (Step 7), target

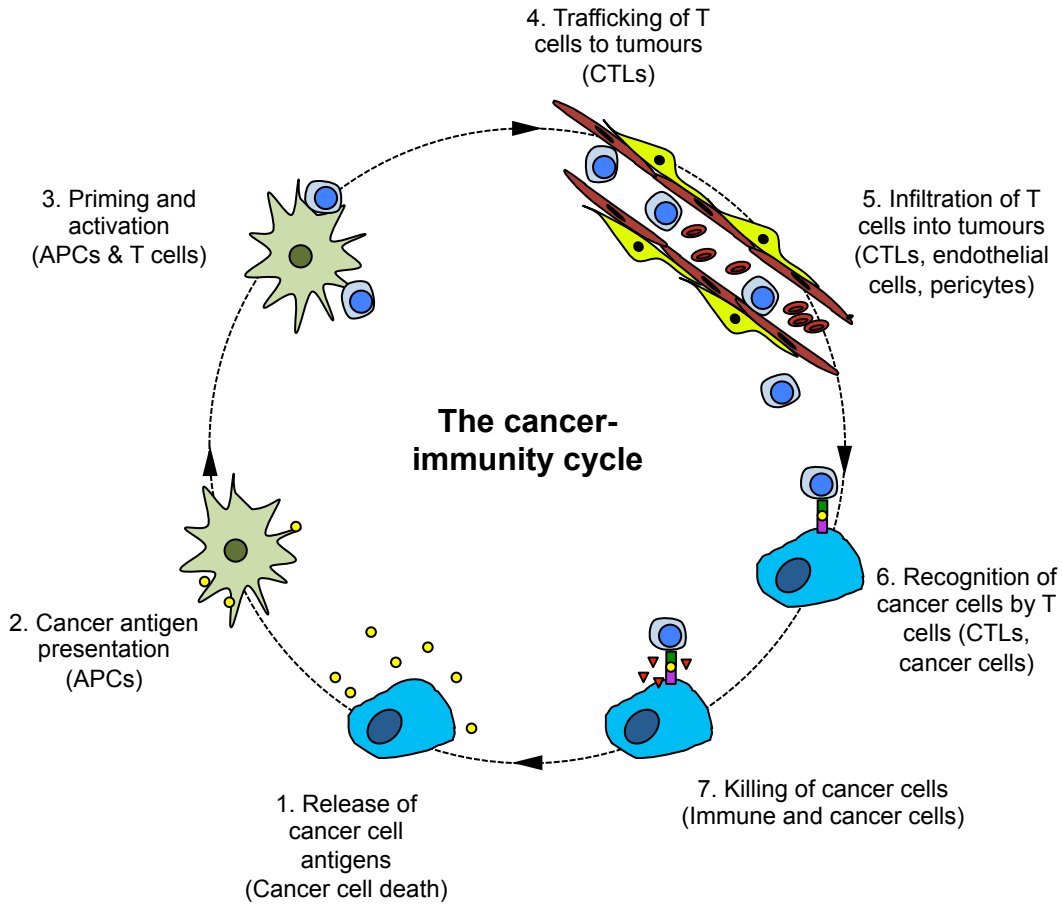

Figure 1.4: The cancer-immunity cycle. The generation of anti-tumour immunity is a cyclic process that can be self propagating, leading to an accumulation of immunostimulatory factors that should theoretically amplify and broaden T cell responses. The cycle is also characterised by inhibitory factors that lead to immune regulatory feedback mechanisms, which can limit immunity. This cycle can be divided into seven major steps, starting with the release of antigens from cancer cells and ending with the killing of cancer cells. Each step is shown above, together with the primary cell types involved. APCs, antigen presenting cells; CTLs, cytotoxic T lymphocytes. Adapted from (Chen and Mellman, 2013).

cancer cells, releasing more tumour neoantigens that should amplify and broaden T cell responses (Garg and Agostinis, 2017).

In cancer patients, one or more of these steps does not occur optimally, allowing cancer cells to evade immunological control. Tumours utilise a number of mechanisms at each step of the cancer-immunity cycle to avoid immune attack. Some tumours lack the mutations necessary to generate tumour neoantigens in the first place. These tumours are said to have low immunogenicity and are poorly controlled by the immune system (Blankenstein et al., 2012). Other mechanisms utilised to avoid

detection by the host immune system include deregulation of APCs, establishment of physical barriers that prevent homing of anti-tumour T cells and the suppression of effector T cells through recruitment of immunosuppressive cells such as myeloid-derived suppressor cells (MDSCs) and T_{regs} (Motz and Coukos, 2013). Some tumours also lose the expression of MHC class I molecules, thus conferring on them the ability to avoid recognition by CTLs. Whilst loss of MHC class I expression may render tumours more susceptible to NK cell attack, some tumour cells are able find a balance between avoiding recognition by CTLs whilst remaining resistant to NK cell attack (Bubenik, 2003). In addition to recruiting immunosuppressive cells, tumours can also evade immune attack directly through expression of cytokines such as TGFβ, cell-surface proteins such as programmed death ligand-1 (PD-L1) and the enzyme indoleamine 2,3-dioxygenase (IDO), all of which contribute to generating a generally immunosuppressive microenvironment (Rabinovich et al., 2007).

The goal of cancer immunotherapy is to interfere with some of these mechanisms in an effort to overcome immune evasion and enhance anti-tumour immune responses. Some of the most effective therapies in the clinic target priming and activation of T cells, but there is also a growing recognition for the powerful role of immunosuppression within the tumour microenvironment in blunting their effectiveness.

1.3.2.2 Cancer immunotherapy

Immunotherapies are a rapidly growing class of drugs that are clinically validated for treatment of many cancer types. Strategies for therapeutically enhancing anti-tumour immune responses include cancer vaccines, oncolytic viruses, adoptive transfer of *ex vivo* activated T cells and administration of antibodies that either co-stimulate cells or block immune checkpoint pathways (Farkona et al., 2016). It has been recognised that infectious diseases could have a beneficial therapeutic effect in cancer since the 1700s; however, the first attempt at exploiting this observation for therapeutic gain did not come about until the late 19th century with the advent of Coley's toxins. By injecting streptococcal organisms into a patient with inoperable cancer, William Coley was the

first to demonstrate an anti-tumour effect of infection, marking the beginning of cancer immunotherapy (McCarthy, 2006).

Though Coley achieved some durable responses in many cancer types including sarcoma and lymphoma, the lack of a known mechanism for his toxins, combined with the risks associated with infecting already sick patients with pathogenic bacteria meant oncologists instead turned to surgery and radiotherapy as standard of care treatments in the early 20th century. The theory of cancer immunosurveillance, discussed earlier and proposed in 1957, marked a return to the idea of using immunotherapy for cancer. However, no new treatments were developed until the 1990s, when the T cell growth factor, IL2 was shown to be effective in treating certain metastatic cancers (Fyfe et al., 1995).

Current strategies for immunotherapy treatment of cancer consist predominantly of cellular immunotherapies and antibody therapies, though immunomodulatory small molecule inhibitors, such as the IDO inhibitor epacadostat, are also being clinically investigated. One type of cellular immunotherapy, known as dendritic cell therapy, utilises the antigen presentation properties of dendritic cells to induce potent immune responses. Sipuleucel-T (Provenge) is a treatment of this type that was approved by the U.S. Food and Drug Administration (FDA) in 2010 for the treatment of metastatic hormone-refractory prostate cancer. Treatment consists of extracting patients immune cells, primarily dendritic cells, and incubating them with a fusion protein known as PA2024. This protein consists of the prostatic acid phosphatase (PAP) antigen, which is present in most prostate cancer cells, and granulocyte-macrophage colony-stimulating factor (GM-CSF) that promotes dendritic cell maturation. The activated blood product is then reinfused into the patient in three courses with the aim of boosting the CTL anti-tumour response (Gardner et al., 2012). A second type of cellular treatment, known as adoptive T cell transfer, involves extracting tumour-infiltrating lymphocytes (TILs) from a tumour biopsy, exposure to tumour antigens from the primary tumour presented on MHC matched B cells alongside high concentration IL2 treatment and enrichment for CD137 expressing

activated T cells. These cells are subsequently implanted into patients in high numbers (Dudley et al., 2003). Early response rates with this treatment in melanoma were limited and costs were extremely high, however, T cell therapy has since advanced significantly (Rosenberg et al., 2011). In 2018, adoptive transfer of autologous TILs reactive against mutant versions of four proteins in conjunction with IL2 and immune checkpoint blockade (Section 1.3.2.3) led to complete tumour regression in a patient with metastatic breast cancer who was refractory to conventional treatment, highlighting the potential of this type of immunotherapy (Zacharakis et al., 2018). Another type of adoptive immunotherapy involves genetically engineering T cells to express novel receptor proteins, known as chimeric antigen receptors (CARs), that give T cells the ability to target specific proteins on the surface of tumour cells. The receptors are chimeric because they combine T cell activating and antigen-binding capabilities into a single receptor. These CAR-T cells are subsequently infused into patients where they use their cytotoxic activity to destroy cells expressing target antigens (Miliotou and Papadopoulou, 2018). This type of therapy has demonstrated curative effects in a variety of cancer types, especially haematological malignancies, but responses in solid tumours, including breast cancer, have been extremely limited to date (Wang and Zhou, 2017).

Antibody therapy for cancer involves developing monoclonal antibodies that either recognise specific tumour-associated antigens or target proteins involved in immunoregulatory mechanisms. For tumour specific antibodies to work optimally, target antigens should be expressed homogenously, consistently and exclusively on the surface of cancer cells (Scott et al., 2012). Further, antigen secretion should be minimal, as secreted antigens can bind antibodies and blunt their effectiveness. The killing of cancer cells by antibodies is a result of several mechanisms: direct action of the antibody either through binding and activating surface receptors that induce apoptosis or through antagonist activity that blocks signalling and affect proliferation; delivery of conjugated payloads such as drugs, toxins or radioisotopes; inducing

immune-mediated cell killing mechanisms such as complement-dependent cytotoxicity and ADCC; and regulation of T cell function (Scott et al., 2012).

Tumour associated antigens recognised by therapeutic antibodies are often cell surface differentiation antigens or growth factors and their receptors. Rituximab, which was approved for medical use in 1997, is a chimeric monoclonal antibody that binds to the cell surface protein CD20 and is used to treat non-Hodgkin's B cell lymphoma (Emer and Claire, 2009). CD20 is expressed exclusively on mature B cells, and antibody binding triggers complement-dependent cytotoxicity, ADCC and apoptosis in both healthy and cancerous B cells. However, anti-CD20 antibodies have no effect on haematopoietic stem cells that can regenerate B cell populations within 6 to 12 months following therapy (Roll et al., 2006).

Striking improvements in survival have been demonstrated in breast cancer patients treated with the monoclonal antibody trastuzumab (Herceptin). Trastuzumab targets the HER2/ErbB2 growth factor receptor that is overexpressed or amplified in about a quarter of breast cancer patients. By blocking ligand binding, trastuzumab inhibits the downstream mitogen-activated protein kinase (MAPK) and phosphoinositide 3-kinase/protein kinase B (PI3K/Akt) intracellular signalling pathways, which leads to suppression of cell growth and proliferation, and an increase in cell cycle arrest (Kroemer et al., 2015). Interestingly, evidence also suggests that ADCC plays a major role in the anti-tumour effects of trastuzumab. Mouse models have demonstrated how NK cells, via their Fc receptors, are able to target HER2-overxpressing cells with bound trastuzumab through a CD16-mediated ADCC mechanism (Clynes et al., 2000). Subsequently, patient samples were used in immunohistochemical evaluation of immune cell infiltration and showed that trastuzumab treatment was associated with significantly increased numbers of tumour-associated NK cells (Arnould et al., 2006).

1.3.2.3 Immune checkpoint blockade

Antibodies can also function to activate or antagonise immunological pathways that control cancer immunosurveillance. One approach, known as immune checkpoint blockade, attempts to interfere with inhibitory signals that regulate lymphocytes. Ordinarily, these immune checkpoints control the duration and amplitude of physiological immune responses and are initiated by ligand-receptor interactions, making them suitable for targeting by therapeutic antibodies. T cells require co-stimulation by B7 proteins, such as CD80 (B7-1) and CD86 (B7-2), found on the surface of professional APCs, to enhance the activity of a MHC-TCR signal between the APC and the T cell. In fact, MHC binding alone, without any stimulatory signal, sends the T cell into a state of inactivity known as anergy (Abe and Macian, 2013). In addition, negative immunological checkpoints exist that also decrease T cell activity, and therapeutically blocking these pathways has resulted in dramatic responses in the clinic (Pardoll, 2012).

Cytotoxic T-lymphocyte-associated protein 4 (CTLA-4) represents an important immune checkpoint for potentially auto-reactive T cells by binding to CD80 (B7-1) and CD86 (B7-2), on dendritic cells (Figure 1.5). This interaction delivers an inhibitory signal to T cells that must be overcome by other stimulatory signals for T cells to become activated. Furthermore, CTLA-4 mediates immunosuppression by competing with the co-stimulatory receptor CD28 for binding to CD80 and CD86 (Figure 1.5). Thus, blocking CTLA-4 function, for example with the anti-CTLA-4 antibody tremelimumab, lowers the threshold for T cell activation, enhances T cell priming and improves anti-tumour immunity (Wei et al., 2018).

Whilst it was initially thought that anti-CTLA-4 antibodies acted solely by regulating effector T cell responses, recent evidence suggests that depletion of T_{regs}, via ADCC, also contributes to anti-CTLA-4 activity. Using a mouse model expressing human Fc receptors, it has recently been demonstrated how surrogate antibodies with isotypes equivalent to the anti-CTLA-4 drugs ipilimumab and tremelimumab mediate intra-tumoural T_{reg} depletion, thus increasing the CTL to T_{reg} ratio and driving tumour rejection (Arce Vargas et al., 2018). However, anti-CTLA-4 therapies have no reported

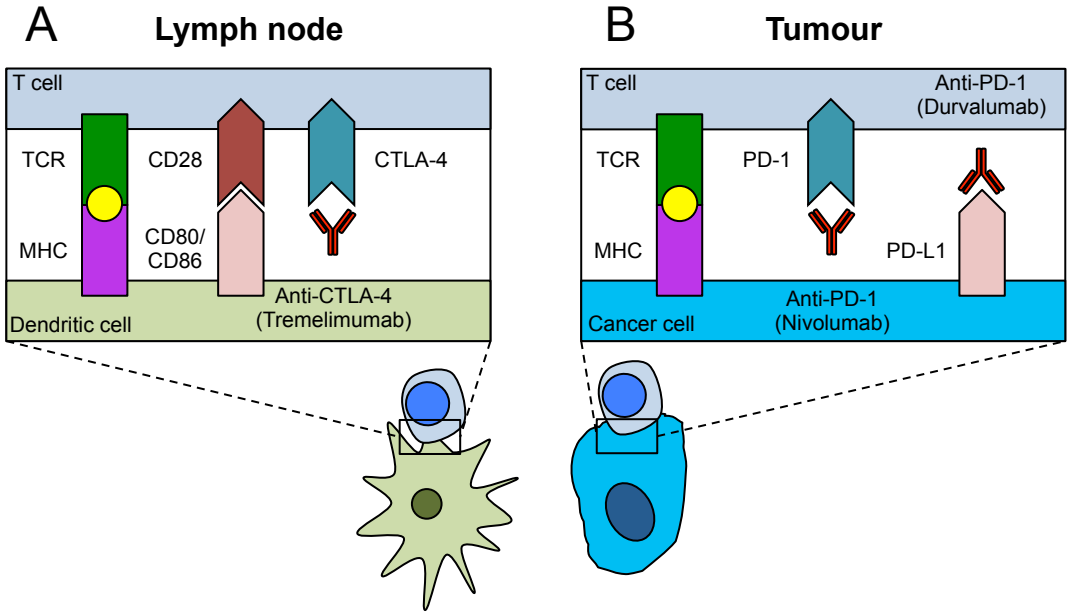

Fig. 1.5: **Blockade of CTLA-4 and of PD-1 and PD-L1 to induce anti-tumour immune responses. A.** CTLA-4 is a negative regulator of co-stimulation that is required for initial activation of anti-tumour T cells in lymph nodes upon recognition of specific tumour antigens presented by antigen-presenting cells such as dendritic cells. CTLA-4 can be blocked with anti-CTLA-4 antibodies such as tremelimumab. **B.** Once T cells are activated they circulate throughout the body to find their cognate antigen presented by cancer cells. Upon recognition, triggering of the TCR leads to expression of the negative regulatory receptor PD-1, and the production of IFNγ results in the reactive expression of PD-L1 on cancer cells, dampening anti-tumour T cell responses. This negative interaction can be blocked by anti-PD-1 or anti-PD-L1 antibodies such as nivolumab and durvalumab, respectively. CTLA-4, cytotoxic T lymphocyte-associated protein 4; IFNγ, interferon gamma; MHC, major histocompatibility complex; PD-1, programmed cell death protein 1; PD-L1, programmed death-ligand 1; TCR, T cell receptor.

effects on the density of T_{regs} in melanoma, prostate or bladder cancer patients, suggesting that their efficacy could be improved by modifying the Fc portions of the antibodies to enhance Fc-mediated depletion of intratumoural T_{regs} (Sharma et al., 2019).

Another T cell checkpoint pathway that is mediated by the interaction of the inhibitory receptor, programmed cell death protein 1 (PD-1) with its ligand programmed death-ligand 1 (PD-L1) (Figure 1.5). Whilst antibodies targeting CTLA-4 affect T cell priming and activation, monoclonal antibodies such as nivolumab and durvalumab that target PD-1 or PD-L1, respectively, have a direct effect on tumour cell killing by T cells in peripheral tissues. Ordinarily, PD-L1 binds to PD-1 receptors on the surface of T cells delivering an inhibitory signal, minimizing the possibility of chronic autoimmune

inflammation (Francisco et al., 2010). This inhibitory function is mediated by the tyrosine phosphatase SHP2, which dephosphorylates signalling molecules downstream of the TCR (Ribas and Wolchok, 2018). PD-1 is upregulated on T cells following their activation and continues to be expressed by effector T cells in the periphery. Inflammatory signals, such as IFNγ production, are known to induce the expression of PD-L1, and this can occur on both cancer cells and tumour-infiltrating immune cells, acting as an adaptive immune resistance mechanism in response to endogenous anti-tumour immune responses (Tumeh et al., 2014). The existence of this mechanism implies that immunosurveillance occurs even in advanced cancers, but that tumours ultimately resist immune elimination by upregulating expression of ligands for inhibitory receptors, inhibiting tumour-specific T cells within the tumour microenvironment (Pardoll, 2012). Furthermore, this inflammation-induced PD-L1 expression results in continuous PD-1 signalling in T cells and induces an epigenetic program of T cell exhaustion (Ribas and Wolchok, 2018). Exhausted T cells are defined by progressive loss of effector function, including defective proliferative capacities and cytokine production, but recent evidence suggests that immune checkpoint blockade treatment can reinvigorate these cells and reverse tumour-induced T cell dysfunction, thus promoting anti-tumour immunity (Twyman-Saint Victor et al., 2015; Zarour, 2016).

Understanding that expression of PD-1 increases on TILs, and how PD-L1 expression is increased in tumour and stromal cells, made targeting this pathway an attractive proposition for anti-cancer treatment. This approach was validated in preclinical models demonstrating that blockade of PD-1 or its ligands enhanced anti-tumour immunity (Dong et al., 2002). Subsequently, clinical trials have demonstrated how monoclonal antibodies targeting this checkpoint pathway can induce powerful and durable therapeutic effects in many cancer types including melanoma and non-small cell lung cancer (Pardoll, 2012). In addition, targeting PD-1 or PD-L1 resulted in higher response rates and fewer side effects when compared to CTLA-4 targeting therapies

(Havel et al., 2019). Currently, there are five anti-PD-1 or anti-PD-L1 antibodies approved by the FDA in 11 types of cancer (Ribas and Wolchok, 2018).

The fully human monoclonal antibody, nivolumab, was the first PD-1 inhibitor to show anti-tumour activity during a phase I single-infusion dose-escalation trial. Out of the 16 patients receiving nivolumab, including those with melanoma, renal cell carcinoma and non-small cell lung cancer, six (37.5%) exhibited objective tumour responses (Sznol et al., 2010). In April 2011, following the clinical success of nivolumab, the efficacy of another anti-PD-1 antibody pembrolizumab was demonstrated in the largest phase I trial ever conducted in oncology, with 1235 patients eventually being enrolled (Garon et al., 2015).

Single-agent PD-1 blockade has proven to be most effective in Hodgkin's lymphoma, in which there is constitutive expression of PD-L1, a result of the amplification of the PD-L1 encoding locus (Ansell et al., 2015). Further, highly mutated cancers also appear to respond particularly well to PD-1 blockade. Mismatch repair-deficient cancers, those that carry mutations in genes involved in correcting mistakes during DNA replication, are known to have large numbers of mutation-associated neoantigens that may be recognised by the immune system (Ribas and Wolchok, 2018). Colorectal cancers of this kind responded well to PD-1 blockade in a small phase II study (Le et al., 2015), providing evidence to suggest a relationship exists between mutational burden and response to treatment.

Since immune checkpoint blockade relies on activating a patient's own immune system, the effects of treatment are not immediately evident. Many immuno-oncology drugs, a result of their delayed action, would fail when assessed in clinical trials based on traditional response evaluation criteria in solid tumours (RECIST). In responses, researchers and drug developers developed a new set of response criteria known as the immune-related response criteria (irRC) (Wolchok et al., 2009), making it possible to design clinical trials that could document the effects of checkpoint blockade. The usefulness of the irRC is well illustrated by the early development of the competing anti-CTLA-4 antibodies, ipilimumab and tremelimumab. Tremelimumab was assessed

using traditional response criteria and interim analysis found no survival advantage, leading to trial termination in April 2008 (Ribas et al., 2008). However, soon after termination, survival curves between treatment and control groups began to separate (Marshall et al., 2010). In contrast, ipilimumab was shown to be effective in treating metastatic melanoma under the new irRC (Hodi et al., 2010), and received FDA approval in 2011. Whilst only about 15% of patients showed a response, the treatment did induce impressive long-term remission in responding patients.

In contrast to targeted oncogene therapies, where tumours initially respond, but often relapse once the cancer manages to reactivate the targeted pathway or utilise pathway redundancies to bypass the blocked oncogene, responses with immune checkpoint blockade are usually durable (Ribas and Wolchok, 2018). Theoretically, immunological memory derived from robust adaptive immune responses to cancer should induce long-term responses, particularly when this response is polyclonal. However, many cancer types, including breast cancer, are often refractory to immune checkpoint blockade, and others develop acquired resistance following a period of response. Most data suggests that patients with a pre-existing anti-tumour T cell response respond better to single-agent anti-PD-1 or anti-PD-L1 therapy than those without. However, many cancers lack any pre-existing T cell infiltration, likely because of low immunogenicity or an active means of T cell exclusion (Sharma et al., 2017).

Anti-CTLA-4 and anti-PD-1/PD-L1 antibodies target non-redundant co-inhibitory signals, making the combined use of these agents for cancer an attractive proposition. Recently, mass cytometry (CyTOF) was used to profile the effects of combined checkpoint blockade on tumour immune infiltrates in both human melanoma and murine tumour models. Whilst anti-PD-1 treatment induced the expansion of specific tumour-infiltrating exhausted-like $CD8^+$ T cell subsets, anti-CTLA-4 induced expansion of an $ICOS^+$ Th1-like $CD4^+$ effector population, proving that these treatments act through distinct cellular mechanisms (Wei et al., 2017). In a phase I trial combining ipilimumab with nivolumab, over 50% of metastatic melanoma patients responded, however, the number of high-grade immune-related toxicities were though higher than

had been observed in previous monotherapy trials (Wolchok et al., 2017), limiting the uptake of combination therapy into the clinic. However, more recently, combined nivolumab and ipilimumab was shown to improve the five-year survival of advanced melanoma patients compared to those receiving ipilimumab alone without any apparent loss of quality of life (Larkin et al., 2019), indicative of improvements in the safety profile of combination immunotherapy.

Immune checkpoint blockade treatment is being investigated in combination with a rapidly increasing number of agents in an effort to increase the number of patients who respond. Chemotherapy, radiotherapy and oncogene-targeted therapies can all modulate the tumour immune microenvironment and potentially act synergistically with immune checkpoint blockade. The efficacy of some of these combinations in the context of breast cancer will be discussed in Section 1.3.2.5, but it clear from evidence both in breast cancer and other cancer types, that combining treatments with immune checkpoint blockade can exert potent anti-tumour effects (Ribas and Wolchok, 2018). However, agents are often combined with only minimal consideration into which combinations may work best in specific patients. Recently, technological, analytical and mechanistic advances in immunology have revealed the complexity and diversity of the tumour microenvironment and its influence on responses to therapy. As a consequence, researchers have started to identify different subclasses of immune environment that have an influence on tumour progression, response to therapy and aid in predicting the most effective combination therapies (Binnewies et al., 2018; Galon and Bruni, 2019).

1.3.2.4 Tumour immune microenvironment subtypes

Although techniques for estimating the composition of tumour immune infiltrates, including flow cytometry and gene expression analysis of bulk tissue, are already used to stratify patients and predict disease outcome, they do not provide detailed information of cellular heterogeneity and spatial distribution (Binnewies et al., 2018). Still, the information that has been gathered has provided a basis for classifying the

tumour immune microenvironment according to the composition of the immune infiltrate and the nature of the inflammatory response. Further technological advancements will expand our understanding of how the immune microenvironment varies both between tumour types, and subtypes.

The tumour immune microenvironment can broadly be divided into three general classes: infiltrated-excluded, infiltrated-inflamed and infiltrated-tertiary lymphoid structures (TLSs) (Binnewies et al., 2018). Excluded tumour immune microenvironments are broadly populated with immune cells but lack infiltration of CTLs into the tumour core. Instead, CTLs are found localised along the border of tumour masses, either in the invasive margin or 'caught' in fibrotic nests. Epithelial cancer such as colorectal cancer and pancreatic ductal adenocarcinoma often have an excluded phenotype, and it is thought this may be in part driven by TAMs preventing CTL infiltration (Beatty et al., 2015). Tumours with an excluded phenotype are often poorly immunogenic or 'cold', and contain CTLs with low expression of the activation markers granzyme B and IFNγ that fail to infiltrate the tumour core (Binnewies et al., 2018).

In contrast, inflamed tumour immune microenvironments are immunologically 'hot' and are characterised by high infiltration of CTLs expressing PD-1. In addition, this class of tumours also contains immune cells and tumour cells expressing PD-L1 and they are often defined by a high rate of nonsynonymous single-nucleotide polymorphisms (SNPs), leading to increased numbers of neoantigens.

The final phenotype represents a subclass of inflamed tumours that display evidence of TLSs: lymphoid aggregates that contain a diversity of lymphocytes including T cells, B cells and dendritic cells. TLSs are often correlated with good prognosis and are normally present at the invasive margin or tumour stroma (Pitzalis et al., 2014).

An understanding of tumour-immune system interactions has already aided in rationally guided stratification of both patients and therapeutic strategies (Galon et al., 2006). The type, density and location of immune cells within tumours can predict

survival in colorectal cancer better than the classical TNM pathological classification of malignant tumours (Mlecnik et al., 2011). This finding led to the development of the Immunoscore - a robust, standardised scoring system based on the quantification of CD3 and CD8 expressing lymphocytes at the tumour centre and the invasive margin of colorectal cancers (Galon and Bruni, 2019). The Immunoscore ranges from 0 (where densities of both cell types are low in both regions) to 4 (where immune cell densities are high in both regions). Naturally, this introduced the notion of 'hot' (highly infiltrated, Immunoscore 4) and 'cold' (non-infiltrated, Immunoscore 0) tumours. These classifications have since become more nuanced with the introduction of the concept of 'immune contexture', which refers to the nature, density, immune functional orientation and distribution of immune cells within tumours (Camus et al., 2009). In an attempt to develop a simplistic, yet comprehensive classification, the notions of 'hot' and 'cold' tumours were extended to include an intermediate classification known as 'altered'. This altered phenotype can be further subdivided into 'excluded' and 'immunosuppressed' (Galon and Bruni, 2019). In 'excluded' tumours, T cells are found at the edge of tumour sites without being able to infiltrate, reflecting the intrinsic ability to mount a T cell-mediated immune response, and the ability of the tumour to evade it by physically hindering infiltration. In 'immunosuppressed' tumours, low immune infiltration is instead a result of an immunosuppressive environment that limits further recruitment and expansion of T cells, particularly CTLs.

Recently, attempts have also been made to stratify and characterise tumour immune microenvironment subtypes in triple-negative breast cancer (TNBC). By integrating spatial resolution of immune cells with laser capture microdissection gene expression profiles, distinct subtypes were defined that will likely have implications for immune checkpoint blockade treatment of breast cancer. TNBCs with an 'immunoreactive' microenvironment were infiltrated with granzyme B^+ CTLs, a type 1 IFN signature and high expression of immune inhibitory molecules such as IDO and PD-L1. These patients had improved outcomes. In contrast, tumours that had an immune 'cold' microenvironment, marked by absence of tumoural CTLs and a fibrotic

stroma had worse outcomes. This work also identified a poor outcome subtype that exhibited stromal restriction of CTLs, stromal expression of PD-L1 and enrichment for signatures of cholesterol biosynthesis (Gruosso et al., 2019).

1.3.2.5 Immunotherapy and breast cancer

A major factor determining cancer progression, including in breast cancer, is the overall proportion and phenotype of immune cells within the tumour immune microenvironment. In early stage $HER2^+$ and TNBC, immune infiltrates are found in 75% of tumours, with around 20% having dense infiltration (Stanton et al., 2016). Consequently, interest in evaluating the number of TILs in breast cancer has increased, and evidence suggests this measure has relevance as an immunological biomarker. Measuring TIL infiltration is becoming increasingly important as a stratifying marker in clinical trials, particularly considering the interest in utilising immunotherapy after neoadjuvant chemotherapy (Salgado et al., 2015).

The quantification of TILs in breast cancer, often via haematoxylin and eosin (H&E) stained tumour sections, shows a positive association between higher TIL numbers and prognosis or response to treatment (Savas et al., 2016). As chemotherapy remains a pillar of breast cancer treatment, it is important to consider its substantial immunomodulatory effects in both adjuvant and neoadjuvant settings. Though chemotherapy is generally thought to induce systemic immunosuppression, it has been argued that it can effectively 'reset' the relationship between the tumour and the immune system, restoring functional immunity (Savas et al., 2016). Furthermore, adaptive immune responses may be triggered by chemotherapy-induced cell death, promoting the elimination of tumour cells both in primary tissues and in distant metastatic sites (Wang et al., 2018).

As discussed in Section 1.3.2.1, the generation of tumour neoantigens is critical in the establishment of robust anti-tumour adaptive immune responses and is linked to mutational rates. Compared to other cancer types such as melanoma and lung cancer, breast tumours have a relatively low mutational burden, though this varies between

subtypes, with TNBCs accumulating mutations more readily than ER^+ disease (Wang et al., 2014b). This results in some breast tumours lacking the immunogenicity that is essential in developing a diverse repertoire of anti-tumour effector T cells. Whilst the presence of T cells in breast cancer confers a favourable prognosis, ultimately, the fact that viable tumour remains suggests that the immune response was inadequate. This could be a result of a number of tumour-induced tolerance mechanisms, characterised by the presence of exhausted, dysfunctional T cells that have high surface expression of inhibitory receptors such as PD-1. Despite their exhausted phenotype, human breast tumour T cells retain their capacity for production of effector cytokines and degranulation, suggesting that with alternative targeting strategies, they could be reinvigorated to produce an anti-tumour response (Egelston et al., 2018).

In the last year, the FDA granted accelerated approval for the anti-PD-L1 immune checkpoint inhibitor, atezolizumab, in combination with chemotherapy for the treatment of advanced TNBC, representing the first approved regimen for breast cancer to include immunotherapy. Approval was based on promising data from a phase III trial where patients with untreated metastatic TNBC received atezolizumab plus the antineoplastic chemotherapy, nab-paclitaxel or placebo plus nab-paclitaxel. Each group included 451 patients, and the median progression-free survival was 7.4 months for patients receiving atezolizumab and 4.8 months for those receiving placebo (Schmid et al., 2018). Furthermore, it was clear from the trial that the patients who benefited from the combination therapy were those whose tumours were PD-L1-positive, with high PD-L1 expression on TILs proving particularly important. The progression of TNBC is known to be particular sensitive to the state of anti-tumour adaptive immunity (Bates et al., 2018), but whether this kind of treatment regimen would work as effectively in other breast cancer subtypes remains to be seen. Even amongst patients with PD-L1 positive tumours, there were those that responded poorly, suggesting that alternative mechanisms of insensitivity exist.

Numerous populations of immune cells have been reported to have suppressive functions in the breast tumour immune microenvironment. Cells such as

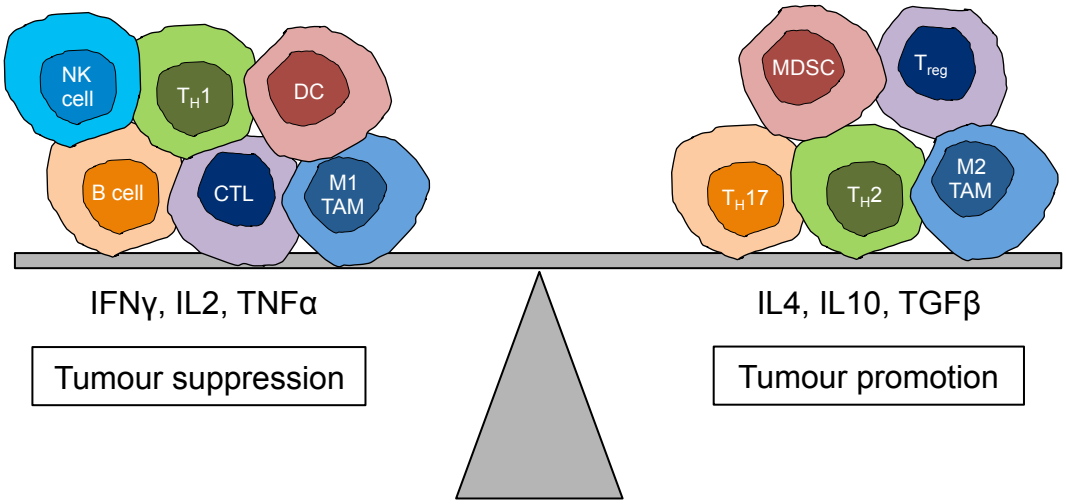

Figure 1.6: The dual role of the immune compartment. Immune cells within a tumour can have tumour-promoting or tumour-suppressing effects depending on their polarisation. Immune polarisation depends on the prevalence of pro- or anti-inflammatory cytokines. Type 1 polarisation is characterised by IFNγ, IL12 and TNFα production by different cell types within the tumour, as well as an increased number of infiltrating CTLs and other pro-inflammatory immune cells. Type 2 polarisation is elicited by IL4, IL10 and TGFβ and is often characterised by increased numbers of infiltrating T_{regs}, as well as other immunosuppressive cells, including MDSCs. The balance of tumour suppression to tumour promotion can be tipped as a result of cytokine secretion by a variety of cell types within the tumour. CTL, cytotoxic T lymphocyte; DC, dendritic cell; IFNγ, interferon gamma; IL, interleukin; MDSC, myeloid-derived suppressor cell; NK, natural killer; TAM, tumour-associated macrophage; T_H, T helper cell; TNF, tumour necrosis factor; T_{reg}, regulatory T cell.

CTLs, NK cells and T_H1 cells, driven by factors such as IFNγ, IL2 and TNFα are generally considered to promote anti-tumour immunity and suppress cancer progression (Figure 1.6). However, the immune infiltrate of breast tumours is often skewed towards a tumour-promoting immune microenvironment through increased expression of factors such as IL4, IL10 and TGFβ (Soria and Ben-Baruch, 2008) and the presence of abundant M2 TAMs, T_{regs} and MDSCs (Figure 1.6). Though numerous populations of immune cells have been reported to have suppressive functions in the breast TME, TAMs are the best studied and characterised. As mentioned previously in Section 1.3.1.1, macrophages can adopt an M1 or M2 polarisation phenotype based on their cytokine and chemokine profiles. In breast cancer, the majority of TAMs have an M2, anti-inflammatory phenotype (Choi et al., 2018), and TAM density correlates with poor prognosis (Laoui et al., 2011). In mouse models of breast cancer, eliminating

TAMs can relieve suppression of CTLs and results in retarded tumour progression (Laoui et al., 2011). Other studies using the MMTV-PyMT breast cancer model have shown that the proportion of exhausted, PD-1^{+} CTLs increases in concordance with increasing proportion of monocyte-derived TAMs (Franklin et al., 2014). Targeting TAMs in human disease is complicated by the plasticity of these cells. However, attempts have been made to therapeutically target the colony-stimulating factor 1 (CSF1)/colony-stimulating factor 1 receptor (CSF1R) axis. CSF1 is a secreted cytokine that causes haematopoietic stem cells to differentiate into macrophages, particularly those with an M2 phenotype (Cannarile et al., 2017). A number of small molecules and antibodies targeting CSF1R or its ligand CSF1 are currently in clinical development, but is too soon to determine their efficacy.

Another cell type associated with driving suppression of the breast tumour immune microenvironment is MDSCs, which are currently difficult to differentiate from neutrophils based on surface marker expression alone. They are a heterogeneous group of immune cells derived from the myeloid lineage that expand in pathological conditions such as chronic infections and cancer. Through multiple mechanisms, MDSCs suppress the function of other immune cells such as T cells and NK cells, and their presence in breast cancer is associated with poor prognosis (Gonda et al., 2017). One driver of MDSC accumulation in cancer is the expression of IDO by tumour cells. In preclinical models, inhibiting IDO reverses tumour immunosuppression by decreasing the number of infiltrating MDSCs and abolishing their suppressive function (Holmgaard et al., 2015). However, a recent clinical trial of the IDO inhibitor, epacadostat, failed to improve progression-free survival or overall survival in metastatic melanoma when combined with anti-PD-1 therapy, suggesting that other factors may be contributing to immunosuppression in patients (Long et al., 2019).

Clearly, the tumour immune microenvironment has a profound impact on both breast cancer progression and responses to immunotherapy. Whilst cancer cells and immune cells undoubtedly play major roles in determining the phenotype of the tumour immune microenvironment, accumulating evidence suggests other non-immune

stromal cells are also key players. One such cell type, known as cancer-associated fibroblasts (CAFs) are discussed in Section 1.4.

1.4 Cancer-associated fibroblasts

Fibroblasts are mesenchymal cells characterised by their spindle like morphology and lack of expression of epithelial, vascular and immune cell markers (Tarin and Croft, 1969). Fibroblasts are crucial in generating the structural framework of tissues through production of extracellular matrix (ECM) components such as collage and fibronectin (Kalluri and Zeisberg, 2006). The ECM is a dynamic structure that exhibits physical, biochemical and biomechanical properties, which define the architecture of tissues, as well as the behaviour of cells that interact with it.

Fibroblasts are highly heterogeneous cells, which reside in most tissues of the body. Recently, single-cell RNA sequencing experiments of human skin have revealed some of this heterogeneity, with five sub-populations of fibroblasts being identified that shared only one common lineage marker (Tabib et al., 2018). Although a number of fibroblast markers exist, none are both exclusively expressed on fibroblasts and common to all fibroblast populations (Sugimoto et al., 2006). A well-established fibroblast marker is the structural protein vimentin, which is expressed by the majority of fibroblast populations, but also by endothelial, myoepithelial and neuronal cells (Goodpaster et al., 2008). Another, desmin, is expressed primarily on fibroblasts of the skin, but is also found on vascular smooth muscle cells (Paulin and Li, 2004). Fibroblast specific protein 1 (FSP1, also known as S100A4) is a cytoplasmic calcium-binding protein identified as a transcript enriched in fibroblasts following comparisons with epithelial cells, however, it can also be expressed by macrophages (Strutz et al., 1995; Österreicher et al., 2011). Other putative markers for fibroblasts include platelet-derived growth factor receptor alpha (PDGFRα), neural/glial antigen 2 (NG2), endosialin, and fibroblast activation protein (FAP) (Kalluri and Zeisberg, 2006)

Ordinarily, fibroblasts remain quiescent and non-proliferative. However, during processes that require tissue remodelling, such as wound healing, fibroblasts are

activated by mechanical stress and TGFβ. These fibroblasts develop characteristics of myoepithelial cells and are known as myofibroblasts. Wound healing requires expansion of the epithelial layer, formation and contraction of granulation tissue, and vascularisation. Myofibroblasts deposit ECM components, secrete growth factors and cytokines and upregulate cellular stress fibres such as alpha smooth muscle actin (αSMA), which increases their contractility. Following successful healing of a wound, myofibroblasts are removed via apoptosis (Darby et al., 2014).

During breast cancer progression, fibroblasts are recruited into developing tumours where they are activated, adopting a myofibroblast like phenotype marked by expression of αSMA. These fibroblasts are known as cancer-associated fibroblasts (CAFs) (Kalluri, 2016). Instead of dying through apoptosis as in wound healing, CAFs remain constitutively active and they represent one of the most abundant components of the tumour microenvironment. Many solid tumours are characterised by extensive fibroblast infiltration and deposition of ECM components like fibrillar collagens, proteoglycans and tenascin C. This 'desmoplastic response' is regularly found in colon, pancreatic, prostate and breast cancer and correlates with invasiveness and poor prognosis (Kalluri, 2016). As a marker of fibroblast activation, αSMA is commonly used as maker for identifying CAFs, though it is also expressed in vascular smooth muscle cells and pericytes (Kalluri and Zeisberg, 2006). Though their functional role in promoting tumour progression is well recognised, the underlying mechanisms are not fully understood.

Unsurprisingly considering the heterogeneity of normal fibroblasts, CAF phenotypes are equally diverse (Sugimoto et al., 2006). The activation of fibroblasts in the TME depends on both the biomechanical properties of tumours and the signalling molecules they release (Thannickal et al., 2003). Consequently, the heterogeneity of tumour cells also contributes to the heterogeneity of neighbouring CAFs. Furthermore, the origin of CAFs also varies. They can arise from activation of resident fibroblasts, epithelial to mesenchymal transition (EMT) of tumour cells or recruited from mesenchymal stem/progenitor cells in the bone marrow or in perivascular niches

(Kalluri and Zeisberg, 2006). Recently, single cell RNA sequencing was used to determine the transcriptome of 768 mesenchymal cells from a genetically engineered mouse model of breast cancer and identified spatially and functionally distinct subsets of breast CAFs (Bartoschek et al., 2018). These subsets were predominantly derived from the perivascular niche, activation of resident mammary fat pad fibroblasts and the transformed epithelium, and gene profiles for each CAF subtype correlated to distinctive functional programs that had prognostic capability in clinical cohorts by association to metastatic disease.

Normal fibroblasts generally have a tumour suppressive phenotype, however, CAFs are known to promote breast cancer progression at various stages. CAFs secrete a range of cytokines and growth factors, in addition to matrix remodelling enzymes and components of the ECM. These factors, which include collagens, C-X-C motif chemokine ligand 2 (CXCL2), stromal cell-derived factor 1 (SDF1), chemokine ligand 2 (CCL2) and vascularisation promoting factors such as vascular endothelial growth factor (VEGF) affect tumour cell proliferation, invasiveness, survival, metabolism and stemness (Ziani et al., 2018). Thus, CAFs have been demonstrated to contribute to tumour growth, metastasis and angiogenesis, which are key hallmarks of cancer (Hanahan and Weinberg, 2011). Correspondingly, quantification of αSMA expression in human breast tumours via immunohistochemistry revealed how high expression correlates with poor clinical prognosis for patients with invasive breast cancer (Yamashita et al., 2012). The role of CAFs within the tumour microenvironment is summarised in Figure 1.7.

The pro-tumour effects of breast CAFs can partly be attributed to CAF-released SDF1, which interacts with CXC-chemokine receptor 4 (CXCR4) on the surface of cancer cells. Using a co-implantation tumour xenograft model, studies have shown how CAFs from human breast carcinomas promoted the growth of admixed breast carcinoma cells more than normal fibroblasts derived from the same patients (Orimo et al., 2005). By secreting SDF1, CAFs directly stimulated tumour growth through interactions with CXCR4, and also promoted angiogenesis through recruitment of

endothelial progenitor cells. A study from our laboratory identified Wnt7a as a key factor secreted by tumour cells that drives CAF activation. Functionally, this resulted in ECM remodelling that created a permissive environment for tumour cell invasion and metastasis (Avgustinova et al., 2016). The activation of CAFs in this model was not dependent on classical Wnt signalling but instead amplified TGFβ signalling. Autocrine TGFβ and SDF1 signalling has also been shown to drive the evolution of CAFs in a co-implantation breast tumour xenograft model. During tumour progression, resident human mammary fibroblasts acquire two signalling loops, mediated by TGFβ and SDF1 cytokines, which act in autocrine and paracrine fashions to initiate and maintain the differentiation of normal fibroblasts into CAFs, driving tumour progression (Kojima et al., 2010). CAFs can also promote invasion of cancer cells through degradation of ECM components. Activated fibroblasts produce matrix-metalloprotease-1 (MMP-1), which acts through protease-activated receptor-1 (PAR1) to promote invasion of breast carcinoma cells in a xenograft model (Eck et al., 2009). Together, whilst direct evidence for CAF-driven carcinogenesis in human cancers is still lacking, the findings above suggest that activated fibroblasts likely play a critical role in promoting tumour growth.

As described above, CAFs interact closely with cancer cells via cell-cell contact and cytokine release. However, in addition to the tumour-stroma crosstalk, crosstalk also exists between CAFs and other cells of the tumour microenvironment (Figure 1.7), adding to the complexity. Accumulating evidence suggests that in addition to their role in shaping cancer progression through directly affecting tumour cell proliferation and invasion, CAFs have an immunomodulatory role. Because of their abundance in the tumour microenvironment, research focused on understanding how CAFs influence immune cell recruitment, function and response to immunotherapeutic agents is increasing. Much of this research is focused on identifying secreted factors, such as TGFβ, that affect both innate and adaptive anti-tumour immune responses (Harper and Sainson, 2014).

1.4.1 CAFs and the immune system

1.4.1.1 CAFs and innate immunity

TAMs are often found in close proximity to CAF-rich areas of the tumour microenvironment, suggesting a close interaction exists between these cell types (Chen and Song, 2018). Prostate CAFs, through secretion of SDF1, are known to promote the differentiation of monocytes into M2 TAMs (Comito et al., 2014). This relationship is a reciprocal one, with M2 TAMs promoting CAF activation and thus, malignancy. In another study, colorectal CAF-derived IL6 and IL8 increased the expression of S100 calcium-binding protein A8 and A9 (S100A8 and S100A9) on tumour-infiltrating myeloid cells, encouraging their differentiation into MDSCs (Kim et al., 2012). Furthermore, in a murine model of breast cancer lung metastasis, mesenchymal stromal cells, following activation by TNFα, promoted metastasis by recruiting CXCR2 expressing neutrophils (Yu et al., 2017).

Breast CAFs have also been implicated in promoting tumour growth by shifting the immune microenvironment towards a T_H2 response. This was shown to be driven in part by CAF-derived chitinase 3-like 1 (Chi3L1), which when genetically deleted from fibroblasts *in vivo* enhanced tumour infiltration of T_H and CTLs, attenuating tumour growth (Cohen et al., 2017). Fibroblast activation protein (FAP) expressing CAFs have also been shown, in a number of cancer types, to enhance recruitment of CCR2-expressing circulating MDSCs through increased monocyte chemoattractant protein-1 (MCP1)/CCL2 expression (Yang et al., 2016).

Galectin-1 expression, which can regulate activation of CAFs, also controls expression of MCP1, facilitating tumour invasion and metastasis primarily through actions on the tumour cells themselves, but also through its role as a potent chemoattractant for monocytes, macrophages and dendritic cells (Wu et al., 2011). In the 4T1 murine breast cancer model, deletion of the *Mcp-1* gene resulted in a significant reduction in tumour residing F4/80 positive macrophages (Yoshimura et al., 2013).

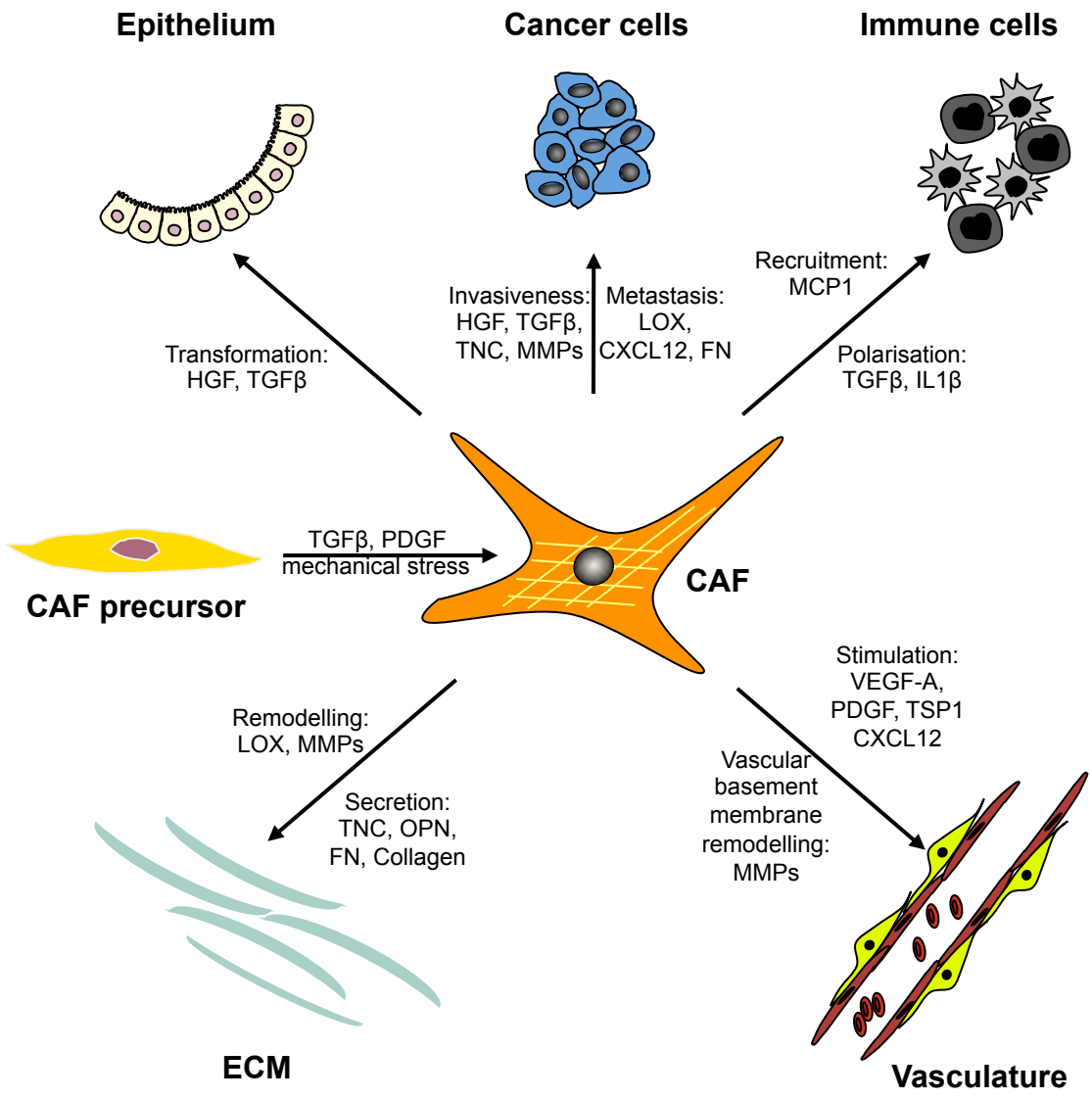

Figure 1.7: Functions of cancer-associated fibroblasts (CAFs) in the tumour microenvironment. CAF activation is mediated by factors including TGFβ, PDGF and mechanical stress. CAFs modify many components of the tumour microenvironment by secretion of ECM components, cytokines and proteases, thereby altering the tumour milieu and affecting tumour progression. Some examples of known CAF-derived factors are shown for each CAF interaction. FN, fibronectin; HGF, hepatocyte growth factor; IL, interleukin; LOX, lysyl oxidase; MMP, matrix metalloproteinase; OPN, osteopontin; PDGF, platelet-derived growth factor; TGF, transforming growth factor; TNC, tenascin C; TSP, thrombospondin; VEGF, vascular endothelial growth factor.

CAFs have also been shown to modulate the function of other innate immune cells in the tumour microenvironment outside those of the myeloid lineage. In co-culture experiments, CAFs isolated from endometrial cancer suppress the cytotoxic activity of NK cells through downregulation of poliovirus receptor (PVR/CD155), a ligand of the activating NK receptor DNAM-1 (Inoue et al., 2016). Similarly, melanoma-

derived fibroblasts can interfere with NK cell cytotoxicity and cytokine production via secretion of prostaglandin E2 (PGE2), thus impairing NK cell-mediated killing of melanoma target cells (Balsamo et al., 2009).

1.4.1.2 CAFs and adaptive immunity

In addition to their crosstalk with the innate immune system, CAFs have been implicated in modulating adaptive tumour immunity. For example, CAFs derived from hepatocellular carcinoma were shown to secrete IL6 that induces IDO-producing regulatory dendritic cells, which secrete immunosuppressive cytokines, impair T cell proliferation and promote T_{reg} expansion thus inducing tumour immune escape (Cheng et al., 2016).

An alternative method for assessing the contribution of CAFs to tumour immune escape *in vivo* is via their depletion, either through vaccination or by employing transgenic mouse models. In a 4T1 murine model of metastatic breast cancer, elimination of CAFs using a DNA vaccine targeted FAP-expressing cells shifted the immune microenvironment in tumours from a tumour-promoting T_H2 to an anti-tumour T_H1 phenotype (Liao et al., 2009). This shift was characterised by increased levels of the T_H1 associated cytokines IL2 and IL7 and suppressed recruitment of immunosuppressive cells including macrophages, MDSCs and T_{regs}. Though these findings demonstrate that CAFs can play a role in immune polarisation of the tumour microenvironment, they do little to reveal a mechanistic understanding of CAF-immune cell biology.

In a different approach, depleting FAP^+ cells in a transgenic model of pancreatic cancer in which FAP^+ cells were selectively susceptible to diphtheria toxin uncovered the anti-tumour effects of anti-PD-L1 immunotherapy (Feig et al., 2013). SDF1 secreted from FAP^+ cells was responsible for their immunosuppressive actions and administering CXCR4 inhibitor, AMD3100, induced T cell accumulation among cancer cells and acted synergistically with anti-PD-L1 treatment. Although this study demonstrated the significance of a single FAP^+ CAF-derived protein, SDF1, in driving

tumour immune evasion, the contribution of CAFs that may not express FAP was not explored. In addition, it is not clear whether CXCR4-mediated exclusion of T cells is a result of T cell apoptosis or a chemo-repulsive effect of SDF1.

It has recently been reported that CAFs can promote immune evasion by inducing antigen-mediated activation-induced cell death of tumour-specific CTLs, which are critical in mounting effective anti-tumour immunity. CAFs can sample, process and cross-present antigen, killing CTLs in an antigen-specific, antigen-dependent manner via PD-L2 and Fas ligand. Expression of T cell inhibitory ligands was also observed on the surface of human CAFs, and neutralisation of the ligands PD-L2 or FAS ligand reactivated T cell cytotoxic capacity both *in vitro* and *in vivo* (Lakins et al., 2018*).*

In a recent seminal study (Costa et al., 2018), four CAF subsets were identified that accumulate differentially in human breast cancer subtypes, with one subset in particular modulating T cell responses and contributing to immunosuppression. CAF subpopulations were identified based on differential expression of the markers CD29, FAP, αSMA, PDGFRβ, FSP1 and caveolin 1 (CAV1). One specific CAF subset, named CAF-S1, promotes immunosuppression by secreting CXCL12, which attracts T_{regs} and retains them through OX40L, PD-L2 and junctional adhesion molecule 2 (JAM2). Furthermore, CAF-S1 populations promote differentiation of T cells into T_{regs}, and enhance their capacity to inhibit CTL proliferation.

Finally, a study focusing on the effects of CAFs on both the function and spatial distribution of CTLs attributed a particularly immunosuppressive capacity to breast CAFs expressing FAP and podoplanin (PDPN). FAP^+ $PDPN^+$ CAFs expressed a TGFβ and fibrosis-related gene signature and were found in direct contact with T cells in the peritumoural stroma of mammary tumours. Additionally, these FAP^+ $PDPN^+$ CAFs could suppress T cell proliferation *in vitro* in a nitric oxide-dependent manner, reminiscent of the role of fibroblast reticular cells (FRCs) in lymph nodes (Cremasco et al., 2018).

In summary, whilst CAFs are known to be key cells in promoting cancer cell growth, invasiveness and angiogenesis, only recently has CAF biology also been

implicated in affecting immune cell recruitment, regulation and responses to immunotherapy. CAFs have pleiotropic effects on both innate and adaptive immune cells and have generally been reported to promote the development of an immunosuppressive tumour microenvironment. Early evidence suggests that the exact mechanisms driving CAF-induced tumour immunosuppression depends largely on cancer type and the subpopulation of CAFs present. Thus, therapeutically modulating CAF biology in specific cancers may represent a novel approach to activating more potent anti-tumour immune responses, particularly when combined with immune checkpoint blockade.

1.5 Conclusions and project aims

In conclusion, there is a growing body of evidence to support a role for the tumour microenvironment in regulating breast cancer progression. Extensive efforts invested into understanding the role of immune cells in carcinogenesis has led to the development of novel immune-based treatments that are effective in many cancer types. However, breast cancer remains largely insensitive to most forms of immunotherapy. The breast tumour microenvironment is often characterised by an abundance of immune cells with known immunosuppressive capacities, inhibiting the efficacy of therapies designed to enhance anti-tumour immunity. Whilst numerous mechanisms have been postulated for contributing to the establishment of an immunologically ‘cold’ microenvironment, CAFs, which makes up a large proportion of stromal cells in breast cancer, have only recently been acknowledged for their immunosuppressive function.

The goal of this project was to use bespoke preclinical syngeneic models to better characterise the role of CAFs in modulating the breast tumour microenvironment, to assess their impact on tumour progression and responses to immunotherapy. Specifically, the aims of the project were:

- To establish suitable models for investigating CAF-immune cell crosstalk in the *in vivo* setting
- To directly demonstrate an immunomodulatory role for CAFs both *in vitro* and *in vivo* within these models
- To characterise the underlying mechanisms involved in CAF-driven immunosuppression
- To investigate whether CAF-driven immunosuppression affects the sensitivity of breast cancer models to immune checkpoint blockade, and whether modulating CAF biology can reverse immunosuppression and improve responses

Chapter 2: Materials and methods

2.1 Materials

All reagents were stored according to manufacturer's instructions. Where not specified, reagents were obtained from the Institute of Cancer Research (ICR) Laboratory Support Services (LSS).

2.1.1 General reagents

β-mercaptoethanol: Sigma-Aldrich (M7154).

Ethanol: VWR (101077Y).

Isopropanol: Thermo Fisher Scientific (BP2618-212).

Methanol: VWR (20847-30).

Nuclease-free water: Ambion (AM9937).

PBS: 137 mM NaCl, 2 mM KCl, 8 mM Na2HPO4, 1.5 mM KH_2PO_4 in H_2O. pH adjusted to 7.4 with HCl (LSS). Stored at 4°C.

Ultra-filtered (UF) water: 17 megaohms filtered water.

2.1.2 Reagents for cell culture and cell-based assays

Antibodies used for flow cytometry, immunostaining and as therapeutic reagents are listed in Tables 2.1-2.7.

Bovine serum albumin (BSA): Sigma-Aldrich (A3059-100G).

Cell freezing medium: 90% FBS, 10% DMSO. Stored at 4°C.

Cell strainers: 40 µm and 100 µm. BD Falcon (352340 and 352360).

Countess automated cell-counter slides: Invitrogen (C10283).

Dimethyl sulphoxide (DMSO): Sigma-Aldrich (D2650).

Dulbecco's modified Eagle's medium (DMEM): Invitrogen (41966-029).

Dynabeads: Sheep anti-rat IgG. Invitrogen (11035).

FACS buffer: 1% FBS in PBS. Stored at 4°C.

Foetal bovine serum (FBS): Invitrogen (10106-169).

HPV-E6/E7-puromycin retrovirus: Cell immortalisation reagent (gift from Fernando Calvo).

HPV-E6/E7-neomycin lentivirus: Applied Biological Materials.

Interferon gamma (IFNγ): Recombinant mouse IFNγ. BioLegend (575306).

JQ1 (+): Active enantiomer. Sigma-Aldrich (SML1524-5MG).

JQ1 (-): Negative control probe. Sigma-Aldrich (SML1525-5MG).

Penicillin/streptomycin (P/S): (1 L) benzylpenicillin sodium 12 g, streptomycin sulphate 20 g.

Polybrene: Sigma-Aldrich (AL-118).

Red blood cell (RBC) lysing buffer: Sigma-Aldrich (R7757).

RPMI 1640 Medium, HEPES: Thermo Fisher Scientific (22400089).

Tissue culture plastics: All tissue culture plastics were purchased from BD Falcon.

Trypan Blue: Invitrogen (T10282).

Trypsin/EDTA: (1 L) NaCl 8 g, KCl 0.2 g, Na_2HPO_4 1.15 g, D-glucose 1 g, KH_2PO_4 0.2 g, EDTA 0.2 g, Tris 3 g, phenol red (1%) 1.5 mL, trypsin (Difco 1:250) 0.5 g, streptomycin sulphate 0.1 g, benzylpenicillin 0.06 g.

2.1.3 Reagents for tissue dissociation

gentleMACS C Tube: Miltenyi Biotec (130-093-237).

MACS SmartStrainer: 70 µm, Miltenyi Biotec (130-098-462).

Tumour dissociation kit: Miltenyi Biotec (130-096-730).

2.1.4 Reagents for flow cytometry cell staining

123count eBeads: eBioscience (01-1234-42).

Anti-mouse CD16/CD32 purified: Fc receptor block. eBioscience (14-0161).

ArC (amine reactive compensation) bead kit: Thermo Fisher Scientific (A10346).

CellTrace CFSE cell proliferation kit: Thermo Fisher Scientific (C34554).

CellTrace Violet cell proliferation kit: Thermo Fisher Scientific (C34557).

Fixable Violet dead cell stain kit: Thermo Fisher Scientific (L34955).

FoxP3/Transcription factor staining buffer set: eBioscience (00-5523-00).

UltraComp eBeads: eBioscience (01-2222).

Table 2.1: Antibodies for flow cytometry (Myeloid Panel)

Antibody (Clone)	Species	Source (Catalogue number)	Dilution	Conjugate
CD11b (M1/70)	Rat	BD Biosciences (563553)	1/794	BUV395
CD11c (N418)	Hamster	eBioscience (25-0114)	1/100	PE/Cy7
CD45 (30-F11)	Rat	BD Biosciences (564225)	1/500	BV786
CD206 (C068C2)	Rat	BioLegend (141715)	1/100	PerCP/Cy5.5
F4/80 (Cl:A3-1)	Rat	Bio-Rad (MCA497A647)	1/100	AF647
Ly6C (HK1.4)	Rat	BioLegend (128035)	1/2941	BV605
Ly6G (1A8)	Rat	BioLegend (127621)	1/400	AF700
MHCII (M5/114.15.2)	Rat	BioLegend (107606)	1/4000	FITC
PD-L1 (10F.9G2)	Rat	BioLegend (124315)	1/100	BV421

Table 2.2: Antibodies for flow cytometry (Lymphoid Panel)

Antibody (Clone)	Species	Source (Catalogue number)	Dilution	Conjugate
CD3 (17A2)	Rat	BioLegend (100229)	1/100	BV650
CD4 (GK1.5)	Rat	BD Biosciences (563790)	1/200	BUV395
CD8a (53-6.7)	Rat	BD Biosciences (564297)	1/833	BUV737
CD45 (30-F11)	Rat	BD Biosciences (564225)	1/500	BV786
FoxP3 (FJK-16s)	Rat	eBioscience (12-5773)	1/200	PE
Granzyme B (GB11)	Mouse	BioLegend (515403)	1/100	FITC
Ki67 (SolA15)	Rat	eBioscience (50-5698)	1/1000	eFluor 660
NKp46 (29A1.4)	Rat	BioLegend (137619)	1/100	BV605
PD-1 (J43)	Hamster	eBioscience (61-9985)	1/100	PE-eFluor 610

Table 2.3: Antibodies for flow cytometry (CAF Panel)

Antibody (Clone)	Species	Source (Catalogue number)	Dilution	Conjugate
αSMA (1A4)	Mouse	eBioscience (50-9760)	1/200	eFluor 660
CD45 (30-F11)	Rat	BD Biosciences (564225)	1/500	BV786
CD90 (53-2.1)	Rat	BioLegend (140327)	1/500	BV421
PDGFRα (APA5)	Rat	BioLegend (135916)	1/200	BV605

Table 2.4: Antibodies for flow cytometry (Plug Panel)

Antibody (Clone)	Species	Source (Catalogue number)	Dilution	Conjugate
CD4 (GK1.5)	Rat	BioLegend (100414)	1/200	APC/Cy7
CD8a (53-6.7)	Rat	BioLegend (100706)	1/200	FITC
CD45 (30-F11)	Rat	BD Biosciences (553082)	1/500	PE/Cy5
F4/80 (BM8)	Rat	eBioscience (25-4801)	1/100	PE/Cy7
NKp46 (29A1.4)	Rat	BioLegend (137607)	1/100	APC

Table 2.5: Antibodies for flow cytometry (Miscellaneous)

Antibody (Clone)	Species	Source (Catalogue number)	Dilution	Conjugate
PD-L1 (10F.9G2)	Rat	BioLegend (124311)	1/100	APC
Isotype (RTK530)	Rat	BioLegend (400612)	1/100	APC
MHCI (28-8-6)	Mouse	BioLegend (114619)	1/100	PerCP/Cy5.5
Isotype (MOPC-173)	Mouse	BioLegend (400257)	1/100	PerCP/Cy5.5
CD4 (GK1.5)	Rat	BioLegend (100408)	1/200	PE
CD8a (53-6.7)	Rat	BioLegend (100734)	1/200	PerCP/Cy5.5
CD45 (30-F11)	Rat	BioLegend (103112)	1/100	APC
CD45 (30-F11)	Rat	BD Biosciences (553082)	1/500	PE/Cy5
CD44 (IM7)	Rat	BioLegend (103012)	1/200	APC
CD62L (MEL-14)	Rat	BioLegend (104448)	1/200	PE/Dazzle 594
PD-1 (J43)	Hamster	eBioscience (12-9985)	1/200	PE

2.1.5 Reagents for immunohistochemistry and immunofluorescence

Antigen retrieval buffer: pH 6.0 citrate target retrieval buffer. Dako (S1699).

4', 6-diamidino-2-phenylindole (DAPI): Diluted 1/10000 in PBS. Stored at 4°C. Invitrogen (D1306).

Paraformaldehyde: 4% w/v paraformaldehyde powder in PBS, dissolved at

50°C on a heated stirrer. Sigma-Aldrich (15812-7).

Hydrophobic barrier pen: Vectorlabs (H-4000).

Immersol immersion oil: Zeiss (518F).

Immunofluorescence buffer (IFF): 1% BSA, 2% FBS in PBS. Sterilised using a 20 µm syringe filter. Stored at -20°C.

Triton X-100: Sigma-Aldrich (T9284).

Vectashield Mounting Medium: Vector Laboratories (H-1000). Stored at 4°C.

Table 2.6: Antibodies for immunofluorescence and immunohistochemistry

Antibody (Clone)	Species	Source (Catalogue number)	Dilution
CD8a (4SM15)	Rat	eBioscience (14-0808)	1/250
αSMA (1A4)	Mouse	Sigma (F3777)	1/1000
GFP	Rabbit	Abcam (ab290)	1/1000
FSP1	Rabbit	Proteintech (16105-1-AP)	1/200
Alexa Fluor 488-anti-mouse IgG	Goat	Molecular Probes (A11001)	1/1000
Alexa Fluor 555-anti-mouse IgG	Goat	Molecular Probes (A21424)	1/1000
Alexa Fluor 555-anti-rabbit IgG	Goat	Molecular Probes (A21429)	1/1000

2.1.6 Reagents for T cell proliferation assay

EasySep mouse T cell isolation kit: Stem Cell Technologies (19851).

Purified anti-mouse CD28 antibody: BioLegend (102102).

Purified anti-mouse CD3e antibody: BioLegend (100302).

Interleukin 2 (IL2; recombinant mouse): BD Biosciences (550069).

2.1.7 Reagents for nucleic acid manipulation

DNeasy Blood and Tissue kit: Qiagen (69504).

RNeasy Mini kit: Qiagen (74104).

RLT buffer: Qiagen (79216).

2.1.8 Cells

CAF-1 cells: Isolated and immortalised during this thesis. See Section 2.2.5.

CAF-2 cells: Previously isolated in the Molecular Cell Biology laboratory (ICR). Immortalised during this thesis. See Section 2.2.5.

NMF cells: Isolated and immortalised during this thesis. See Section 2.2.5 below.

4T07: Mouse mammary carcinoma cells (Jean-Christophe Bourdon, University of Dundee). Derived from spontaneously arisen mammary tumour in BALB/cfC3H female mouse (Aslakson and Miller, 1992). Ethyl methanesulphonate treated, thioguanine and oubain resistant.

4T1: Mouse mammary carcinoma cells (Jean-Christophe Bourdon, University of Dundee). Derived from spontaneously arisen mammary tumour in BALB/cfC3H female mouse (Aslakson and Miller, 1992). Thioguanine resistant.

D2A1: Mouse mammary carcinoma cells (Ann Chambers, Western University, Canada). Derived from a spontaneous mammary tumour that originated from a precancerous D2 hyperplastic alveolar nodule in a BALB/c mouse (Morris et al., 1993).

D2A1-m2: Mouse mammary carcinoma cells derived by serial inoculation of D2A1 cells in BALB/c mice followed by recovery from the lung tissue *ex vivo* (Jungwirth et al., 2018). Generated in the Molecular Cell Biology laboratory (ICR).

2.1.9 Equipment

BD FACSAria: BD Biosciences.

gentleMACS Octo Dissociator with heaters: Miltenyi Biotec (130-096-427).

IVIS Illumina II: Caliper-Life Sciences as PerkinElmer.

LSR II flow cytometer: BD Biosciences.

LSRFortessa: BD Biosciences.

Nanodrop Spectrophotometer: Thermo Fisher Scientific (ND-8000-GL).

NanoZoomer-XR digital slide scanner: Hamamatsu (C12000-01).

2.1.10 *In vivo* studies

Endo180 knockout (KO) BALB/c mice: Generated in the Molecular Cell Biology laboratory (ICR) (East et al., 2003) and backcrossed for > 6 generation onto a BALB/c background.

Endosialin knockout (KO) mice: Generated by David Huso (Johns Hopkins Medical Institutions, Baltimore, MD) (Nanda et al., 2006) and backcrossed for > 6 generations onto a BALB/c background.

Hydroxypropylbetacyclodextrin: Sigma-Aldrich (C0926-10G).

Isoflurane: IsoFlo, Abbot (05260-05).

JQ1 (+): Used at 50 mg/kg in 10% DMSO in 10% w/v hydroxypropylbetacyclodextrin. Selleckchem (S7110).

Matrigel: Growth factor reduced basement membrane matrix, phenol red-free. BD Biosciences (356231).

NOD-scid mice: 6-8-week old female mice. Charles River.

NOD-scid gamma (NSG) mice: 6-8-week old female mice. Charles River.

Ub-GFP BALB/c mice: 6-8-week old female BALB/c mice expressing green fluorescent protein (GFP) under the control of the human ubiquitin C promoter (Schaefer et al., 2001). Swain laboratory (ICR).

Wild-type (WT) BALB/c mice: 6-8-week old female mice. Charles River.

Table 2.7: Therapeutic antibodies for *in vivo* studies

Antibody (Clone)	Isotype	Source	Dose
Anti-CTLA-4 (9D9)	mIgG1 kappa	MedImmune/AZ (SP17-038)	10mg/kg
Anti-PD-L1 (AB740080)	mIgG1 D265A	MedImmune/AZ (SP16-138)	10mg/kg
NIP228 isotype control	mIgG1 kappa	MedImmune/AZ (SP17-095)	10mg/kg
NIP228 isotype control	mIgG1 D265A	MedImmune/AZ (SP16-017)	10mg/kg

Table 2.8: Cell information for *in vivo* studies

Cell line	Mouse strain	Culture conditions	Cell number implanted
4T07	BALB/c	DMEM, 10% FBS, 0.5% P/S	5×10^5
4T1	BALB/c	DMEM, 10% FBS, 0.5% P/S	5×10^4
D2A1	BALB/c	DMEM, 10% FBS, 0.5% P/S	2×10^5
D2A1-m2	BALB/c	DMEM, 10% FBS, 0.5% P/S	2×10^5

2.2 Methods

2.2.1 Tissue culture

2.2.1.1 Culture conditions

Adherent cells were cultured at 37°C in a tissue culture incubator with humidified air, supplemented with CO_2 to 5%. Unless otherwise stated, cells were grown in complete media (DMEM plus 10% FBS and 1/200 penicillin/streptomycin). All cell lines used were cultured to limited passage and were periodically screened to confirm the absence of mycoplasma.

2.2.1.2 Passaging of cells

Adherent cells were cultured in tissue culture flasks until 90% confluent. The growth medium was removed, the cells rinsed with PBS and incubated at 37°C with trypsin/EDTA until detachment. Cells were then fully removed by pipetting with 5-15 mL of fresh culture medium and, depending on the rate of growth and cell type, re-plated at a 1/2 to 1/20 dilution in a fresh tissue culture flask. For all tissue culture based experiments described below, suspension cells were stained with 0.4% Trypan Blue and counted using a Countess automated cell counter system prior to replating.

2.2.1.3 Frozen storage of cells

Cells growing in a 75 cm^2 flask were detached using trypsin/EDTA, resuspended in culture medium and pelleted by centrifugation for 5 minutes. The cells were resuspended in 2 mL of cell freezing medium, and 1 mL of cell suspension was added

to CryoTube vials. Vials were then placed in polystyrene insulated boxes at -80°C for at least 24 hours before transfer to liquid nitrogen for long-term storage.

2.2.1.4 Conditioned medium

Conditioned medium was collected from cells grown in complete RPMI medium for 72 hours. Cells were grown to a final confluency of 75%. 10 mL conditioned medium was collected from a single 75 cm^2 flask, filtered using 40µm filters and used immediately or frozen at -20°C.

2.2.2 Cellular assays

2.2.2.1 Tumour cell proliferation assay

5 x 10^4 4T1 cells were stained with a CellTrace Violet cell proliferation kit and cultured for 48 hours at 37^{o}C either alone or in the presence of 1 x 10^5 NMF or CAF-1 cells. CellTrace Violet signal intensity of 4T1 cells was measured by flow cytometry (LSRII Flow Cytometer, BD Biosciences).

2.2.2.2 T cell proliferation assay

Spleens from naïve WT BALB/c mice were isolated and dissociated through 40 µm filters to generate a single-cell suspension. After red blood cell (RBC) lysis, T cells were isolated using the EasySep mouse T cell isolation kit, and labelled with 1 mM CFSE in pre-warmed PBS for 10 minutes at 37^{o}C. The CFSE-labelled T cells were then plated in complete RPMI media supplemented with 50 mM β-mercaptoethanol into 96-well plates coated with 1 µg/mL anti-CD3ε antibody. Naïve CFSE-stained T cells were cultured for 4 days at 37^{o}C with 5 µg/mL anti-CD28 antibody and 10 ng/mL IL2 in complete RPMI media or conditioned complete RPMI media collected from CAF-1 cultures. After 4 days, cells were stained with an anti-mouse CD16/CD32 antibody for 10 minutes at room temperature to block non-specific binding of staining antibodies. APC-conjugated anti-CD45, PE-conjugated anti-CD4 and PerCP/Cy5.5-conjugated anti-CD8 antibodies were added to cells at specified dilutions (Table 2.4) and

incubated at 4^{o}C for 30 minutes. Cells were stained with DAPI and the CFSE signal in gated live CD4^{+} (T_H) and CD8^{+} cells (CTLs) was measured by flow cytometry (LSRII flow cytometer, BD Biosciences).

2.2.2.3 PD-L1 upregulation assay

D2A1 and D2A1-m2 cells were cultured in complete media supplemented with 10 ng/mL recombinant mouse IFNγ. After 24 hours, cells were stained with APC-conjugated anti-PD-L1 and PerCP/Cy5.5-conjugated anti-MHCI antibodies, or isotype control antibodies, at specified dilutions (Table 2.5) and incubated at 4 ^{o}C for 30 minutes. Cells were stained with DAPI and live cells were assessed for expression of PD-L1 and MHCI by flow cytometry (LSRII flow cytometer, BD Biosciences).

2.2.3 *In vivo* studies

2.2.3.1 Animal husbandry

All animal work was carried out under UK Home Office Project licences 70/7413 and P6AB1448A (Establishment License, X702B0E74 70/2902) and was approved by the Animal Welfare and Ethical Review Body at the ICR. All mice were housed in groups of 5 mice in individually vented cages (IVC). Bedding, food and water were replenished twice per week, and all animals were monitored on a daily basis by staff from the ICR Biological Service Unit (BSU) for signs of ill health. During the course of experiments mice were weighed at least two times per week.

2.2.3.2 Tumour models

Unless otherwise stated, 50 µL of cells in PBS were injected orthotopically into the 4th mammary fat pad of 6-8-week old female mice. Cell numbers injected are listed in Table 2.8. Tumour dimensions were recorded using callipers and tumour volumes were calculated using the formula (width^2 x length)/2.

2.2.3.3 4T07 tumour fragment study

5 x 10^5 4T07 cells were injected orthotopically into the 4th mammary fat pad of 6-8-week old female NSG mice (Figure 3.2A). 19 days post cell injection, 4T07 tumours were cut into 2-3 mm^3 fragments and implanted subcutaneously into the flank of 6-8-week old female WT BALB/c mice. Resultant tumours were processed to single cell suspensions and frozen as described in Section 2.2.1.3. 5 x 10^5 thawed 4T07 cells isolated *ex vivo* from a fragment-derived tumour were subsequently injected orthotopically into the 4th mammary fat pad of 6-8-week old female WT BALB/c mice.

2.2.3.4 Co-implantation models

5 x 10^5 4T07 cells were injected orthotopically into the 4th mammary fat pad of 6-8-week old female WT BALB/c mice, with or without 6 x 10^5 CAF-1 cells. 2 x 10^5 D2A1 cells were injected orthotopically into the 4th mammary fat pad of 6-8-week old female WT BALB/c mice, with or without 6 x 10^5 NMF or CAF-1 cells.

2.2.3.5 Immune checkpoint blockade treatment

Tumours were established in female WT BALB/c mice as described in Section 2.2.3.2. Mice received, via intraperitoneal injection, 10 mg/kg of either anti-CTLA-4 or anti-PD-L1 antibodies (Table 2.7) either as single agents or in combination (COMBO). Unless otherwise stated, anti-CTLA-4 was given on days 7, 11, 14, 18, 21 and 25 post cell implant, and anti-PD-L1 was given on days 5, 7, 11, 14, 18 and 21 post cell implant. Treatment regimens for individual experiments are also illustrated in Figures 5.2A and 5.5A. Control mice received 10 mg/kg of respective isotype controls antibodies (ISO) (Table 2.7). For survival analysis, mice were culled upon reaching protocol-defined humane endpoints.

2.2.3.6 JQ1 treatment

D2A1-m2 tumours were established in female WT BALB/c mice as described in Section 2.2.3.2. Combination immune checkpoint blockade treatment (COMBO) was given as described in Section 2.2.3.5. JQ1 (Selleckchem, S7110) was administered

daily by intraperitoneal injection at 50 mg/kg in 10% DMSO in 10% w/v hydroxypropylbetacyclodextrin either alone (JQ1) or in combination with immune checkpoint blockade (JQ1 + COMBO). JQ1 treatment began 7 days post cell implant and continued for 22 days.

2.2.3.7 Matrigel plug immune cell recruitment assay

2 x 10^6 NMF, CAF-1 or CAF-2 cells were resuspended in 100 µL PBS, mixed with 300 µL Matrigel, and 300 µL was injected subcutaneously into the right flank of 6-8-week old female WT BALB/c mice. Control mice were injected with the PBS/Matrigel mixture alone. After 7 days, Matrigel plugs were processed to single-cell suspensions using a tumour dissociation kit in combination with a gentleMACS Octo Dissociator according to the manufacturer's protocol. Cell suspensions were resuspended in FACS buffer and stained with Fixable Violet Dead Cell Stain for 20 minutes at 4^{o}C. Cells were subsequently stained with an anti-mouse CD16/CD32 antibody for 10 minutes at room temperature to block non-specific binding of staining antibodies to Fc receptor expressing cells. Panels of directly conjugated antibodies against cell surface markers were added to cell suspensions at specified dilutions (Table 2.4) and incubated at 4^{o}C for 30 minutes. Cells were resuspended in FACS buffer and samples were analysed by flow cytometry (LSRII Flow Cytometer, BD Biosciences). Data analysis was performed using FlowJo software (Tree Star Inc.).

2.2.4 Immunohistochemical and immunofluorescent imaging

2.2.4.1 Immunohistochemistry

Tumours were removed and fixed overnight at room temperature in 4% paraformaldehyde and embedded in paraffin wax after processing in a Tissue-Tek VIP automatic tissue processor (Sakura, Finland). For immunohistochemical staining, 3-4 µm sections were cut from formalin-fixed paraffin-embedded (FFPE) tissue blocks, and dewaxed in xylene, rehydrated through ethanol washes and were stained using haematoxylin and eosin (H&E) or were subjected to high-temperature antigen retrieval,

depending on the primary antibody requirements. Slides were cooled at room temperature before incubation with the primary antibody (see Table 2.6 for antibody dilutions). Detection was performed using chemi-luminescence horseradish peroxidase (HRP) based methods. The Breast Cancer Now (BCN) Histopathology Core Facility performed all immunohistochemical staining. Slides were scanned on the Hamamatsu microscope with a NanoZoomer XR camera. For quantitative spatial analysis of $CD8^+$ cell infiltration, QuPath software was used to count the number of positively stained cells in 8 x peripheral and 8 x central 1 mm^2 regions of viable tumour tissue.

2.2.4.2 Immunofluorescence

Cells were cultured on glass coverslips, fixed for 40 minutes in 4% formaldehyde, rinsed in PBS and then permeabilised in 0.5% Triton X-100 for 10 minutes. Cells were washed twice in PBS and stored in PBS at 4˚C.

Confocal microscopy of FFPE material was performed as previously described (Robertson et al., 2008). Briefly, sections were dewaxed and rehydrated. Antigen retrieval was performed at 95°C in citrate pH 6.0 antigen retrieval buffer for 30 minutes followed by 20 minutes at room temperature and 5 minutes under running water. Slides were removed from water and sections were outlined with a hydrophobic barrier pen. Care was taken to keep sections wet at all times. Labeling was performed as described below. Unstained pre-cut sections were stored at 4˚C in nitrogen gas. For fluorescent labeling, cells or sections were blocked in IFF for 15 minutes. Primary antibodies (Table 2.6) were diluted in IFF and incubated for 1 hour at room temperature on a rocking platform or overnight at 4°C.

Cells or sections were then washed for 15 minutes in 3 rinses of PBS and incubated with secondary antibody (Table 2.6) diluted in IFF for 1 hour at room temperature on a rocking platform. Nuclei were counterstained for 15 minutes in 3 washes of 14 nM DAPI in PBS. Cells or sections were mounted using 4-8 µL Vectashield and sealed using clear nail varnish. Images were collected immediately or stained sections were stored at -20˚C. Fluorescent images were collected sequentially

in up to four channels on a TCS SP2 confocal microscope (Leica) or using an EVOS fluorescence microscope (Thermo Fisher Scientific).

2.2.5 Fibroblast isolation

2.2.5.1 Isolation of normal mammary fibroblasts

Normal mammary fibroblasts (NMFs) were isolated from the mammary fat pads of naïve 6-8-week old female Ub-GFP BALB/c mice. Mammary fat pads were cut into small chunks and cultured in complete medium. After 10 days, mammary fat pad chunks were discarded and migratory fibroblasts were cultured separately and immortalised as outlined in Section 2.2.5.3.

2.2.5.2 Isolation of cancer-associated fibroblasts

CAFs were isolated from 4T1 tumours grown bilaterally in the 4^{th} mammary fat pads of 6-8-week old female Ub-GFP BALB/c mice implanted with 5 x 10^4 4T1 cells. Tumours were processed to single-cell suspensions using a tumour dissociation kit in combination with a gentleMACS Octo dissociator according to the manufacturer's protocol. Unlabelled primary antibodies against mouse CD24 and CD45 were added and samples were incubated at 4^{o}C for 20 minutes. Cells were washed once in FACS buffer. Depletion of antibody bound cells was performed using anti-rat immunoglobulin G (IgG) dynabeads according to manufacturer's depletion protocol. Prior to sorting, samples were passed through a 40 µm cell strainer. GFP^+ cells were sorted into complete medium using a FACSAria cell sorter (BD Biosciences) and cultured in tissue culture plates.

2.2.5.3 Immortalisation of primary fibroblasts

Fibroblasts isolated from 4T1 tumours (CAF-1 and CAF-2 cells) were immortalised using an HPV-E6/E7-puromycin retrovirus. Normal mammary fibroblasts (NMF cells) were immortalised using an HPV-E6/E7-neomycin lentivirus. Virus-containing media was added at a 1:1 dilution with fresh complete media to primary fibroblasts in one well

of a 6-well plate and left to incubate for 48 hours. Polybrene was also added at a concentration of 8 µg/mL. After 48 hours, the virus-containing media was removed and cells were cultured in complete media for a further 24 hours.

2.2.5.4 Flow cytometry analysis of CAF markers

D2A1, NMF, CAF-1 and CAF-2 cells were stained with antibodies listed in Table 2.3 at specified dilutions and incubated at 4^{o}C for 30 minutes. Cells were stained with DAPI and live cells were assessed for expression of αSMA, CD45, CD90 and PDGFRα by flow cytometry (LSRII flow cytometer, BD Biosciences).

2.2.6 Immune profiling

2.2.6.1 Tissue dissociation

Tumours were removed and a single-cell suspension generated using a tumour dissociation kit in combination with a gentleMACS Octo Dissociator according to the manufacturer's protocol. Specified volumes of supplied enzymes were added to tumour samples before running each sample on the Octo Dissociator with the program 37C_m_TDK_2. Samples were subsequently applied to a 70 µm MACS SmartStrainer and washed in PBS. Red blood cells were removed from tumour samples by suspension in RBC lysis buffer for 5 minutes at room temperature. Samples were resuspended in FACS buffer for FACS or flow cytometry staining.

2.2.6.2 Cell staining and flow cytometry

Tumours were processed to single-cell suspensions as described in Section 2.2.6.1, resuspended in FACS buffer and stained with Fixable Viability Dye eFluor 455UV for 20 minutes at 4^{o}C. Cells were subsequently stained with an anti-mouse CD16/CD32 antibody for 10 minutes at room temperature to block non-specific binding of staining antibodies to Fc receptor expressing cells. Panels of directly conjugated antibodies against cell surface markers were added to cell suspensions at specified dilutions (Tables 2.1-2.4) and incubated at 4^{o}C for 30 minutes. Cells were washed twice in PBS

before being fixed and permeabilised overnight using the FoxP3/Transcription factor staining buffer set. Panels of directly conjugated antibodies against intracellular markers were then added to cells for 60 minutes at 4^{o}C. Following further washing, cells were fixed in 4% paraformaldehyde solution for 15 minutes at 4^{o}C. Finally, cells were resuspended in FACS buffer, counting beads were added and samples were analysed on a BD LSRFortessa or BD LSRII flow cytometer. Data analysis was performed using FlowJo software (Tree Star Inc.). Gates were set using appropriate fluorescence minus one (FMO) controls. Absolute cell counts were calculated as follows: absolute count (cells/uL) = (cell count x counting bead volume) / (counting bead count x cell volume) x counting bead concentration. Tumours were weighed before processing to permit calculation of cell counts per mg of tumour.

2.2.7 Whole-exome sequencing

DNA was extracted from tumour cell lines or BALB/c mouse spleen tissue using the DNeasy Blood and Tissue kit. DNA samples were physically sheared to the desired size using a Covaris E Serires instrument (Covaris). Paired-end multiplexed library preparation was performed by the Tumour Profiling Unit (TPU) at the ICR using the SureSelect^{XT} Library Prep and Capture System (Agilent Technologies) following the standard protocol workflow, before multiplex sequencing on an NovaSeq 6000 flow cell (Illumina).

Bioinformatics and statistical analyses were performed using custom R scripts and a bespoke DNA sequencing pipeline based on the Nextflow framework (Tommaso et al., 2017). Whole exome sequencing FASTQ files were aligned to the mouse genome assembly build GRCm38 with the Burrows-Wheeler Aligner (BWA) v0.7.12 (Li and Durbin, 2010). BWA was run with default parameters, utilising 5 threads. The resulting SAM file was converted to BAM and sorted with SAMtools v1.5 (Li et al., 2009). Duplicate reads were removed from the sample files with the Picard v2.8.1 suite of tools (http://broadinstitute.github.io/picard/). Insert size and coverage metrics were also calculated with Picard. Lastly, base scores were recalibrated with the Genome

Analysis Toolkit (GATK) v4.0.3.0 (McKenna et al., 2010) according to the GATK Best Practices pipeline.

Copy number analysis (CNA) was carried out with CNVkit v0.9.3 (Talevich et al., 2016), utilising the batch command. A cancer-free sample taken from BALB/c mouse spleen tissue was used as a normal reference for each cell line sample. Copy number $\log_2$ ratios from CNVkit were used to create CNA plots in R statistical programming language v3.5.0 (R Core Team, 2018).

LoFreq (Wilm et al., 2012) was used to call somatic variants. As in CNA, the same healthy BALB/c sample was used as a normal reference. Common variants were removed before annotating the remaining variants with ANNOVAR (01/02/2016 release) (Wang et al., 2010). The output from ANNOVAR was further processed in R for comparisons between samples and visualisations. Adam Mills of the Breast Cancer Now (BCN) Bioinformatics Facility performed data analysis.

2.2.8 NanoString gene expression analysis

Tumours were established as described in 2.2.3.2. At the end of the experiment, tumours were harvested and immediately frozen in CryoTubes in liquid nitrogen. Cryo-preserved tissue was stored at -80^{o}C. Frozen tissue was lysed in RLT buffer containing 1/100 β-mercaptoethanol in Hard-Tissue homogenising CK28 tubes and homogenised using a Precellys tissue homogeniser (Bertin-Corp) for 2 minutes. RNA was extracted and purified using the Qiagen Rneasy kit according to the manufacturer's protocol. RNA was hybridised with the PanCancer Mouse IO 360 Panel or the PanCancer Mouse Immune Profiling Panel (NanoString) by Richard Buus of the BCN NanoString facility.

Raw NanoString data was pre-processed using R package NanoStringNorm (v1.2.1) (Bankhead et al., 2017). Differential mRNA abundance analysis was performed using voom (TMM normalisation), with R package limma (v3.34.9) (Ritchie et al., 2015) Genes with absolute $\log_2$ fold change > 1 and adjusted *P* value < 0.05 were considered significant. For cell type abundance analysis, NanoString curated

genesets representing specific cell types were used. For each cell type, genesets with more than two genes were further reduced to the largest positively correlated cluster of genes by running hierarchical clustering on Spearman's correlation distance, followed by identification of optimal number of clusters using Silhouette score. Genes were kept if they all showed pairwise Spearman's $P > 0.5$. A similar approach was used for the comparison of CD8 T effector, Pan-F-TBRS, TGF-beta Signalling and Wnt Signalling signatures. All analyses were performed in R statistical programming language (v3.4.4). Visualisations were generated using in-house plotting libraries implemented in R. Syed Haider of the BCN Bioinformatics Facility performed downstream data analysis of NanoString datasets.

2.2.9 Statistical analysis

All statistical tests were performed in GraphPad Prism 7. Error bars indicate ± standard error of the mean (SEM). All tests were two-tailed, with a confidence interval of 95%. For multiple comparisons, a one-way analysis of variance (ANOVA) was used followed by Dunnett's multiple comparisons test, with confidence intervals of 95%. Tumour growth curves were analysed with two-way ANOVA followed by Bonferroni post-test with confidence intervals of 95%. For survival analysis, Kaplan-Meier curves were compared using the log-rank test.

Chapter 3: CAF-rich mouse mammary carcinomas have a 'colder' tumour immune microenvironment

3.1 Introduction

A better understanding of the influential role of the immune system in dictating cancer progression has ushered in a new era of cancer treatment (Pardoll, 2012). By focusing on overcoming immunological checkpoints that suppress anti-tumour immunity and lead to cancer immune evasion, immunotherapy has changed the way cancer is treated. However, as described in Chapter 1.3.2.5, despite the clinical success of immunotherapy in a variety of cancer types, many breast cancer patients continue to experience limited or no benefit with drugs of this kind (Vonderheide et al., 2017b).

The mechanisms driving the poor response of breast cancer to immunotherapy remain unclear. Key to improving responses will be attempting to unravel the complexities within the tumour immune microenvironment. Advances in techniques such as flow cytometry have already identified subsets of tumour-infiltrating immune cells with contrasting roles in cancer immunity (Gajewski et al., 2013). It is well established that cytotoxic T lymphocytes (CTLs) are critical in driving anti-tumour adaptive immune responses and their presence in breast cancers is often associated with a favourable clinical outcome (Blake-Mortimer et al., 2004). Conversely, tumour-associated macrophages (TAMs), particularly those with an M2-polarised, immunosuppressive phenotype, can blunt CTL responses and accelerate cancer progression (Choi et al., 2018). This diversity within the tumour immune microenvironment has been intensively investigated preclinically, and data from the bench has supported improvements in treatment in the clinical scenario (Budhu et al., 2014).

More recently, accumulating evidence implicates other stromal cells in the generation of an immunosuppressive tumour immune microenvironment (Harper and

Sainson, 2014). Activated tumour-resident fibroblasts, known as cancer-associated fibroblasts (CAFs), can promote cancer cell proliferation, invasion and metastasis (Kalluri and Zeisberg, 2006). However, their role in modulating anti-tumour immunity is less clear. Research has implicated fibroblasts, and fibrosis in general, in inhibiting T cell activity, particularly during wound healing (Larouche et al., 2018). With cancer now viewed as a 'wound that doesn't heal' (Dvorak, 1986), there are increasing efforts to describe the role of CAFs in contributing to the composition and polarisation of the tumour immune microenvironment.

In this chapter, the tumour immune microenvironments of two, paired syngeneic mouse mammary tumour models, which differ in their CAF infiltration and activation status, were characterised.

3.2 Results

3.2.1 Characterisation of 4T07 and 4T1 tumours

The aim of this project was firstly to determine the role that CAFs play in modulating the tumour immune microenvironment and affecting breast cancer progression, and secondly, to determine whether CAFs can modulate responses to immunotherapy. To address both of these aims, *in vivo* models were required that differed in their CAF content and activation that could be interrogated for any differences in immune composition. Recently, a phenotypically comparable pair of mouse mammary carcinoma cell lines has been described that exhibit differences in CAF content *in vivo*. When implanted orthotopically into the mammary fat pads of syngeneic BALB/c mice, 4T1 cells give rise to metastatic tumours that are abundant in αSMA^+ CAFs (Avgustinova et al., 2016). In contrast, 4T07 cells, which are derived from the same spontaneous mammary adenocarcinoma in a BALB/cfC3H mouse as 4T1 cells (Miller et al., 1983), form less metastatic, slower growing tumours with a paucity of CAFs. In additional unpublished experiments, CAFs directly isolated from 4T07, but not 4T1 tumours, expressed a gene signature associated with activation of the adaptive immune system.

To confirm these differences in CAF content between 4T07 and 4T1 tumours, and to investigate differences in immune cell composition, 4T07 and 4T1 cells were injected orthotopically into the 4th mammary fat pad of wild-type BALB/c mice to form syngeneic tumours. Resultant primary tumours were formalin-fixed, paraffin-embedded and FFPE sections were stained for the CAF marker, αSMA, and the CTL marker, CD8 (Figure 3.1A). Compared to 4T07 tumours, 4T1 tumours exhibited significantly higher levels of CAF infiltration/activation (Figure 3.1B). The reverse was true of CTL infiltration - the density of CD8$^+$ cells was lower in CAF-rich 4T1 tumours (Figure 3.1C).

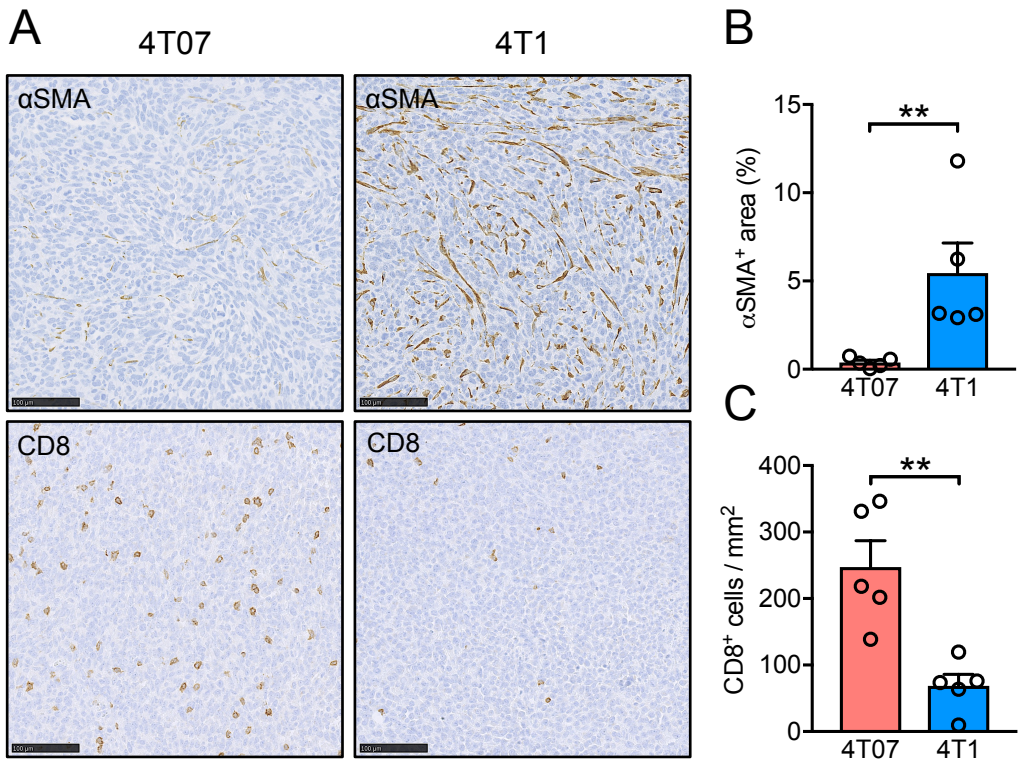

Figure 3.1: Characterisation of primary 4T07 and 4T1 tumours. 5 x 10^5 4T07 or 5 x 10^4 4T1 cells were injected orthotopically into the 4th mammary fat pad of wild-type BALB/c mice (*n* = 5 mice per group). Mice were culled and tumours removed 17 days later and formalin-fixed and paraffin-embedded. FFPE sections were stained with anti-αSMA or anti-CD8 antibodies (Table 2.6), and positive staining quantified in a blinded fashion using QuPath software. Positive staining of viable tissue was assessed in 6, randomly selected, 1 mm^2 fields of view (FOV) per tumour section and the mean value per FOV was calculated for each section. **A.** Representative images. Scale bar, 100 μm. **B.** Quantification of αSMA$^+$ staining expressed as the percentage of αSMA$^+$ stained area per FOV. **C.** Quantification of CD8$^+$ staining expressed as the number of CD8$^+$ cells per FOV. Data in **B** and **C** are mean ± SEM. Statistical analysis was performed using an unpaired *t*-test: ** = $P < 0.01$.

To determine whether the immune system plays a role in modulating growth of 4T07 and 4T1 tumours, 4T07 and 4T1 cells were implanted orthotopically into the 4th

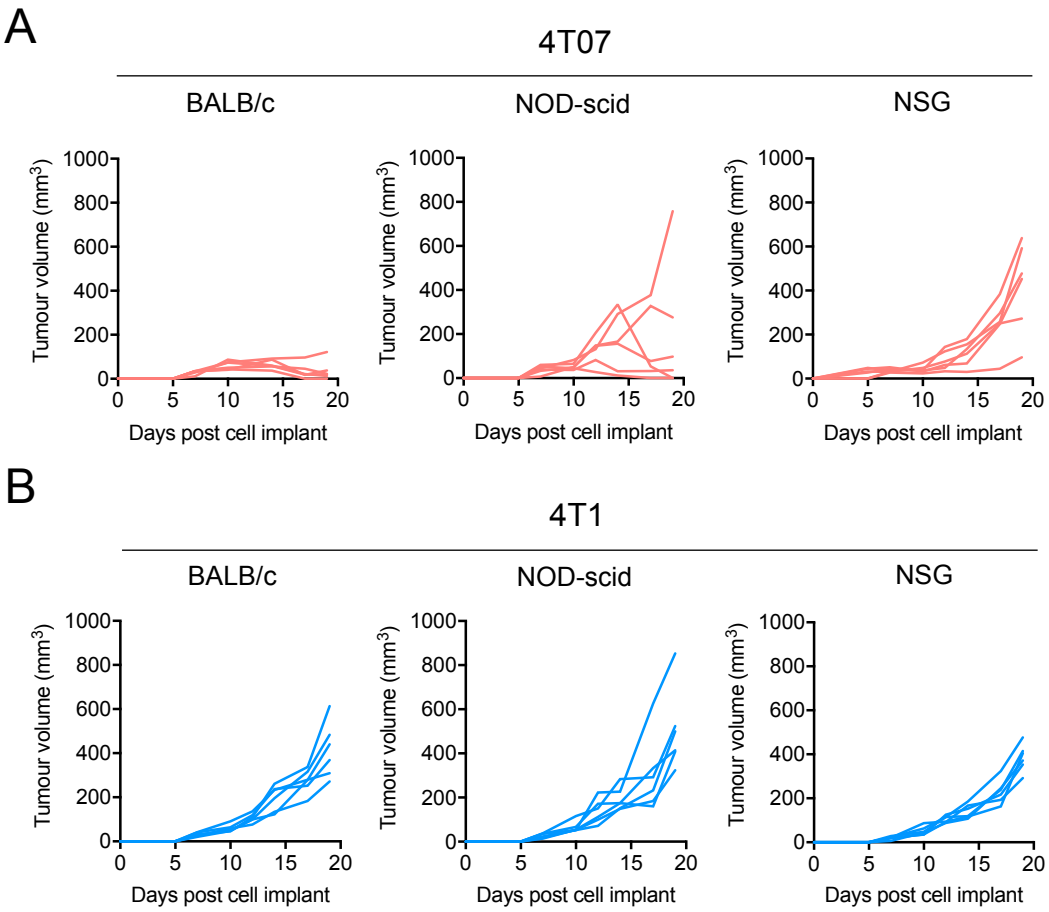

Figure 3.2: Growth of primary 4T07 and 4T1 tumours in immunocompetent and immunodeficient mice. A, B. (**A**) 5 x 10^5 4T07 or (**B**) 5 x 10^4 4T1 cells were injected orthotopically into the 4th mammary fat pad of immunocompetent wild-type BALB/c mice and immunodeficient NOD-scid and NSG mice (*n* = 6 mice per group). Shown are tumour growth curves for individual mice.

mammary fat pad of wild-type BALB/c, NOD.CB17-Prkdcscid/J (hereafter referred to as NOD-scid) and NOD.Cg-Prkdcscid Il2rgtm1Wjl/SzJ (hereafter referred to as NSG) mice. NOD-scid mice are immunodeficient and have impaired T and B cell development, whilst NSG mice, are, T, B and natural killer (NK) cell deficient, and also carry mutations affecting macrophage and dendritic cell functions (Shultz et al., 1995). 4T07 cells grew slowly in BALB/c mice, and by day 19, the majority of tumours (83%) had regressed (Figure 3.2A). Strikingly, growth of 4T07 tumours was enhanced in immunodeficient NOD-scid mice, and was further enhanced in the highly immunodeficient NSG mice (Figure 3.2A). In contrast, 4T1 tumours grew at similar rates in immunocompetent and immunodeficient recipient mice (Figure 3.2B). These

findings, together with the higher density of CTLs observed in 4T07 tumours, suggest that induction of a strong adaptive immune response is a major growth-restricting factor in 4T07, but not 4T1 tumours.

3.2.2 The 4T07 and 4T1 innate tumour immune microenvironments

The main components of the innate immune system include physical epithelial barriers, macrophages, granulocytes, NK cells and dendritic cells (DCs). Though difficulties can arise in unambiguously identifying innate immune cell subsets within the tumour immune microenvironment, particularly macrophages and neutrophils (Kather and Halama, 2019), an understanding of the role of innate immune cells in modulating cancer progression has led to the development of novel immunotherapeutic agents that are beginning to reach the clinic (Chapter 1.3.2.5).

To assess differences in infiltration of innate immune cells between the 4T07 and 4T1 models, primary tumours were processed to single-cell suspensions and stained with panels of antibodies against a range of immune cell markers and analysed by flow cytometry (Chapter 2.2.6). Panels were optimised using mouse splenocytes (data not shown), and the final panels used are shown in Tables 2.1 and 2.2. The number of viable immune cells was determined using a viability dye (Fixable Viability Dye eFluor 455UV) and gating on cells expressing the pan-leukocyte marker, CD45 (Donovan and Koretzky, 1993) (Figure 3.3A). In an effort to control for temporal changes in immune cell composition in 4T07 and 4T1 tumours, tumours were collected simultaneously. This meant that 4T07 tumours were significantly smaller than 4T1 tumours (Figure 3.3B). Nonetheless, there were no significant differences in the overall immune content ($CD45^+$ cells) of 4T07 and 4T1 tumours, assessed either by actual counts (Figure 3.3C) or as a proportion of live cells (Figure 3.3D).

A subset of cells that has recently been demonstrated to have a profound effect on cancer progression is myeloid-derived suppressor cells (MDSCs) (Chapter 1.3.2.5). They are a group of pathologically activated immature myeloid cells that are defined by their ability to suppress T cell function and support tumour growth and metastasis

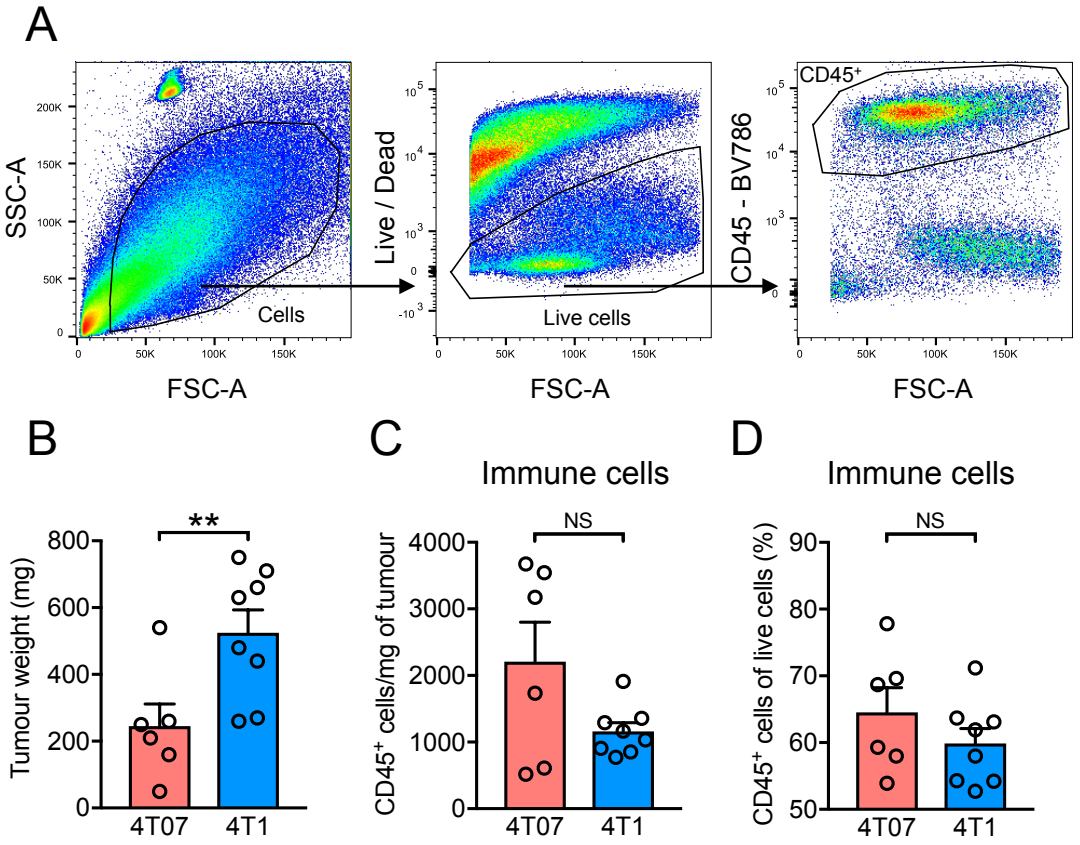

Figure 3.3: Immune profiling of primary 4T07 and 4T1 tumours. 5 x 10^5 4T07 or 5 x 10^4 4T1 cells were injected orthotopically into the 4th mammary fat pad of wild-type BALB/c mice (4T07: *n* = 6 mice; 4T1: *n* = 8 mice). All mice were culled and tumours removed 16 days later. Primary tumours were processed to a single cell suspension, stained with panels of antibodies (Tables 2.1 and 2.2), and analysed on a BD LSRFortessa flow cytometer. Gating for identifying live immune cells was performed using FlowJo software. **A.** Representative plots of the gating strategy employed for identification of live immune cells. Live cells were identified using a fixable viability dye. $CD45^+$ immune cells were identified using a BV786-conjugated anti-CD45 antibody. **B.** Weights of tumours used for immune profiling. **C.** Number of $CD45^+$ cells per mg of tumour. **D.** Proportion of $CD45^+$ cells gated on live cells. Data in **B**-**D** are mean ± SEM. Statistical analysis was performed using an unpaired *t*-test: NS = not significant; ** = $P < 0.01$.

(Marvel and Gabrilovich, 2015). Two major subsets of murine MDSCs are $CD11b^+$ $Ly6C^{high}$ $Ly6G^-$ monocytic MDSCs (mMDSCs) and $CD11b^+$ $Ly6C^{low}$ $Ly6G^+$ granulocytic MDSCs (gMDSCs) (Figure 3.4). However, gMDSCs share common markers with neutrophils, making it impossible to separate them from their immature precursors by cell surface expression markers alone (Coffelt et al., 2016). With this in mind, $CD11b^+$ $Ly6C^{low}$ $Ly6G^+$ cells will herein be referred to as neutrophils.

A higher proportion of the immune cell infiltrate in 4T07 tumours consisted of mMDSCs than in 4T1 tumours (Figure 3.5A). Neutrophils made up a larger proportion

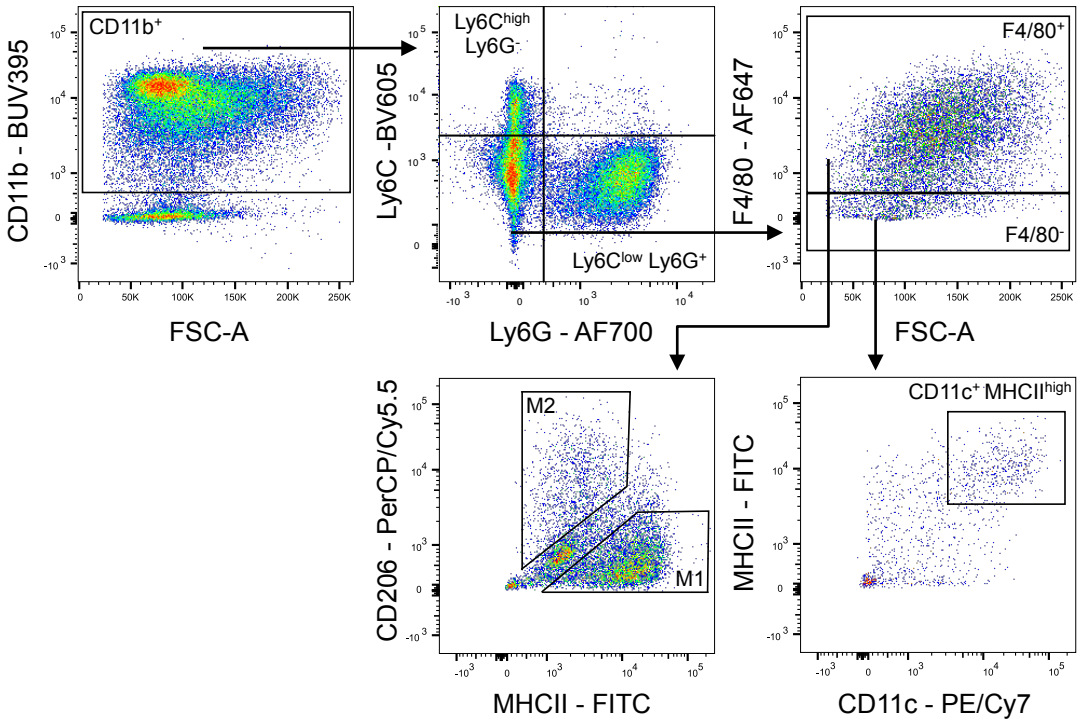

Figure 3.4: Gating strategy for identification of innate immune cell subsets. Representative plot of gating strategy employed for identification of innate immune cell subsets in the 4T07 (*n* = 6) and 4T1 (*n* = 8) tumours from Figure 3.3. $CD45^+$ immune cells, as in Figure 3.3, were gated based on staining with: a BUV395-conjugated anti-CD11b antibody, a BV605-conjugated anti-Ly6C antibody, an AF700-conjugated anti-Ly6G antibody, an AF647-conjugated anti-F4/80 antibody, a FITC conjugated anti-MHCII antibody, a PE/Cy7-conjugated anti-CD11c antibody and a PerCP/Cy5.5-conjugated anti-CD206 antibody (Table 2.1). Gating for was performed using FlowJo software.

of immune cells present in both 4T07 and 4T1 tumours than mMDSCs, but no significant differences in their levels of infiltration were observed (Figure 3.5B).

TAMs also play an important role in the tumour immune microenvironment and have consistently been shown to contribute to immunosuppression and blunt effective immunotherapy treatment (Chapter 1.3.2.5). Thus, the infiltration of TAMs, defined by their expression of CD11b and F4/80 and lack of Ly6C and Ly6G expression (Figure 3.4) was assessed in 4T07 and 4T1 tumours. As has been previously reported in breast cancer (Williams et al., 2016), TAMs made up a large proportion (up to 70%) of all immune cells in both models. However, no model-specific differences in TAM content were observed (Figure 3.5C).

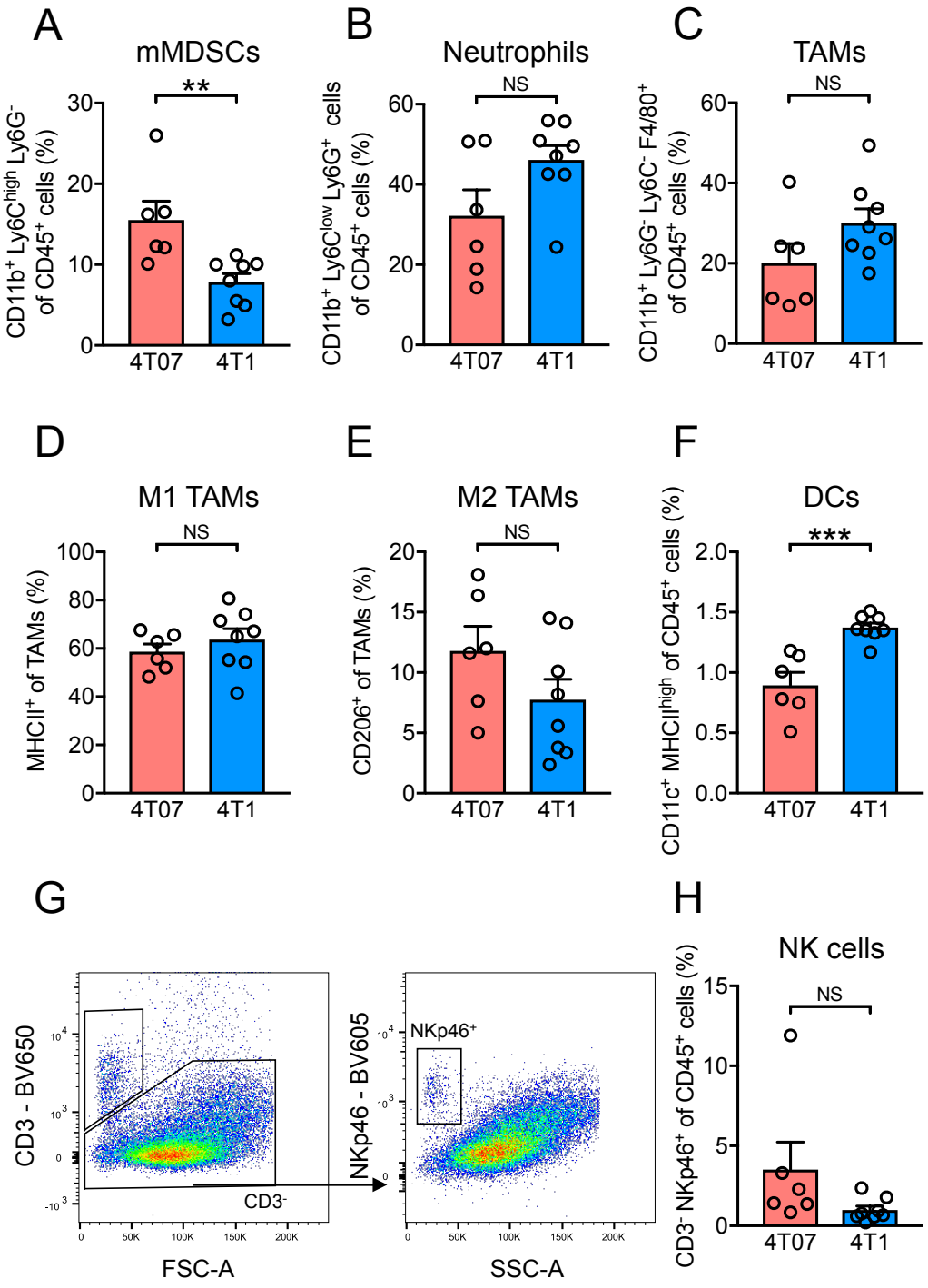

Figure 3.5: Innate immune cell content of primary 4T07 and 4T1 tumours. **A-C.** Proportion of (**A**) mMDSCs, (**B**) neutrophils, and (**C**) TAMs gated on CD45$^+$ cells in 4T07 (*n* = 6) and 4T1 (*n* = 8) tumours from Figure 3.3. **D, E.** Proportion of (**D**) M1-polarised and (**E**) M2-polarised TAMs gated on TAMs. **F.** Proportion of DCs gated on CD45$^+$ cells. **G**. Representative plot of gating strategy employed for identification of NK cells. Cells were gated based on staining with a BV650-conjugated anti-CD3 antibody and a BV605-conjugated anti-NKp46 antibody (Table 2.2). Data in **A-F, H** are mean ± SEM. Statistical analysis was performed using an unpaired *t*-test: NS = not significant; ** = $P < 0.01$; *** = $P < 0.001$.

TAM subpopulations are often described as either classically activated (M1) or alternatively activated (M2) (Chapter 1.3.1.1). Generally, M1-polarised TAMs are proinflammatory and have anti-tumour properties, whilst M2-polarised TAMs are immunosuppressive and contribute to tumour growth (Sousa et al., 2015). M1 TAMs express high levels of MHCII, whilst M2 TAMs can be identified based on their expression of the mannose receptor, CD206 (Choi et al., 2010). There were no significant differences between 4T07 and 4T1 tumours in terms of the proportion of M1 or M2 polarised TAMs (Figures 3.5D and E).

DCs are professional antigen-presenting cells (APCs) that play a crucial role in tumour immunity through the presentation of tumour antigens, and they form a crucial link between the innate and adaptive immune systems (Chapter 1.3.1.1). DCs made up a larger proportion of immune cells in 4T1 tumours than they do in 4T07 tumours, though they represented a minor proportion in both models (Figure 3.5F).

NK cells lack antigen-specific cell surface receptors, so are part of the innate immune system (Chapter 1.3.1.1). They are able to kill cancer cells directly without deliberate immunisation or activation, and in animal studies they play a critical role in the control of tumour growth and metastasis (Wu and Lanier, 2003). NK cells were identified by their lack of CD3 expression and expression of the activation receptor, NKp46 (Figure 3.5G). No significant differences in NK cell infiltration were observed between models (Figure 3.5H).

3.2.3 The 4T07 and 4T1 adaptive tumour immune microenvironments

Research into immunotherapeutic strategies designed to enhance anti-tumour immunity has focused intensively on harnessing the cytotoxic activity of lymphocytes of the adaptive immune system. This is not without good reason, as antibody-based drugs targeting inhibitory T cell checkpoints have proven remarkably successful in the clinic (Chapter 1.3.2.3). Though assessing CTL infiltration via immunohistochemistry (IHC) of tissue sections provides a clinically relevant assessment of the magnitude of anti-tumour immune responses, a more in-depth understanding of adaptive immune

cell diversity within the tumour microenvironment would aid in identifying subsets or phenotypes responsible for driving the aforementioned differences between the 4T07 and 4T1 models.

Single-cell suspensions of the same 4T07 and 4T1 tumours used for investigating innate immune cell composition (Figure 3.3B) were also stained with antibodies to interrogate the content of lymphoid lineage cells (Table 2.2). T cells were identified based on expression of the common T cell marker CD3, and cells were also stained for the surface markers CD4, CD8, and the transcription factor FoxP3 (Figure 3.6A). As discussed in Chapter 1.3.2.1, CTLs, that express CD8, contribute significantly to tumour eradication. Likewise, $CD4^+$ T helper (T_H) cells also support anti-tumour immunity, primarily through modulating other immune cells, including the priming of CTLs (Chapter 1.3.1.2). In contrast, regulatory T cells (T_{regs}), which are defined as $CD4^+$ cells expressing FoxP3, are considered immunosuppressive and promote tumour escape of immune control, primarily through suppression of CTLs (Chapter 1.3.1.2). The proportion of $CD4^+$ $FoxP3^-$ T_H cells and $CD4^+$ $FoxP3^+$ T_{regs} did not differ between 4T07 and 4T1 tumours (Figures 3.6B and C). However, 4T07 tumours exhibited a significantly higher proportion of CTLs than 4T1 tumours (Figure 3.6D), consistent with earlier IHC analysis (Figure 3.1C) and indicative of a more inflamed tumour immune microenvironment (Binnewies et al., 2018).

Whilst numerous preclinical investigations and clinical studies have established that the presence of tumour-reactive CTLs is associated with better prognosis, understanding their activity states and cytotoxic capacity is also important when assessing the magnitude of anti-tumour adaptive immune responses. Thus, tumour cell suspensions were also stained with antibodies against granzyme B, Ki67 and PD-1 (Table 2.2). Granzyme B is a serine protease most commonly found in CTLs that, together with perforin, mediates apoptosis of target cells and is a marker of a more inflamed tumour immune microenvironment (Binnewies et al., 2018). A significantly higher proportion of CTLs expressed granzyme B in 4T07 compared to 4T1 tumours (Figure 3.6E), confirming their more activated, cytotoxic phenotype. However, there

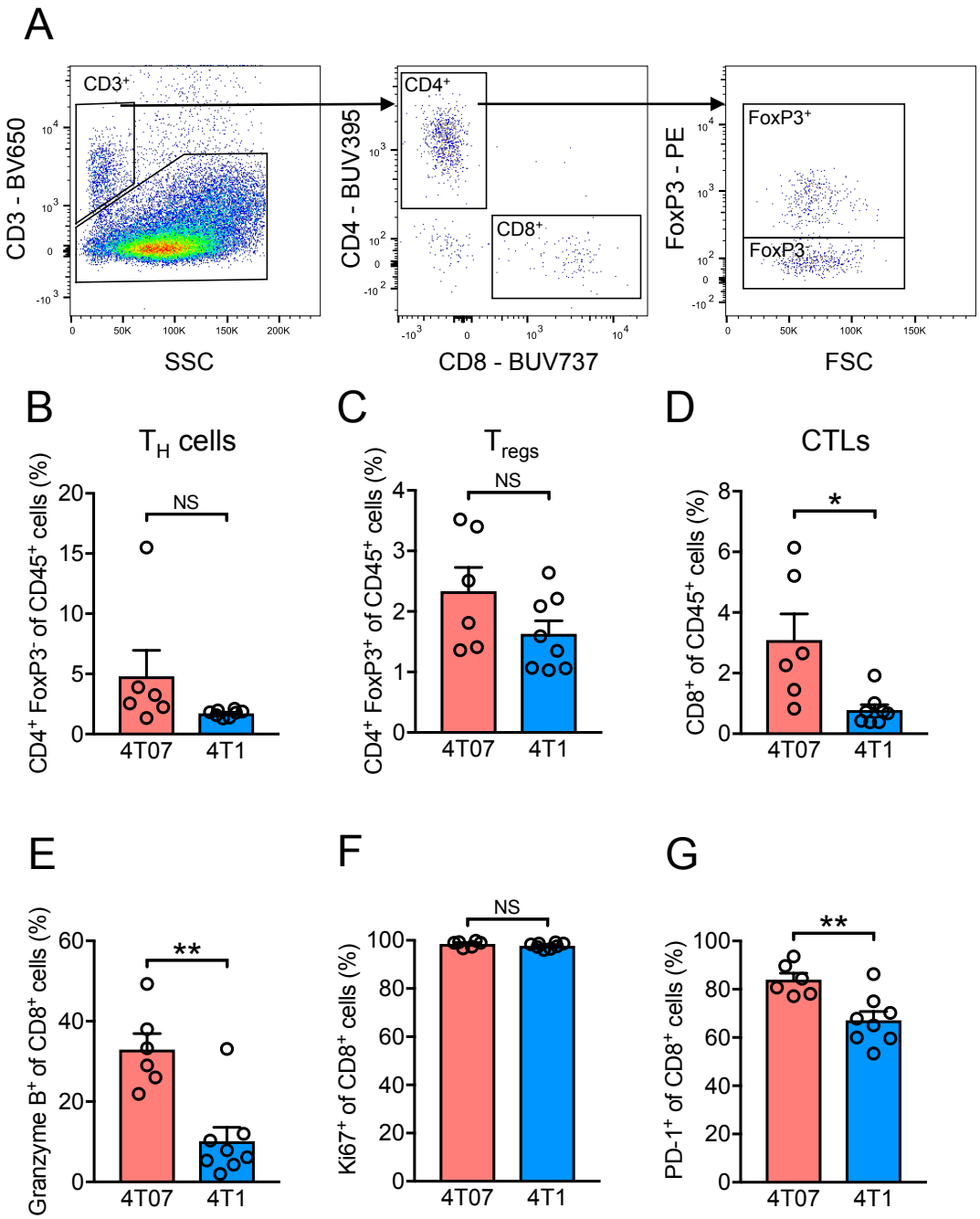

Figure 3.6: Adaptive immune cell content of primary 4T07 and 4T1 tumours. **A**. Representative plot of gating strategy employed for identification of adaptive immune cell subsets in the 4T07 (*n* = 6) and 4T1 (*n* = 8) tumours from Figure 3.3. $CD45^+$ immune cells, as in Figure 3.3A, were gated based on staining with a BV650-conjugated anti-CD3 antibody, a BUV395-conjugated anti-CD4 antibody, a BUV737-conjugated anti-CD8 antibody and a PE-conjugated anti-FoxP3 antibody (Table 2.2). **B**-**D**. Proportion of (**B**) T_H cells, (**C**) T_{regs}, and (**D**) CTLs gated on $CD45^+$ cells. **E**-**G**. Proportion of (**E**) granzyme B, (**F**) Ki67, and (**G**) PD-1 expressing CTLs. Data in **B**-**G** are mean ± SEM. Statistical analysis was performed using an unpaired *t*-test: NS = not significant; * = $P < 0.05$; ** = $P < 0.01$.

were no differences in the proportion of CTLs expressing the proliferation marker, Ki67, which was high in both models (Figure 3.6F).

As discussed in Chapter 1.3.2.3, PD-1 on the surface of CTLs, upon engagement with PD-L1, induces suppression of T cell activity and function. However, although PD-1 is a potent inhibitory receptor, PD-1 upregulation is indicative of prior T cell activity and T cell exhaustion - a hyporesponsive state of T cells prompted by chronic exposure to antigens (Jiang et al., 2015). Thus, infiltration of CTLs expressing PD-1 is another characteristic of immunologically 'hot' tumours with an inflamed immune microenvironment (Binnewies et al., 2018). Accordingly, these tumours tend to respond better to drugs such as pembrolizumab (Merck), an anti-PD-1 antibody that antagonises the PD-1/PD-L1 axis. A significantly higher proportion of CTLs expressed PD-1 in 4T07 tumours compared to 4T1 tumours (Figure 3.6G), providing further evidence to suggest that, in contrast to the more immunologically 'cold', CAF-rich 4T1 tumours, 4T07 tumours have a more inflamed phenotype.

3.2.4 Characterisation of D2A1 and D2A1-m2 tumours

Similarly to the 4T07 and 4T1 cell lines, the parental D2A1 cell line was also derived from a spontaneous BALB/c mouse mammary tumour (Morris et al., 1993). Recently, the D2A1-m2 subline was generated from the D2A1 cell line by serial inoculation of tumour cells in BALB/c mice followed by recovery from the lung tissue ex vivo (Jungwirth et al., 2018). In contrast to the non-metastatic parental D2A1 cell line, D2A1-m2 tumours are highly metastatic.

To determine whether D2A1 and D2A1-m2 models differed in their CAF content to a similar degree as the 4T07 and 4T1 models, D2A1 and D2A1-m2 cells were injected orthotopically into the 4th mammary fat pad of wild-type BALB/c mice to form syngeneic tumours as described in Chapter 2.2.3.2. Resultant primary tumours were formalin-fixed, paraffin-embedded and FFPE sections were stained with αSMA and CD8 antibodies (Figure 3.7A). Similarly to the differences observed between 4T07 and 4T1 tumours (Figure 3.1A), the more metastatic D2A1-m2 tumours had significantly

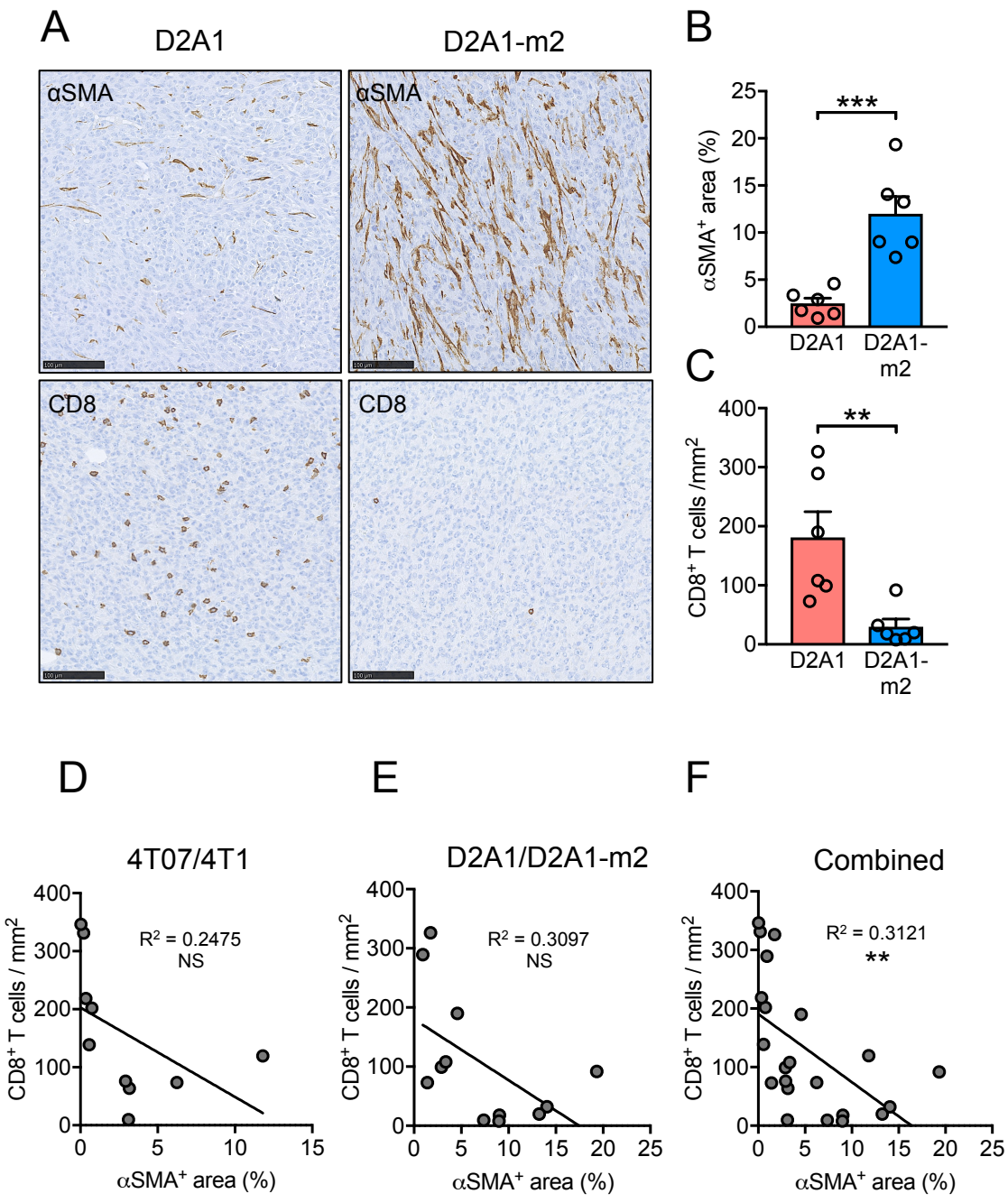

Figure 3.7: Characterisation of primary D2A1 and D2A1-m2 tumours. 2 x 10^5 D2A1 or D2A1-m2 cells were injected orthotopically into the 4th mammary fat pad of wild-type BALB/c mice (*n* = 6 mice per group). Mice were culled and tumours removed 35-45 days later. Primary D2A1 and D2A1-m2 tumours were formalin-fixed and paraffin-embedded. FFPE sections were stained with anti-αSMA or anti-CD8 antibodies (Table 2.6), and positive staining quantified in a blinded fashion using QuPath software. Positive staining of viable tissue was assessed in 6, randomly selected, 1 mm^2 fields of view (FOV) per tumour section and the mean value per FOV was calculated for each section. **A.** Representative images. Scale bar, 100 μm. **B.** Quantification of αSMA⁺ staining expressed as the percentage of αSMA⁺ stained area per FOV. **C.** Quantification of CD8⁺ staining expressed as the number of CD8⁺ cells per FOV. Data in **B** and **C** are mean ± SEM. Statistical analysis was performed using an unpaired *t*-test: ** = $P < 0.01$; *** = $P < 0.001$. **D, E, F.** Correlation between CAF content (% αSMA⁺ area) and CTL content (CD8⁺ T cells / mm^2) of primary (**D**) 4T07 and 4T1, (**E**) D2A1 and D2A1-m2, and (**F**) 4T07, 4T1, D2A1 and D2A1-m2 tumours. R^2 values were calculated from the Pearson correlation coefficient: NS = not significant; ** = $P < 0.01$.

higher CAF content, and a lower CTL content, than D2A1 tumours (Figures 3.7B and C). No significant correlation between CAF and CTL infiltration was observed when looking at the 4T07/4T1 and D2A1/D2A1-m2 models separately (Figures 3.7D and E). However, a significant inverse correlation between CAF content and CTL infiltration was observed when data from all models was combined (Figure 3.7F), indicative of a biological relationship between the two cell types.

3.2.5 The D2A1 and D2A1-m2 innate tumour immune microenvironments

To assess differences in the infiltration of immune cells between the D2A1 and D2A1-m2 models, primary tumours were processed to single-cell suspensions and stained with panels of antibodies against a range of immune cell markers (Tables 2.1 and 2.2) and analysed by flow cytometry as with 4T07 and 4T1 tumours in Section 3.2.2. In contrast to 4T07 and 4T1 tumours, D2A1 and D2A1-m2 tumours grew at similar rates *in vivo*, and tumours analysed were of a similar weight (Figure 3.8A). D2A1-m2 tumours contained significantly fewer immune ($CD45^+$) cells than D2A1 tumours, whether assessed by actual counts (Figure 3.8B) or as a proportion of live cells (Figure 3.8C).

As a proportion of immune cells, D2A1-m2 tumours also contained significantly higher levels of immunosuppressive mMDSCs than D2A1 tumours (Figure 3.8D). In contrast, neutrophils made up a bigger proportion of infiltrating immune cells in the D2A1 model (Figure 3.8E). No differences in the proportion of TAMs was observed (Figure 3.8F), however, TAMs were phenotypically different. TAMs in D2A1 tumours exhibited higher expression of PD-L1 (Figure 3.8G) and were also M1-polarised (Figure 3.8H). PD-L1 is upregulated on tumour and stromal cells in response to T-cell activity, primarily through IFNγ, and is another indication of an inflamed tumour immune microenvironment (Binnewies et al., 2018).

3.2.6 The D2A1 and D2A1-m2 adaptive tumour immune microenvironments

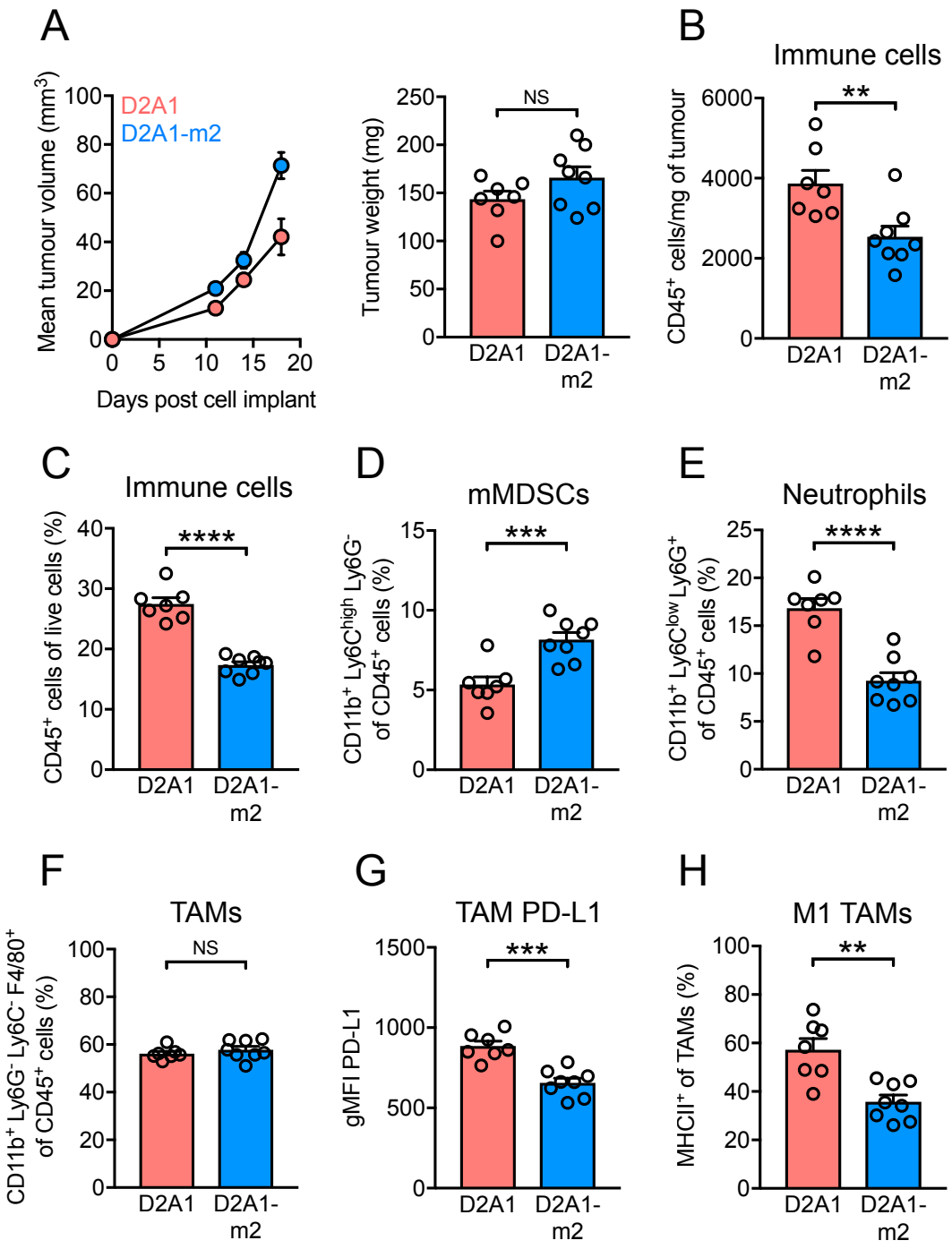

Figure 3.8: Innate immune cell content of primary D2A1 and D2A1-m2 tumours. 2 x 10^5 D2A1 or D2A1-m2 cells were injected orthotopically into the 4th mammary fat pad of wild-type BALB/c mice (D2A1: *n* = 7 mice; D2A1-m2: *n* = 8 mice). All mice were culled and tumours removed 19 days later. Primary tumours were processed to a single cell suspension, stained with panels of antibodies (Tables 2.1 and 2.2) and analysed on a BD LSRFortessa flow cytometer. Gating for identifying live immune cells was performed using FlowJo software. Identification of CD45+ immune cells was performed as in Figure 3.3A. Innate immune cell subsets were identified as illustrated in Figure 3.4. **A**. Mean tumour volume growth curves and weights of tumours used for immune profiling. **B**. Number of CD45+ cells per mg of tumour. **C**. Proportion of CD45+ cells gated on live cells. **D**-**F**. Proportion of (**D**) mMDSCs, (**E**) neutrophils, and (**F**) TAMs gated on CD45+ cells. **G**. Geometric mean fluorescence intensity (gMFI) of PD-L1 expression on TAMs. **H**. Proportion of M1-polarised TAMs. Data in **A**-**H** are mean ± SEM. Statistical analysis was performed using an unpaired *t*-test: NS = not significant; ** = $P < 0.01$; *** = $P < 0.001$; **** = $P < 0.0001$.

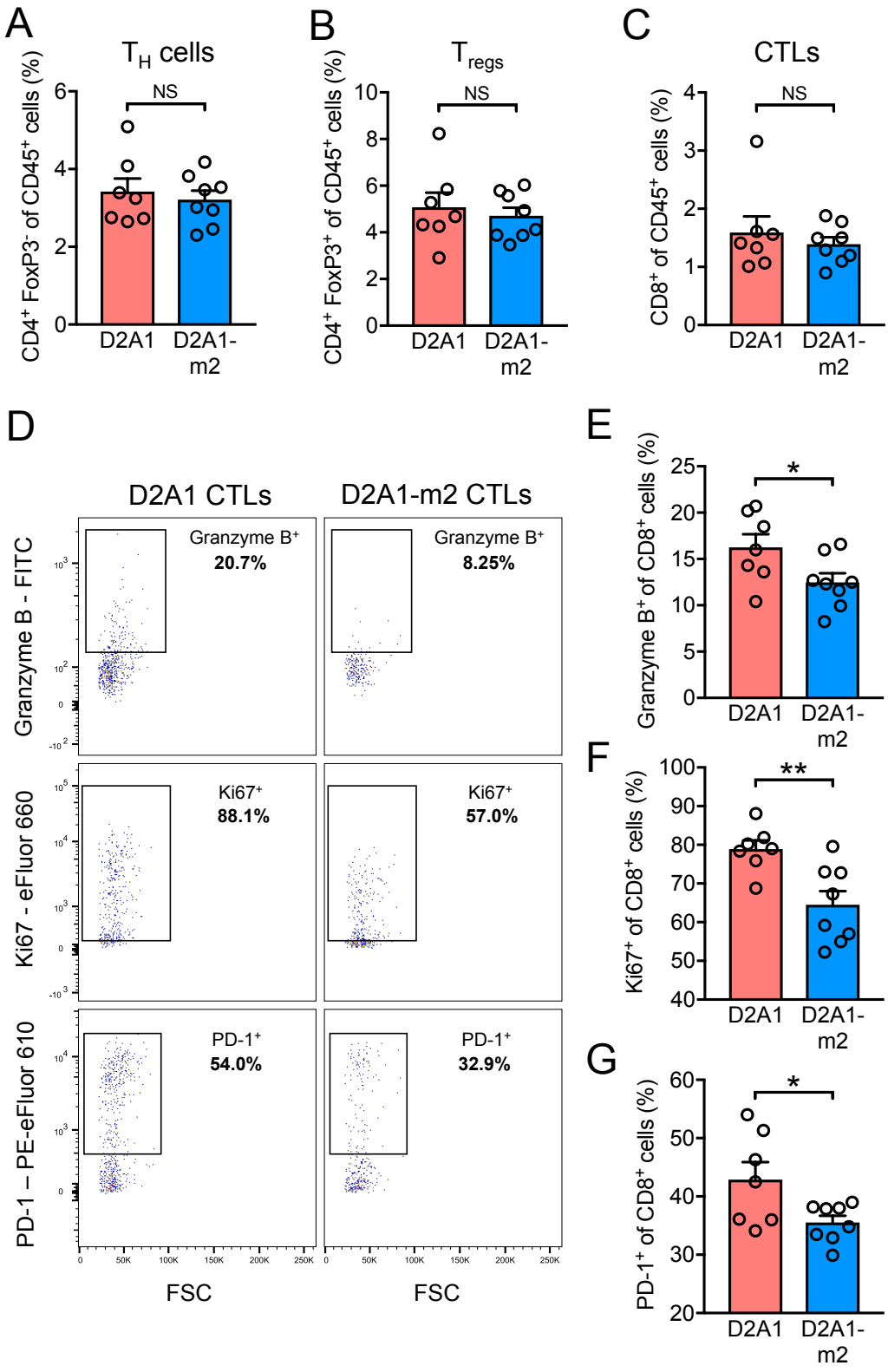

Figure 3.9: Adaptive immune cell content of primary D2A1 and D2A1-m2 tumours. CD45$^+$ cells as in Figure 3.8 were gated for the identification of adaptive immune cell subsets as in Figure 3.6A. **A-C.** Proportion of (**A**) T_H cells, (**B**) T_{regs}, and (**C**) CTLs gated on CD45$^+$ cells. **D**. Representative plot of gating strategy employed for identification of CTLs expressing granzyme B, Ki67, and PD-1. Proportion of (**E**) granzyme B, (**F**) Ki67, and (**G**) PD-1 expressing CTLs in D2A1 and D2A1-m2 tumours. Data in **A-C, E-G** are mean ± SEM. Statistical analysis was performed using an unpaired *t*-test: NS = not significant; * = $P < 0.05$; ** = $P < 0.01$.

Surprisingly, despite the differences in CTL infiltration observed via IHC (Figure 3.7A), no significant differences in infiltration of T_H cells, T_{regs} or CTLs were observed between D2A1 and D2A1-m2 tumours when assessed via flow cytometry (Figures 3.9A-C). However, a significantly higher proportion of D2A1 CTLs expressed the markers granzyme B, Ki67 and PD-1 compared to CTLs in D2A1-m2 tumours (Figures 3.9D-G), indicative of increased CTL activation and proliferation in D2A1 tumours.

3.3 Discussion

Accumulating evidence suggests that adaptive immunity mediated by T cells is essential in generating effective and sustained anti-tumour responses (Salgado et al., 2015). However, the presence of tumour-infiltrating lymphocytes (TILs) in many clinical tumours indicates that they are incapable of fully eradicating tumours and that cancers are able to evade anti-tumour immunity. Clinically approved immune checkpoint inhibitors, that enhance the activity of tumour-specific T cells, can tip the balance in favour of the development of an immunostimulatory milieu. Although these therapies focus on enhancing the anti-tumour capabilities of CTLs, it is important not to overlook the influence of other immune cells that can have pro- or anti-carcinogenic properties. Furthermore, a number of recent studies suggest that CAFs may also be capable of shaping the tumour immune microenvironment (Cohen et al., 2017; Cremasco et al., 2018). In both *in vitro* and *in vivo* studies, evidence overwhelmingly points to an immunosuppressive role for CAFs, generating interest in targeting them in efforts to enhance anti-tumour immune responses evoked by immunotherapy (Chapter 1.4.1).

As discussed in Chapter 1.3.2.4, the immune microenvironment of tumours can generally be divided into two categories based on their cellular and molecular characteristics. Inflamed, or immunologically 'hot' tumours exhibit infiltrating CTLs, broad chemokine profiles and type I interferon signalling, and immune evasion in tumours of this phenotype is driven by the effects of PD-L1, T_{regs} and T cell exhaustion (Gajewski et al., 2013). In contrast, excluded, or immunologically 'cold' tumours are characterised by a lack of CTL infiltration, poor chemokine expression and evidence

suggests these tumours tend to have denser stroma and an abundance of M2 TAMs (Gajewski et al., 2013). Tumours with an inflamed phenotype, that resist immune attack through the inhibitory effects of immune system-suppressive pathways, tend to respond favourably to immune checkpoint inhibitors compared to excluded/cold tumours (Binnewies et al., 2018). Thus, distinct therapeutic strategies are required for maximising the effect of immunotherapy in excluded/cold tumours.

To investigate CAF-immune cell crosstalk in the breast cancer setting, and to determine whether CAFs promote the development of an immunologically 'cold' tumour immune microenvironment, the 4T07/4T1 and D2A1/D2A1-m2 mouse mammary carcinoma models were utilised. Staining of primary tumour sections with an anti-αSMA antibody revealed how 4T1 and D2A1-m2 tumours have higher levels of CAF infiltration/activation than paired 4T07 and D2A1 tumours (Figures 3.1B and 3.7B). Strikingly, the density of CTLs was lower in CAF-rich 4T1 and D2A1-m2 tumours than in 4T07 and D2A1 tumours (Figures 3.1C and 3.7C), suggesting that CAFs contribute to poor CTL infiltration.

To assess the characteristics of the tumour immune microenvironment with greater granularity, tumours were also analysed using flow cytometry. Immune profiling revealed how a major proportion of immune cells within 4T07/4T1 and D2A1/D2A1-m2 tumours were CD11b-expressing myeloid cells, including mMDSCs, neutrophils and TAMs. This suggests that the innate immune system detects a perturbation of tissue homeostasis, possibly a result of damage- or pathogen-associated molecular patterns (DAMP/PAMP) released by necrotic cell death occurring within the tumour core (Gajewski et al., 2013; Nowarski et al., 2013). The composition of myeloid cell subsets in 4T07 and 4T1 tumours was broadly similar, though there were some differences in mMDSC infiltration (Figure 3.5A). Similarly, D2A1 and D2A1-m2 tumours differed in their mMDSC content, but also in their neutrophil content (Figures 3.8D and E). Both mMDSCs and neutrophils have been shown to contribute to resistance to immunotherapy through inhibition of CTL activity, and their abundance is linked to poor prognosis in breast cancer patients (Coffelt et al., 2016; Gonda et al., 2017). However,

in these murine tumour models, levels of mMDSC or neutrophil accumulation were disparate, and did not directly relate to previously observed differences in CTL infiltration assessed via IHC.

Immune profiling also revealed that 4T07 and 4T1 tumours did not differ in terms of their TAM density or polarisation (Figures 3.5C-E). D2A1 and D2A1-m2 tumours also had similar TAM content, but TAMs in D2A1 tumours were polarised towards a proinflammatory M1 phenotype (Figure 3.8H). In addition, TAMs in D2A1 tumours expressed significantly higher levels of PD-L1 than those in D2A1-m2 tumours (Figure 3.8G). As previously mentioned, PD-L1 expression is a hallmark of an inflamed tumour immune microenvironment, and CTL-secreted IFNγ largely drives its upregulation on both tumour and immune cells (Abiko et al., 2015). Furthermore, PD-L1 expression on TAMs is associated with a proinflammatory M1 phenotype that drives anti-tumour immunity (Loke and Allison, 2003).

As discussed, tumours with an inflamed phenotype are characterised by robust CTL infiltration and expression of T cell activity markers such as granzyme B and PD-1 (Binnewies et al., 2018). Flow cytometry analysis demonstrated how, compared to CAF-rich 4T1 tumours, 4T07 tumours were more heavily infiltrated with CTLs (Figure 3.6D). Furthermore, a higher proportion of CTLs in 4T07 tumours expressed granzyme B (Figure 3.6F) and PD-1 (Figure 3.6H). Similarly, compared to CTLs in CAF-rich D2A1-m2 tumours, a higher proportion of those present in D2A1 tumours expressed granzyme B (Figure 3.9E), Ki67 (Figure 3.9F) and PD-1 (Figure 3.9G). Surprisingly, given the differences in CTL infiltration observed between the D2A1 and D2A1-m2 models when assessed via IHC, analysis via flow cytometry revealed no significant differences in CTL abundance (Figure 3.9C). This is likely a result of differences in the size of tumours used for these analyses, but may also reflect differences in the spatial distribution of CTLs in D2A1 and D2A1-m2 tumours, rather than overall abundance.

Together, these findings implicate CAFs in promoting establishment of an immunologically 'cold' or excluded tumour immune microenvironment, and raise questions as to whether CAF modulation may reverse this phenotype. One challenge

in addressing this question is the availability of isolated CAF populations for functional studies. This challenge is addressed in the next chapter of this thesis.

Chapter 4: Isolation and characterisation of cancer-associated fibroblasts

4.1 Introduction

Fibroblasts are mesenchymal cells that synthesise components of the extracellular matrix (ECM) and play an important physiological role in wound healing. In cancer, fibroblasts acquire a modified phenotype and are often the predominant non-haematopoietic stromal cell type in breast carcinomas (Kalluri and Zeisberg, 2006). These cancer-associated fibroblasts (CAFs) are a heterogeneous population of cells, and accumulating evidence suggests they modulate cancer progression. Whilst some studies have postulated a protective, tumour-suppressive role for CAFs (Ozdemir et al., 2014), the vast majority of research points to a tumour-promoting role through stimulating angiogenesis, tumour cell proliferation and metastasis (Cohen et al., 2017). In human breast cancer, the abundance of CAFs (identified based on expression of the commonly used marker, αSMA) is associated with poorer prognosis and predicts disease recurrence (Yamashita et al., 2012). The biology of CAFs is described in greater detail in Chapter 1.4.

Having established in Chapter 3 that murine breast tumours abundant in CAFs have a 'colder' tumour immune microenvironment than related tumours with a paucity of CAFs, this chapter explores efforts to disentangle CAF-immune crosstalk. The functional relationship between CAFs and immune cells remains largely unknown, partly due to issues in identifying and isolating CAFs for functional analysis. Furthermore, CAFs are recognised as a heterogeneous population (Bartoschek et al., 2018; Costa et al., 2018; Cremasco et al., 2018), and the absence of specific markers makes their exact identity unclear and presents difficulties in comparing different studies. Most commonly, markers such as αSMA, fibroblast activation protein (FAP), fibroblast specific protein-1 (FSP1) and platelet-derived growth factor receptor alpha

(PDGFRα), have been utilised either individually, or in combination, to identify, therapeutically target, or isolate, CAF populations.

As demonstrated in Chapter 3, 4T1 tumours are abundant in αSMA^+ cells and thus represent a good source for the isolation and culture of CAFs. However, as described above, isolating CAFs based on their expression of specific markers would likely omit subsets of CAFs that may have influential roles in modulating the immune microenvironment. With this in mind, this chapter describes a CAF isolation technique based on negative selection and the characterisation of resulting CAF populations to determine their role in modulating the tumour immune microenvironment and breast cancer progression.

4.2 Results

4.2.1 Isolation of CAFs from 4T1 tumours

To generate tumours in which host-derived cells could be readily distinguished from tumour cells, Ub-GFP BALB/c mice were used. In these animals, green fluorescent protein (GFP) is under the expression of the human ubiquitin C promoter, resulting in GFP expression in all cells and tissues (Schaefer et al., 2001). When injected orthotopically into the 4^{th} mammary fat pad of Ub-GFP BALB/c mice, 4T1 cells give rise to tumours with equivalent growth kinetics to tumours grown in wild-type BALB/c mice (data not shown, for wild-type BALB/c data see Figure 3.2B).

To confirm that 4T1 tumours grown in Ub-GFP BALB/c mice were abundant in CAFs, formalin-fixed and paraffin-embedded (FFPE) sections of 4T1 tumours from Ub-GFP mice were stained with an anti-αSMA antibody. Furthermore, to assess whether these CAFs were host-derived, as opposed to transdifferentiated tumour cells, sections were also stained with an anti-GFP antibody. Tumours were indeed abundant in αSMA^+ CAFs that were also GFP^+ and therefore host-derived (Figure 4.1A). Detected αSMA^- GFP^+ cells likely represent cells of haematopoietic origin.

To allow fluorescence-activated cell sorting (FACS)-based isolation of CAFs, 4T1 tumours from BALB/c mice were processed to single cell suspensions and

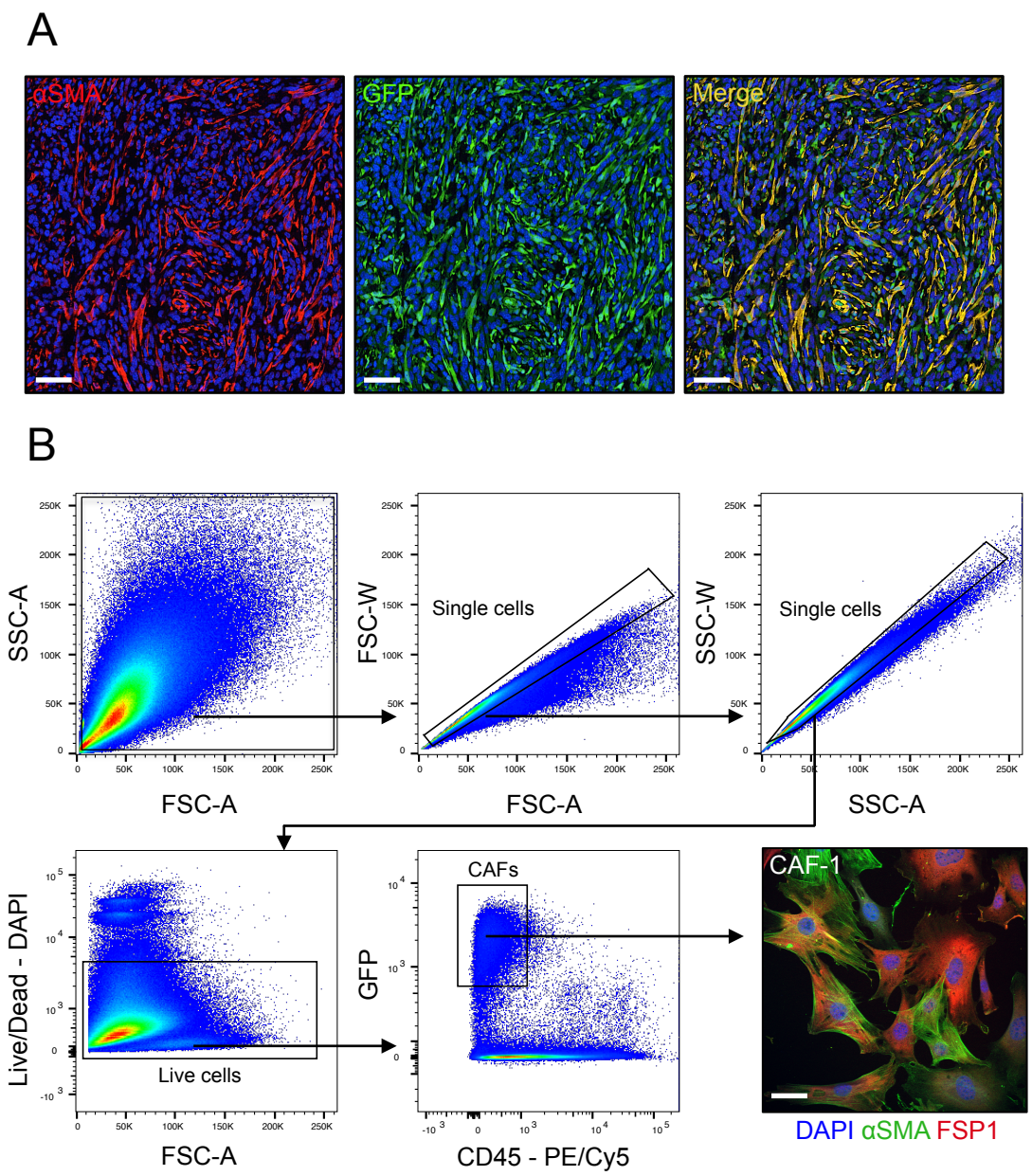

Figure 4.1: Isolation of CAFs from 4T1 tumours. **A**. 5 x 10^4 4T1 cells were injected orthotopically into the 4th mammary fat pad of Ub-GFP BALB/c mice. Mice were culled and tumours removed 17 days later and formalin-fixed and paraffin-embedded. FFPE sections were stained with anti-αSMA and anti-GFP antibodies (Table 2.6), followed by Alexa Fluor 555 (red) and Alexa Fluor 488 (green) secondary antibodies (Table 2.6), respectively. Nuclei were counterstained with DAPI (blue). Representative images are shown. Scale bar, 100 μm. **B**. Representative plots of the gating strategy employed for identification, and isolation, of CAFs. Live cells were identified using the viability dye, DAPI. CAFs were identified as GFP$^+$ CD45$^-$ cells. Isolated CAFs (CAF-1 cells) were cultured and stained with anti-αSMA and anti-FSP-1 antibodies (Table 2.6), followed by staining with Alexa Fluor 488 (green) and Alexa Fluor 555 (red) secondary antibodies (Table 2.6), respectively. Nuclei were counterstained with DAPI (blue). Scale bar, 75 μm.

subjected to Dynabead-based separation to deplete CD24$^+$ epithelial cells and CD45$^+$ immune cells (Chapter 2.2.5.2). Prior to sorting, cell suspensions were stained with a PE/Cy5-conjugated anti-CD45 antibody, permitting superior omission of immune cells

from the final isolation. Tumour cells were excluded from sorting based on their lack of GFP expression, and CAFs were identified as GFP^+ $CD45^-$ cells (Figure 4.1B). Isolated CAFs were immortalised as described in Chapter 2.2.5.3 and are hereafter referred to as CAF-1 cells. Cultured CAF-1 cells displayed an elongated, stellate shaped morphology and exhibited variable expression of αSMA and FSP1 (Figure 4.1B).

To confirm their identity, CAF-1 cells were stained with a panel of antibodies against selected CAF markers and analysed via flow cytometry. D2A1 tumour cells, normal mammary fibroblast (NMF) cells and a second, 4T1 tumour-derived, CAF population (CAF-2) were analysed in parallel. NMF cells were isolated from the normal mouse mammary glands of Ub-GFP BALB/c mice as described in Chapter 2.2.5.1, and CAF-2 cells were independently isolated by the Isacke laboratory from 4T1 tumours using methods analogous to those used for isolating CAF-1 cells (Figure 4.1B). NMF, CAF-1 and CAF-2 cells were immortalised as described in Chapter 2.2.5.3.

As expected, all three fibroblast populations expressed GFP, whilst D2A1 tumour cells did not (Figure 4.2A). All four cell-lines lacked expression of CD45, confirming their non-haematopoietic nature (Figure 4.2B), and had variable expression of αSMA, PDGFRα and CD90 (Figure 4.2C). Though a proportion of D2A1 cells expressed low levels of αSMA, expression was higher in NMF cells, and higher still in both CAF populations (Figure 4.2D). Considering αSMA is a protein involved in fibroblast activation and contraction, it is unsurprising that CAFs, which are known to share phenotypic features with myofibroblasts (Desmouliere et al., 2004), express higher levels of αSMA than NMF cells. That NMF cells express any αSMA is likely a result of their propagation *in vitro* on stiff, plastic tissue culture flasks, as matrix stiffness has been linked to fibroblast activation (Calvo et al., 2013).

PDGFRα has been proposed as a surface marker for isolation of fibroblasts from both mouse and human tissue, and is abundantly expressed by both normal fibroblasts and CAFs (Sharon et al., 2013). Expression of PDGFRα was evident in NMF, CAF-1 and CAF-2 cells at levels higher than those found in D2A1 cells (Figure

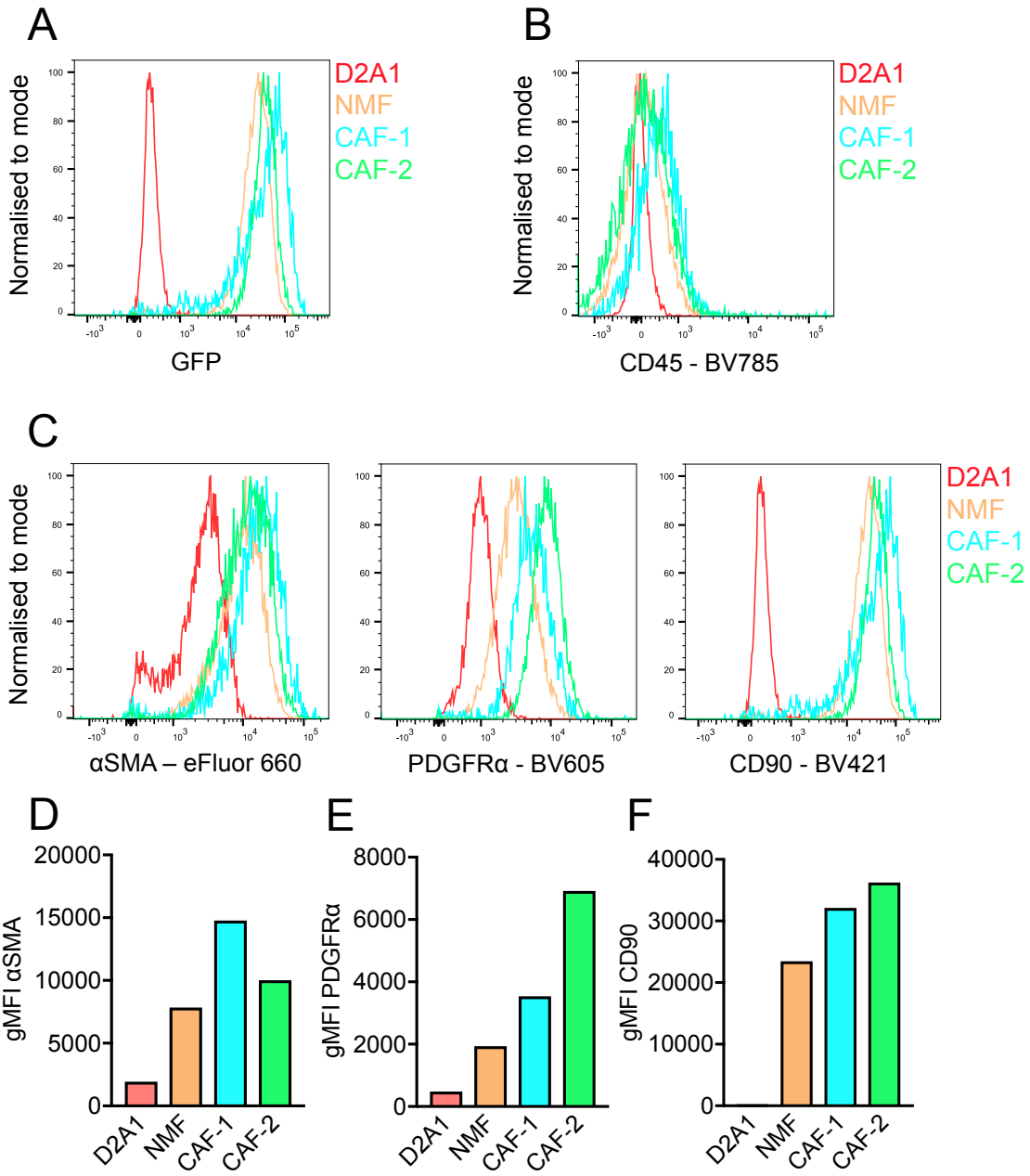

Figure 4.2: Flow cytometry profiling of isolated CAFs. D2A1, NMF, CAF-1 and CAF-2 cells were permeabilised and stained with a BV786-conjugated anti-CD45 antibody, an APC-conjugated anti-αSMA antibody, a BV605-conjugated anti-PDGFRα antibody and a BV421-conjugated anti-CD90 antibody (Table 2.3). **A-C.** Histograms of (**A**) GFP, (**B**) CD45, and (**C**) αSMA, PDGFRα, and CD90 expression in indicated cell populations. **D-F.** Geometric mean fluorescence intensity (gMFI) of (**D**) αSMA, (**E**) PDGFRα, and (**D**) CD90 expression in indicated cell populations as determined by flow cytometry. Values were normalised by subtracting gMFI values for unstained cells from values for stained cells.

4.2E), supporting its use as a surface marker for isolation for at least a proportion of CAFs.

All three fibroblast populations expressed high levels of CD90, whilst D2A1 cells were CD90$^-$ (Figure 4.2F). Although CD90 (also known as Thy-1) is also expressed on

some mouse haematopoietic cells, considering the striking differences in expression between tumour cells and fibroblasts, it may represent a robust marker for fibroblast identification when combined with negative selection for CD45 staining.

In conclusion, CAFs were successfully isolated and immortalised from 4T1 tumours using techniques based on negative selection. Isolated CAFs were GFP^+, $CD45^-$, and exhibited variable expression of the markers αSMA, PDGFRα and CD90, confirming their identity and simultaneously illustrating CAF heterogeneity.

4.2.2 Investigating *in vivo* CAF-mediated immune cell recruitment

The number of studies investigating the role of CAFs in modulating the tumour immune microenvironment has increased considerably in the last decade, particularly in the context of trying to understand their impact on resistance to immune checkpoint blockade. However, few studies have directly assessed the contribution of CAFs to the diversity of the immune microenvironment in the absence of tumour cells.

A Matrigel plug assay, often employed for evaluating angiogenic processes in response to known pro- or anti-angiogenic molecules, was used to directly assess the recruitment of immune cells by fibroblasts (Coltrini et al., 2013). NMF, CAF-1 or CAF-2 cells were re-suspended in a Matrigel:PBS (3:1) solution and injected orthotopically into wild-type BALB/c mice to establish Matrigel plugs. Control plugs containing no cells were also established. After 7 days, plugs were removed, dissociated into single cell suspensions and stained with a panel of antibodies against immune cell markers (Table 2.4). Analysis was performed via flow cytometry, and immune cell subsets were identified as previously described (Chapter 3).

Plugs containing fibroblasts contained more live cells than Matrigel-only control plugs (Figure 4.3A). The majority of cells in all plugs were $CD45^+$ immune cells, and CAF-1 and CAF-2 cells recruited a significantly higher proportion of immune cells than NMF cells (Figure 4.3B). $NKp46^+$ natural killer (NK) cells and $F4/80^+$ tumour-associated macrophages (TAMs) made up a large proportion of immune cells in fibroblast-containing plugs (Figures 4.3C and D). No differences in the proportion of NK cells

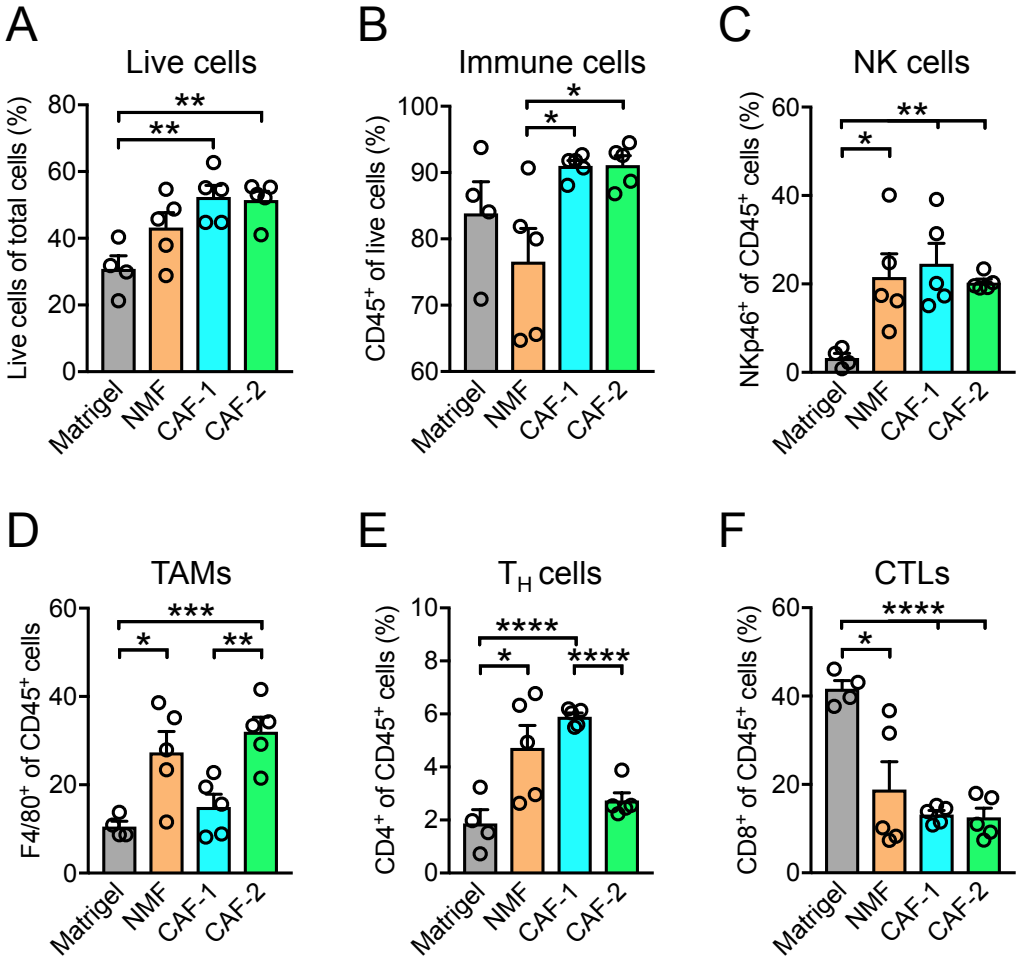

Figure 4.3: Matrigel plug immune cell recruitment. 2 x 10^6 NMF, CAF-1 or CAF-2 cells were resuspended in 100 µL PBS, mixed with 300 µL Matrigel, and 300 µL was injected subcutaneously into the right flank of 6-8-week old female wild-type BALB/c mice to establish Matrigel plugs (*n* = 5 mice per group). Plugs containing no cells were established as a control (*n* = 4 mice). After 7 days, plugs were removed, dissociated into single cell suspensions and stained with a panel of antibodies against immune cell markers (Table 2.4). Immune cell subsets were identified as described previously (Chapter 3). **A.** Proportion of live cells gated on total cells. **B**. Proportion of $CD45^+$ cells gated on live cells. **C**-**F.** Proportion of (**C**) NK cells, (**D**) TAMs, (**E**) T_H cells, and (**F**) CTLs gated on $CD45^+$ cells. All data are mean ± SEM. Statistical analysis was performed using an unpaired *t*-test: * = $P < 0.05$; ** = $P < 0.01$; *** = $P < 0.001$; **** = $P < 0.0001$.

were observed between fibroblast-containing plugs (Figure 4.3C), but a significantly higher proportion of immune cells were TAMs in CAF-2 plugs, compared to CAF-1 plugs (Figure 4.3D).

The recruitment of the major T cell subsets, $CD4^+$ T helper (T_H) cells and $CD8^+$ CTLs was also assessed. All fibroblast-containing plugs recruited higher proportions of T_H cells than plugs containing matrigel alone, though CAF-2 cells recruited significantly fewer than CAF-1 cells (Figure 4.3E). Strikingly, immune cells in Matrigel control plugs

were primarily CTLs, but NMF, CAF-1 and CAF-2 cells recruited a significantly lower proportion of CTLs (Figure 4.3F).

In conclusion, these experiments demonstrate that CAFs can directly contribute to the modulation and composition of the tumour immune microenvironment. Compared to both NMF and CAF-1 cells, CAF-2 cells recruited a higher proportion of macrophages and fewer T cells, perhaps indicative of a particularly immunosuppressive CAF population. The differences in recruitment of CTLs was particularly noteworthy, with both CAF populations dramatically decreasing CTL recruitment compared to control plugs. Whether this exclusion of CTLs is due to a direct interaction with CAFs, or a result of the differences in recruitment of other immune cell subsets, remains to be investigated.

4.2.3 CAFs promote *in vitro* proliferation of tumour cells

CAFs have multiple mechanisms through which they promote tumour growth, one being their ability to promote cancer cell proliferation (Jahangiri et al., 2019). To investigate whether this was true of isolated NMF and CAF populations *in vitro*, a co-culture system was utilised. 4T1 tumour cells labelled with CellTrace Violet were cultured either alone or with NMF or CAF-1 cells as described in Chapter 2.2.2.1 (Figure 4.4A). After 48 hours, 4T1 cells were identified based on their expression of CellTrace Violet, and NMF or CAF-1 cells excluded from analysis based on their expression of GFP (Figure 4.4B). Representative histograms show a decrease in CellTrace Violet fluorescence intensity in 4T1 cells cultured with NMF or CAF-1 cells compared to 4T1 cells cultured alone (Figure 4.4B). Quantification of geometric mean fluorescence intensity (gMFI) confirmed how both NMF and CAF-1 cells, cultured at either 1:1 or 1:2 (4T1:NMF/CAF-1), significantly decreased the gMFI of 4T1 cells, indicative of an increase in cell proliferation (Figure 4.4C). Moreover, CAF-1 cells decreased the gMFI of 4T1 cells to a greater extent than NMF cells, suggesting that CAFs have more pro-proliferative activity (Figure 4.4C).

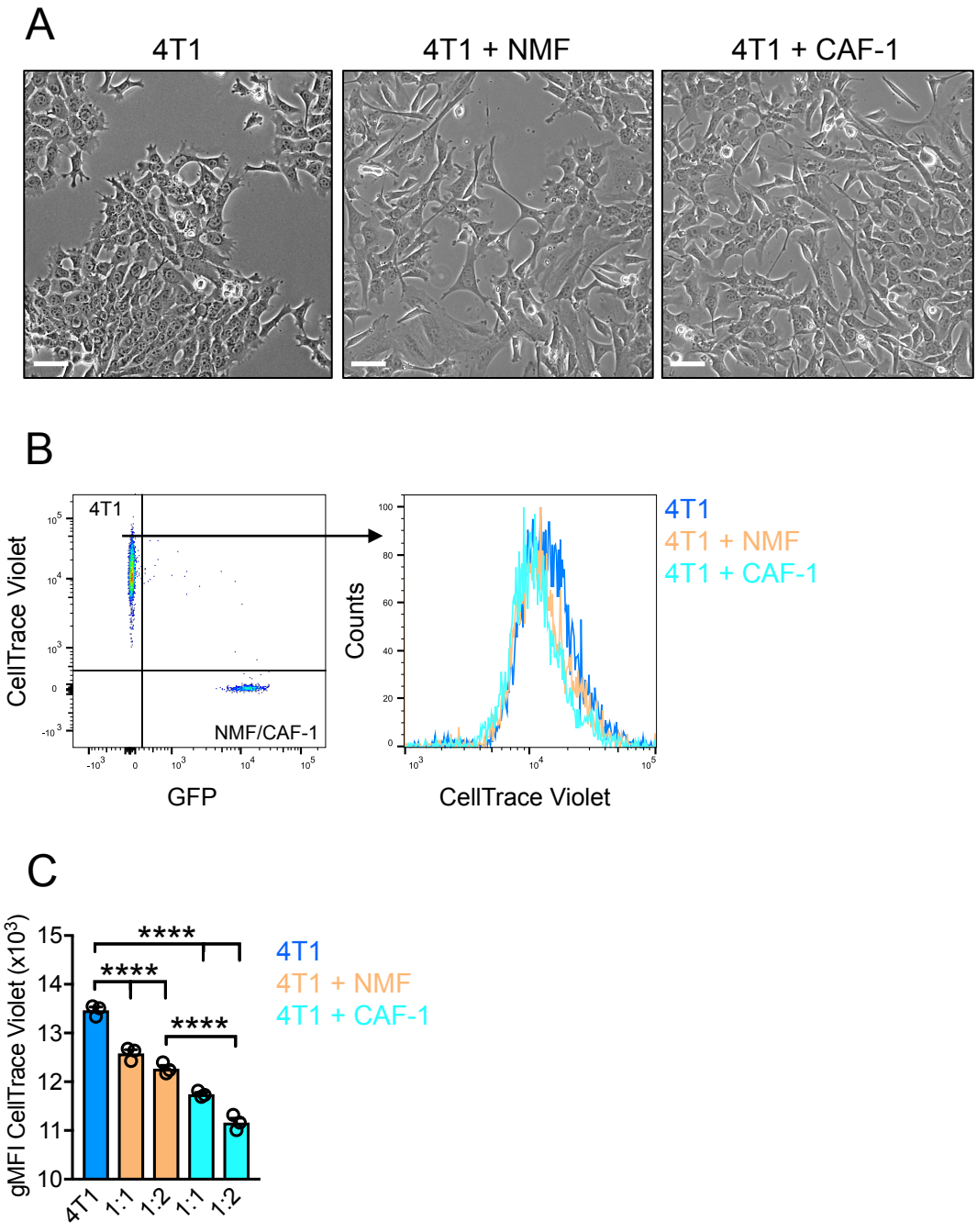

Figure 4.4: CAFs promote *in vitro* tumour cell proliferation. 5 x 10^4 4T1 tumour cells were stained with CellTrace Violet and cultured for 48 hours at 37°C either alone or in the presence of 5 x 10^4 or 1 x 10^5 NMF or CAF-1 cells. CellTrace Violet fluorescence intensity was measure by flow cytometry. **A.** Phase contrast images of co-cultured cells. Scale bar, 200 µm. **B.** Gating strategy for identification of CellTrace Violet$^+$ 4T1 cells and representative histograms of their CellTrace Violet intensity. **C.** Geometric mean fluorescence intensity (gMFI) of 4T1 cells cultured alone or in the presence of NMF or CAF-1 cells, at indicated ratios. Data are mean ± SEM. Statistical analysis was performed with an ordinary one-way ANOVA followed by Dunnett's multiple comparisons test: **** = $P < 0.0001$.

4.2.4 CAFs induce *in vitro* inhibition of T cell proliferation

The tumour immune microenvironment is often rich in soluble factors such as interleukin 10 (IL10) and transforming growth factor beta (TGFβ) that can suppress T cell activity (Oh and Li, 2013; Taga and Tosato, 1992). To directly assess the role of the CAF secretome in inhibiting T cell proliferation, T cells isolated from naïve BALB/c mouse spleens were stained with carboxyfluorescein succinimidyl ester (CFSE) and stimulated through culture in anti-CD3 antibody coated plates supplemented with anti-CD28 antibody and recombinant IL2. Cells were cultured either in normal complete media (NM (+αCD3)) or conditioned media from CAF-1 cells (CAF-1 CM). Some cells were also cultured in normal complete media without anti-CD3 stimulation (NM (-αCD3)). Following 4 days in culture, cells were stained with fluorescently conjugated antibodies against CD45, CD4 and CD8, and T_H cells ($CD4^+$) and CTLs ($CD8^+$) were identified via flow cytometry. Gates were used to identify the percentage of T_H cells and CTLs with diminished CFSE signal intensity, indicative of cell proliferation (Figures 4.5A and B). Culture of T_H cells or CTLs in CAF-1 CM significantly inhibited their proliferation compared to those cultured in NM (+αCD3), directly implicating the CAF secretome in suppression of T cell proliferation (Figures 4.5C and D).

4.2.5 CAFs modulate the tumour immune microenvironment

Following demonstration that CAF-1 cells promote tumour cell proliferation and induce T cell inhibition *in vitro,* experiments were performed to assess whether they could promote the growth of tumours *in vivo*. As discussed in Chapter 1.4, CAFs are noted for their ability to promote tumour growth via multiple distinct mechanisms. To determine whether CAF-1 cells alter tumour growth kinetics, they were co-injected into wild-type BALB/c mice together with 4T07 or D2A1 cells at a ratio of 1:3 (4T07/D2A1:CAF-1). Both 4T07 and D2A1 tumours ordinarily contain a paucity of CAFs (Chapter 3), making them good models to study the response to exogenously added CAFs. Strikingly, co-injection of CAF-1 cells significantly increased the growth of

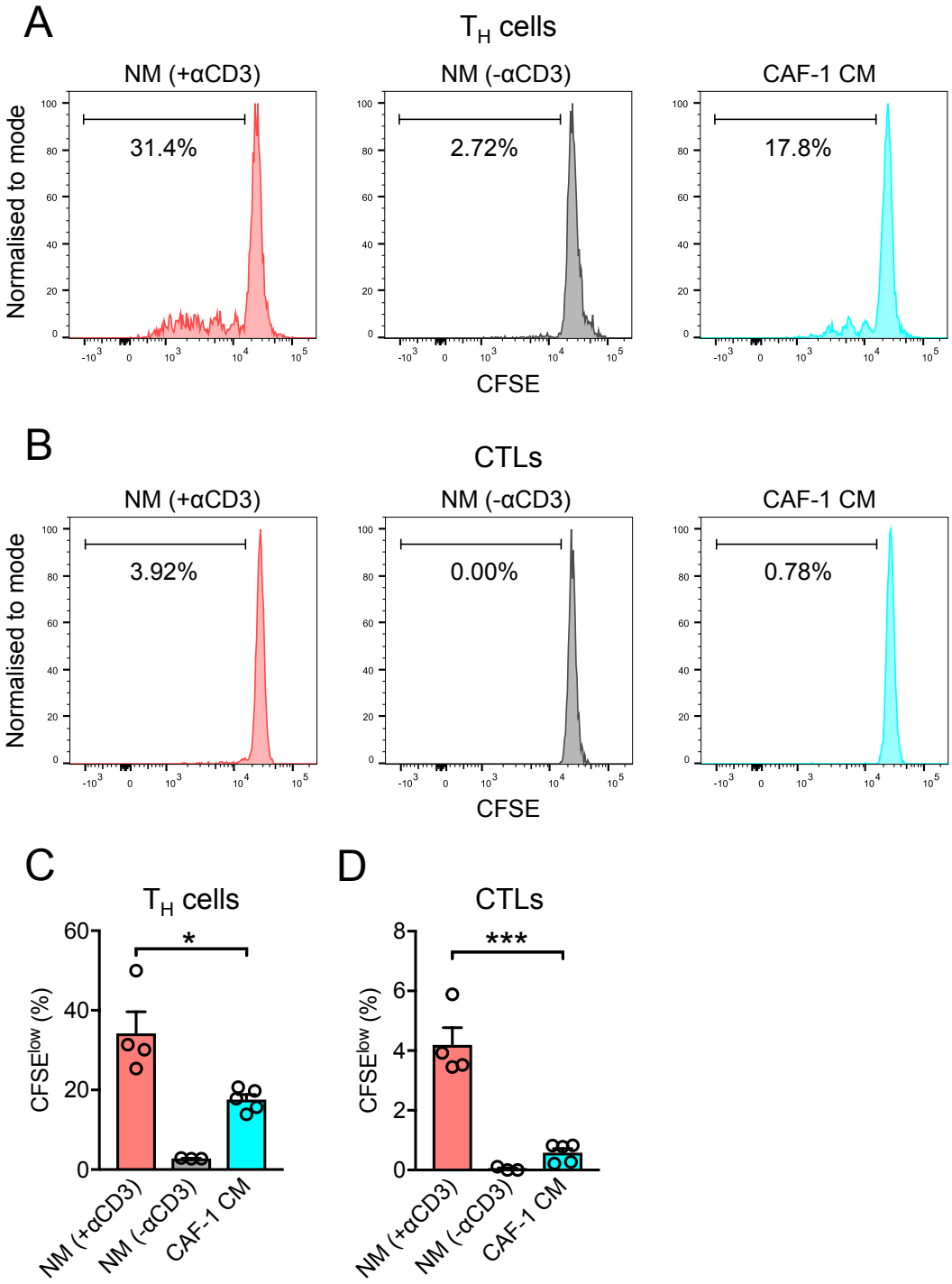

Figure 4.5: CAF-1 conditioned medium inhibits *in vitro* T cell proliferation. T cells isolated from the spleens of naïve 6-8 week female wild-type BALB/c mice using an EasySep mouse T cell isolation kit were labelled with 1 mM CFSE and cultured in normal complete medium with 5 µg/mL anti-CD28 antibody and 10 ng/mL IL2 in standard (NM (-αCD3)), or anti-CD3 coated (NM (+αCD3)), 96-well plates. Isolated T cells were also cultured in CAF-1 conditioned media (Chapter 2.2.1.4) with 5 µg/mL anti-CD28 antibody and 10 ng/mL IL2, in anti-CD3 coated 96-well plates (CAF-1 CM). After 4 days, cells were stained with DAPI and fluorescently conjugated anti-CD45, anti-CD4 and anti-CD8 antibodies (Table 2.5). CFSE signal in $CD4^+$ (T_H) and $CD8^+$ cells (CTLs) was assessed using flow cytometry. **A**-**B.** Representative histograms of CFSE signal in (**A**) $CD4^+$ (T_H cells) and (**B**) $CD8^+$ (CTLs). Gates identifying the percentage of cells with diminished CFSE signal intensity ($CFSE^{low}$) are shown. **C**-**D.** Mean percentage of $CFSE^{low}$ (**C**) $CD4^+$ (T_H cells) and (**D**) $CD8^+$ (CTLs). Statistical analysis was performed using an unpaired *t*-test: * = $P < 0.05$; *** = $P < 0.001$.

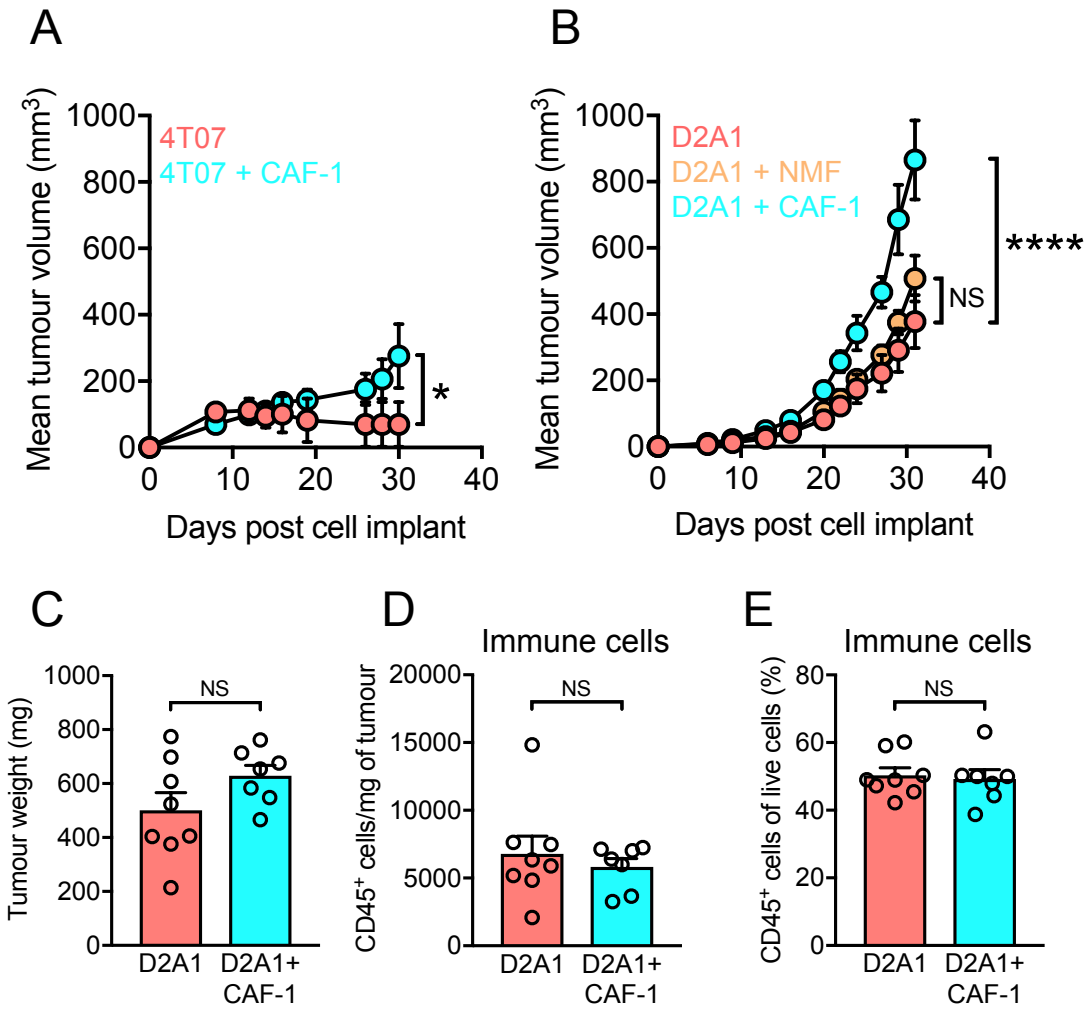

Figure 4.6: CAFs promote *in vivo* tumour growth. **A-B.** (**A**) 5 x 10^5 4T07 cells with or without 5 x 10^5 CAF-1 cells, and (**B**) 2 x 10^5 D2A1 cells with our without 6 x 10^5 NMF or CAF-1 cells were injected into the 4th mammary fat pad of wild-type BALB/c mice (*n* = 6-8 mice per group). Tumour growth was monitored by caliper measurements. Data in **A-B** are the mean tumour volume ± SEM. Statistical analysis was performed with a two-way ANOVA: * = $P < 0.05$; **** = $P < 0.0001$. **C-E.** 2 x 10^5 D2A1 cells with our without 6 x 10^5 CAF-1 cells were injected into the 4th mammary fat pad of wild-type BALB/c mice (*n* = 7-8 mice per group). All mice were culled and tumours removed 27 days later. Primary tumours were processed to a single cell suspension, stained with panels of antibodies (Tables 2.1 and 2.2), and analysed on a BD LSRFortessa flow cytometer. Gating for identifying immune cells was performed using FlowJo software as described in Chapter 3. (**C**) Weights of tumours used for immune profiling. (**D**) Number of CD45$^+$ cells per mg of tumour. (**E**) Proportion of CD45$^+$ cells gated on live cells. Data in **C-E** are mean ± SEM. Statistical analysis was performed using an unpaired *t*-test: NS = not significant.

both 4T07 and D2A1 tumours (Figures 4.6A and B). NMF cells had no effect on D2A1 tumour growth (Figure 4.6B).

Having previously demonstrated that both the 4T07 and D2A1 models have an inflamed phenotype, and how growth of 4T07 tumours is under considerable immune control (Chapter 3), it is tempting to speculate that co-injection with CAF-1 cells

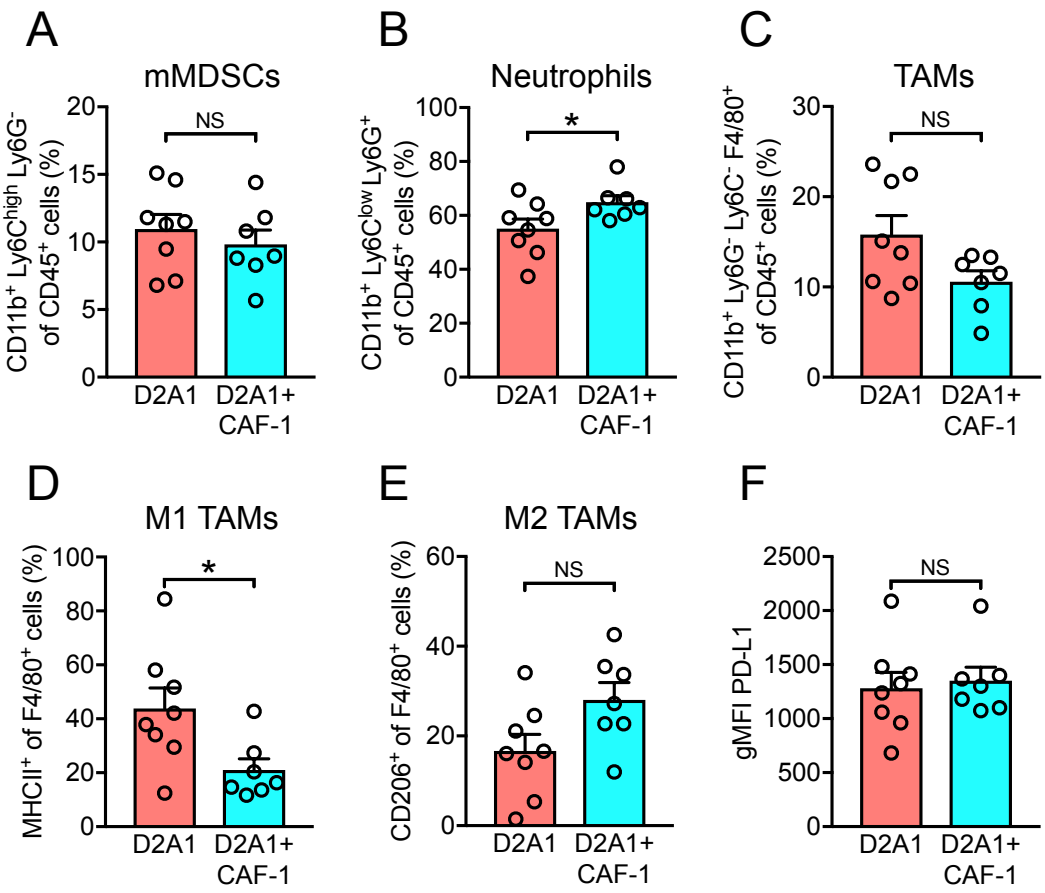

Figure 4.7: Innate immune cell content of primary D2A1 and D2A1 + CAF-1 tumours. **A**-**E.** CD45+ cells as in Figure 4.6 were gated for the identification of innate immune cell subsets as described in Chapter 3. The proportion of (**A**) mMDSCs, (**B**) neutrophils, (**C**) TAMs, (**D**) M1 TAMs, and (**E**) M2 TAMs gated on indicated cell populations is shown. **F.** Geometric mean fluorescence intensity (gMFI) of TAM PD-L1 expression. All data are mean ± SEM. Statistical analysis was performed using an unpaired *t*-test: NS = not significant; * = $P < 0.05$.

promotes the growth of 4T07 and D2A1 cells at least in part through the immunosuppressive effect of CAFs. To determine whether CAF-1 cells alter the immune microenvironment of D2A1 tumours, a co-injection experiment analogous to the one described above was employed. Resultant tumours were removed 27 days post implant when they were of a similar weight (Figure 4.6C), before being processed to single-cell suspensions and stained with a panel of antibodies against a range of immune cell markers (Tables 2.1 and 2.2). Analysis by flow cytometry revealed no differences in the total infiltration of immune cells, whether assessed by actual counts (Figure 4.6D) or as a proportion of live cells (Figure 4.6E).

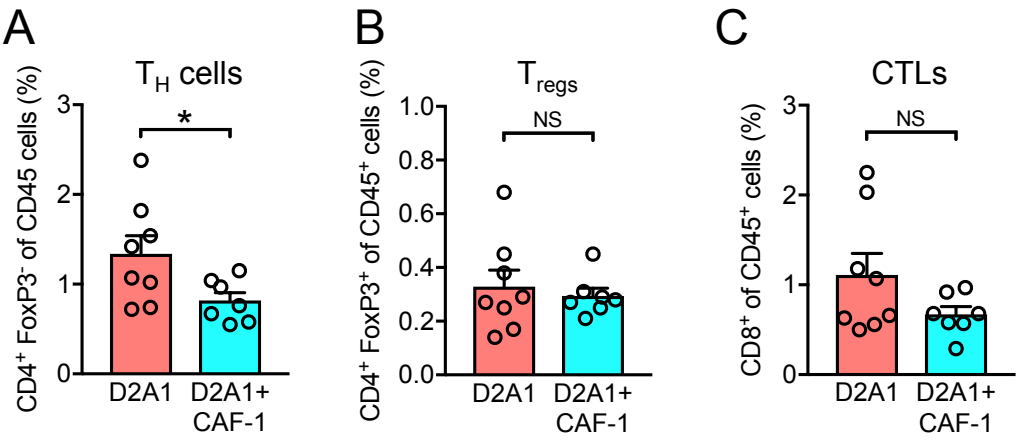

Figure 4.8: Adaptive immune cell content of primary D2A1 and D2A1 + CAF-1 tumours. **A**-**C.** $CD45^+$ cells as in Figure 4.6 were gated for the identification of adaptive immune cell subsets as described in Chapter 3. The proportion of (**A**) T_H cells, (**B**) T_{regs}, and (**C**) CTLs gated on $CD45^+$ cells is shown. All data are mean ± SEM. Statistical analysis was performed using an unpaired *t*-test: NS = not significant; * = $P < 0.05$.

To identify major immune cell subsets, gating strategies analogous to those illustrated in Chapter 3 were used. No differences in infiltration of monocytic myeloid-derived suppressor cells (mMDSCs) were observed (Figure 4.7A). However, neutrophils, an immune cell subset associated with poor prognosis in the clinic (Soto-Perez-de-Celis et al., 2017), were enriched in D2A1 tumours co-injected with CAF-1 cells (Figure 4.7B). Though the infiltration of TAMs in both models was similar (Figure 4.7C), D2A1 + CAF-1 tumours exhibited a significant reduction in infiltration of TAMs with a pro-inflammatory, M1 phenotype (Figure 4.7D). No differences in the infiltration of M2 TAMs, or TAM expression of programmed death-ligand 1 (PD-L1) expression were observed (Figures 4.7E and F).

Tumours were also analysed for the infiltration of T cell subsets. D2A1 tumours co-injected with CAF-1 cells exhibited a significant decrease in T_H cells (Figure 4.8A), which orchestrate a range of effector activities during the adaptive tumour immune response (Knutson and Disis, 2005). No differences in the infiltration of regulatory T cells (T_{regs}) or CTLs were observed (Figures 4.8B and C).

Together, these findings suggest that CAF-1 cells promote the growth of mouse mammary carcinomas with an inflamed phenotype at least in part through modulating the tumour immune microenvironment. In the D2A1 model, co-injection of CAF-1 cells

promoted the accumulation of neutrophils and a decrease in the abundance of pro-inflammatory M1 TAMs and T_H cells.

4.3 Discussion

Emerging evidence indicates a potentially key role for CAFs in altering the composition and polarisation of the tumour immune microenvironment. CAFs, isolated using an anti-PDGFRα antibody, have been shown to express a pro-tumourigenic inflammatory signature, driving the recruitment of TAMs in addition to promoting both neovascularisation and *in vivo* tumour growth (Erez et al., 2010). Likewise, genetic ablation of FAP^+ fibroblasts in lung and pancreatic tumours induced immunological control of tumours via an IFNγ-dependent mechanism (Kraman et al., 2010). Furthermore, in a 4T1 model, ablation of FAP^+ cells using a DNA vaccine has been shown to polarise the immune microenvironment to a pro-inflammatory phenotype (Liao et al., 2009). These, and other similar studies, have contributed to revealing an immunosuppressive role for CAFs, however they only characterise the immunomodulatory effect of CAFs expressing one specific marker and may not be representative of the diversity of CAF populations within tumours.

Recently, the identification of different human and murine CAF subsets using a combination of putative CAF markers has provided an insight into the marked diversity in their biological functions (Kalluri, 2016). Utilising a negative selection strategy similar to the one used in this study, single-cell RNA sequencing of mesenchymal cells from a genetically engineered mouse model of breast cancer identified three distinct subpopulations of CAFs (Bartoschek et al., 2018). Validation experiments, both in mouse models and in human tissue, revealed separation of the subpopulations attributable to different origins including the perivascular niche, resident mammary fat pad and the transformed epithelium. These subtypes had distinct functional programs and held independent prognostic capabilities. Similar work has identified CAF subsets that accumulate differentially in human triple-negative breast cancer (TNBC). Using a panel of antibodies against several fibroblast markers, four CAF subsets were

identified, with one subset promoting immunosuppression by promoting the accumulation and retention of regulatory T cells (Costa et al., 2018). In principle, developing specific CAF-targeted anticancer therapies is an attractive proposition. However, in the context of immunotherapy, determining the general mechanisms through which CAFs, particularly specific CAF subsets, contribute to immunosuppression remains a priority. Key to any successes will be developing appropriate mouse models that allow hypothesis-driven research.

In these experiments, CAFs were isolated from the 4T1 mouse mammary carcinoma model using a negative selection strategy outlined in Figure 4.1B. Difficulties arose due to the need to isolate fibroblast populations with very high purity - any contaminating tumour cells quickly overwhelmed CAF populations when placed in culture. This was particularly true of efforts to isolate CAFs from 4T07 tumours, likely a result of the paucity of CAFs in this model and the more mesenchymal nature of these tumour cells (Drasin et al., 2011), making purification techniques less effective.

The purity of sorted cells was verified by expression of commonly used fibroblast markers and by lack of expression of immune cell markers (Figure 4.2). Whilst it is well established that CAF-released chemokines can enhance the proliferative, migratory and invasive properties of CAFs through cross-talk with tumour cells (Mishra et al., 2011), the type of immune cells recruited by CAF-derived mediators is less clear. To untangle the immunomodulatory role of CAFs from that of the tumour cells with which they ordinarily reside, normal mammary fibroblasts (NMF) and CAFs (CAF-1/CAF-2) were implanted in Matrigel plugs. Flow cytometry analysis, utilising only a relatively basic panel of immune cell marker antibodies, revealed significant diversity in immune cell recruitment (Figure 4.3), perhaps reflective of the contribution of different CAF subsets within isolated populations. TAMs and NK cells represented a major proportion of Matrigel plug infiltrating cells, but a key finding was the significant reduction in recruitment of CTLs in plugs containing CAFs, compared to those containing Matrigel alone (Figure 4.3F). Whether this is a result of suppression of CTL proliferation within plugs, or due to direct exclusion of CTLs remains to be investigated.

Importantly, these results demonstrate that CAFs are not only critical to the recruitment of immune cells, but that they can also mediate these effects in the absence of tumour cells.

Having established *in vitro* that isolated CAF-1 cells promoted the proliferation of cancer cells (Figure 4.4), and how CAF-1 secreted factors could inhibit T cell proliferation (Figure 4.5), a well-established co-injection assay was adopted allowing the effects of CAFs on tumour growth in a syngeneic host to be assessed. CAF-1 cells promoted the growth of ordinarily immunogenic 4T07 and D2A1 tumours (Figures 4.6A and B), suggesting that CAF-induced immunosuppression may play a role in driving tumour growth. To determine the veracity of this hypothesis, similar co-injection assays were established for immune profiling experiments. Though the immune profiles of D2A1 tumours and those co-injected with CAF-1 cells were fairly similar, differences in some key immune cell subsets were revealed. CAF-1 cells drove increased accumulation of neutrophils in D2A1 tumours (Figure 4.7B). Neutrophils were long considered inert bystanders in the cancer setting, but are increasingly considered to promote tumour growth by inducing angiogenesis or through specific cytokine release, facilitating a tumour promoting, immunosuppressive tumour microenvironment (Coffelt et al., 2016). Furthermore, CAF-1 cells decreased infiltration of pro-inflammatory TAMs and $CD4^+$ T_H cells into D2A1 tumours (Figures 4.7D and 4.8A). This decrease in $CD4^+$ T_H cells is particularly noteworthy, as these cells are critical in coordinating tumour-reactive adaptive immune responses that are a feature of drugs targeting immunological checkpoints (Wei et al., 2018).

In conclusion, these experiments provide direct evidence for the immunomodulatory role of CAFs in breast cancer. Whether these effects contribute to the resistance to immunotherapy observed in the majority of breast cancer patients will be addressed in following chapters. Though it was tempting to propose utilising the co-injection assays described in this chapter to address these questions, it was anticipated that the variation inherent to these assays would have made assessing any therapeutic intervention difficult. Furthermore, other experiments performed during this

research project have provided evidence to suggest that although co-injected CAFs are observed early on in tumour development, they are not readily detected in larger tumours (data not shown). Thus, this would make it difficult to draw conclusions regarding their role in response to therapy. As a consequence, it was judged that the established 4T07/4T1 and D2A1/D2A1-m2 models characterised in Chapter 3 likely represent better models for assessing the role of CAFs in insensitivity to immunotherapy.

Chapter 5: Response of the 4T07/4T1 and D2A1/D2A1-m2 models to immune checkpoint blockade

5.1 Introduction

In order to develop into clinically detectable masses, it is now appreciated that cancers must successfully escape immune control. Though cancers can evade the immune system through numerous mechanisms, by far the most understood to date is their ability to co-opt immune-checkpoint pathways. Physiologically, immune checkpoints are important in controlling the magnitude of immune responses and maintaining self-tolerance, primarily by dampening the activation or function of T cells (Pardoll, 2012). However, cancers can exploit these same mechanisms, driving immune resistance and promoting tumour progression.

As discussed in Chapter 1.3.2.3, T cells, which can directly recognise and kill antigen-expressing cells and coordinate diverse immune responses, have been the focus of efforts to therapeutically magnify a patient's endogenous anti-tumour immune response and promote immunological control of cancer. The checkpoints controlling T cell activity are initiated by ligand-receptor interactions, and are therefore amenable to being targeted by agnostic or antagonistic antibodies. This approach has resulted in impressive response rates in small subsets of cancer patients, particularly using antibodies to block the inhibitory receptors cytotoxic T-lymphocyte associated antigen 4 (CTLA-4) and programmed cell death protein 1 (PD-1) or its ligand PD-L1 (Wei et al., 2018). However, breast cancer remains largely refractory to these forms of immune checkpoint blockade (ICB) (Vonderheide et al., 2017a).

It has been suggested that the lack of response to ICB in breast cancer is a result of its relatively low-mutational load, thus limiting the acquisition of neoantigens and rendering tumours somewhat non-immunogenic, particularly when compared to melanoma and lung cancer (Miller et al., 2016). Nevertheless, numerous studies have

demonstrated that the presence of tumour infiltrating cytotoxic T lymphocytes (CTLs) in breast cancer, particularly in triple-negative breast cancer (TNBC), can predict clinical outcome (Gruosso et al., 2019; Salgado et al., 2015; Savas et al., 2016). Furthermore, the anti-PD-L1 antibody, atezolizumab, has recently been approved for use in combination with nab-paclitaxel in patients with PD-L1-positive, metastatic triple-negative, based on data from the Phase III Impassion130 trial (Schmid et al., 2018). Though this represents major progress in harnessing the power of immunotherapy in treating breast cancer, a number of patients still responded poorly. Similar studies are also yet to be performed in patients with other sub-types of breast cancer that lack the infiltration of CTLs seen in TNBC and are likely less susceptible to immunotherapeutic intervention.

Increasingly, evidence suggests that the tumour stroma in breast cancer, particularly cancer-associated fibroblasts (CAFs), plays a key role in modulating responses to immunotherapy (Binnewies et al., 2018). Having described the immunomodulatory capabilities of CAFs and demonstrated that CAF-rich mouse mammary carcinoma models exhibit more of an immunologically 'cold' tumour microenvironment than those with a paucity of CAFs, the aim of this chapter was to determine the responses of these models to ICB. As discussed in Chapter 1.3.2.3, combination therapy with the anti-PD-1 antibody, nivolumab, plus the anti-CTLA-4 antibody, ipilimumab, is more efficacious in advanced melanoma than ipilimumab alone (Larkin et al., 2019). Thus, this chapter also explored the efficacy of combination ICB treatment in the 4T1, D2A1 and D2A1-m2 models.

5.2 Results

5.2.1 Response of the 4T07 and 4T1 models to ICB

As previously described, CAF-rich 4T1 tumours are more immunologically 'cold' than 4T07 tumours, exhibiting significantly lower levels of CTL infiltration and lower expression of CTL activation markers including granzyme B and PD-1 (Chapter 3.2.3). These immune profiling experiments were performed using relatively small tumours

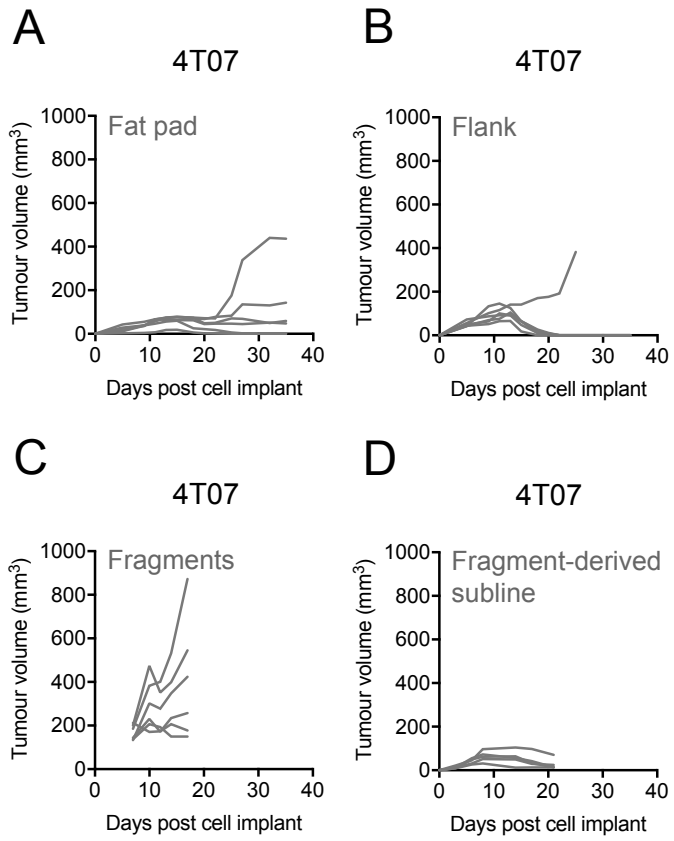

Figure 5.1: Growth kinetics of primary 4T07 tumours. A-B. 5 x 10^5 4T07 cells were injected into the (**A**) 4th mammary fat pad or (**B**) flank of 6-8 week old female wild-type BALB/c mice (*n* = 6 mice per group). **C.** Tumour fragments freshly resected from 4T07 tumour-bearing NSG mice in Figure 3.2A were implanted into the flank of wild-type 6-8 week old female BALB/c mice (*n* = 6 mice). **D.** 5 x 10^5 4T07 cells isolated from tumours in Figure 5.1C were injected into the 4th mammary fat pad of wild-type 6-8 week old female BALB/c mice (*n* = 6 mice). Tumour growth was monitored by caliper measurements. Shown are the tumour growth curves for individual mice.

(~200 mm^3) resected from mice soon after cell implantation. However, in order to assess the response of these models to ICB treatment, it was important to first determine their long-term growth kinetics without treatment. This was particularly necessary for 4T07 tumours, which in contrast to 4T1 tumours grew poorly and eventually regressed when implanted into syngeneic BALB/c mice (Chapter 3.2.1), making it difficult to evaluate any anti-tumour effects of treatment.

It is well established that the site of tumour cell implantation affects the metastatic profile and, importantly, the growth kinetics of resultant tumours in mouse models of cancer (Du et al., 2014; Zhang et al., 2018). Thus, 4T07 cells were injected orthotopically into the 4th mammary fat pad, or subcutaneously into the flank of

syngeneic BALB/c mice. As before, 4T07 tumours grew poorly when cells were injected either into the fat pad (Figure 5.1A) or subcutaneously into the flank (Figure 5.1B). Although in both models some individual tumours did grow well, the highly variable growth kinetics observed would not facilitate proper evaluation of treatment efficacy.

Recently, preclinical tumour models have been described where fragments of tumours from genetically engineered models, such as KrasG12D; Trp53R172H; Pdx-1C (KPC) mice, were implanted into syngeneic mice and developed into tumours with consistent growth rates (Majumder et al., 2016). To determine whether implanting tumour fragments improved the growth of 4T07 tumours, freshly resected tumour pieces from established 4T07 tumours grown in immunodeficient NSG mice (Figure 3.2A) were implanted into the flank of immunocompetent BALB/c mice as described in Chapter 2.2.3.3. The implanted fragments developed into tumours with improved growth kinetics compared to models where cells alone were implanted (Figure 5.1C). However, although the implanted fragments were of a similar size, the growth rates of resultant tumours were again highly variable. A tumour cell subline derived from established 4T07 tumours in Figure 5.1C was subsequently injected into naïve BALB/c mice as described in Chapter 2.2.3.3, but regressed (Figure 5.1D), suggesting that the tumour-associated stroma in implanted fragments was essential in promoting 4T07 tumour growth, perhaps by protecting the tumour from immune destruction.

The variable growth kinetics of 4T07 tumours meant that the susceptibility of this model to ICB could not be determined. However, the 4T1 model is a better-established preclinical model of breast cancer and grows reproducibly in BALB/c mice (Figure 3.2B). To determine the response of the 4T1 model to ICB, 4T1 cells were injected orthotopically into the 4th mammary fat pad of syngeneic BALB/c mice and treated with an anti-CTLA-4 antibody (10 mg/kg, IP), an anti-PD-L1 antibody (10 mg/kg, IP) or a combination of both (hereafter referred to as COMBO), as described in Chapter 2.2.3.5 and illustrated in Figure 5.2A. Of note, the anti-PD-L1 antibody used was an IgG1 antibody harbouring a D265A mutation known to attenuate Fc effector

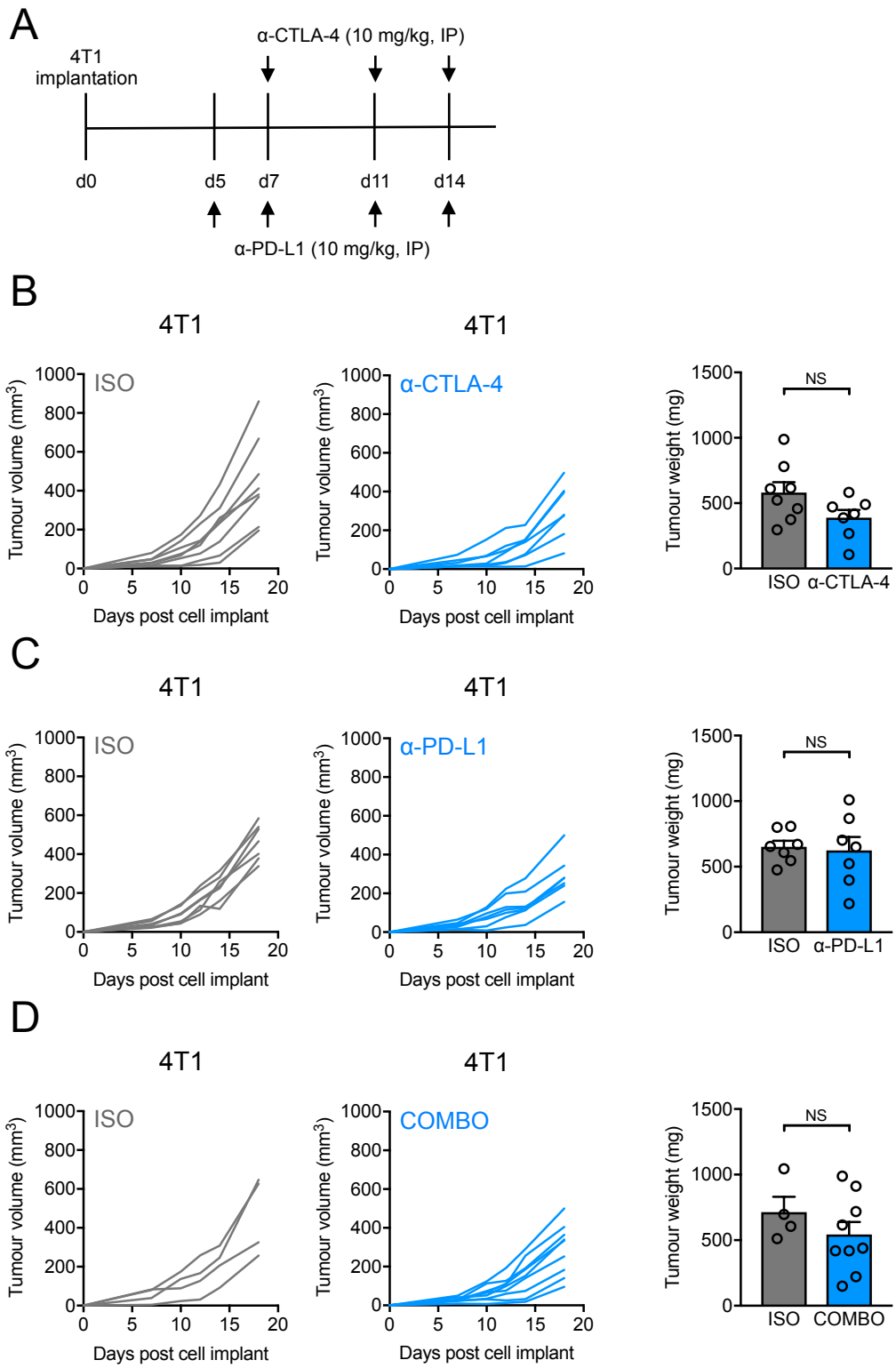

Figure 5.2: The anti-tumour activity of immune checkpoint blockade treatment in the 4T1 tumour model. 5 x 10^4 4T1 cells were implanted into the 4th mammary fat pad of 6-8 week old female wild-type BALB/c mice. Mice were treated with an anti-CTLA-4 antibody (10 mg/kg, IP), an anti-PD-L1 antibody (10 mg/kg, IP) or a combination of both (COMBO). Control mice received relevant isotype control antibodies (ISO). *n* = 4-9 mice per group. Tumour growth was monitored by caliper measurements and tumour growth curves are shown for individual mice. Tumour weight was measured post-mortem on day 18. **A.** Dosing regimen for immune checkpoint blockade treatment. **B**-**D.** Individual tumour growth curves and tumour weights for 4T1 tumour-bearing mice treated with (**B**) anti-CTLA-4, (**C**) anti-PD-L1 or (**D**) a combination of both. Data are mean ± SEM. Statistical analysis was performed using an unpaired *t*-test: NS = not significant.

function (Chen et al., 2019b). This mutation is present in the clinically approved anti-PD-L1 antibody, durvalumab (AstraZeneca), and functions to limit the depletion of PD-L1$^+$ CTLs and antigen-presenting cells (APCs) that are critical to anti-tumour immunity. Control mice received isotype control antibodies listed in Table 2.7 (hereafter referred to as ISO) that lack specific target binding, either alone or in combination. Mice were randomised between treatment groups by tumour volume on the first day of treatment. ICB treatment, either as single agents or in combination had a little effect on 4T1 tumour growth, with no mice completely responding to treatment (Figures 5.2 B-D). ICB treatment also had no significant effect on final tumour weight (Figures 5.2 B-D), confirming the insensitivity of the 4T1 model to ICB therapy.

In conclusion, whilst the immunogenic nature of the 4T07 model made it difficult to assess its response to ICB, these experiments confirmed that the CAF-high, immunologically 'cold' 4T1 model is insensitive to anti-CTLA-4 and anti-PD-L1 treatment, given either alone or in combination.

5.2.2 Response of the D2A1 and D2A1-m2 models to ICB

D2A1 tumours, much like 4T07 tumours, have low numbers of CAFs within their tumour microenvironment (Figures 3.7A and B). Furthermore, D2A1 tumours exhibit a more inflamed immune microenvironment than CAF-rich D2A1-m2 tumours, marked by increased immune cell infiltration (Figures 3.8B and C) and an increased expression of the activity markers granzyme B, Ki67 and PD-1 on infiltrating CTLs (Figures 3.9D-G). Retrospective analyses of patients treated with ICB have revealed how these indicative markers are associated with tumours with enhanced responses (Binnewies et al., 2018).

More recently, improved outcomes have been observed in breast cancer patients with high PD-L1 expression when receiving the PD-1 axis targeting treatments atezolizumab, pembrolizumab or avelumab (Schmid et al., 2018). In particular, PD-L1 expression on tumour-infiltrating immune cells held considerable prognostic value in triple-negative breast cancer (TNBC). However, whether PD-L1 expression itself is a

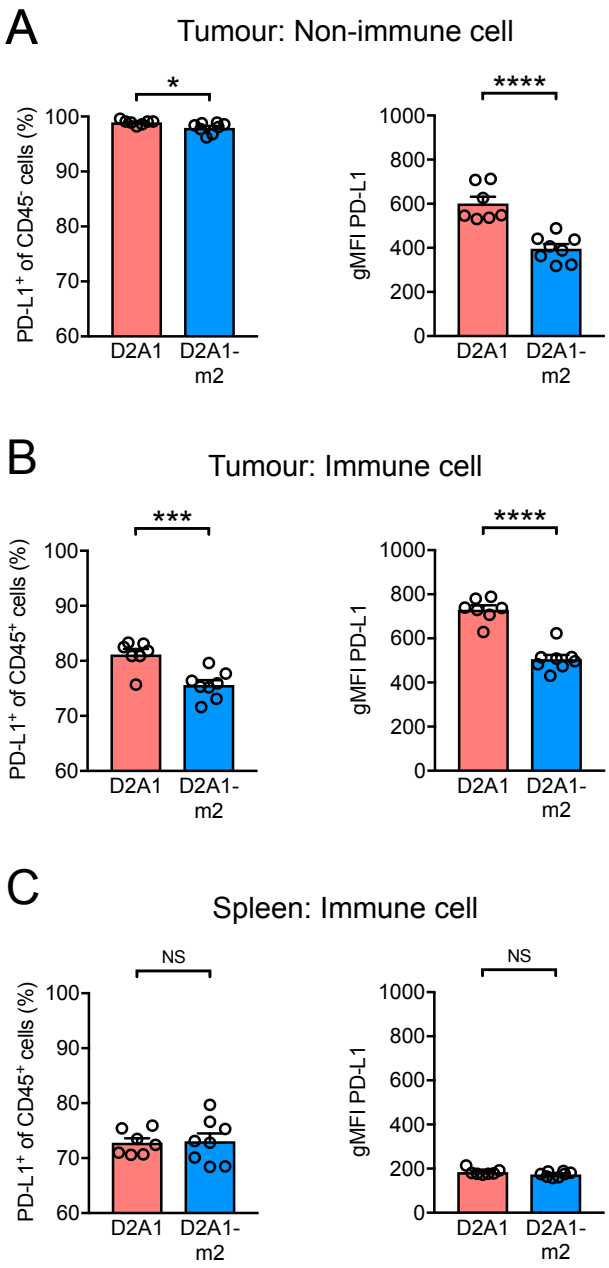

Figure 5.3: PD-L1 expression in the D2A1 and D2A1-m2 tumour models. 2 x 10^5 D2A1 or D2A1-m2 cells were injected orthotopically into the 4th mammary fat pad of 6-8 week old female wild-type BALB/c mice (D2A1: *n* = 7 mice; D2A1-m2; *n* = 8 mice). Primary tumours and spleens were processed to single cell suspensions and stained with BV786-conjugated anti-CD45 and BV421-conjugated anti-PD-L1 antibodies (Table 2.1). **A**-**C.** Proportion of PD-L1 expressing cells and PD-L1 expression levels expressed as geometric mean fluorescence intensity (gMFI) for (**A**) tumour-derived CD45$^-$ non-immune cells, (**B**) tumour-derived CD45$^+$ immune cells, and (**C**) spleen-derived CD45$^+$ immune cells. Data are mean ± SEM. Statistical analysis was performed using an unpaired *t*-test: NS = not significant; * = $P < 0.05$; *** = $P < 0.001$; **** = $P < 0.0001$.

key predictor of clinical outcomes, or whether PD-L1 expression is simply indicative of an active T cell response, remains unclear (Sharma and Allison, 2015).

With this in mind, D2A1 and D2A1-m2 tumours were assessed for PD-L1 expression via flow cytometry. A higher proportion of CD45$^-$ cells, that includes both

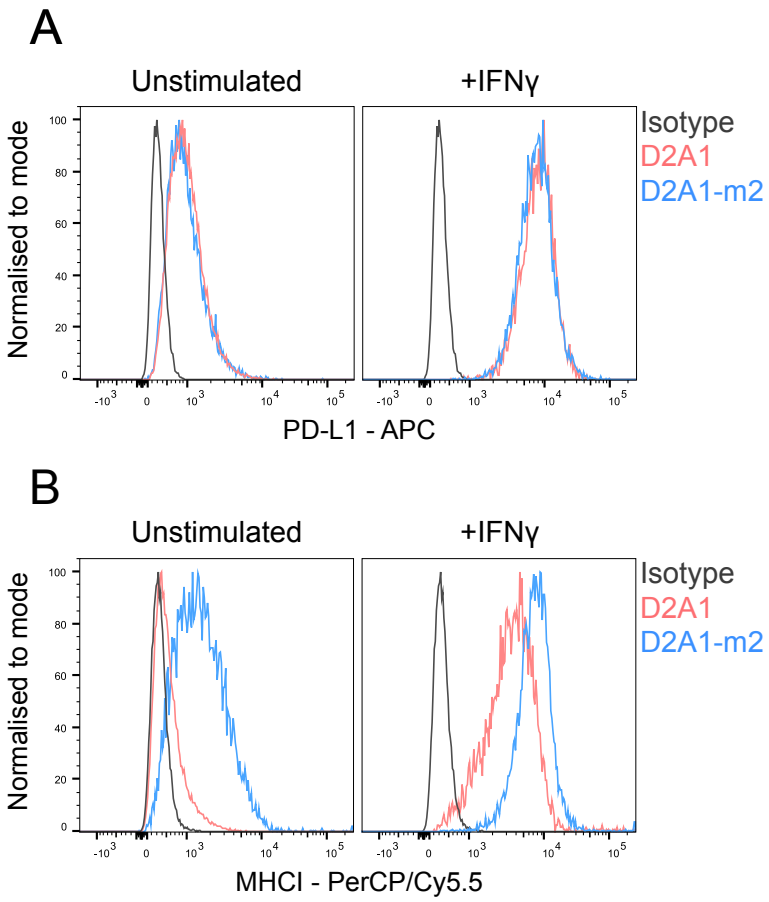

Figure 5.4: PD-L1 and MHCI expression in D2A1 and D2A1-m2 cells *in vitro*. A-B. D2A1 and D2A1-m2 cells were stimulated for 24 hours with 10 ng/mL IFNγ and stained with (**A**) an APC-conjugated anti-PD-L1 antibody, and (**B**) a PerCP/Cy5.5-conjugated anti-MHCI antibody, or relevant isotype control antibodies (Table 2.5), and analysed via flow cytometry. Analysis of unstimulated cells is also shown.

tumour cells and non-immune stromal cells, expressed PD-L1 in D2A1 tumours (Figure 5.3A). Cells also expressed higher levels of PD-L1, as determined by geometric mean fluorescence intensity, in D2A1 tumours, compared to D2A1-m2 tumours (Figure 5.3A). Similarly, a higher proportion of $CD45^+$ immune cells expressed PD-L1 in D2A1 tumours, and cells again expressed higher levels of PD-L1 (Figure 5.3B). In contrast, a similar proportion of splenocytes from both models expressed PD-L1 and no significant differences in the levels of PD-L1 expression were observed (Figure 5.3C), suggesting that the differential PD-L1 expression between models was tumour-specific.

Cancer-cell surface expression of PD-L1 can be constitutive, attributed to cell intrinsic genetic alterations, or inducible and attributed to external factors in the microenvironment. Upon activation, T cells, in addition to up-regulating expression of

immune checkpoints such as PD-1, also produce cytokines such as interferon gamma (IFNγ) that promote expression of PD-L1 on tumour cells and other cells in tumour tissues (Dong et al., 2002). To determine whether the differences in PD-L1 expression observed between D2A1 and D2A1-m2 tumours are a result of intrinsic differences in tumour cells or are a result of microenvironmental factors such as IFNγ production, D2A1 and D2A1-m2 tumour cells were assessed for PD-L1 expression *in vitro*. Prior to IFNγ stimulation, D2A1 and D2A1-m2 cells exhibited similar constitutive expression of PD-L1 (Figure 5.4A). In response to stimulation with 10ng/mL IFNγ, both D2A1 and D2A1-m2 cells upregulated PD-L1 expression to similar levels (Figure 5.4A). These similar expression patterns of PD-L1 expression *in vitro* suggest that the higher levels of PD-L1 observed in D2A1 tumours is reflective of increased T cell activity.

IFNγ also regulates tumour cell expression of MHC class I (MHCI) molecules (Zhou, 2009). MHCI is crucial in antigen presentation and plays a key role in initiating anti-tumour CTL responses. Furthermore, loss of MHCI expression is a common mechanism of immune evasion by tumours, as CTLs preferentially kill $MHCI^{+}$ tumour cells, and are unable to kill tumours homogeneously deficient or completely negative for MHCI expression (Bubenik, 2003). MHCI expression has also been validated as a surrogate marker of immunogenicity and correlates with response to ICB treatment in some preclinical models (Lechner et al., 2013). Conversely, it is also well established that natural killer (NK) cells can recognise and kill cells that have down-regulated MHCI expression (Bubenik, 2003). Interestingly, MHCI expression was higher in D2A1-m2 cells, than in D2A1 cells, both constitutively and in response to IFNγ stimulation (Figure 5.4B).

Based on characterisation of the immune microenvironment of D2A1 and D2A1-m2 tumours, it was hypothesised that the D2A1 model would exhibit better responses to ICB treatment. To determine whether this was accurate, D2A1 cells were injected orthotopically into the 4^{th} mammary fat pad of syngeneic BALB/c mice and treated with a combination of anti-CTLA-4 (10 mg/kg, IP) and anti-PD-L1 (10 mg/kg, IP) antibodies (hereafter referred to as COMBO), as described in Chapter 2.2.3.5 and illustrated in

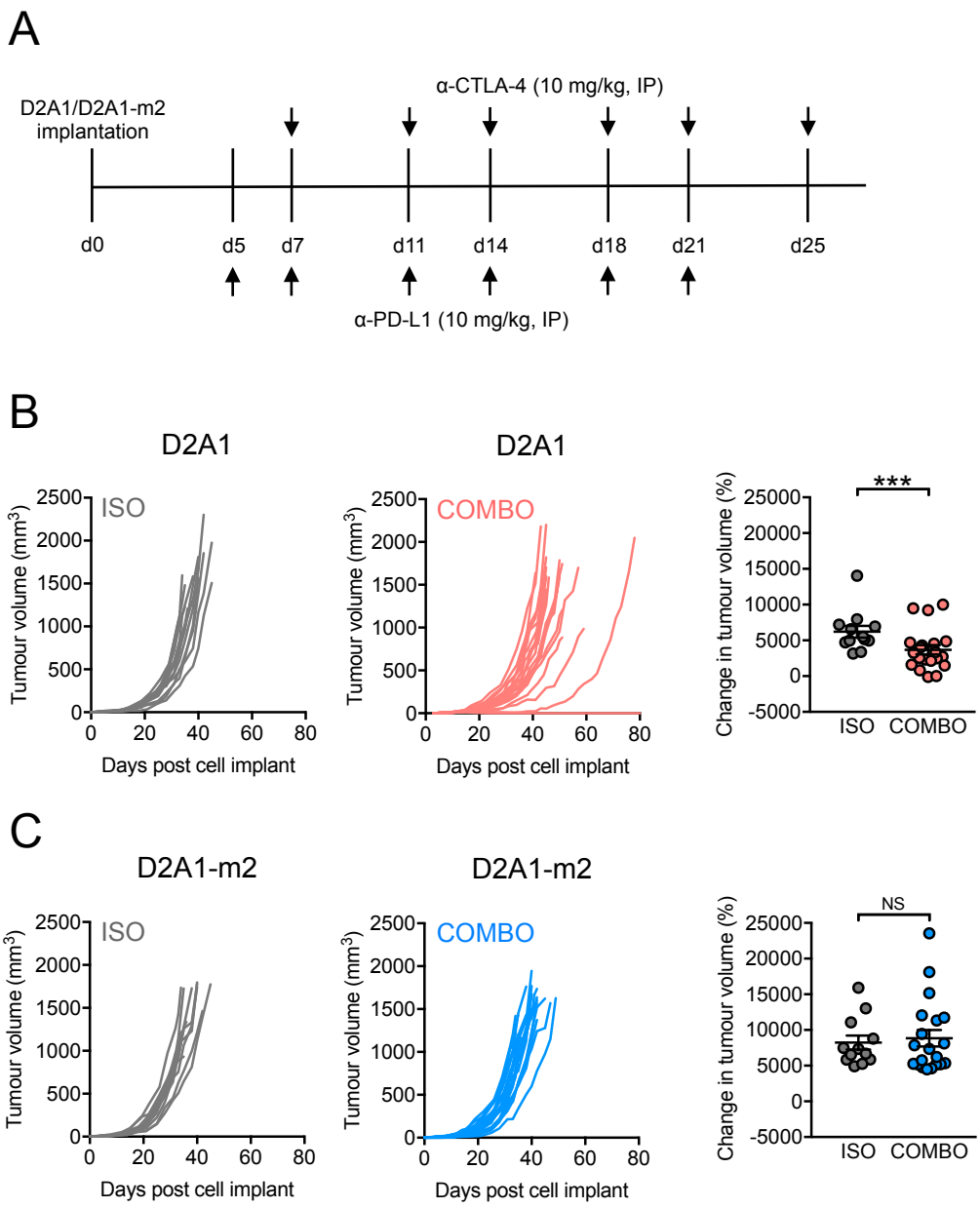

Figure 5.5: The anti-tumour activity of immune checkpoint blockade treatment in the D2A1 and D2A1-m2 tumour models. 2 x 10^5 D2A1 or D2A1-m2 cells were injected into the 4th mammary fat pad of 6-8 week old female wild-type BALB/c mice. Mice were treated with a combination of anti-CTLA-4 (10 mg/kg, IP) and anti-PD-L1 (10 mg/kg, IP) antibodies (COMBO) (*n* = 20-21 mice per group; from 2 independent experiments). Control mice received relevant isotype control antibodies (ISO) (*n* = 12 mice per group; from 2 independent experiments). **A.** Dosing regimen for immune checkpoint blockade treatment. **B**-**C.** Individual tumour growth curves and changes in tumour volume from initial measurement of palpable tumours to 33 days post cell injection for (**B**) D2A1, and (**C**) D2A1-m2 tumour-bearing mice receiving a combination of anti-CTLA-4 and anti-PD-L1 treatment (COMBO), or relevant isotype control treatment (ISO). Tumour growth was monitored by caliper measurements. Data are mean ± SEM. Statistical analysis was performed using an unpaired *t*-test: NS = not significant; *** = $P < 0.001$.

Figure 5.5A. Control mice received a combination of isotype control antibodies listed in Table 2.7 (hereafter referred to as ISO). Mice were randomised between treatment groups by tumour volume on the first day of treatment. COMBO treatment delayed the growth of individual D2A1 tumours, and one mouse exhibited complete tumour regression (Figure 5.5B). COMBO treatment also significantly inhibited the increase in tumour volume from when tumours were first palpable, to day 33, when some mice were sacrificed due to tumour volume restrictions (Figure 5.5B). In contrast, COMBO treatment had no effect on the growth, or change in the volume of D2A1-m2 tumours (Figure 5.5C).

In addition to monitoring tumour growth, the effect of COMBO treatment on survival was also assessed. COMBO treatment significantly extended the survival of D2A1 (increase in median survival from 40 to 45 days), but not D2A1-m2 (increase in median survival from 37 to 40 days) tumour-bearing mice (Figures 5.6A and B). As previously mentioned, one D2A1 tumour-bearing mouse exhibited complete tumour regression and survived to 80 days post cell implant. To confirm that ICB treatment had induced an immunological memory, the responding mouse was re-challenged with D2A1 cells injected into the opposite mammary fat pad. Implanted D2A1 cells failed to establish a tumour in the re-challenged mouse (Re-challenge), but did form tumours in control naïve BALB/c mice (Naïve) implanted with the same cells (Figure 5.6C).

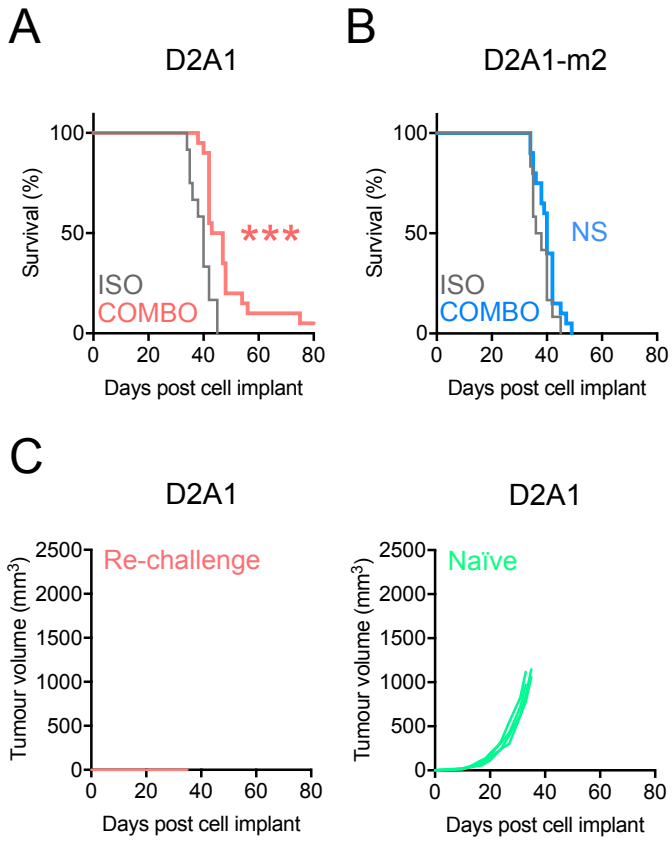

Figure 5.6: Survival analysis of immune checkpoint blockade treatment in the D2A1 and D2A1-m2 tumour models. A-B. Kaplan-Meier curves for (**A**) D2A1, and (**B**) D2A1-m2 tumour-bearing mice shown in Figure 5.5 receiving a combination of anti-CTLA-4 and anti-PD-L1 treatment (COMBO), or isotype control treatment (ISO). Mice were sacrificed upon reaching a humane endpoint. Curves were compared using the log-rank test: NS = not significant; *** = $P < 0.001$. **C.** 2 x 10^5 D2A1 cells were injected into the opposite mammary fat pad of a surviving wild-type BALB/c mouse from Figure 5.6A exhibiting complete tumour regression (Re-challenge), or bilaterally into 2 naïve wild-type BALB/c mice (Naïve). Individual tumour growth curves are shown.

5.3 Discussion

5.3.1 Challenges in establishing the 4T07 model for ICB efficacy studies

To determine the effects of CAF abundance within the tumour microenvironment on responses to ICB treatment, the 4T07 and 4T1 cell lines, which share a single origin but give rise to primary tumours with striking differences in CAF content (Figures 3.1A and B), were initially employed. However, whilst 4T1 tumours exhibited consistent growth-kinetics in syngeneic BALB/c mice, 4T07 tumour growth was highly variable and tumours often regressed soon after cell implantation, making the 4T07 model unsuitable for use in assessing the efficacy of ICB treatment.

In attempts to enhance the tumourigenicity of 4T07 cells *in vivo*, cells were implanted both orthotopically into the mammary fat pad and subcutaneously into the flank of BALB/c mice (Figures 5.1A and B). Furthermore, growth pilot studies were also initiated where 4T07 cells were implanted with an extract of reconstituted basement membrane (Matrigel) or at increased cell numbers. However, neither of these approaches improved 4T07 tumour growth (Data not shown).

Although 4T07 tumour growth was enhanced in NSG mice (Figure 3.2A), this model would not permit studying the efficacy of ICB treatment, which targets elements of the host immune system absent in these immunodeficient mice. It has been long recognised that tumour fragments containing stromal elements are not as readily rejected immunologically as tumour cell suspensions when implanted into mice *in vivo* (Singh et al., 1992). The stroma of solid tumours consists of fibroblasts, macrophages and vascular endothelial cells, in addition to extracellular matrix, all of which contribute to supporting tumour growth (Gajewski et al., 2013). Thus, it was hypothesised that implanting 4T07 tumour fragments, with their established stromal components, from tumours grown in NSG mice into immunocompetent BALB/c mice, would promote 4T07 tumour progression. Whilst this was confirmed, resultant tumours continued to display high variability in their growth kinetics, making them unsuitable for ICB efficacy studies (Figure 5.1C). Nevertheless, this did serve as a striking demonstration of the tumour-promoting properties of the stroma, particularly when considered alongside previous experiments where co-injection of CAFs also enhanced the growth of highly immunogenic 4T07 tumours (Figure 4.5A). Though the differences in 4T07 and 4T1 tumour growth in an immunocompetent setting may be being driven by cell-intrinsic factors, the aforementioned experiments utilising stromal elements to improve 4T07 growth suggest otherwise.

5.3.2 Response of the 4T1, D2A1 and D2A1-m2 models to ICB

The anti-tumour activity of anti-CTLA-4 and anti-PD-L1 treatment, given either alone or in combination, was assessed in selected mouse models using dosing regimens similar to those previously described (Mosely et al., 2016).

Having previously demonstrated that CAF-rich 4T1 and D2A1-m2 tumours exhibited an immunologically 'cold' microenvironment, it was hypothesised that these tumours would respond more poorly to ICB treatment than comparatively inflamed 4T07 and D2A1 tumours. As expected, ICB treatment was ineffective in delaying tumour growth in both the 4T1 (Figures 5.2B-C) and D2A1-m2 (Figure 5.5C) models. In contrast to the D2A1-m2 model, ICB treatment delayed tumour growth (Figure 5.5B), improved survival (Figure 5.6A) and led to an instance of complete tumour regression (Figure 5.5B) in the D2A1 model. Furthermore, this responsive animal developed an immunological memory to re-challenge with D2A1 cells, indicative of an adaptive anti-tumour immune response (Figure 5.6C). Though it is conceivable that these differences in susceptibility to ICB treatment between the D2A1 and D2A1-m2 models could be attributed to tumour cell-intrinsic factors, these cell lines are closely related and exhibit very similar primary tumour growth kinetics (Jungwirth et al., 2018). Furthermore, PD-L1 expression, a major influencing factor on the responsiveness of tumours to ICB treatment, was similar in D2A1 and D2A1-m2 cells *in vitro* (Figure 5.4A), and only differed *in vivo* (Figures 5.3A-B), indicative of a microenvironmental-driven difference rather than a cell-intrinsic one.

Although D2A1-m2 tumours are significantly more metastatic than D2A1 tumours (data not shown), animals were sacrificed for survival analysis based exclusively on tumour volume restrictions, not as result of metastasis-induced illness. Thus, any treatment-induced improvements in survival were a result of effects on primary tumour growth alone.

Transcriptomic differences between D2A1 and D2A1-m2 cells may also underlie observed differences in responsiveness to ICB treatment. However, both cell lines have recently been subjected to gene expression analysis and, using Ingenuity Pathway Analysis (IPA), this revealed that although the cell lines had distinct top

canonical pathways, the upstream regulators and molecular and cellular functions were highly overlapping (Jungwirth et al., 2018). Furthermore, transforming growth factor beta 1 (TGFβ1), known to induce fibroblast activation (Clark et al., 1997), was identified as an upstream regulator only in D2A1-m2 cells, potentially accounting for the increased stromal activation observed in D2A1-m2 tumours. Of note, a signature of TGFβ signalling in fibroblasts has recently been linked to attenuation of tumour response to PD-L1 blockade by contributing to T cell exclusion (Mariathasan et al., 2018), a phenomenon explored in the next chapter.

5.3.3 Improving responses of breast cancer to ICB treatment

Though drugs targeting CTLA-4, PD-1 and PD-L1 are widely used both as a standard of care and in numerous clinical trials for a variety of cancer types, much remains to be learned about how they may best be utilised to maximise their anti-tumour effects, and broaden their benefits. Attempts to increase the clinical benefit of ICB agents have generally focused on identifying novel immune checkpoints for targeting, or, combining existing ICB agents. Increasingly, combination treatment is being evaluated preclinically, and has demonstrated some impressive results (Nolan et al., 2017). In the clinic, ICB agents are often combined with more traditional chemotherapeutic agents. As previously discussed, the PD-L1 targeting drug atezolizumab was recently approved for treating TNBC in combination with nab-paclitaxel (Schmid et al., 2018). Thus, when studying mechanisms of resistance to ICB treatment preclinically, it will be important to try and mimic clinical treatment schedules as closely as possible. Additional ICB experiments using the models examined in this chapter could include a range of other agents to determine whether the CAF-driven differences in responsiveness persist.

In addition to developing novel treatment combinations, much research is focused on identifying biomarkers of responsiveness to ICB treatment. As discussed in Chapter 1.3.2.4, defining tumours based on their immunological microenvironment, even crudely, has proven particularly useful in predicting responses to ICB treatment.

The data in this chapter supports the notion that a better understanding of the CAF content of tumours may also aid in making informed clinical decisions when treating breast cancer patients with ICB. To fully elucidate the role of CAFs in promoting resistance to ICB treatment, and to identify novel stromal targets, it will be important to integrate different techniques for assessing the microenvironmental composition of breast cancer, some of which will be explored in the following chapter.

Chapter 6: Genomic, transcriptomic and histopathological characterisation of the D2A1 and D2A1-m2 models

6.1 Introduction

Immune checkpoint blockade (ICB) therapies, particularly those targeting the programmed cell death protein 1 (PD-1)/programmed death ligand-1 (PD-L1) axis, have delivered significant clinical benefit for patients with a variety of cancer types, however, there is still an unmet clinical need for the overwhelming majority who do not respond. As discussed in Chapter 1.3.2.4, technological advances have improved our understanding of the biological diversity within the tumour microenvironment, helping to identify putative biomarkers for predicting therapeutic responses, whilst simultaneously revealing new levels of complexity that are yet to be fully characterised. Clinically validated biomarkers predictive of response to anti-PD-1 therapy include expression of the PD-1 ligand, PD-L1, and the presence of microsatellite instability that results from impaired DNA mismatch repair (Cristescu et al., 2018). Further, tumour mutational burden and the presence of an inflamed, immunologically 'hot' tumour microenvironment are emerging biomarkers for response to ICB therapy, highlighting how resistance to these agents is driven by both tumour-intrinsic and tumour-extrinsic factors (Pitt et al., 2016). Thus, an integrative approach to characterising the tumour immune microenvironment will be required to reveal the mechanisms promoting resistance to ICB in breast cancer and identify novel therapeutic targets. Having established that the CAF-low, immunologically 'hot' D2A1 model responds more favourably to combination ICB than the CAF-high, immunologically 'cold' D2A1-m2 model, this chapter describes further experiments undertaken to understand the mechanisms driving these differences in response.

Whilst the accumulation of mutations in tumour cells can confer a selective advantage through increased genetic diversity, somatic mutations also result in increased generation of neoantigens that may be recognised by the adaptive immune system. Tumour mutational burden, often defined as the number of nonsynonymous mutation per megabase (Mb) of total genomic DNA, is associated with improved survival in patients receiving ICB treatment across multiple cancer types (Goodman et al., 2017), however, only modest associations have been observed in breast cancer which lacks the mutational load of cancers such as melanoma and lung cancer (Alexandrov et al., 2013). Nevertheless, in breast cancers exhibiting favourable immune infiltration, high tumour mutational burden is associated with better survival (Goodman et al., 2017) and the treatment of preclinical *BRCA1*-mutant breast cancer models with cisplatin increases their mutational load and enhances the efficacy of combination anti-CTLA-4 and anti-PD-1 treatment (Nolan et al., 2017), suggesting that tumour mutational burden should be considered when investigating the response of breast cancer to ICB.

Highly mutated tumours should theoretically incite more robust anti-tumour immune responses and lead to the development of a more inflamed tumour immune microenvironment. Whilst immune profiling via flow cytometry is useful in providing an overview of the nature of the tumour immune microenvironment, advances in transcriptomic technologies have facilitated a heightened interest in using gene expression profiling to characterise the immune phenotype of cancers. The relationship between tumour mutational burden and an inflamed tumour immune microenvironment is poorly characterised, but the utility of using immune gene expression signatures from bulk tumour tissue alone to predict responses to ICB is well established (Ayers et al., 2017). These signatures often include genes related to antigen presentation, chemokine expression, cytotoxic activity and adaptive immune resistance, but accumulating evidence suggests that CAF-related gene signatures may also be useful in identifying tumours with an immune-excluded phenotype that may respond poorly to ICB (Jiang et al., 2018). Indeed, a signature of transforming growth factor beta (TGFβ)

signalling in fibroblasts was recently linked to an immune-excluded tumour phenotype that attenuated responses to anti-PD-L1 treatment. Blocking TGFβ signalling in preclinical models enhances T cell infiltration and improves responses to anti-PD-L1 (Mariathasan et al., 2018), highlighting how gene expression profiling can provide mechanistic insights with therapeutic relevance.

To determine the genomic and transcriptomic profiles of the D2A1 and D2A1-m2 models, the cell lines and tumours were subjected to whole exome sequencing (WES) and gene expression profiling using the NanoString platform, respectively. Subsequent analysis explored differences in tumour mutational burden and the expression of immune and stromal gene signatures. Furthermore, the spatial arrangement of cytotoxic T lymphocytes (CTLs) within both models was determined and indicated a role for CAFs in these models in driving an immune excluded phenotype.

6.2 Results

6.2.1 Whole-exome sequencing of the D2A1 and D2A1-m2 cell lines

Having demonstrated in Chapter 5 that the D2A1 model is more responsive to a combination of anti-CTLA-4 and anti-PD-L1 therapies than the D2A1-m2 model, it was important to determine whether cell-intrinsic genetic differences existed between the cell lines that could affect their inherent immunogenicity.

To characterise mutational differences, D2A1 and D2A1-m2 cell lines were analysed using WES. WES is a genomic technique for sequencing the protein-coding regions of a genome, known as the exome. Though the exome represents only around 2% of an entire genome, mutations in these coding regions are the primary source of neoantigens that the immune system can target.

One type of genetic variation that can be assessed through WES data is copy-number variation (CNV), where sections of a genome are gained/amplified or lost/deleted. When compared to a reference BALB/c mouse genome, the D2A1 and D2A1-m2 cell lines displayed similar copy number variation profiles (Figure 6.1A). This

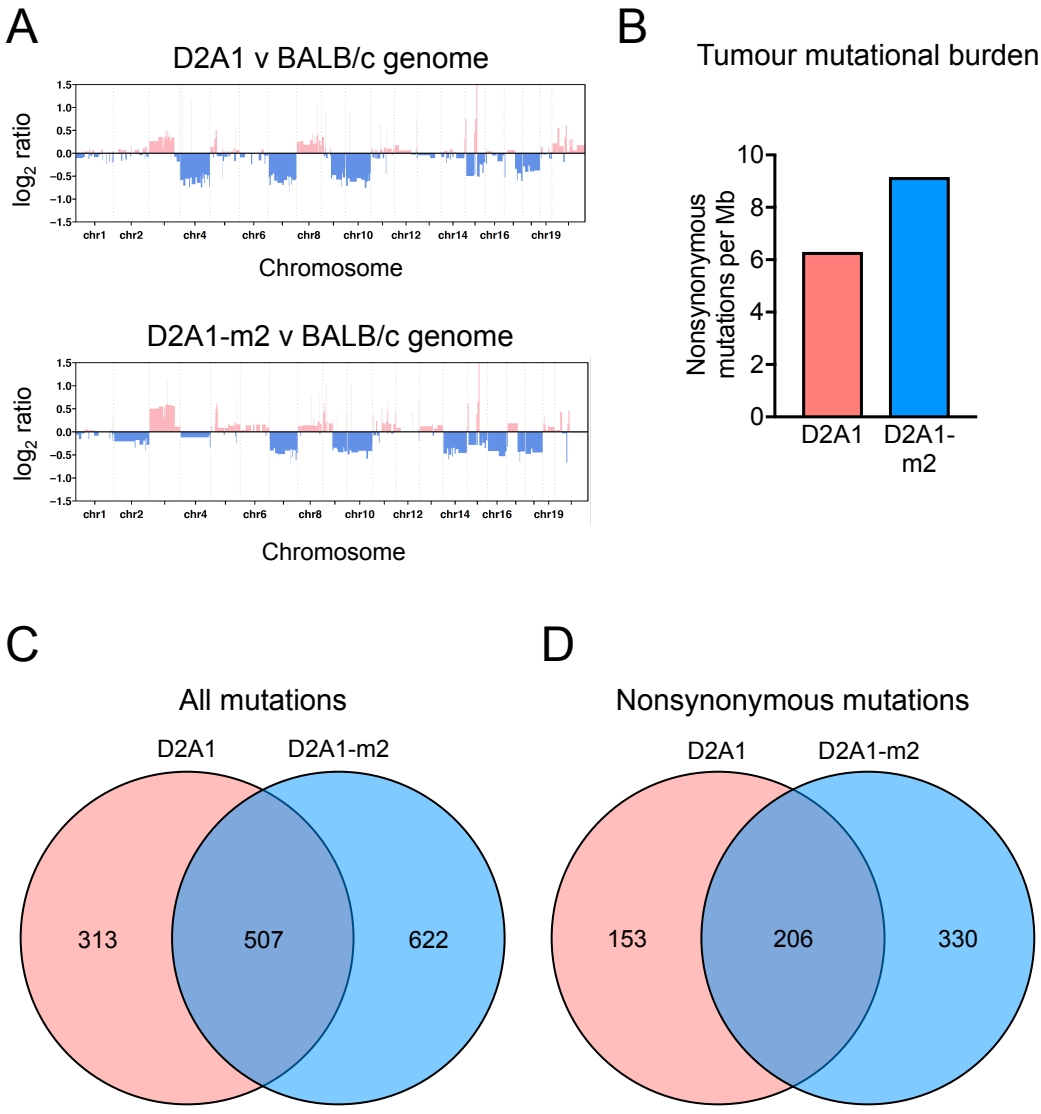

Figure 6.1: Genomic characterisation of the D2A1 and D2A1-m2 cell lines. D2A1 and D2A1-m2 cell lines and normal BALB/c mouse DNA (isolated from the spleen) were subjected to whole exome sequencing (WES). **A.** Copy number variation (CNV) plots (log_2 ratio) for D2A1 and D2A1-m2 cell lines using the normal BALB/c genome as reference. **B**. Tumour mutational burden of D2A1 and D2A1-m2 cell lines. The number of protein-coding nonsynonymous mutations per megabase (Mb) of exome is shown. **C**-**D.** Venn diagrams illustrating the number of (**C**) total mutations, and (**D**) nonsynonymous mutations in common between the D2A1 and D2A1-m2 cell lines.

was expected given that the cell lines are closely related. As discussed in Chapter 3, the metastatic D2A1-m2 subline was derived by serial inoculation of parental D2A1 cells in BALB/c mice followed by recovery from lung tissue *ex vivo* (Jungwirth et al., 2018). Next, to determine whether mutational status contributes to the differences observed in terms of both metastatic potential and ICB responsiveness between D2A1 and D2A1-m2 cells *in vivo,* the number of nonsynonymous mutations in both cell lines

was determined. Comparison of their mutational profiles revealed how D2A1-m2 cells had a higher tumour mutational burden than parental D2A1 cells (Figure 6.1B). Many of these mutations were shared, but both cell lines also carried distinct mutations (Figure 6.1C and D), suggesting that the D2A1 cell line is a heterogeneous population, and confirms that the D2A1-m2 cell line likely derives from selection of a subset of D2A1 cell clones during *in vivo* passage.

6.2.2 Transcriptomic comparison of the D2A1 and D2A1-m2 models

Having demonstrated in Chapter 3 how the D2A1 and D2A1-m2 models differ in terms of their immune profiles, the transcriptomes of established, untreated D2A1 and D2A1-m2 tumours were analysed to investigate additional baseline characteristics that may underlie their differential responsiveness to ICB treatment. RNA was extracted from bulk D2A1 and D2A1-m2 tumours of similar weights (Figure 6.2A) and was analysed using the NanoString nCounter platform. The PanCancer IO 360 gene expression panel was used, which measures the expression of 770 genes involved in the interplay between the tumour, its microenvironment and the immune response. Raw NanoString data were processed using R package NanoStringNorm (v1.2.1) and differential mRNA abundance analysis was performed using voom (TMM normalisation), with R package limma (v3.34.9). Genes with absolute $\log_2$ fold change > 1 and adjusted *P* value < 0.05 were considered significant (Figures 6.2B and C). Genes significantly increased in D2A1 tumours, compared to D2A1-m2 tumours, included inflammation-related genes such as interferon-induced transmembrane protein 1 (*Ifitm1*), whose expression is induced by interferons, and chemoattractant genes such as chemokine (C-C motif) ligand 12 (*Ccl12*) and chemokine (C-C motif) ligand 17 (*Ccl17*). Whilst some immune genes were also increased in D2A1-m2 tumours, compared to D2A1 tumours, there was a noticeable increase in genes related to TGFβ and Wnt signalling including inhibitor of DNA binding 4 (*Id4*), inhibin, beta A (*Inhba*) and Wnt family member 11 (*Wnt11*). Furthermore, interleukin 11 (*Il11*) also had higher expression in D2A1-m2 tumours and has been shown to stimulate collagen production downstream of

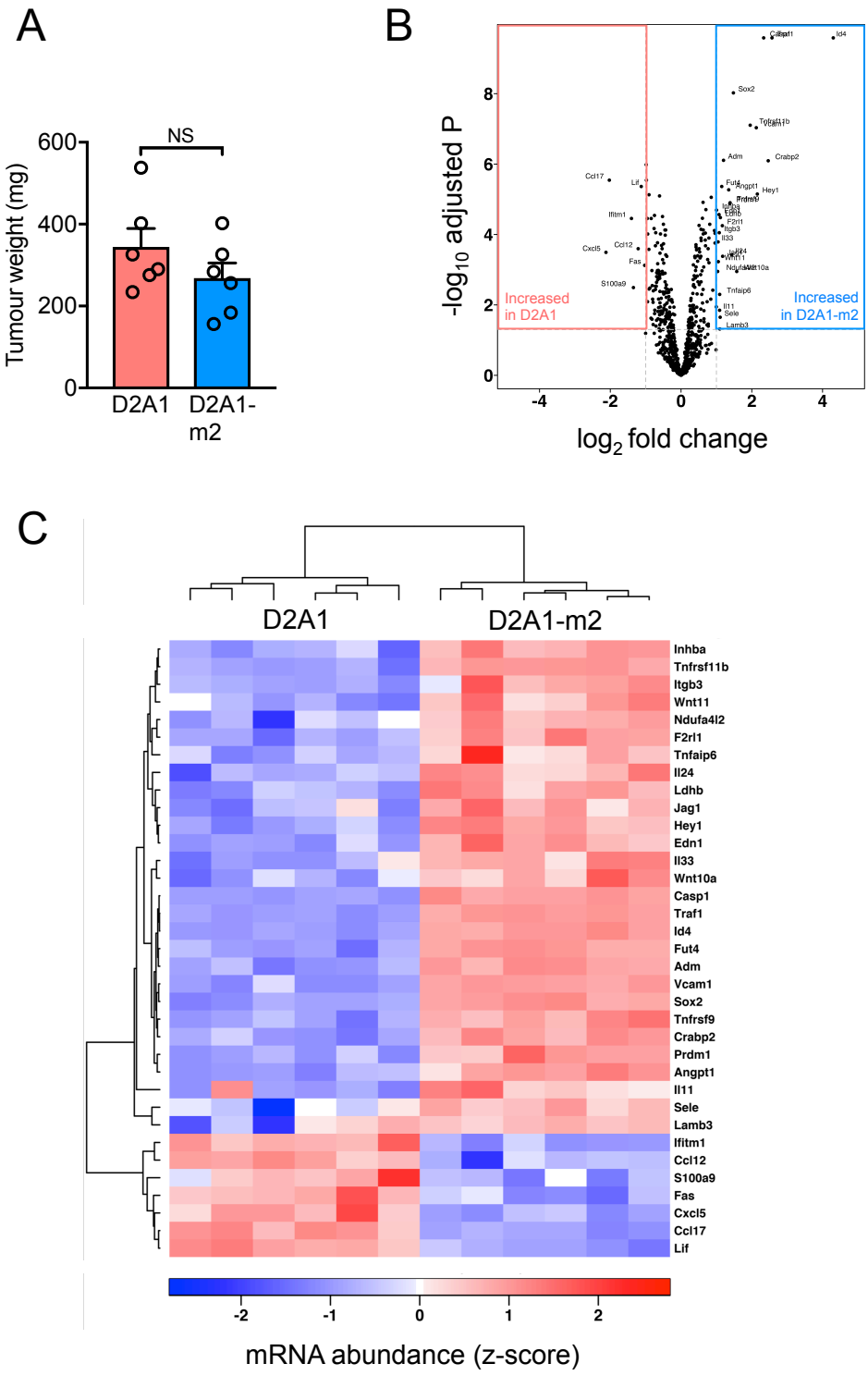

Figure 6.2: Differentially expressed genes in D2A1 and D2A1-m2 tumours. Gene expression profiling of D2A1 and D2A1-m2 tumours was performed using the targeted NanoString PanCancer IO 360 gene expression panel. **A.** Weights of tumours used for gene expression profiling. Data are mean ± SEM. Statistical analysis was performed using an unpaired *t*-test: NS = not significant. **B.** Volcano plots showing differentially expressed genes between D2A1 and D2A1-m2 tumours. Genes with absolute $\log_2$ fold change > 1 and adjusted *P* value < 0.05 were considered significant. **C.** Heat map of genes differentially expressed between D2A1 and D2A1-m2 tumours.

transforming growth factor beta 1 (*Tgfb1*) and is secreted by cancer-associated fibroblasts (CAFs), driving chemoresistance (Tao et al., 2016).

The expression of selected fibroblast, inflammatory and chemoattractant genes are shown in Figure 6.3. Compared to D2A1 tumours, D2A1-m2 tumours also exhibited increased expression of fibroblast genes including *Tgfb1* and lysyl oxidase-like 2 (*Loxl2*), but not fibroblast activation protein (*Fap*) (Figure 6.3A). In contrast, the expression of granzyme A (*Gzma*), granzyme B (*Gzmb*) and interferon gamma (*Ifng*), genes associated with T cell activity, was higher in D2A1 tumours (Figure 6.3B). Expression of the chemokines C-X-C motif chemokine ligand 9 (*Cxcl9*) and C-X-C motif chemokine ligand 10 (*Cxcl10*), which facilitate chemotactic recruitment of tumour-infiltrating lymphocytes, was increased in D2A1 tumours, but expression of C-X-C motif chemokine ligand 12 (*Cxcl12*) was increased in D2A1-m2 tumours (Figure 6.3C).

Increasingly, gene expression data is used to measure the intratumoural abundance of immune cell populations. This type of analysis is based on historic studies of gene expression in purified immune cells that demonstrated enrichment of specific genes within single immune cell subtypes. For cell type abundance analysis, NanoString curated genesets representing cell types were used, and genesets with more than two genes were further reduced to the largest positively correlated cluster of genes by first running hierarchical clustering on Spearman's correlation distance, followed by identification of optimal number of clusters using Silhouette score. The original NanoString genesets for each cell type are shown, with kept genes (that showed pairwise Spearman's $P > 0.5$) in bold (Figure 6.4A), and a similar approach was used for the comparison of selected stromal biology signatures (Figure 6.4B). Figures 6.4C and D illustrate correlation plots for the CD8 T effector and Pan-fibroblast TGFβ response signature (Pan-F-TBRS), respectively. Expression of genes from the CD8 T effector signature, particularly the interferon gamma (IFNγ)-inducible T-helper-1-type chemokine, CXCL9, is associated with responses to the anti-PD-L1 agent atezolizumab in patients with metastatic urothelial carcinoma (Rosenberg et al., 2016). Genes comprising the Pan-F-TBRS signature used here were selected from a wider,

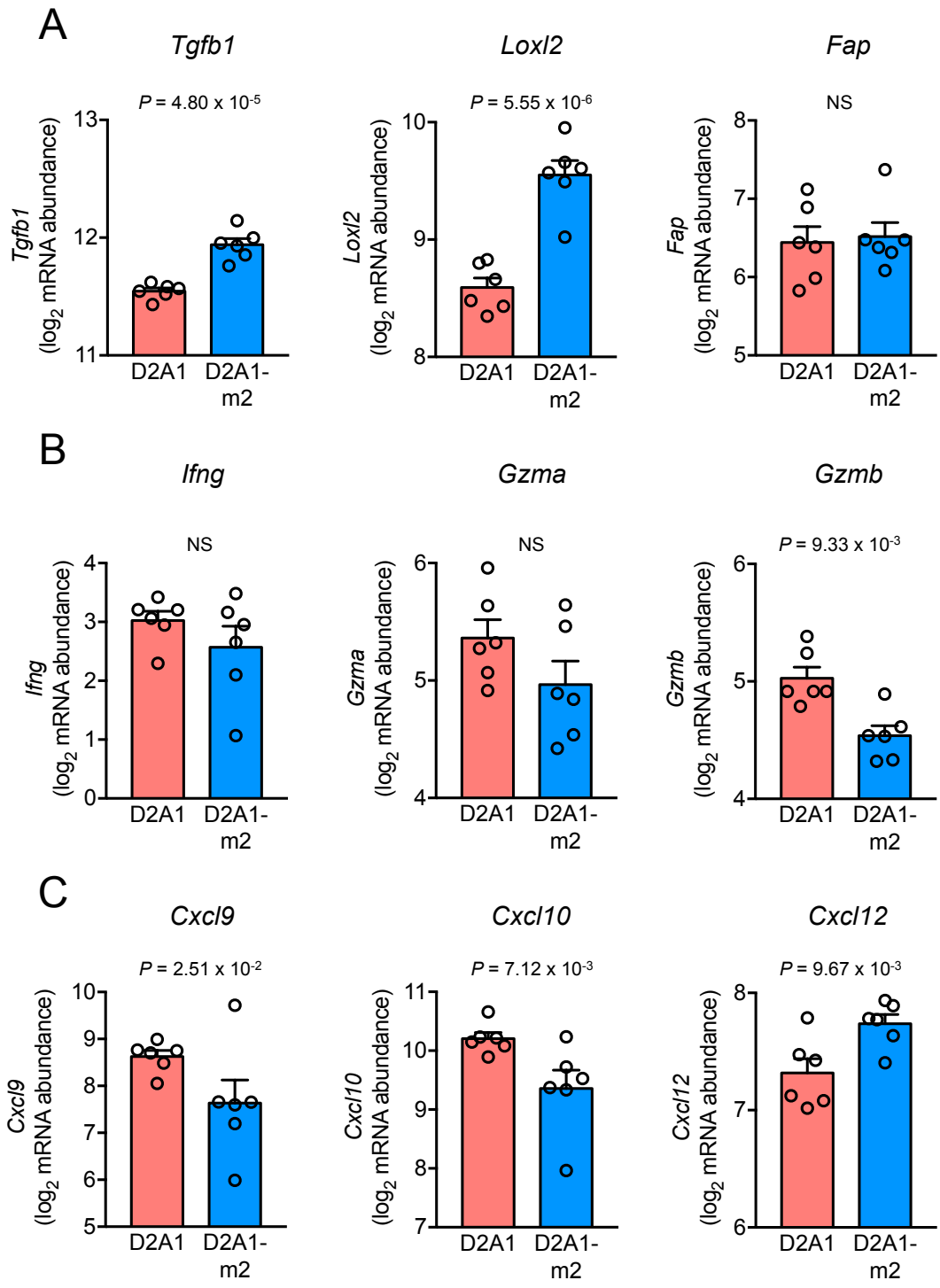

Figure 6.3: Expression of selected genes in D2A1 and D2A1-m2 tumours. **A-C.** Expression of selected (**A**) fibroblast, (**B**) inflammatory, and (**C**) chemoattractant genes from the NanoString PanCancer IO 360 gene expression panel from Figure 6.2. All data are mean ± SEM. Statistical analysis was performed using an unpaired *t*-test: NS = not significant.

A

NanoString immune cell abundance signatures

Cell type	Genes
B cells	***Blk***, *Cd19*, ***Fcrlb***, *Ms4a1*, *Pnoc*, ***Spib***, *Tcl1*, ***Tnfrsf17***
CD45	***Ptprc***
CD8 T cells	***Cd8a***, ***Cd8b1***
Cytotoxic cells	*Ctsw*, ***Gzma***, ***Gzmb***, ***Klrb1***, ***Klrd1***, ***Klrk1***, ***Nkg7***, ***Prf1***
DC	***Ccl2***, *Cd209e*, ***Hsd11b1***
Exhausted CD8	*Cd244*, ***Eomes***, ***Lag3***, ***Ptger4***
Macrophages	*Cd163*, ***Cd68***, ***Cd84***, *Ms4a4a*
Mast cells	***Cpa3***, ***Hdc***, *Ms4a2*
Neutrophils	*Ceacam3*, ***Csf3r***, ***Fcgr4***, ***Fpr1***
NK CD56dim cells	*Il21r*, ***Kir3dl1***, ***Kir3dl2***
NK cells	***Ncr1***, ***Xcl1***
T cells	*Cd3d*, *Cd3e*, *Cd3g*, ***Cd6***, ***Sh2d1a***, *Trat1*
Th1 cells	***Tbx21***
Treg	***Foxp3***

B

Selected stromal biology signatures

Signature	Genes
[1] CD8 T effector	***Cd8a***, ***Cxcl9***, ***Gzma***, ***Gzmb***, *Ifng*, ***Prf1***, *Tbx21*
[2] Pan-F-TBRS	***Adam12***, ***Fstl3***, ***Tgfb1***, ***Tpm1***
[3] TGF-beta signalling	***Acvr1c***, ***Bambi***, ***Bmp2***, *Cdkn2b*, ***Chd9***, ***Id4***, *Ifng*, ***Inhba***, *Myc*, *Rbl2*, ***Rock1***, ***Rps6kb1***, ***Smad5***, ***Tgfb1***, ***Tgfb2***, ***Tgfb3***, *Tgfbr1*, *Tgfbr2*, ***Thbs1***, *Tnf*, *Ubb*
[3] Wnt signalling	*Apc*, ***Axin1***, *Ccnd1*, *Ccnd2*, ***Ccnd3***, *Ctnnb1*, ***Dkk1***, ***Fosl1***, ***Fzd8***, ***Fzd9***, ***Gpc4***, ***Map3k7***, *Mapk10*, ***Mdm2***, *Mmp7*, *Nfatc2*, ***Prkacb***, *Prkca*, ***Sfrp1***, ***Sfrp4***, ***Sox11***, ***Sox2***, ***Trp53***, ***Wnt10a***, ***Wnt11***, ***Wnt2***, ***Wnt2b***, ***Wnt3a***, *Wnt4*, ***Wnt5a***, ***Wnt5b***, *Wnt7b*, ***Bambi***, *Myc*

[1] Signature obtained from Mariathasan et al, 2018.
[2] Signature obtained from Mariathasan et al, 2018.
[3] NanoString curated gene lists

C

CD8 T effector

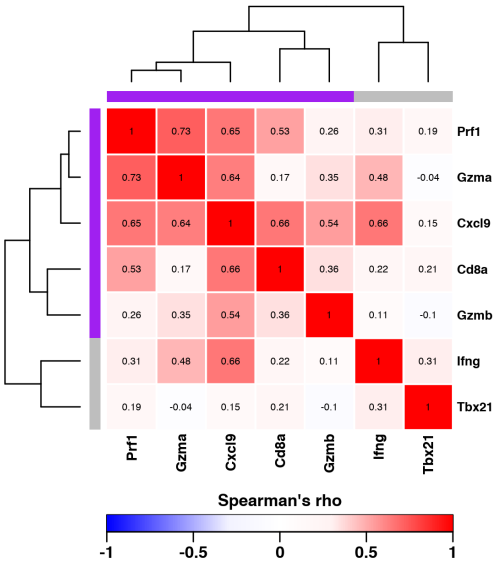

D

Pan-F-TBRS

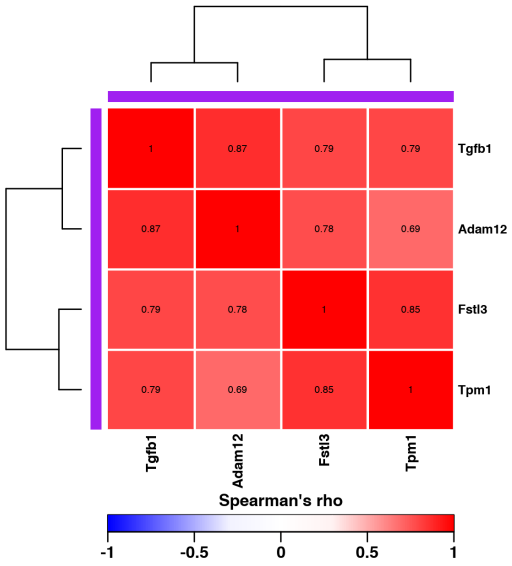

Figure 6.4: Curation of immune cell abundance and stromal gene expression signatures. A-D. NanoString gene expression profiling from Figure 6.2 was analysed for (**A**) immune cell subtype, and (**B**) selected stromal biology signatures. As illustrated in (**C**) and (**D**) for the CD8 T effector gene signature and pan-fibroblast TGFβ response signature (Pan-F-TBRS), genes within individual signatures were analysed by hierarchical clustering on Spearman's correlation distance, followed by identification of optimal clusters using Silhouette score. Genes within signatures that were significantly correlated are indicated in purple in panels (**C**) and (**D**), and in bold in panels (**A**) and (**B**).

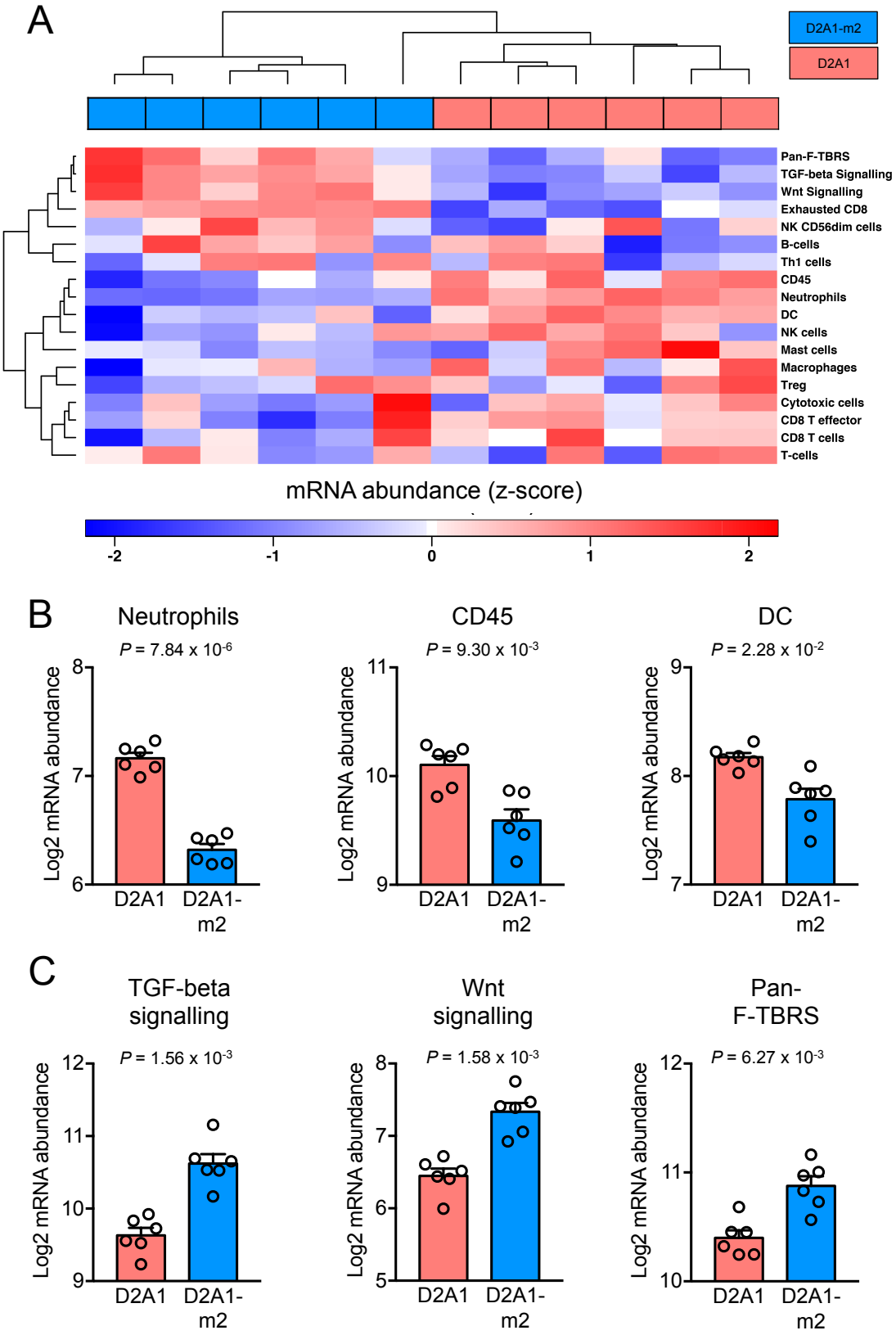

Figure 6.5: Differentially expressed immune cell abundance and stromal biology signatures in D2A1 and D2A1-m2 tumours. A. Unsupervised hierarchical clustering of D2A1 and D2A1-m2 tumours based on expression of annotated signatures from Figure 6.4. **B**-**C.** Expression signatures significantly increased in (**B**) D2A1, and (**C**) D2A1-m2 tumours. Data are mean ± SEM. Statistical analysis was performed using an unpaired *t*-test.

experimentally determined, set of genes upregulated in fibroblasts in response to TGFβ (Mariathasan et al., 2018). The TGF-beta signalling and Wnt signalling signatures were curated by NanoString.

Unsupervised hierarchical cluster analysis based on the immune cell abundance and stromal signatures listed in Figures 6.4A and B revealed that the majority of D2A1 and D2A1-m2 samples clustered separately, with one D2A1-m2 clustering with D2A1 tumours (Figure 6.5A). Interestingly, this D2A1-m2 tumour sample was more abundant in cytotoxic cells and $CD8^+$ T cells than other D2A1-m2 samples, and had lower expression of fibroblast-related signatures (Figure 6.5A). The abundance of neutrophils, CD45 (total immune) and DCs (dendritic cells) was significantly higher in D2A1 tumours (Figure 6.5B). By contrast, TGF-beta signalling, Wnt signalling and Pan-F-TBRS signatures were significantly increased in D2A1-m2 tumours (Figure 6.5C).

In an effort to determine whether specific cell types contribute to suppression of CTL responses and thus resistance to ICB treatment, the correlation between immune cell type-specific gene expression and expression of the CD8 T effector signature was analysed for each D2A1 and D2A1-m2 tumour sample. When grouping all tumours together, it was observed that the abundance of neutrophils, macrophages, mast cells and T_{regs}, all known to possess immunosuppressive functions, did not correlate with expression of the CD8 T effector signature suggesting these cell types had limited effect on CTL activity within D2A1 and D2A1-m2 tumours (Figure 6.6A). However, expression of both the Pan-F-TBRS and TGF-beta signalling signatures was inversely correlated with expression of the CD8 T effector signature (Figure 6.6B) supporting the hypothesis that CAFs play a role in suppressing CTL activity.

6.2.3 Spatial analysis of CTL infiltration in D2A1 and D2A1-m2 tumours

A TGFβ-activated stroma has recently been associated with exclusion of T cells in an EMT6 mouse mammary carcinoma model (Mariathasan et al., 2018). To determine whether physical exclusion of T cells also plays a role in the differential response of

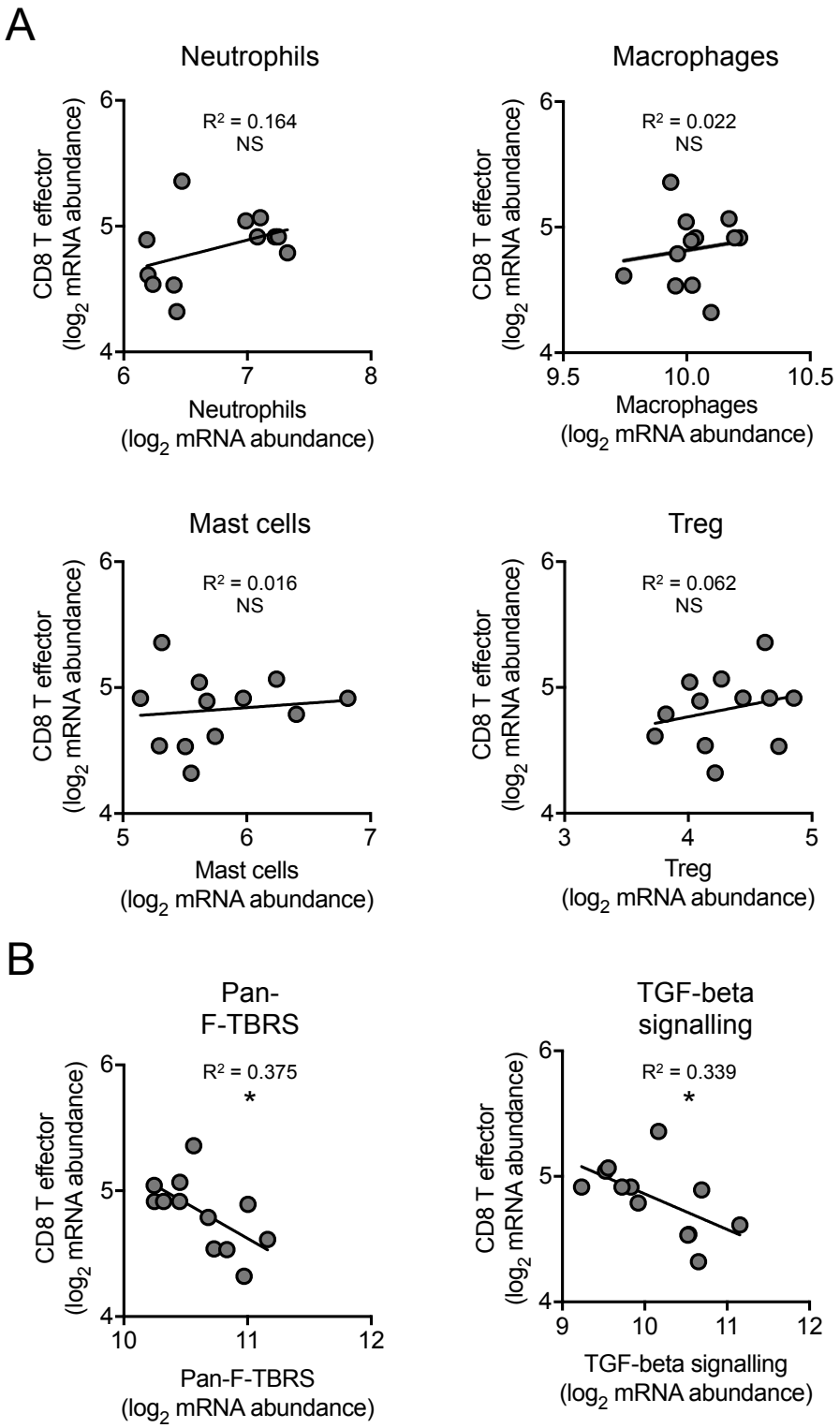

Figure 6.6: Correlation of selected immune cell abundance and stromal biology signatures with CD8 T effector signature expression. A-B. Correlation analysis of selected (**A**) immune cell type signatures, and (**B**) stromal biology signatures, with CD8 T effector signature expression in all experimental D2A1 and D2A1-m2 tumours. R^2 values were calculated from the Pearson correlation coefficient: NS = not significant, * = $P < 0.05$.

D2A1 and D2A1-m2 tumours to ICB treatment, tumour sections from mice treated with isotype control antibodies (ISO) or combination anti-CTLA-4 and anti-PD-L1 treatment (COMBO) were stained for CD8. Quantitative histopathology using QuPath software confirmed the findings presented in Chapter 3 that demonstrated significantly increased $CD8^+$ cell (CTL) infiltration in D2A1 tumours compared to D2A1-m2 tumours, but also revealed how D2A1-m2 tumours have an immune-excluded phenotype, with few CTLs penetrating the tumour centre (Figures 6.7A-C). Combination ICB treatment increased the total density of CTLs in D2A1 tumours from a mean of 67 cells/mm^2 to 120 cells/mm^2, but this effect was not statistically significant (Figure 6.7C). In D2A1-m2 tumours, total CTL density increased from 10 cells/mm^2 to only 11 cells/mm^2 upon treatment (Figure 6.7C). Quantification of CTL density in the periphery and centre of tumour sections revealed how D2A1 tumours had more central then peripheral CTLs, whilst the opposite was true of D2A1-m2 tumours (Figure 6.7D). The distribution of CTLs was unchanged with ICB treatment in D2A1 tumours, and treatment was unable to promote infiltration of CTLs into the centre of D2A1-m2 tumours (Figure 6.7D).

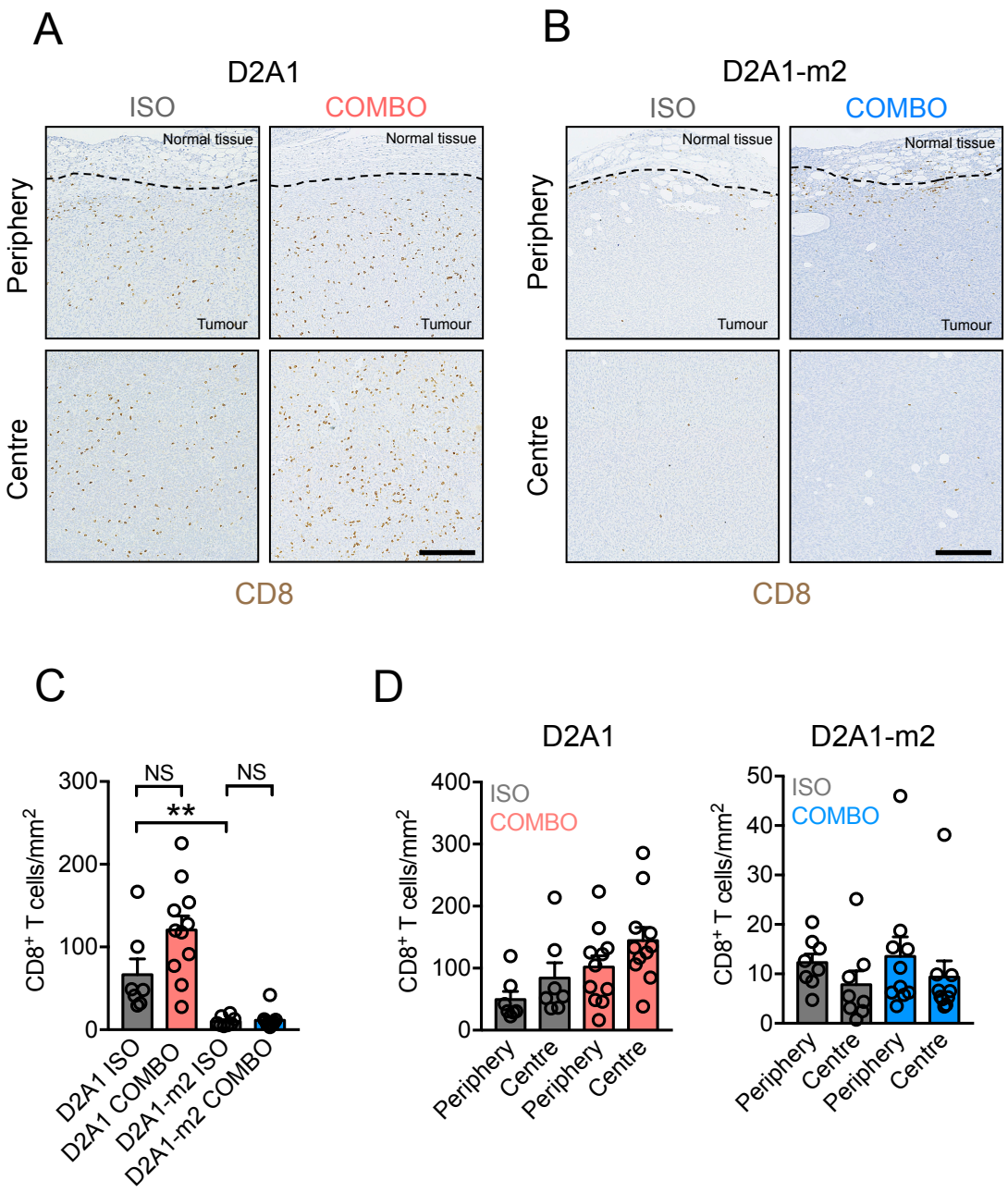

Figure 6.7: Quantitative histopathological analysis of CD8⁺ T cell infiltration. A-B. Representative immunohistochemistry images of (**A**) D2A1, and (**B**) D2A1-m2 tumours from Figure 5.5 stained for CD8. Peripheral and central tumour regions are shown. Tumours were from mice treated with either isotype control antibodies (ISO) or combination anti-CTLA-4 and anti-PD-L1 treatment (COMBO). Dotted line indicates tumour-stroma boundary. Scale bar, 250 μm. **C**. Quantification of overall CD8⁺ T cell density in ISO or COMBO treated D2A1 and D2A1-m2 tumours. Data are mean ± SEM. Statistical analysis was performed using unpaired *t*-tests: NS = not significant, ** = $P < 0.01$. **D**. Quantification of CD8⁺ T cell density in peripheral and central regions of ISO or COMBO treated D2A1 and D2A1-m2 tumours. Data are mean ± SEM.

6.3 Discussion

This chapter explored genetic, transcriptomic and histopathological differences between the D2A1 and D2A1-m2 tumour models that may account for their differential responsiveness to ICB treatment.

Although breast cancers in the clinic typically harbour lower mutational loads than melanoma and lung cancer, averaging around one mutation per Mb of genome, this varies both within and across breast cancer subtypes and the mutational landscape of preclinical models of breast cancer often differs significantly to that found in the human disease (Yang et al., 2017). Still, a higher tumour mutational burden has been explicitly linked to generation of more neoantigens and improved responsiveness to ICB treatment, so it was important to determine whether the D2A1 and D2A1-m2 cell lines possess different mutational profiles.

Accumulating evidence proposes the usefulness of measuring tumour mutational burden as a biomarker for immunotherapy, particularly in melanoma, lung cancer, urothelial cancer and mismatch-repair deficient colorectal cancers (Fancello et al., 2019). Despite observations in Chapter 5 that D2A1 tumours respond preferentially to ICB treatment compared to D2A1-m2 tumours, D2A1 cells exhibited a lower mutational burden compared to D2A1-m2 cells, and only some of these mutations were shared between cell lines (Figures 6.1B-D). During the generation of the D2A1-m2 cell line, it is likely that D2A1 cell clones were selected that possessed mutations conferring a selective advantage by promoting immune evasion and rendering D2A1-m2 cells less immunogenic than D2A1 cells. However, in experimental metastasis assays, both D2A1 and D2A1-m2 cells give rise to significantly increased metastatic burden in the lungs in immunocompromised mice (Jungwirth et al., 2018), suggesting that both cell lines are under a degree of immune control.

Although highly mutated tumours are more likely to produce tumour-specific mutant epitopes functioning as neoantigens, not all mutations give rise to immunogenic peptides. The additional mutations found in D2A1-m2 cells compared to D2A1 cells may not necessarily give rise to neoantigens, and would therefore not play a role in

modulating their immunogenicity. Recently, particularly in the field of cancer vaccines, increasing emphasis has been assigned to recognising mutations that generate neoantigens through the use of predictive algorithms. Identifying candidate neoantigens in the clinic involves exon sequencing of a cancer biopsy, detecting missense mutations in tumour-expressed proteins and predicting which mutant proteins are processed into 8- to 11-reside peptides and loaded onto major histocompatibility complex class I (MHCI) for recognition by CTLs. Often, prediction strategies employ *in silico* analysis to predict the binding affinity of epitopes to MHC molecules (Lu and Robbins, 2016). These techniques are expensive, time-consuming and have not been extensively trialled in murine models of cancer, however, predicting the neoantigens in the D2A1 and D2A1-m2 cell lines would help in determining whether intrinsic cell differences affect responses to immunotherapy.

Regardless of any differences in the mutational profile of the D2A1 and D2A1-m2 cell lines, data presented in Chapters 3 and 4 suggest that the differential CAF content of tumours contributes to shaping their immune microenvironment. To gain a better understanding of the role of the stromal biology of the D2A1 and D2A1-m2 models, primary tumours were subjected to targeted gene expression profiling. Analysis of data acquired from a NanoString Pan Cancer IO 360 panel revealed how D2A1 tumours, compared to D2A1-m2 tumours, have more of an inflamed phenotype, characterised by increased expression of genes such as *Ifng*, *Gzmb* and *Cxcl9*, an increased abundance of immune cells and higher expression of a CD8 T effector signature (Figures 6.3 and 6.5). In contrast, D2A1-m2 tumours are characterised by lower levels of inflammatory gene expression, an increased expression of genes associated with a fibrotic stroma including *Tgfb1* and *Loxl2* and higher expression of TGF-beta signalling and Pan-F-TBRS gene signatures (Figures 6.3 and 6.5). Furthermore, expression of fibroblast-related gene signatures was inversely correlated with a CD8 T effector signature, implicating CAFs in inhibiting CTL activity.

Studies of bulk tumour gene expression lose information on compartment-specific signals within the tumour core and therefore do not reflect the spatial

landscape of the tumour immune microenvironment (Gruosso et al., 2019). Quantitative histopathology revealed how D2A1-m2 tumours have an immune-excluded phenotype, characterised by the presence of CTLs primarily in the tumour border. This suggests that an anti-tumour T cell response is generated, but the T cells are physically unable to reach the tumour bed. This may be a result of a lack of T cell recruiting signals, including chemokines directing T cell trafficking such as Cxcl9 and Cxcl10 (Trujillo et al., 2018), but recent evidence suggests an activated fibrotic stroma plays a key role in limiting CTL infiltration (Anderson et al., 2017; Chen et al., 2019a; Lanitis et al., 2017).

Key to improving the broad potential of immunotherapy is an understanding of the nature of the tumour microenvironment and what factors contribute to development of a non-inflamed phenotype. Therapeutic strategies designed to enhance the efficacy of ICB treatment will likely differ depending on these causative factors. Converting tumours from a non-inflamed to an inflamed phenotype can be achieved preclinically by enhancing tumour antigen presentation, innate immune components or chemokine production. However, the data presented in this chapter suggest that eliminating or altering the fibrotic stroma may also promote immune infiltration and enhance ICB responsiveness. Thus, the D2A1-m2 model represents a powerful preclinical model for assessing the efficacy of CAF modulation, an approach explored further in Chapter 7.

Chapter 7: CAF modulation and the tumour immune microenvironment

7.1 Introduction

Currently, the majority of breast cancer treatments are designed to eradicate tumour cells themselves, but this approach fails to acknowledge the role of the cancer stroma in modulating tumour growth and promoting therapeutic resistance. Cancer-associated fibroblasts (CAFs) are some of the most abundant stromal cells present in the breast tumour microenvironment and have a key involvement in cancer progression. CAFs can directly promote tumour cell growth, invasion and metastasis, but as demonstrated in previous chapters, they can also impair anti-tumour immunity and contribute to resistance to immunotherapy through multiple mechanisms.

Recently, characterisation of CAFs based on specific cell markers has deepened our understanding of their phenotypic heterogeneity and has revealed significant functional diversity and how they can have tumour-suppressive or tumour-promoting activity (Chen and Song, 2018). In theory, targeting specific CAF subsets with known pro-tumourigenic functions could represent a novel approach to treating breast cancer. Furthermore, identifying and therapeutically targeting sub-populations of CAFs with immunosuppressive functions may amplify anti-tumour immune responses and enhance the activity of existing immunotherapeutic strategies. Whilst precisely targeting CAFs is complicated by a lack of specific markers making it difficult to avoid damaging normal tissue, a number of preclinical studies have provided a proof of concept for this strategy. General approaches to targeting CAFs preclinically include: inhibiting their activation and/or function by disrupting crucial chemokine and growth factor pathways, normalising CAFs and encouraging them to adopt an inactive phenotype through the use of molecules such as calciptriol, targeting CAF-derived

extracellular matrix (ECM) proteins and associated signalling and directly depleting CAFs by transgenic technologies (Chen and Song, 2018).

The majority of studies to date have focused on directly depleting specific CAF populations in an effort to elucidate their role in carcinogenesis. More recently, research has focused on unravelling CAF heterogeneity and has revealed how sub-populations of CAFs can have context dependent functions. For example, whilst a subset of αSMA-expressing human breast CAFs was recently identified and shown to promote the generation of an immunosuppressive tumour microenvironment (Costa et al., 2018), earlier experiments in mouse model of spontaneous pancreatic ductal adenocarcinoma (PDAC) demonstrated how depleting αSMA-expressing cells increased the infiltration of immunosuppressive T_{regs}, leading to reduced animal survival (Ozdemir et al., 2014).

An alternative approach to studying the role of CAFs in carcinogenesis is by interrogating the role of stromal or CAF restricted molecules. Because depleting CAFs or reversing their functional states remains challenging, it may be more feasible to identify specific molecular targets that drive CAF biology. Endosialin (CD248) is a transmembrane glycoprotein that was originally described as a cell surface marker for tumour endothelial cells (Rettig et al., 1992), but is now known to be expressed by tumour-associated pericytes and myofibroblasts. Comparative experiments in wild type and endosialin-deficient mice have revealed how stromal endosialin does not affect primary breast tumour growth but does promote spontaneous metastasis (Viski et al., 2016), making it an attractive therapeutic target in breast cancer. Importantly, resting mesenchymal cells in healthy adult tissues have low or undetectable expression of endosialin (Rettig et al., 1992)

A second potential target expressed primarily in the stroma of breast cancer is Endo180 (MRC2, uPARAP), a collagen-binding receptor that plays a key role in the turnover of collagen by various mesenchymal cells (Melander et al., 2015). Endo180 is predominantly expressed by stromal fibroblasts. Mice with a genetic deletion of Endo180 have no overt phenotype (East et al., 2003), however, when implanted with

syngeneic tumour cells they display reduced CAF activation, as determined by the abundance αSMA$^+$ cells, and impaired tumour growth at both primary and metastatic sites (Isacke laboratory; unpublished data). These unpublished data indicate that Endo180 expression is required to support the establishment of a tumour supportive microenvironment

Single-cell RNA-sequencing experiments have recently been employed to define functionally distinct subclasses of CAFs isolated from mouse models of breast cancer (Bartoschek et al., 2018). Interestingly, expression of endosialin is found primarily in CAFs of perivascular origin, whilst Endo180 is expressed mainly in CAFs involved in remodelling of the extracellular matrix (ECM), suggesting that these two markers may be useful in defining, and potentially therapeutically targeting, different breast CAF subsets.

As discussed above, reverting the activated state of pro-tumourigenic CAFs also represents an attractive therapeutic strategy. However, the precise mechanisms through which CAFs are activated and maintained in an active state remain poorly understood. Accumulating evidence suggests that the activated CAF phenotype is regulated through epigenetic modifications (Albrengues et al., 2015). One class of epigenetic targets is the bromodomain and extraterminal (BET) proteins, a protein family known to be overexpressed in multiple cancer types (Doroshow et al., 2017). Whilst inhibitors of BET proteins have proven anti-tumour activity, the mechanisms underling these effects are not clear. Recently, the BET inhibitor JQ1 was shown to inhibit Hedgehog and TGFβ pathways, two major pathways implicated in CAF activation, attenuating desmoplasia and delaying tumour growth (Yamamoto et al., 2016). Whilst BET inhibition has also been implicated in promoting anti-tumour immunity through suppression of PD-L1 expression (Zhu et al., 2016), it is not known whether the stromal modulating effects of JQ1 may also promote anti-tumour immunity in breast cancer.

Given the roles of endosialin and Endo180 in promoting breast cancer progression, the aim of experiments described in this chapter was to determine

whether these stromal receptors contributed to modulation of the breast tumour immune microenvironment and responses to immunotherapy. Furthermore, the efficacy of the stromal modulator JQ1 was assessed in combination with immune checkpoint blockade.

7.2 Results

7.2.1 The role of endosialin in modulating the immune microenvironment

To investigate the role of stromal endosialin on the breast cancer immune microenvironment, 4T1 cells were injected orthotopically into the 4th mammary fat pads of BALB/c wild-type (WT) and endosialin-deficient (EN^{KO}) mice to form syngeneic tumours. Resultant primary tumours were formalin-fixed, paraffin-embedded (FFPE) and sections were stained for the cytotoxic T lymphocyte (CTL) marker CD8. Compared to tumours from WT mice, those from EN^{KO} mice exhibited higher levels of CTL infiltration, though this difference was not significant (Figure 7.1A).

To characterise the immune microenvironment in greater depth, primary tumours of comparable size (Figures 7.1B and C) from a similar experiment were processed to single-cell suspensions, stained with panels of antibodies against a range of immune cell markers (Tables 2.1 and 2.2) and analysed by flow cytometry. The number of viable cells was determined using a LIVE/DEAD Fixable Violet Dead Cell Stain Kit. There were no significant differences in the overall immune (CD45^{+}) content of 4T1 tumours from WT or EN^{KO} mice, assessed either as a proportion of live cells (Figure 7.1D) or by actual counts (Figure 7.1E).

As CTLs are key players in generation of a robust anti-tumour immune response, their abundance and phenotype was also assessed. There were no significant differences in the infiltration of CTLs in 4T1 tumours from WT or EN^{KO} mice (Figure 7.1F) and a similar proportion of infiltrating CTLs expressed the immune checkpoint, programmed cell death protein 1 (PD-1) (Figure 7.1G), and the proliferation marker, Ki67 (Figure 7.1H).

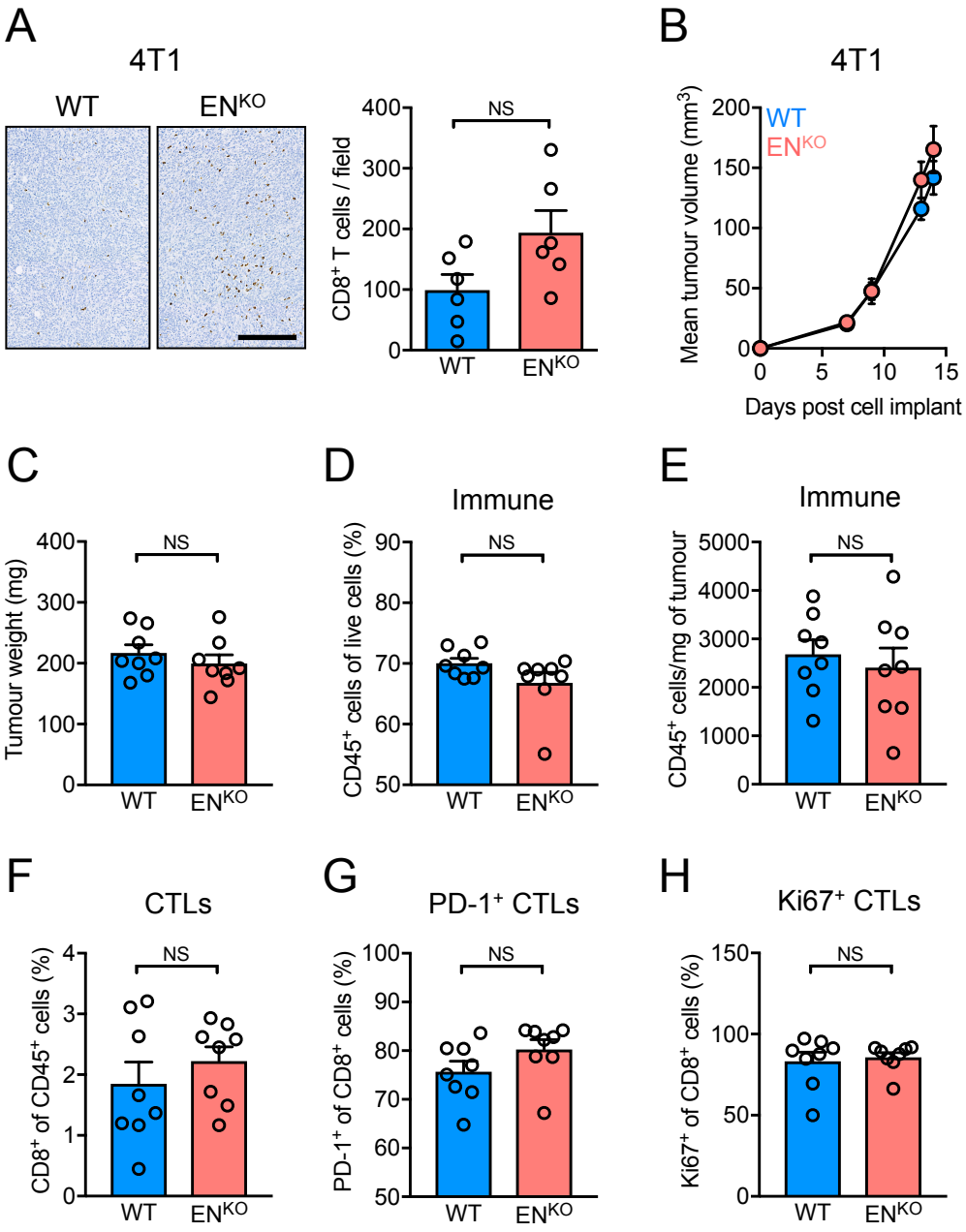

Figure 7.1: Effect of stromal endosialin expression on the 4T1 immune microenvironment. A. 5 x 10^4 4T1 cells were injected orthotopically into the 4th mammary fat pad of BALB/c wild-type (WT) or endosialin-deficient (EN^{KO}) mice (*n* = 6 mice per group). Mice were culled and tumours removed, formalin-fixed and paraffin-embedded. FFPE sections were stained with an anti-CD8 antibody, and positive staining quantified in a blinded fashion using FIJI software. Positive staining of viable tissues was assessed in 6, randomly selected fields of view (FOV) per tumour section and the mean value per field was calculated for each section. Scale bar = 250 µm. **B**-**H**. 5 x 10^4 4T1 cells were injected orthotopically into the 4th mammary fat pad of BALB/c WT or EN^{KO} mice (*n* = 8 mice per group). Mice were culled and tumours removed on day 14. Primary tumours were processed to a single cell suspension, stained with panels of antibodies (Tables 2.1 and 2.2) and analysed on a BD LSRFortessa flow cytometer. Gating for identifying immune cells was performed using FlowJo software as described in Chapter 3. **B**. Mean tumour volume growth curves. **C**. Tumour weights. **D**. Proportion of $CD45^+$ cells gated on live cells. **E**. Number of $CD45^+$ cells per mg of tumour. **F**. Proportion of cytotoxic T lymphocytes (CTLs) gated on $CD45^+$ cells. **G**. Proportion of PD-1 expressing CTLs. **H**. Proportion of Ki67 expressing CTLs. All data are mean ± SEM. Statistical analysis was performed using an unpaired *t*-test: NS = not significant.

Historic microarray studies of purified immune cells have revealed how individual immune cell populations are enriched in specific genes (Newman et al., 2015). Thus, an alternative technique for measuring the abundance of immune cell populations within solid tumours is through multiplex gene expression analysis. RNA extracted from bulk primary tumours of a similar size (Figure 7.2A) was analysed using the NanoString nCounter platform. The PanCancer Immune Profiling Panel was used, which interrogates 770 genes from 24 different immune cell types of the innate and adaptive immune systems. Raw NanoString data was pre-processed using R package NanoString Norm (v1.2.1) and differential mRNA abundance was performed using voom (TMM normalisation), with R package limma (v3.34.9). For immune cell type abundance analysis, NanoString curated genesets representing cell types were used, and genesets with more than two genes were further reduced to the largest positively correlated cluster of genes by first running hierarchical clustering on Spearman's correlation distance, followed by identification of optimal number of clusters using Silhouette score. The original NanoString genesets for each cell type are shown, with kept genes (that showed Spearman's $P > 0.5$) in bold (Figure 7.2B). Example correlation plots for T-cells (Figure 7.2C) and CD8 T-cells (Figure 7.2D) are shown, with kept genes highlighted by purple panels.

Unsupervised hierarchical cluster analysis based on abundance of the 24 immune cell types revealed how 4T1 tumour samples did not fully cluster based on whether they were derived from WT or EN^{KO} mice (Figure 7.3A). Correspondingly, the abundance of all 24 immune cells was similar in tumours, irrespective of their origin. Though abundance values for dendritic cells (DC), eosinophils and neutrophils were higher in WT-derived 4T1 tumours (Figure 7.3B), and values for CTLs (CD8 T-cell), T cells and natural killer cells (NK cell) higher in EN^{KO}-derived 4T1 tumours (Figure 7.3C), these differences were not significant.

Although stromal endosialin has a proven role in promoting breast cancer progression, particularly metastasis (Viski et al., 2016), these data demonstrate how

A

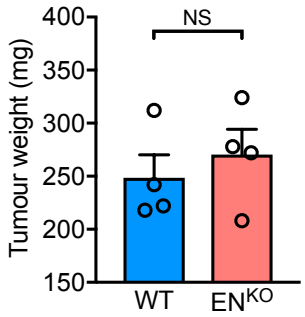

B

NanoString immune cell abundance signatures

Cell type	Genes
aDC	***Oas3***, ***Ido1***, *Ccl1*, *Ebi3*
B-cell	***Ms4a1***, ***H2-Ob***, *Cd19*, *Cr2*
CD8 T-cell	***Cd8b1***, ***Cd8a***, ***Prf1***, *Flt3l*, *Gzmm*
Cytotoxic cell	***Klrd1***, ***Gzma***
DC	***Hsd11b1***, ***Ccl22***, ***Ccl17***
Eosinophils	*Ccr3*, ***Ptgdr2***, ***Smpd3***, ***Thbs1***
iDC	***Syt17***, *F13a1*, ***Cd1d2***
Macrophages	***Ccl7***, ***Msr1***, ***Cd68***, *Chit1*, *Cxcl5*, *Apoe*, *Marco*
Mast cell	***Ms4a2***, ***Tpsab1***, ***Cma1***, *Prg2*, *Kit*
Neutrophils	***Fpr2***, ***Csf3r***
NK CD56bright cell	*Rrad*, ***Pla2g6***, ***Foxj1***
NK CD56dim cell	***Il21r***, ***Gzmb***, *Gtf3c1*
NK cell	***Bcl2***, *Ncr1*, ***Zfp13***
T helper cell	***Cd28***, ***Icos***, ***Batf***, *Nup107*, *Anp32b*
T-cell	***Cd3e***, ***Cd3g***, ***Cd6***, ***Cd2***
Tcm	***Reps1***, ***Atm***, *Nefl*, ***Dock9***
Tem	***Ewsr1***, ***Nfatc4***, ***Ltk***, ***Akt3***, *Ccr2*
TFH	***Bcl6***, *Pdcd1*, ***Maf***
Tgd	***Fez1***, ***Cd160***
Th1 cell	***Ifng***, ***Ctla4***, *Cd38*, *Lta*, *Csf2*, ***Tbx21***, ***Stat4***, ***Il12rb2***
Th2 cell	***Smad2***, ***Stat6***, *Cxcr6*, ***Pmch***, ***Gata3***
Th17 cell	***Il17ra***, ***Rorc***, *Il17a*

C

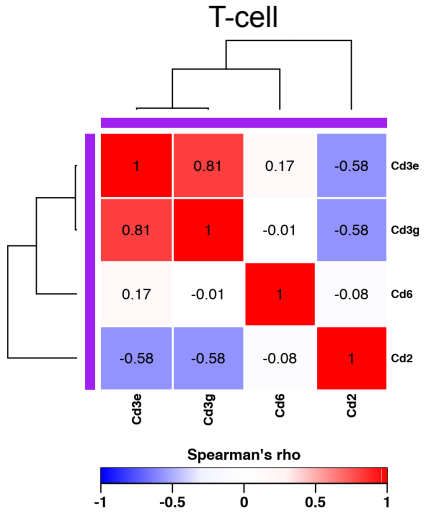

D

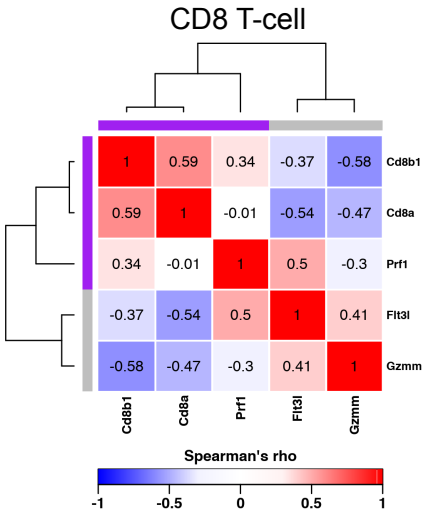

Figure 7.2: Curation of immune cell abundance signatures. Gene expression profiling of 4T1 tumours from wild-type BALB/c (WT) and endosialin-deficient (EN^{KO}) mice (n = 4 mice per group) was performed using the targeted NanoString PanCancer Immune Profiling panel. **A.** Weights of tumours used for gene expression profiling. Data are mean ± SEM. Statistical analysis was performed using an unpaired t-test: NS = not significant. **B-D.** NanoString gene expression profiling data was analysed for immune cell type abundance signatures. As illustrated in (**C**) and (**D**) for the T-cell and CD8 T-cell signatures, genes within individual signatures were analysed by hierarchical clustering on Spearman's correlation distance, followed by identification of optimal clusters using Silhouette score. Genes within signatures that were significantly correlated are indicated in purple in panels (**C**) and (**D**), and in bold in panel (**B**).

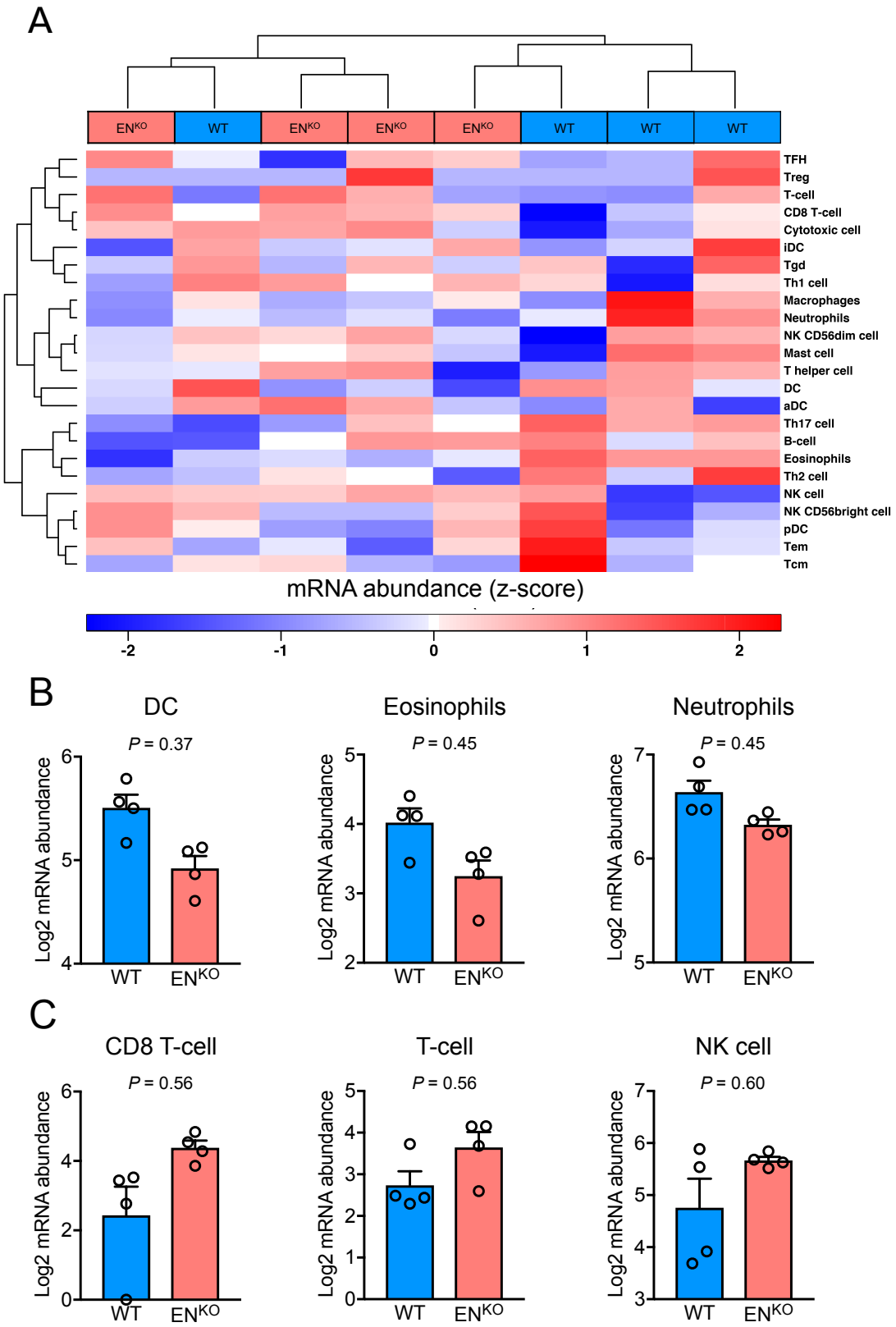

Figure 7.3: Differentially expressed immune cell abundance signatures. A. Unsupervised hierarchical clustering of NanoString gene expression profiling data from Figure 7.2. **B**-**C.** Selected expression signatures increased in 4T1 tumours from BALB/c (**B**) WT and (**C**) EN^{KO} mice. Data are mean ± SEM. Statistical analysis was performed using an unpaired *t*-test.

this metastasis phenotype is not driven by differences in the immune profile of primary tumours.

7.2.2 The role of Endo180 in modulating the immune microenvironment

Genetic deletion of Endo180 in host mice reduces the abundance of αSMA^{+} cells in orthotopic D2A1-m2 tumours (Isacke laboratory; unpublished data). To investigate the role of stromal Endo180 on the breast cancer immune microenvironment and responses to immune checkpoint blockade, D2A1-m2 cells were injected orthotopically into the 4^{th} mammary fat pads of BALB/c wild-type (WT) and Endo180-deficient ($E180^{KO}$) mice to form syngeneic tumours. Once tumours were established, mice were treated with a combination of anti-PD-L1 and anti-CTLA-4 antibodies (COMBO) or a combination of equivalent isotype control antibodies (ISO) (Figures 7.4A and B). COMBO treatment of tumours in $E180^{KO}$ mice did not affect tumour growth alone and although there was a significant reduction in the weight of D2A1-m2 tumours grown in COMBO treated $E180^{KO}$ mice compared to D2A1-m2 tumours grown in ISO treated WT mice, these differences were small and would need further validation (Figure 7.4C).

To further investigate the immune landscape, primary tumours from Figure 7.4 were processed to single-cell suspensions, stained with panels of antibodies against a range of immune cell markers (Tables 2.4 and 2.5) and analysed by flow cytometry. The number of viable cells was determined using a LIVE/DEAD Fixable Violet Dead Cell Stain Kit, and tumours with < 10% viable cells were excluded from subsequent analysis. Only two WT COMBO tumours had > 10% viable cells, so these were excluded from statistical analysis. There were no significant differences in the abundance of total T cells (Figure 7.5A) or CTLs (Figure 7.5B). To characterise the tumour-infiltrating T cells, T cells were also examined for expression of CD44 and CD62L (Figure 7.5C). CD44 is expressed by a variety of cell types, but is rapidly up-regulated in T cells following antigen encounter and its expression is maintained in memory T cells (Schumann et al., 2015). CD62L, also known as L-selectin, is an adhesion molecule found on naïve T cells, that is cleaved from antigen-activated T

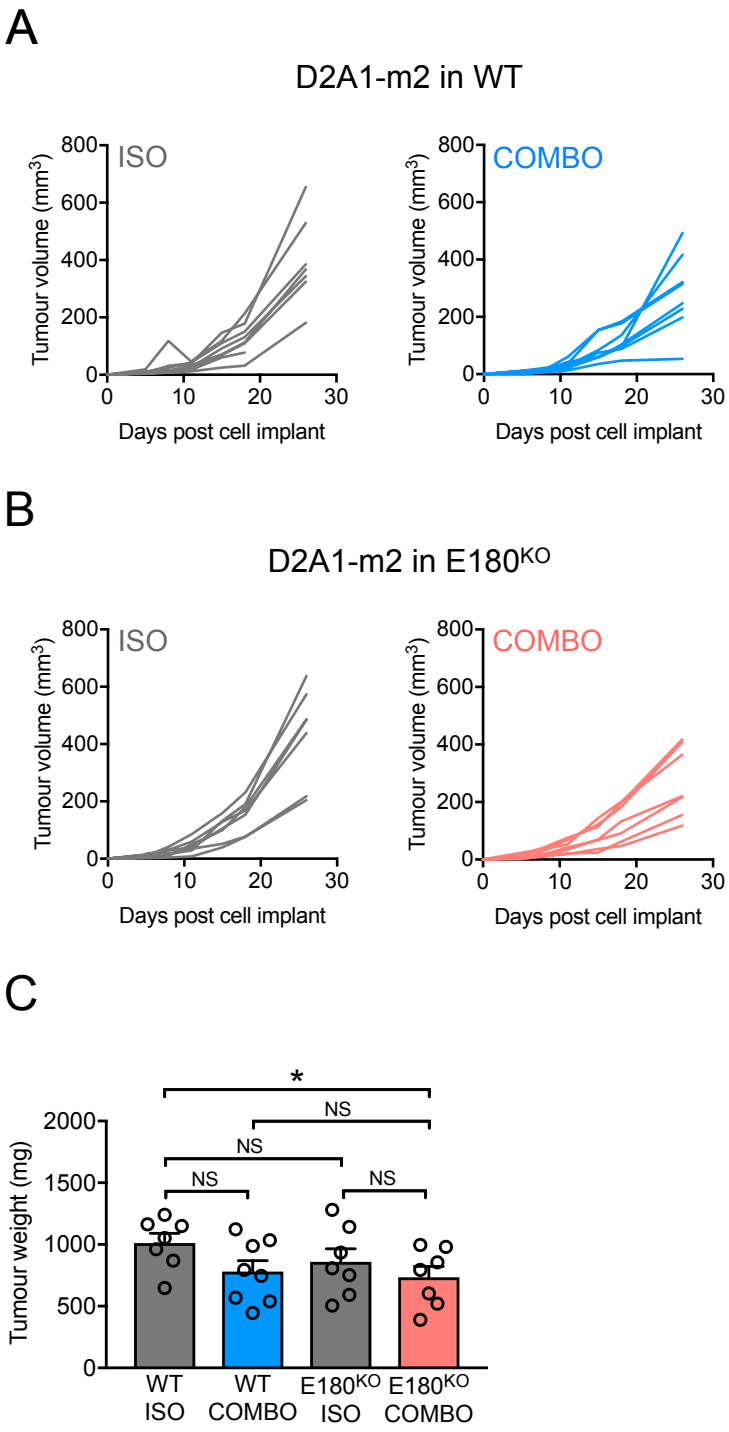

Figure 7.4: Immune checkpoint blockade treatment of D2A1-m2 tumours in BALB/c wild-type or Endo180-deficient mice. 2 x 10^5 D2A1-m2 tumour cells were injected orthotopically into the 4th mammary fat pad of BALB/c wild-type (WT) or Endo180-deficient ($E180^{KO}$) mice (*n* = 7-8 mice per group). Mice were treated with a combination of anti-CTLA-4 (10 mg/kg, IP) and anti-PD-L1 (10 mg/kg, IP) antibodies (COMBO) as described in Chapter 2.2.3.5. Control mice received isotype control antibodies (ISO). **A-B.** Individual tumour growth curves. **C**. Final tumour weights. Data are mean ± SEM. Statistical analysis was performed using an unpaired *t*-test: NS = not significant; * = $P < 0.05$.

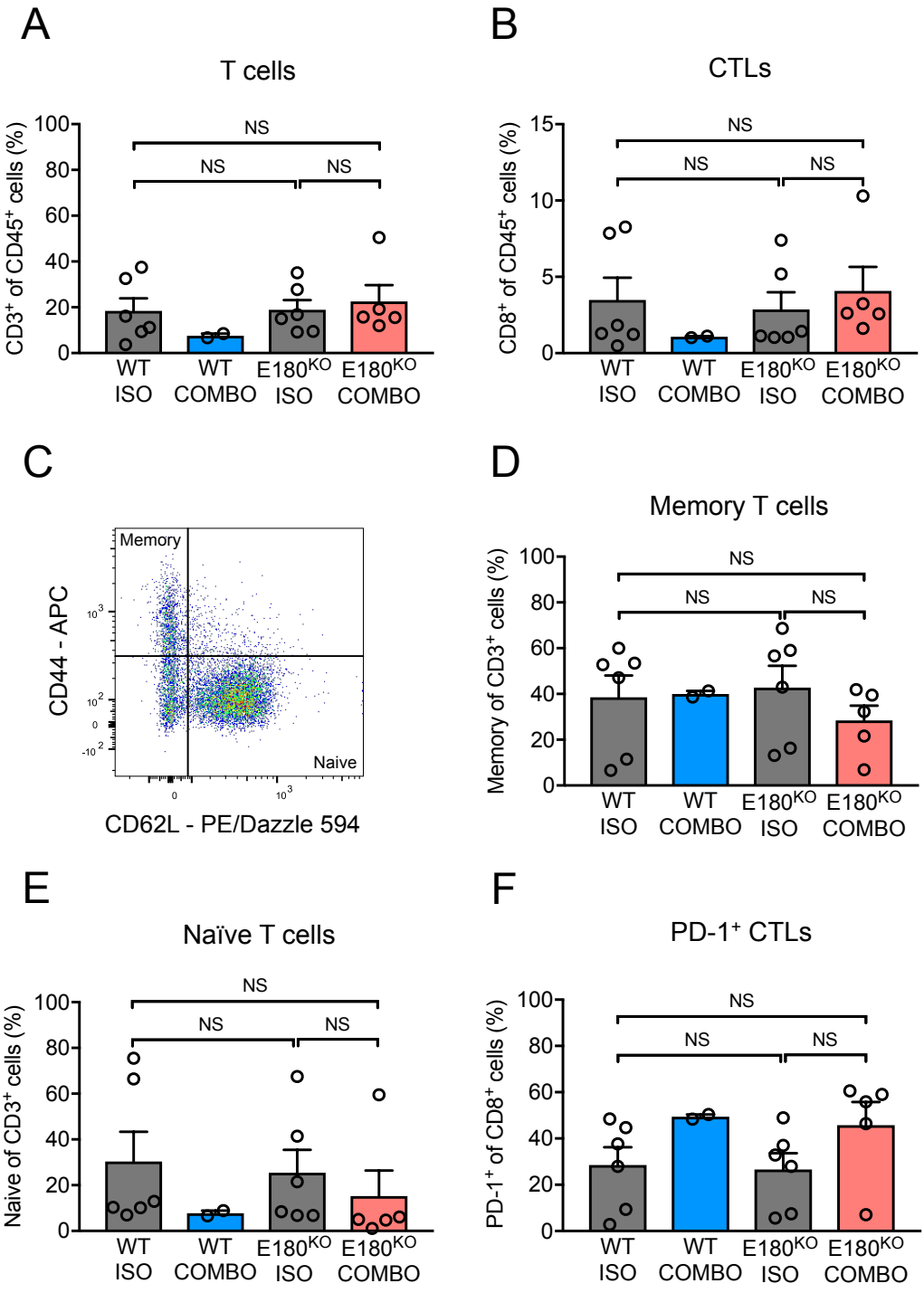

Figure 7.5: Adaptive immune cell content of primary D2A1-m2 tumours from BALB/c wild-type or Endo180-deficient mice treated with immune checkpoint blockade. Primary tumours from Figure 7.4 were processed to single-cell suspensions, stained with panels of antibodies listed in Tables 2.4 and 2.5, and analysed on a BD LSRFortessa flow cytometer. Gating for identification of T cell subsets was performed using FlowJo software as illustrated in Figure 3.6. **A**-**B.** Proportion of (**A**) T cell, and (**B**) CTLs gated on $CD45^+$ cells. **C.** Representative plot of gating strategy employed for identification of naïve and memory T cell subsets. **D**-**E.** Proportion of (**D**) memory, and (**E**) naïve T cells gated on $CD3^+$ cells. **F.** Proportion of PD-1 expressing CTLs. All data are mean ± SEM. Statistical analysis was performed using an unpaired *t*-test: NS = not significant.

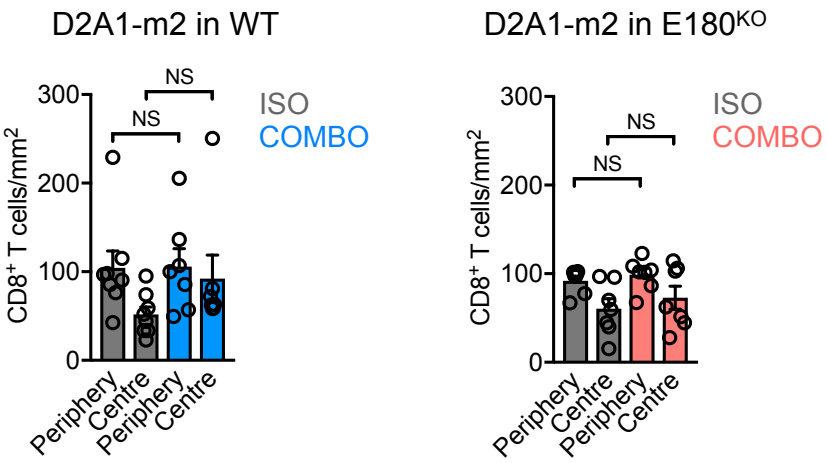

Figure 7.6: Quantitative histopathological analysis of CD8⁺ T cell infiltration in D2A1-m2 tumours from BALB/c wild-type or Endo180-deficient mice. CD8⁺ T cell density in peripheral and central regions of D2A1-m2 tumours from Figure 7.4. Quantification was performed as described in Figure 7.5. Data are mean ± SEM. Statistical analysis was performed using an unpaired *t*-test: NS = not significant.

cells in lymph nodes, allowing them to re-enter the circulation where they can exert their helper or effector functions (Yang et al., 2011). In mice, increased expression of CD44 distinguishes memory T cells from naïve T cells which express higher levels of CD62L (Samji and Khanna, 2017). No significant differences in the abundance of memory or naïve T cell subsets were observed between groups (Figures 7.5 D and E). COMBO treatment increased the proportion of PD-1 expressing CTLs in D2A1-m2 tumours from both WT and E180^{KO} mice, but these differences were not statistically significant (Figure 7.5F).

To determine the spatial distribution of CTLs, tumours in Figure 7.4 were also analysed for the presence of CD8^{+} cells by immunohistochemistry. COMBO treatment had no significant effect on the distribution of CTLs in BALB/c WT or E180^{KO} mice (Figure 7.6).

Together, these data suggest that Endo180 expression has a limited effect on the immune microenvironment of primary D2A1-m2 tumours. However, subtle differences in both tumour growth and the T cell landscape of tumours warrant further investigation.

7.2.3 The role of JQ1 in modulating the immune microenvironment

Treatment with the BET inhibitor, JQ1, was recently reported to suppress expression of CAF effector genes in stromal fibroblasts of pancreatic ductal adenocarcinoma (PDAC) and attenuate tumour growth (Yamamoto et al., 2016). To determine whether JQ1 treatment affected the activation of CAFs *in vitro*, CAF-1 cells (Chapter 4) were treated with 1 μM of the active JQ1 enantiomer, (+) JQ1, or a negative control, (-) JQ1 (Figure 7.7A). After 72 hours, CAF-1 cells were stained with antibodies against alpha smooth muscle actin (αSMA), and cell nuclei were stained with DAPI. JQ1 treatment did not affect the viability of CAFs, and immunofluorescent microscopy revealed loss of αSMA expression in CAF-1 cells (Figure 7.7A), suggesting that JQ1 disrupted CAF activation rather than triggering their depletion.

Having previously demonstrated how D2A1-m2 tumours, which are abundant in activated CAFs, have an immunologically 'cold' tumour microenvironment, pilot experiments were initiated to determine whether JQ1 could reverse this phenotype either alone or in combination with immune checkpoint blockade. D2A1-m2 tumour-bearing mice were treated with anti-PD-L1 and anti-CTLA-4 antibodies (COMBO), JQ1 (JQ1) or a combination of all three agents (COMBO + JQ1) (Figure 7.7B). Control mice received no treatment (Untreated). All treatments were well tolerated and any weight loss was within acceptable limits. Whilst COMBO treatment had little effect on tumour growth, treatment with JQ1 and COMBO + JQ1 delayed tumour growth.

Data described in Chapter 6 suggests that CAFs may be responsible for driving the CTL exclusion phenotype observed in D2A1-m2 tumours. Given the potential of JQ1 to alter the tumour immune cell landscape through CAF modulation, FFPE tumours sections from Figure 7.7 were stained for the CTL marker CD8 (Figure 7.8A). D2A1-m2 tumours from untreated mice exhibited low levels of CTL infiltration and those present were found primarily in peripheral regions of tumours (Figure 7.8B). Whilst treatment with COMBO or JQ1 increased the abundance of CTLs, the majority were still found in the tumour periphery. In contrast, treatment with COMBO + JQ1

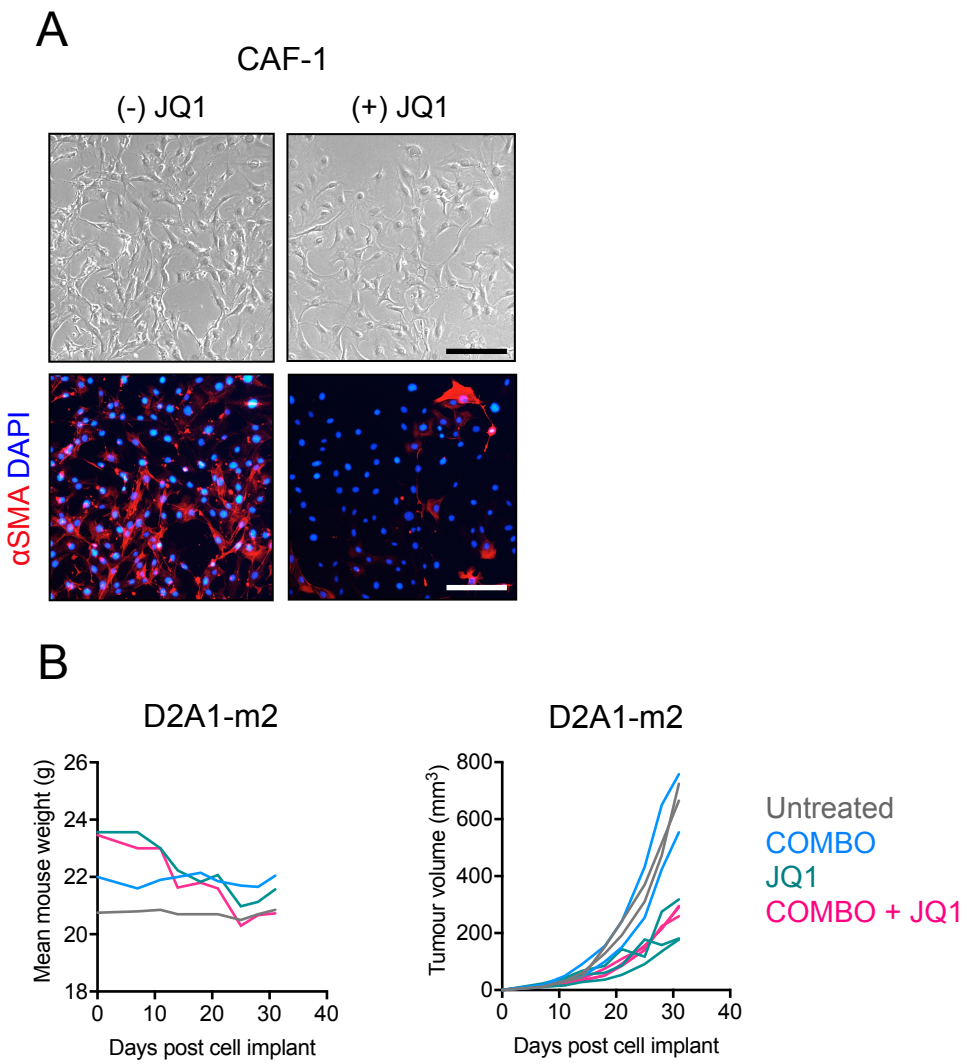

Figure 7.7: Effect of JQ1 on CAF activation and D2A1-m2 tumour growth. A. Immunofluorescent images of CAF-1 cells stained with an anti-αSMA antibody and an Alex Fluor 555 (red) secondary antibody (Table 2.6), following culture in 1 μM active JQ1, (+) JQ1, or a negative control, (-) JQ1, for 72 hours. Nuclei were counterstained with DAPI (blue). Scale bar, 200 μm. **B.** 2 x 10^5 D2A1-m2 cells were injected orthotopically into the 4th mammary fat pad of wild-type BALB/c mice. Mice were either untreated or treated with a combination of anti-CTLA-4 (10 mg/kg, IP) and anti-PD-L1 (10 mg/kg, IP) antibodies (COMBO), JQ1 (50 mg/kg, IP) or a combination of both (COMBO + JQ1) as described in Chapters 2.2.3.5 and 2.2.3.6 (Untreated: *n* = 2 mice; COMBO: *n* = 2 mice; JQ1: *n* = 3 mice; COMBO + JQ1: *n* = 3 mice). Shown are mean mouse weights per group and tumour growth curves for individual mice.

increased CTL infiltration and resulted in redistribution of CTLs from peripheral regions into the centre of D2A1-m2 tumours.

Although primarily a tolerability study, the data described in this section suggests that combining immune checkpoint blockade with JQ1 may reverse the CTL exclusion phenotype and promote anti-tumour immunity.

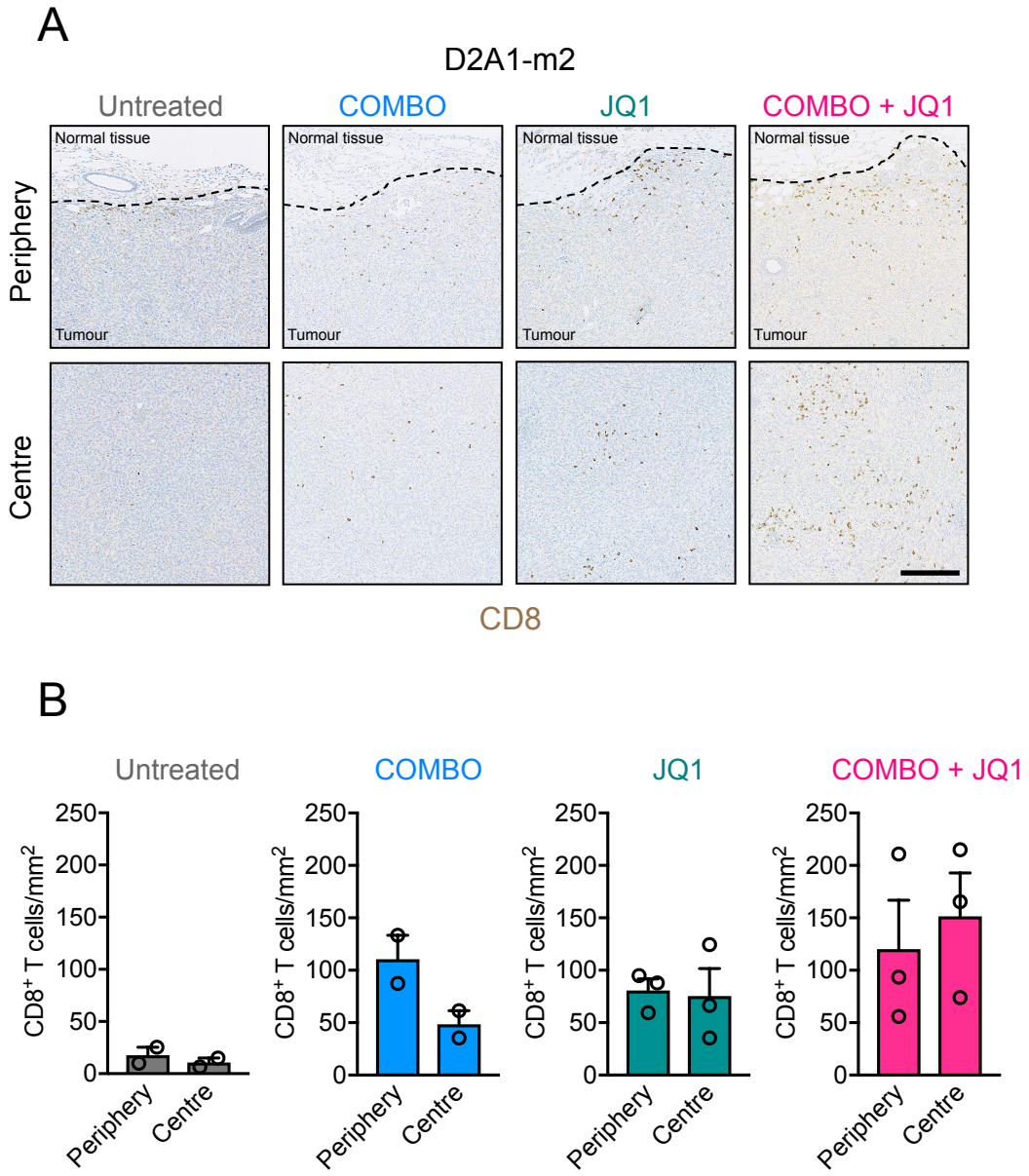

Figure 7.8: Quantitative histopathological analysis of CD8⁺ T cell infiltration in JQ1 treated D2A1-m2 tumours. **A.** Representative immunohistochemistry images of D2A1-m2 tumours from Figure 7.4 from mice treated with combination anti-CTLA-4 and anti-PD-L1 treatment (COMBO), JQ1 (JQ1) or a combination of anti-CTLA-4, anti-PD-L1 and JQ1 treatment (COMBO + JQ1). Tumours were stained for CD8. Peripheral and central tumour regions are shown. Dotted line indicates tumour-stroma boundary. Scale bar, 250 μm. **B.** Quantification of CD8⁺ T cell density in peripheral and central regions of D2A1-m2 tumours. Data are mean ± SEM.

7.3 Discussion

The aim of the experiments described in this chapter was to determine whether CAF modulation, either by altering host expression of stromal receptors known to promote breast cancer progression or through the use of compounds known to normalise CAFs, could modulate the immune microenvironment and improve responses to immune checkpoint blockade.

7.3.1 Endosialin does not affect the breast tumour immune microenvironment

Since presence of stromal endosialin is known to promote spontaneous metastasis in the 4T1 mouse mammary carcinoma model (Viski et al., 2016), and given the well defined role for certain tumour-infiltrating immune cells in promoting metastasis (Coffelt et al., 2015; Kitamura et al., 2015; Qian et al., 2011), it was hypothesised that endosialin may play a role in modulating the immune profile of primary 4T1 tumours. Whilst not a statistically significant difference, initial findings demonstrating a mean increase in CTL density from 99 $CD8^+$ T cells / field for 4T1 tumours from WT mice, to 194 $CD8^+$ T cells / field for 4T1 tumours from EN^{KO} mice (Figure 7.1B), warranted further exploration of potential differences in the immune compartments of these models. Given these differences in CTL infiltration, it was anticipated that a lack of stromal endosialin might skew the immune microenvironment of 4T1 tumours from a 'cold' phenotype (Chapter 3), to a more immunologically 'hot' phenotype.

To explore this prospect, WT- and EN^{KO}-derived primary 4T1 tumours were immune profiled in greater depth using flow cytometry and gene expression analysis. Employing these techniques revealed how the composition and characteristics of immune cells in both models was very similar (Figures 7.1-7.3). Together, these results suggest that endosialin plays a negligible role in modulating the breast tumour immune microenvironment.

Whilst stromal endosialin expression has no effect on the abundance and phenotype of immune cells in 4T1 tumours, it would be of interest to determine whether it plays a role in their distribution within tumours. To explore this possibility, the D2A1-

m2 model, which has a T cell excluded phenotype (Figure 6.7), would be useful. Furthermore, whilst lack of stromal endosialin expression alone does little to alter the composition of the tumour immune microenvironment, using endosialin as a marker for depletion of perivascular CAFs, possibly through the use of anti-endosialin antibodies or anti-endosialin CAR T cells, would likely have a greater impact on the immune microenvironment and could work synergistically with immunotherapeutic strategies.

7.3.2 Endo180 has a limited effect on the breast tumour immune microenvironment

Given the role of Endo180 in CAF activation and the development and maintenance of the extracellular matrix (Melander et al., 2015), it was hypothesised that Endo180 may play a role in modulating the immune profile of D2A1-m2 tumours and affecting their sensitivity to immune checkpoint blockade. Whilst D2A1-m2 tumour growth was not significantly affected by immune checkpoint blockade or Endo180 deletion alone, a combination of these two conditions did significantly decrease the final weight of D2A1-m2 tumours compared to those from ISO treated WT mice (Figure 7.4C), suggesting that combining immune checkpoint blockade with Endo180 targeted therapies could have therapeutic value for breast cancer.

The leukocyte adhesion molecule L-selectin (CD62L) plays an important role in T cell homing, and its expression is downregulated following T cell activation. Paradoxically, $CD62L^+$ expressing T cells are known to have improved anti-tumour capabilities over T cells with full effector activity, with some studies reporting a critical role for CD62L in T cell homing to lymph nodes (Gattinoni et al., 2005; Klebanoff et al., 2005; Watson et al., 2019). However, neither immune checkpoint blockade treatment nor Endo180 expression significantly affected the abundance of $CD44^+$ $CD62L^-$ (Memory) or $CD44^-$ $CD62L^+$ (Naïve) T cells in D2A1-m2 tumours (Figures 7.5D and E).

Immune checkpoint blockade using anti-CTLA-4 and anti-PD-1 antibodies is known to drive expansion of a PD-1 expressing exhausted-like CD8 T cell population in murine tumour models (Wei et al., 2017). Correspondingly, D2A1-m2 tumours from WT and $E180^{KO}$ mice exhibited an increase in the abundance of $PD\text{-}1^+$ CTLs upon COMBO

treatment, though these differences were not statistically significant (Figure 7.5F). The abundance of PD-1^{+} CTLs was similar in both WT and E180^{KO} mice, suggesting that Endo180 expression does not affect this population of T cells.

The density and distribution of CTLs in D2A1-m2 tumours was also assessed using flow cytometry and immunohistochemistry. The CTL landscape of D2A1-m2 tumours was not affected by either immune checkpoint blockade treatment or Endo180 expression (Figures 7.5B and 7.6).

In conclusion, expression of Endo180 had limited effects on the immune microenvironment of D2A1-m2 tumours. However, the tumour growth data described in this section suggests that therapeutically targeting the Endo180 receptor, or possibly depleting Endo180-expressing cells, may synergise with immune checkpoint blockade.

7.3.3 JQ1 modulates CAF activation, delays tumour growth and re-distributes CTLs

An alternative approach to modulating the stroma is through reprogramming CAFs or altering their activation status. Recently, deleting C-X-C chemokine receptor type 4 (*CXCR4*) in αSMA^{+} cells, or pharmacologically inhibiting CXCR4 using the FDA approved drug plerixafor (AMD3100), was shown to alleviate desmoplasia, reduce immunosuppression and sensitised mouse breast cancers to immune checkpoint blockade (Chen et al., 2019a). Though this was one of the first studies to demonstrate in breast cancer how pharmacologically altering CAF activity can reverse immunosuppression, many other agent CAF-modulating agents have exhibited anti-tumour properties through altering the CAF secretome or modulating their extracellular matrix (ECM) remodelling properties (Chen and Song, 2018).

BET inhibition is an approach to stromal remodelling that has proven anti-desmoplastic and anti-tumour activity, and *in vitro* experiments have demonstrated how JQ1 can reverse CAF activation (Figure 7.7A). In addition, D2A1-m2-tumour bearing mice receiving JQ1 either alone or in combination with anti-PD-L1 and anti-CTLA-4 treatment displayed delayed tumour growth and altered the spatial distribution of CTLs (Figures 7.7B and 7.8B). However, whether these effects are dependent on the CAF-

altering activity of JQ1, or are as a result of direct anti-tumour effects of JQ1 reported in other cancer types (Sakaguchi et al., 2018), is unclear. Assessing the abundance of CAFs following *in vivo* JQ1 treatment, either through immunohistochemistry (IHC) or flow cytometry, and performing *in vitro* experiments examining the sensitivity of D2A1-m2 cells to JQ1 treatment, would provide mechanistic insights. Furthermore, BET inhibition is also known to suppress the expression of PD-L1 and promote anti-tumour immunity (Melaiu et al., 2017; Zhu et al., 2016), whilst other studies have demonstrated an anti-inflammatory role for JQ1 (Wagner et al., 2018), suggesting that JQ1 may also directly influence the immune compartment and has broad activity in the context of the tumour microenvironment.

Chapter 8: Discussion and future perspectives

Breast cancer remains a major cause of cancer-associated death in women despite attempts to provide effective therapies. Although the mortality rate for breast cancer is generally declining due to improvements in early detection and the development of novel treatments, only limited successes have been achieved in advanced breast cancer. Thus, there remains a critical need for innovative approaches to treating breast cancer that reduce relapse and death due to this disease. In recent years, accumulating evidence has supported a role for the immune system in determining the long-term survival of breast cancer patients and their responses to standard therapy (Savas et al., 2016). Together with the clinical success of immune checkpoint inhibitors in other solid cancer types, these data have initiated increased efforts to develop immune-based strategies for breast cancer treatment and prevention (Emens, 2018).

Breast cancers are characterised by tremendous molecular complexity (Chapter 1.2), and this is reflected in the diversity of the breast tumour microenvironment. Early on in mammary carcinogenesis, cells of the innate and adaptive immune systems, including natural killer (NK) cells and cytotoxic T lymphocytes (CTLs), work together to eradicate breast cancer cells. However, specific cancer cell variants can escape immune control and develop into breast tumours that possess a microenvironment rich in immunosuppressive cells, such as regulatory T cells (T_{regs}) and myeloid-derived suppressor cells (MDSCs), that promote immune escape and drive tumour progression. Furthermore, established tumours are often characterised by the upregulation of immune checkpoint proteins on both cancer cells and immune cells that serve to inhibit anti-tumour T cell responses. Together, these forces establish a network of immunosuppression within the breast tumour microenvironment that is not easily overcome using immune checkpoint blockade alone.

A major component of the tumour microenvironment, cancer-associated fibroblasts (CAFs), drive breast tumour progression by promoting cancer cell

proliferation and invasion, angiogenesis and extracellular matrix (ECM) remodelling (Costa et al., 2018). In human breast tumours, an abundance of alpha smooth muscle actin (αSMA) expressing stromal myofibroblasts is associated with poor prognosis and predicts disease recurrence (Orimo et al., 2005; Toullec et al., 2010). Furthermore, stromal expression of platelet-derived growth factor receptor beta (PDGFRβ), an important regulator of fibroblasts, is linked to a reduced benefit of tamoxifen in ER^+ breast cancer patients, suggesting that CAFs also contribute to drug resistance (Paulsson et al., 2017).

An accumulating body of evidence now suggests that CAFs can also indirectly affect cancer progression through interactions with other stromal cells, particularly immune cells (Harper and Sainson, 2014). Though CAFs are generally considered to drive immunosuppression within the tumour microenvironment, their contribution to insensitivity to immunotherapy, particularly in breast cancer, remains unclear. Mechanisms describing CAF-immune cell crosstalk within breast cancer have been postulated, but the heterogonous nature of CAFs means that these vary depending on the subset studied (Costa et al., 2018).

This project had four major aims. First, to establish a suitable system for modelling CAF-immune cell crosstalk. Second, to demonstrate an immunomodulatory role for CAFs. Third, to characterise the underlying biology of CAF-driven immunosuppression. And finally, to investigate whether CAF-driven immunosuppression affects responses to immune checkpoint blockade and whether this can be reversed through CAF modulation. These aims were addressed as described in the following sections.

8.1 Modelling CAF-immune cell crosstalk

Early efforts in cancer drug development relied on conventional xenograft models, where human tumour cell lines are implanted into immunodeficient mice. These models allow the efficacy of cytotoxic or targeted drugs to be assessed *in vivo*, primarily by monitoring primary tumour growth. However, cancer immunotherapies are designed to

modulate a patient's own immune system and increase anti-tumour responses, thus, the immunocompromised status of xenograft models means they lack relevance in this setting.

Syngeneic mouse models, in contrast, utilise tumour cells derived from the same genetic background as a given mouse strain and therefore can be implanted into immunocompetent mice. These models have been fundamental in determining the anti-tumour activity of approved immune checkpoint inhibitors that target cytotoxic T lymphocyte-associated protein 4 (CTLA-4), programmed cell death protein 1 (PD-1) or programmed cell death-ligand 1 (PD-L1) (Sanmamed et al., 2019). Mouse mammary carcinoma cell lines, such as 4T1 cells, have also been used extensively in studies that describe the underlying immunobiology of breast cancer. Specifically, the 4T1 model has been used to demonstrate the immunosuppressive role of tumour-associated macrophages (TAMs), MDSCs and T_{regs}, often by observing the effects of their depletion from the tumour microenvironment (Chen et al., 2007; Hamilton et al., 2014; Yoshimura et al., 2013). In addition to their role in the development of immunotherapeutic drugs, the 4T1 model has been employed in efforts to understand CAF biology (Avgustinova et al., 2016; Liao et al., 2009; Takai et al., 2016). Thus, the 4T1 model allows interrogation of the crosstalk between cancer cells and their microenvironment in a molecularly compatible and fully immunocompetent setting.

For this thesis, the 4T07 cell line was also used, as it shares a single origin with the 4T1 cell line but gives rise to primary tumours in BALB/c mice with strikingly different CAF contents (Avgustinova et al., 2016). Reminiscent of the human disease, mice bearing CAF-rich 4T1 tumours exhibit poorer survival than mice bearing 4T07 tumours. This is also true of the D2A1 cell line and the recently generated D2A1-m2 subline, both of which were utilised in this thesis. Mice bearing CAF-rich D2A1-m2 tumours succumb to metastatic disease more readily than those bearing D2A1 tumours (Jungwirth et al., 2018), suggesting that the stromal biology of these two model systems is representative of that in human breast cancers.

Using a combination of immunohistochemistry and flow cytometry, data presented in this thesis demonstrates how, compared to paired tumours with a paucity of CAFs, CAF-rich 4T1 and D2A1-m2 tumours exhibit tumour immune microenvironments characterised by low levels of CTL infiltration and activity (Chapter 3). Interestingly, despite these striking differences in CTL content, the abundance of TAMs and T_{regs} did not differ significantly between models, indicative of a role for CAFs in driving an immunologically 'cold' or immune excluded tumour phenotype.

Caveats to experiments of this kind include determining at what stage to harvest tumours for immune profiling and limitations in capturing the huge diversity of the immune microenvironment using only a subset of immune cell markers. It is widely acknowledged that the immune landscape of breast cancer evolves over time, and that significant heterogeneity in immune composition is observed across tumour subtypes and patients (Azizi et al., 2018). However, of particular importance in studying anti-tumour immunity are changes in the characteristics of T cells, which readily adopt an exhausted phenotype in the tumour microenvironment, marked by downregulation of effector cytokines and diminished responsiveness to antigens (Wei et al., 2018). Whilst data presented in this thesis demonstrate how CTL activity and proliferation is diminished in CAF-rich tumours, the expression levels other markers of CTL exhaustion such as CTLA-4, T cell immunoglobulin and mucin-domain containing (TIM-3) and lymphocyte-activation gene 3 (LAG-3) were not assessed. Both reversible and irreversible states of T cell exhaustion have been identified, and the immunosuppressive effect of CAFs in these models would be better appreciated by more detailed assessment of infiltrating T cells at different time points during tumour progression.

As discussed in Chapter 1.2, metastatic disease remains the underlying cause of death in the majority of breast cancer patients who succumb to the disease. Whilst the role of stromal cells in the primary tumour in promoting cancer cell migration and invasion are well described, fewer studies have focused on understanding the role of the stromal cells at secondary sites (Psaila and Lyden, 2009). Though both CAFs and

immune cells have independently been implicated in modulating the microenvironment at secondary sites and permitting malignant cells to realise their metastatic potential, the role of CAF-immune cell crosstalk at these sites is poorly understood. The models described in this thesis, particularly the more metastatic 4T1 and D2A1-m2 models, could also be used in efforts to determine whether CAFs also play a role in establishing an immunosuppressive metastatic niche that favours metastatic tumour growth. Early experiments suggest that metastatic lesions in the lungs of D2A1-m2 tumour-bearing mice exhibit stromal activation and an immune exclusion phenotype similar to that of primary D2A1-m2 tumours (data not shown). However, detailed examination of the immune composition of metastatic sites has not been performed, and whether CAF-immune crosstalk at secondary sites affects the response of these lesions to immunotherapy remains to be seen.

8.2 Can targeting CAFs reverse immunosuppression?

8.2.1 CAF heterogeneity

Experiments described in Chapter 4 of this thesis showed how CAFs isolated from 4T1 tumours can both promote *in vitro* cancer cell proliferation, and directly inhibit T cell proliferation. Furthermore, co-inoculated CAFs also promote the *in vivo* growth of normally immunogenic tumours and can modulate the tumour immune microenvironment, decreasing the infiltration of T helper (T_H) cells and increasing the accumulation of neutrophils. However, additional experiments also described in Chapter 4 demonstrate how two populations of CAFs (CAF-1 and CAF-2) exhibited differential expression of CAF markers and recruited different immune cell subsets in Matrigel plug assays. This provides a striking illustration of CAF diversity, as both CAF populations were isolated from 4T1 tumours with the same negative selection technique. Thus, although the immunosuppressive and pro-tumour functions of CAFs described in this thesis suggest they may represent a good target for therapeutic intervention, CAF heterogeneity, and the lack of specific CAF markers makes this challenging, particularly in determining how to target CAFs without damaging normal

tissue. Furthermore, approaches to targeting CAFs have given contradicting results, at times promoting worse outcomes (Ozdemir et al., 2014). This suggests that different subtypes of CAFs exist with distinct roles in the pathophysiology of cancer.

Since the initiation of this PhD project, significant progress has been made in attempting to elucidate CAF heterogeneity. In pancreatic cancer, two spatially separated, reversible and mutually exclusive CAF subtypes have recently been identified (Ohlund et al., 2017). Characterised by low levels of αSMA expression, inflammatory CAFs (iCAFs) were located away from neoplastic cells and exhibited elevated expression of cytokines and chemokines known to drive cancer progression including IL6 and IL11. In contrast, myofibroblastic CAFs (myCAFs), defined by high αSMA expression and their periglandular location, lacked expression of inflammatory CAFs. Further experiments showed how these CAFs could dynamically reverse from one phenotype to the other, though the mechanisms governing these changes were not explored.

As discussed in Chapter 1.4, single-cell RNA sequencing and flow cytometry have recently been used to identify CAF subsets in murine and human breast cancer, respectively (Bartoschek et al., 2018; Costa et al., 2018). These CAF subsets exhibited diverse transcriptomic and functional differences, with some directly contributing to immunosuppression within the tumour microenvironment. Similarly, identification of fibroblast activation protein (FAP) expressing stromal cells in mouse and human breast tumours revealed how expression of podoplanin (PDPN) delineates CAF subsets with different origins and functions (Cremasco et al., 2018). Utilising similar flow cytometry-based techniques to those used in Chapter 4, assessing the relative abundance of CAF subsets in the models characterised in this thesis would aid in determining subsets driving immunosuppression in breast cancer and could reveal novel subsets for therapeutic targeting. Furthermore, co-implantation models similar to those used in Chapter 4 could be useful in determining mechanisms of immunosuppression driven by specific, isolated CAF subsets. However, determining the relative contributions of host-

derived versus implanted CAFs in shaping the tumour immune microenvironment continues to be challenging.

In efforts to determine whether expression of stromal restricted receptors, that may identify specific CAF subsets, plays a role in modulating the breast tumour immune microenvironment, primary tumours from wild-type BALB/c and endosialin- or Endo180- deficient mice were immune profiled as part of this thesis. Whilst data described in Chapter 7 suggests that expression of these receptors alone does little to affect the immune landscape of primary tumours, experimentally depleting endosialin- or Endo180-expressing cells may aid in revealing other novel CAF subsets that contribute to immunosuppression and breast cancer progression.

8.2.2 CAF depletion

Given the immunosuppressive role of CAFs described in this thesis and elsewhere, combining therapeutic targeting of CAFs with conventional immunotherapy represents an attractive approach to treating breast cancer. As discussed in Chapter 1.3.2, it has been suggested that combinatorial strategies for enhancing the efficacy of immune checkpoint blockade rely on a comprehensive understanding of the tumour immune landscape. Whilst inflamed tumours are more likely to respond to combinations of immune checkpoint inhibitors that enhance the activity of pre-existing tumour-specific T cells, it is thought that combinatorial strategies targeting CAFs would be most effective in immunologically 'cold' or excluded tumours such as those in the 4T1 and D2A1-m2 models characterised in Chapter 3. Mechanisms postulated for the immunosuppressive functions of CAFs include: abrogation of CTL function (Khalili et al., 2012), inhibition of dendritic cell function (Cheng et al., 2016), promotion of myeloid-derived suppressor cell accumulation (Cheng et al., 2018), induction of PD-L1^{+} neutrophils (Cheng et al., 2018), antigen-specific depletion CTLs (Lakins et al., 2018) and, as discussed further in Section 8.2.3 below, through direct physical exclusion of immune cells (Salmon et al., 2012). Thus, selecting the optimal CAF-targeting therapies will rely on understanding the exact immunosuppressive mechanisms driven by specific CAF

subsets. Furthermore, it will be important not to target any CAF subsets with immunostimulatory or tumour-suppressive functions.

Although a number of preclinical studies demonstrating the rationality of depleting CAFs have been described, few CAF targeting drugs have reached the clinic, likely because they also deplete normal fibroblasts that have many physiological functions. Those that have been tested in patients, including the anti-FAP antibody sibrotuzumab, have demonstrated little anti-tumour efficacy alone (Hofheinz et al., 2003). However, only relatively recently has the immunosuppressive function of CAFs been appreciated. Thus, contemporary studies involving CAF-targeting therapeutic modalities place increased emphasis on understanding any induced alterations in the tumour immune microenvironment.

Recently, the oncolytic adenovirus, enadenotucirev, was engineered to express a stroma-targeted bi-specific T cell engager (BiTE) that binds to FAP on CAFs, and CD3ε on T cells, leading to fibroblast death and potent T cell activation (Freedman et al., 2018). Treatment of fresh clinical biopsies, including malignant ascites, induced T cell-mediated CAF killing, led to depletion of CAF-associated immunosuppressive factors and upregulated expression of proinflammatory cytokines, and clinical trials have now commenced (Machiels et al., 2019).

FAP has proved a particularly attractive target, and other approaches to targeting FAP^+ CAFs include pharmacological inhibitors, monoclonal antibodies, FAP-targeting immunotoxins and a DNA FAP vaccine (Monteran and Erez, 2019). A chimeric antigen receptor (CAR) T cell specific for FAP has also exhibited anti-tumour efficacy in murine mesothelioma and lung cancer models through augmentation of CTL responses (Wang et al., 2014a). However, it remains to be seen whether targeting FAP^+ CAFs can improve the sensitivity of breast cancer to immunotherapy.

8.2.3 Modulating CAF biology

As described in Chapter 5 of this thesis, D2A1-m2 tumours exhibit an immune excluded phenotype, with $CD8^+$ CTLs accumulating around the tumour periphery,

rather than in the vicinity of cancer cells towards the tumour centre. There are two means by which CAFs are thought to mediate this immune restriction: either through physical exclusion mediated by the components of the extracellular matrix they produce or through production of chemokines such as C-X-C motif chemokine ligand 12 (CXCL12) (Joyce and Fearon, 2015; Massague, 2008). Attempts to reverse this phenotype generally involve inhibiting the fibrotic or desmoplastic response associated with activated CAFs, or by targeting downstream effectors of CAFs. Chapter 7 of this thesis describes how JQ1, a BET inhibitor with proven anti-fibrotic functions (Yamamoto et al., 2016), reversed the immune exclusion phenotype of D2A1-m2 tumours and inhibited primary tumour growth, even in a small pilot study. However, in this pilot study there was no evidence of JQ1 treatment acting synergistically with immune checkpoint blockade, and whether the observed anti-tumour effects were a direct result of CAF modulation remains to be seen. More comprehensive *in vivo* studies will aid in determining JQ1's mechanism of action and effects on long-term survival in these preclinical models

The regulatory cytokine transforming growth factor beta (TGFβ) has been intensively studied and is a key player in shaping cancer development. TGFβ exerts tumour-suppressive effects that cancer cells must escape for malignant evolution yet, paradoxically, TGFβ also modifies the tumour microenvironment and promotes cell invasion (Massague, 2008). As discussed in Chapters 1.3 and 1.4, TGFβ signalling also has a role both in CAF activation and immunosuppression. Recently, a TGFβ gene signature in fibroblasts was reported to be associated with poor response to anti-PD-L1 treatment in metastatic urothelial cancer. Response to treatment was associated with $CD8^+$ T effector cell phenotype and a higher mutational burden. Fibroblast TGFβ signalling also correlated with exclusion of CTLs from the tumour parenchyma, instead, CTLs were found in the fibroblast- and collagen-rich peritumoural stroma. In mouse models that recapitulated this immune-excluded phenotype, combining TGFβ-blocking and anti-PD-L1 antibodies reduced stromal cell TGFβ

signalling, promoted T cell penetration into the centre of tumours and caused tumour regression (Mariathasan et al., 2018).

In a similar study, genetically engineered mice that develop metastatic intestinal tumours were shown to display hallmarks of human microsatellite-stable colorectal cancer, including low mutational burden, T cell exclusion and a TGFβ activated stroma. Strikingly, although inhibition of the PD-1/PD-L1 axis had limited efficacy in this system, inhibiting TGFβ induced a potent and enduring tumour cell specific CTL response that could prevent metastasis (Tauriello et al., 2018). Thus, these studies suggest that CAF-derived TGFβ plays a critical role in promoting T cell exclusion, and suggests that targeting TGFβ signalling may have beneficial effects in combination with immunotherapy. Having demonstrated in Chapter 6 how, compared to D2A1 tumours, D2A1-m2 tumours exhibit increased expression of genes associated with TGFβ signalling, and how these inversely correlate with a signature for CTL function, it would be of interest to determine whether these models also respond differently to TGFβ inhibition.

Together, the studies discussed in this section offer varied mechanisms to reduce CAF-induced immunosuppression in the breast tumour microenvironment. This offers exciting opportunities for anti-CAF therapies in the clinic (Chen and Song, 2018), creating the possibility that combining such agents with immune checkpoint blockade could reverse immune exclusion and enhance anti-tumour immune responses. Future research challenges will be to determine the role of different CAF subsets, how best to administer anti-CAF therapies and determining whether CAFs in metastatic lesions can also be modulated to limit breast cancer metastasis.

8.3: Conclusions

To conclude, the data presented in this thesis have demonstrated a direct role for breast CAFs in promoting *in vitro* cancer cell proliferation and in inhibiting T cell proliferation. Through modulation of the tumour immune microenvironment, breast CAFs also promote the growth of normally immunogenic tumours. Furthermore, mouse

mammary carcinomas rich in CAFs display an immunologically ‘cold’ or immune excluded phenotype, are resistant to immune checkpoint blockade and exhibit increased expression of stromal genes, including those involved in TGFβ and Wnt signalling pathways. Finally, early attempts to reverse CAF-induced immunosuppression will inform future investigations into therapeutically targeting breast CAFs in an effort to enhance T cell activation and infiltration and, ultimately, responses to immune checkpoint blockade.

Bibliography

Abe, B. T., and Macian, F. (2013). Uncovering the mechanisms that regulate tumor-induced T-cell anergy. In Oncoimmunology.

Abiko, K., Matsumura, N., Hamanishi, J., Horikawa, N., Murakami, R., Yamaguchi, K., Yoshioka, Y., Baba, T., Konishi, I., and Mandai, M. (2015). IFN-gamma from lymphocytes induces PD-L1 expression and promotes progression of ovarian cancer. British journal of cancer *112*, 1501-1509.

Aboussekhra, A. (2011). Role of cancer-associated fibroblasts in breast cancer development and prognosis. Int J Dev Biol *55*, 841-849.

Albrengues, J., Bertero, T., Grasset, E., Bonan, S., Maiel, M., Bourget, I., Philippe, C., Herraiz Serrano, C., Benamar, S., Croce, O*., et al.* (2015). Epigenetic switch drives the conversion of fibroblasts into proinvasive cancer-associated fibroblasts. In Nat Commun.

Alcover, A., Alarcon, B., and Di Bartolo, V. (2018). Cell Biology of T Cell Receptor Expression and Regulation. Annu Rev Immunol *36*, 103-125.

Alexandrov, L. B., Nik-Zainal, S., Wedge, D. C., Aparicio, S. A., Behjati, S., and Biankin, A. V. (2013). Signatures of mutational processes in human cancer. Nature *500*.

Ali, H. R., Chlon, L., Pharoah, P. D., Markowetz, F., and Caldas, C. (2016). Patterns of Immune Infiltration in Breast Cancer and Their Clinical Implications: A Gene-Expression-Based Retrospective Study. PLoS Med *13*, e1002194.

Anderson, K. G., Stromnes, I. M., and Greenberg, P. D. (2017). Obstacles posed by the tumor microenvironment to T cell activity: a case for synergistic therapies. Cancer Cell *31*, 311-325.

Ansell, S. M., Lesokhin, A. M., Borrello, I., Halwani, A., Scott, E. C., Gutierrez, M., Schuster, S. J., Millenson, M. M., Cattry, D., Freeman, G. J.*, et al.* (2015). PD-1 blockade with nivolumab in relapsed or refractory Hodgkin's lymphoma. N Engl J Med *372*, 311-319.

Antonia, S. J., Villegas, A., Daniel, D., Vicente, D., Murakami, S., Hui, R., Yokoi, T., Chiappori, A., Lee, K. H., de Wit, M*., et al.* (2017). Durvalumab after Chemoradiotherapy in Stage III Non–Small-Cell Lung Cancer. http://dxdoiorg/101056/NEJMoa1709937.

Arce Vargas, F., Furness, A. J. S., Litchfield, K., Joshi, K., Rosenthal, R., Ghorani, E., Solomon, I., Lesko, M. H., Ruef, N., Roddie, C*., et al.* (2018). Fc Effector Function Contributes to the Activity of Human Anti-CTLA-4 Antibodies. Cancer Cell *33*, 649-663.e644.

Arnould, L., Gelly, M., Penault-Llorca, F., Benoit, L., Bonnetain, F., Migeon, C., Cabaret, V., Fermeaux, V., Bertheau, P., Garnier, J*., et al.* (2006). Trastuzumab-based treatment of HER2-positive breast cancer: an antibody-dependent cellular cytotoxicity mechanism? In Br J Cancer, pp. 259-267.

Aslakson, C. J., and Miller, F. R. (1992). Selective events in the metastatic process defined by analysis of the sequential dissemination of subpopulations of a mouse mammary tumor. Cancer Res *52*, 1399-1405.

Avgustinova, A., Iravani, M., Robertson, D., Fearns, A., Gao, Q., Klingbeil, P., Hanby, A. M., Speirs, V., Sahai, E., Calvo, F., and Isacke, C. M. (2016). Tumour cell-derived Wnt7a recruits and activates fibroblasts to promote tumour aggressiveness. Nat Commun *7*.

Ayers, M., Lunceford, J., Nebozhyn, M., Murphy, E., Loboda, A., Kaufman, D. R., Albright, A., Cheng, J. D., Kang, S. P., Shankaran, V*., et al.* (2017). IFN-gamma-related mRNA profile predicts clinical response to PD-1 blockade. J Clin Invest *127*, 2930-2940.

Azizi, E., Carr, A. J., Plitas, G., Cornish, A. E., Konopacki, C., Prabhakaran, S., Nainys, J., Wu, K., Kiseliovas, V., Setty, M.*, et al.* (2018). Single-Cell Map of Diverse Immune Phenotypes in the Breast Tumor Microenvironment. Cell.

Badwe, R., Hawaldar, R., Nair, N., Kaushik, R., Parmar, V., Siddique, S., Budrukkar, A., Mittra, I., and Gupta, S. (2015). Locoregional treatment versus no treatment of the primary tumour in metastatic breast cancer: an open-label randomised controlled trial. Lancet Oncol *16*, 1380-1388.

Balsamo, M., Scordamaglia, F., Pietra, G., Manzini, C., Cantoni, C., Boitano, M., Queirolo, P., Vermi, W., Facchetti, F., Moretta, A.*, et al.* (2009). Melanoma-associated fibroblasts modulate NK cell phenotype and antitumor cytotoxicity. Proc Natl Acad Sci U S A *106*, 20847-20852.

Bankhead, P., Loughrey, M. B., Fernández, J. A., Dombrowski, Y., McArt, D. G., Dunne, P. D., McQuaid, S., Gray, R. T., Murray, L. J., Coleman, H. G.*, et al.* (2017). QuPath: Open source software for digital pathology image analysis. Scientific Reports *7*, 1-7.

Bartoschek, M., Oskolkov, N., Bocci, M., Lovrot, J., Larsson, C., Sommarin, M., Madsen, C. D., Lindgren, D., Pekar, G., Karlsson, G.*, et al.* (2018). Spatially and functionally distinct subclasses of breast cancer-associated fibroblasts revealed by single cell RNA sequencing. Nat Commun *9*, 5150.

Bates, J. P., Derakhshandeh, R., Jones, L., and Webb, T. J. (2018). Mechanisms of immune evasion in breast cancer. In BMC Cancer.

Beatty, G. L., Winograd, R., Evans, R. A., Long, K. B., Luque, S. L., Lee, J. W., Clendenin, C., Gladney, W. L., Knoblock, D. M., Guirnalda, P. D., and Vonderheide, R. H. (2015). Exclusion of T Cells From Pancreatic Carcinomas in Mice Is Regulated by Ly6C(low) F4/80(+) Extratumoral Macrophages. Gastroenterology *149*, 201-210.

Binnewies, M., Roberts, E. W., Kersten, K., Chan, V., Fearon, D. F., Merad, M., Coussens, L. M., Gabrilovich, D. I., Ostrand-Rosenberg, S., Hedrick, C. C.*, et al.* (2018). Understanding the tumor immune microenvironment (TIME) for effective therapy. Nat Med *24*, 541-550.

Blake-Mortimer, J. S., Sephton, S. E., Carlson, R. W., Stites, D., and Spiegel, D. (2004). Cytotoxic T lymphocyte count and survival time in women with metastatic breast cancer. Breast J *10*, 195-199.

Blankenstein, T., Coulie, P. G., Gilboa, E., and Jaffee, E. M. (2012). The determinants of tumour immunogenicity. Nature Reviews Cancer *12*, 307-313.

Bubenik, J. (2003). Tumour MHC class I downregulation and immunotherapy (Review). Oncol Rep *10*, 2005-2008.

Budhu, S., Wolchok, J., and Merghoub, T. (2014). The importance of animal models in tumor immunity and immunotherapy. Curr Opin Genet Dev *24*, 46-51.

Buell, J. F., Gross, T. G., and Woodle, E. S. (2005). Malignancy after transplantation. Transplantation *80*, S254-264.

Burnet, M. (1957). Cancer: a biological approach. III. Viruses associated with neoplastic conditions. IV. Practical applications. Br Med J *1*, 841-847.

Burstein, H. J., Polyak, K., Wong, J. S., Lester, S. C., and Kaelin, C. M. (2004). Ductal carcinoma in situ of the breast. N Engl J Med *350*, 1430-1441.

Calvo, F., Ege, N., Grande-Garcia, A., Hooper, S., Jenkins, R. P., Chaudhry, S. I., Harrington, K., Williamson, P., Moeendarbary, E., Charras, G., and Sahai, E. (2013). Mechanotransduction and YAP-dependent matrix remodelling is required for the generation and maintenance of cancer-associated fibroblasts. Nature Cell Biology *15*, 637.

Camus, M., Tosolini, M., Mlecnik, B., Pages, F., Kirilovsky, A., Berger, A., Costes, A., Bindea, G., Charoentong, P., Bruneval, P.*, et al.* (2009). Coordination of intratumoral immune reaction and human colorectal cancer recurrence. Cancer Res *69*, 2685-2693.

Cannarile, M. A., Weisser, M., Jacob, W., Jegg, A.-M., Ries, C. H., and Rüttinger, D. (2017). Colony-stimulating factor 1 receptor (CSF1R) inhibitors in cancer therapy. Journal for ImmunoTherapy of Cancer *5*, 1-13.

Chambers, A. F., Groom, A. C., and MacDonald, I. C. (2002). Dissemination and growth of cancer cells in metastatic sites. Nat Rev Cancer *2*, 563-572.

Charles A Janeway, J., Travers, P., Walport, M., and Shlomchik, M. J. (2001). Principles of innate and adaptive immunity.

Cheang, M. C., Chia, S. K., Voduc, D., Gao, D., Leung, S., Snider, J., Watson, M., Davies, S., Bernard, P. S., Parker, J. S.*, et al.* (2009). Ki67 index, HER2 status, and prognosis of patients with luminal B breast cancer. J Natl Cancer Inst *101*, 736-750.

Chen, D. S., and Mellman, I. (2013). Oncology meets immunology: the cancer-immunity cycle. Immunity *39*, 1-10.

Chen, I. X., Chauhan, V. P., Posada, J., Ng, M. R., Wu, M. W., Adstamongkonkul, P., Huang, P., Lindeman, N., Langer, R., and Jain, R. K. (2019a). Blocking CXCR4 alleviates desmoplasia, increases T-lymphocyte infiltration, and improves immunotherapy in metastatic breast cancer. Proc Natl Acad Sci U S A.

Chen, L., Huang, T. G., Meseck, M., Mandeli, J., Fallon, J., and Woo, S. L. (2007). Rejection of metastatic 4T1 breast cancer by attenuation of Treg cells in combination with immune stimulation. Mol Ther *15*, 2194-2202.

Chen, X., and Song, E. (2018). Turning foes to friends: targeting cancer-associated fibroblasts. Nat Rev Drug Discov.

Chen, X., Song, X., Li, K., and Zhang, T. (2019b). FcγR-Binding Is an Important Functional Attribute for Immune Checkpoint Antibodies in Cancer Immunotherapy. Front Immunol *10*.

Cheng, J. T., Deng, Y. N., Yi, H. M., Wang, G. Y., Fu, B. S., Chen, W. J., Liu, W., Tai, Y., Peng, Y. W., and Zhang, Q. (2016). Hepatic carcinoma-associated fibroblasts induce IDO-producing regulatory dendritic cells through IL-6-mediated STAT3 activation. Oncogenesis *5*, e198.

Cheng, Y., Li, H., Deng, Y., Tai, Y., Zeng, K., Zhang, Y., Liu, W., Zhang, Q., and Yang, Y. (2018). Cancer-associated fibroblasts induce PDL1+ neutrophils through the IL6-STAT3 pathway that foster immune suppression in hepatocellular carcinoma. Cell Death Dis *9*, 422.

Chiarella, P., Bruzzo, J., Meiss, R. P., and Ruggiero, R. A. (2012). Concomitant tumor resistance. Cancer Lett *324*, 133-141.

Choi, J., Gyamfi, J., Jang, H., and Koo, J. S. (2018). The role of tumor-associated macrophage in breast cancer biology. Histol Histopathol *33*, 133-145.

Clark, R. A., McCoy, G. A., Folkvord, J. M., and McPherson, J. M. (1997). TGF-beta 1 stimulates cultured human fibroblasts to proliferate and produce tissue-like fibroplasia: a fibronectin matrix-dependent event. J Cell Physiol *170*, 69-80.

Clynes, R. A., Towers, T. L., Presta, L. G., and Ravetch, J. V. (2000). Inhibitory Fc receptors modulate in vivo cytotoxicity against tumor targets. Nat Med *6*, 443-446.

Coffelt, S. B., Kersten, K., Doornebal, C. W., Weiden, J., Vrijland, K., Hau, C. S., Verstegen, N. J., Ciampricotti, M., Hawinkels, L. J., Jonkers, J., and de Visser, K. E. (2015). IL-17-producing gammadelta T cells and neutrophils conspire to promote breast cancer metastasis. Nature *522*, 345-348.

Coffelt, S. B., Wellenstein, M. D., and de Visser, K. E. (2016). Neutrophils in cancer: neutral no more. Nature reviews Cancer *16*, 431-446.

Cohen, N., Shani, O., Raz, Y., Sharon, Y., Hoffman, D., Abramovitz, L., and Erez, N. (2017). Fibroblasts drive an immunosuppressive and growth-promoting microenvironment in breast cancer via secretion of Chitinase 3-like 1. Oncogene.

Coltrini, D., Di Salle, E., Ronca, R., Belleri, M., Testini, C., and Presta, M. (2013). Matrigel plug assay: evaluation of the angiogenic response by reverse transcription-quantitative PCR. Angiogenesis *16*, 469-477.

Comito, G., Giannoni, E., Segura, C. P., Barcellos-de-Souza, P., Raspollini, M. R., Baroni, G., Lanciotti, M., Serni, S., and Chiarugi, P. (2014). Cancer-associated fibroblasts and M2-polarized macrophages synergize during prostate carcinoma progression. Oncogene *33*, 2423-2431.

Corthay, A. (2009). How do Regulatory T Cells Work? Scand J Immunol *70*, 326-336.

Costa, A., Kieffer, Y., Scholer-Dahirel, A., Pelon, F., Bourachot, B., Cardon, M., Sirven, P., Magagna, I., Fuhrmann, L., Bernard, C.*, et al.* (2018). Fibroblast Heterogeneity and Immunosuppressive Environment in Human Breast Cancer. Cancer Cell *33*, 463-479.e410.

Cremasco, V., Astarita, J. L., Grauel, A. L., Keerthivasan, S., MacIsaac, K., Woodruff, M. C., Wu, M., Spel, L., Santoro, S., Amoozgar, Z.*, et al.* (2018). FAP Delineates Heterogeneous and Functionally Divergent Stromal Cells in Immune-Excluded Breast Tumors. Cancer Immunol Res *6*, 1472-1485.

Cristescu, R., Mogg, R., Ayers, M., Albright, A., Murphy, E., Yearley, J., Sher, X., Liu, X. Q., Lu, H., Nebozhyn, M.*, et al.* (2018). Pan-tumor genomic biomarkers for PD-1 checkpoint blockade-based immunotherapy. Science *362*.

Curtis, C., Shah, S. P., Chin, S. F., Turashvili, G., Rueda, O. M., Dunning, M. J., Speed, D., Lynch, A. G., Samarajiwa, S., Yuan, Y.*, et al.* (2012). The genomic and transcriptomic architecture of 2,000 breast tumours reveals novel subgroups. Nature *486*, 346-352.

Darby, I. A., Laverdet, B., Bonté, F., and Desmoulière, A. (2014). Fibroblasts and myofibroblasts in wound healing. In Clin Cosmet Investig Dermatol, pp. 301-311.

Desmouliere, A., Guyot, C., and Gabbiani, G. (2004). The stroma reaction myofibroblast: a key player in the control of tumor cell behavior. The International journal of developmental biology *48*, 509-517.

Disis, M. L., and Stanton, S. E. (2015). Triple-negative breast cancer: immune modulation as the new treatment paradigm. Am Soc Clin Oncol Educ Book, e25-30.

Dong, H., Strome, S. E., Salomao, D. R., Tamura, H., Hirano, F., Flies, D. B., Roche, P. C., Lu, J., Zhu, G., Tamada, K.*, et al.* (2002). Tumor-associated B7-H1 promotes T-cell apoptosis: a potential mechanism of immune evasion. Nat Med *8*, 793-800.

Donovan, J. A., and Koretzky, G. A. (1993). CD45 and the immune response. J Am Soc Nephrol *4*, 976-985.

Dorfman, D. M., Hwang, E. S., Shahsafaei, A., and Glimcher, L. H. (2005). T-bet, a T cell-associated transcription factor, is expressed in Hodgkin's lymphoma. Hum Pathol *36*, 10-15.

Doroshow, D. B., Eder, J. P., and LoRusso, P. M. (2017). BET inhibitors: a novel epigenetic approach. Ann Oncol *28*, 1776-1787.

Drasin, D. J., Robin, T. P., and Ford, H. L. (2011). Breast cancer epithelial-to-mesenchymal transition: examining the functional consequences of plasticity. Breast Cancer Research *13*, 1-13.

Dudley, M. E., Wunderlich, J. R., Shelton, T. E., Even, J., and Rosenberg, S. A. (2003). Generation of tumor-infiltrating lymphocyte cultures for use in adoptive transfer therapy for melanoma patients. J Immunother *26*, 332-342.

Dunn, G. P., Old, L. J., and Schreiber, R. D. (2004). The three Es of cancer immunoediting. Annu Rev Immunol *22*, 329-360.

Dvorak, H. F. (1986). Tumors: wounds that do not heal. Similarities between tumor stroma generation and wound healing. N Engl J Med *315*, 1650-1659.

East, L., McCarthy, A., Wienke, D., Sturge, J., Ashworth, A., and Isacke, C. M. (2003). A targeted deletion in the endocytic receptor gene Endo180 results in a defect in collagen uptake. EMBO Rep *4*, 710-716.

Eck, S. M., Blackburn, J. S., Schmucker, A. C., Burrage, P. S., and Brinckerhoff, C. E. (2009). Matrix Metalloproteinase and G Protein Coupled Receptors: Co-conspirators in the pathogenesis of autoimmune disease and cancer. J Autoimmun *33*, 214-221.

Egelston, C. A., Avalos, C., Tu, T. Y., Simons, D. L., Jimenez, G., Jung, J. Y., Melstrom, L., Margolin, K., Yim, J. H., Kruper, L.*, et al.* (2018). Human breast tumor-infiltrating CD8+ T cells retain polyfunctionality despite PD-1 expression. In Nat Commun.

Elston, C. W., and Ellis, I. O. (1991). Pathological prognostic factors in breast cancer. I. The value of histological grade in breast cancer: experience from a large study with long-term follow-up. Histopathology *19*, 403-410.

Emens, L. A. (2018). Breast Cancer Immunotherapy: Facts and Hopes.

Emer, J. J., and Claire, W. (2009). Rituximab: A Review of Dermatological Applications. J Clin Aesthet Dermatol *2*, 29-37.

Erez, N., Truitt, M., Olson, P., Arron, S. T., and Hanahan, D. (2010). Cancer-Associated Fibroblasts Are Activated in Incipient Neoplasia to Orchestrate Tumor-Promoting Inflammation in an NF-kappaB-Dependent Manner. Cancer Cell *17*, 135-147.

Fancello, L., Gandini, S., Pelicci, P. G., and Mazzarella, L. (2019). Tumor mutational burden quantification from targeted gene panels: major advancements and challenges. Journal for ImmunoTherapy of Cancer *7*, 1-13.

Farkona, S., Diamandis, E. P., and Blasutig, I. M. (2016). Cancer immunotherapy: the beginning of the end of cancer? BMC Medicine *14*, 73.

Feig, C., Jones, J. O., Kraman, M., Wells, R. J., Deonarine, A., Chan, D. S., Connell, C. M., Roberts, E. W., Zhao, Q., Caballero, O. L.*, et al.* (2013). Targeting CXCL12 from FAP-expressing carcinoma-associated fibroblasts synergizes with anti-PD-L1 immunotherapy in pancreatic cancer. Proceedings of the National Academy of Sciences of the United States of America *110*, 20212-20217.

Francisco, L. M., Sage, P. T., and Sharpe, A. H. (2010). The PD-1 pathway in tolerance and autoimmunity. Immunol Rev *236*, 219-242.

Franklin, R. A., Liao, W., Sarkar, A., Kim, M. V., Bivona, M. R., Liu, K., Pamer, E. G., and Li, M. O. (2014). The cellular and molecular origin of tumor-associated macrophages. Science *344*, 921-925.

Freedman, J. D., Duffy, M. R., Lei-Rossmann, J., Muntzer, A., Scott, E. M., Hagel, J., Campo, L., Bryant, R. J., Verrill, C., Lambert, A.*, et al.* (2018). An Oncolytic Virus Expressing a T-cell Engager Simultaneously Targets Cancer and Immunosuppressive Stromal Cells. Cancer Res *78*, 6852-6865.

Fyfe, G., Fisher, R. I., Rosenberg, S. A., Sznol, M., Parkinson, D. R., and Louie, A. C. (1995). Results of treatment of 255 patients with metastatic renal cell carcinoma who received high-dose recombinant interleukin-2 therapy. J Clin Oncol *13*, 688-696.

Gajewski, T. F., Schreiber, H., and Fu, Y. X. (2013). Innate and adaptive immune cells in the tumor microenvironment. Nat Immunol *14*, 1014-1022.

Galon, J., and Bruni, D. (2019). Approaches to treat immune hot, altered and cold tumours with combination immunotherapies. Nat Rev Drug Discov.

Galon, J., Costes, A., Sanchez-Cabo, F., Kirilovsky, A., Mlecnik, B., Lagorce-Pagès, C., Tosolini, M., Camus, M., Berger, A., Wind, P.*, et al.* (2006). Type, Density, and Location of Immune Cells Within Human Colorectal Tumors Predict Clinical Outcome. Science *313*, 1960-1964.

Gardner, T. A., Elzey, B. D., and Hahn, N. M. (2012). Sipuleucel-T (Provenge) autologous vaccine approved for treatment of men with asymptomatic or minimally symptomatic castrate-resistant metastatic prostate cancer. Hum Vaccin Immunother *8*, 534-539.

Garg, A. D., and Agostinis, P. (2017). Cell death and immunity in cancer: From danger signals to mimicry of pathogen defense responses. Immunol Rev *280*, 126-148.

Garon, E. B., Rizvi, N. A., Hui, R., Leighl, N., Balmanoukian, A. S., Eder, J. P., Patnaik, A., Aggarwal, C., Gubens, M., Horn, L.*, et al.* (2015). Pembrolizumab for the treatment of non-small-cell lung cancer. N Engl J Med *372*, 2018-2028.

Gattinoni, L., Klebanoff, C. A., Palmer, D. C., Wrzesinski, C., Kerstann, K., Yu, Z., Finkelstein, S. E., Theoret, M. R., Rosenberg, S. A., and Restifo, N. P. (2005). Acquisition of full effector function in vitro paradoxically impairs the in vivo antitumor efficacy of adoptively transferred CD8+ T cells. J Clin Invest *115*, 1616-1626.

Gonda, K., Shibata, M., Ohtake, T., Matsumoto, Y., Tachibana, K., Abe, N., Ohto, H., Sakurai, K., and Takenoshita, S. (2017). Myeloid-derived suppressor cells are increased and correlated with type 2 immune responses, malnutrition, inflammation, and poor prognosis in patients with breast cancer. Oncol Lett *14*, 1766-1774.

Goodman, A. M., Kato, S., Bazhenova, L., Patel, S. P., Frampton, G. M., and Miller, V. (2017). Tumor mutational burden as an independent predictor of response to immunotherapy in diverse cancers. Mol Cancer Ther *16*.

Goodpaster, T., Legesse-Miller, A., Hameed, M. R., Aisner, S. C., Randolph-Habecker, J., and Coller, H. A. (2008). An Immunohistochemical Method for Identifying Fibroblasts in Formalin-fixed, Paraffin-embedded Tissue. In J Histochem Cytochem, pp. 347-358.

Griguolo, G., Dieci, M. V., Guarneri, V., and Conte, P. (2018). Olaparib for the treatment of breast cancer. Expert Rev Anticancer Ther *18*, 519-530.

Gruosso, T., Gigoux, M., Manem, V. S. K., Bertos, N., Zuo, D., Perlitch, I., Saleh, S. M. I., Zhao, H., Souleimanova, M., Johnson, R. M.*, et al.* (2019). Spatially distinct tumor immune microenvironments stratify triple-negative breast cancers. J Clin Invest *129*, 1785-1800.

Hamilton, M. J., Bosiljcic, M., Lepard, N. E., Halvorsen, E. C., Ho, V. W., Banath, J. P., Krystal, G., and Bennewith, K. L. (2014). Macrophages are more potent immune suppressors ex vivo than immature myeloid-derived suppressor cells induced by metastatic murine mammary carcinomas. J Immunol *192*, 512-522.

Hanahan, D., and Weinberg, R. A. (2000). The hallmarks of cancer. Cell *100*, 57-70.

Hanahan, D., and Weinberg, R. A. (2011). Hallmarks of cancer: the next generation. Cell *144*, 646-674.

Harper, J., and Sainson, R. C. (2014). Regulation of the anti-tumour immune response by cancer-associated fibroblasts. Semin Cancer Biol *25*, 69-77.

Havel, J. J., Chowell, D., and Chan, T. A. (2019). The evolving landscape of biomarkers for checkpoint inhibitor immunotherapy. Nature Reviews Cancer *19*, 133.

Heath, W. R., and Carbone, F. R. (2001). Cross-presentation in viral immunity and self-tolerance. Nat Rev Immunol *1*, 126-134.

Hoadley, K. A., Yau, C., Hinoue, T., Wolf, D. M., Lazar, A. J., Drill, E., Shen, R., Taylor, A. M., Cherniack, A. D., Thorsson, V.*, et al.* (2018). Cell-of-Origin Patterns Dominate the Molecular Classification of 10,000 Tumors from 33 Types of Cancer. Cell *173*, 291-304.e296.

Hodi, F. S., O'Day, S. J., McDermott, D. F., Weber, R. W., Sosman, J. A., Haanen, J. B., Gonzalez, R., Robert, C., Schadendorf, D., Hassel, J. C.*, et al.* (2010). Improved survival with ipilimumab in patients with metastatic melanoma. N Engl J Med *363*, 711-723.

Hofheinz, R. D., al-Batran, S. E., Hartmann, F., Hartung, G., Jager, D., Renner, C., Tanswell, P., Kunz, U., Amelsberg, A., Kuthan, H., and Stehle, G. (2003). Stromal antigen targeting by a humanised monoclonal antibody: an early phase II trial of sibrotuzumab in patients with metastatic colorectal cancer. Onkologie *26*, 44-48.

Holmgaard, R. B., Zamarin, D., Li, Y., Gasmi, B., Munn, D. H., Allison, J. P., Merghoub, T., and Wolchok, J. D. (2015). Tumor-Expressed IDO Recruits and Activates MDSCs in a Treg-Dependent Manner. Cell Rep *13*, 412-424.

Inoue, T., Adachi, K., Kawana, K., Taguchi, A., Nagamatsu, T., Fujimoto, A., Tomio, K., Yamashita, A., Eguchi, S., Nishida, H.*, et al.* (2016). Cancer-associated fibroblast suppresses killing activity of natural killer cells through downregulation of poliovirus receptor (PVR/CD155), a ligand of activating NK receptor. Int J Oncol *49*, 1297-1304.

Jackson, S. P., and Bartek, J. (2009). The DNA-damage response in human biology and disease. Nature *461*, 1071-1078.

Jahangiri, B., Khalaj-Kondori, M., Asadollahi, E., and Sadeghizadeh, M. (2019). Cancer-associated fibroblasts enhance cell proliferation and metastasis of colorectal cancer SW480 cells by provoking long noncoding RNA UCA1. J Cell Commun Signal *13*, 53-64.

Jeanes, A., Gottardi, C. J., and Yap, A. S. (2008). Cadherins and cancer: how does cadherin dysfunction promote tumor progression? Oncogene *27*, 6920-6929.

Jiang, P., Gu, S., Pan, D., Fu, J., Sahu, A., Hu, X., Li, Z., Traugh, N., Bu, X., Li, B.*, et al.* (2018). Signatures of T cell dysfunction and exclusion predict cancer immunotherapy response. Nat Med *24*, 1550-1558.

Jiang, Y., Li, Y., and Zhu, B. (2015). T-cell exhaustion in the tumor microenvironment. Cell Death & Disease *6*.

Joyce, J. A., and Fearon, D. T. (2015). T cell exclusion, immune privilege, and the tumor microenvironment. Science *348*, 74-80.

Jungwirth, U., van Weverwijk, A., Melake, M. J., Chambers, A. F., Gao, Q., Fivaz, M., and Isacke, C. M. (2018). Generation and characterisation of two D2A1 mammary cancer sublines to model spontaneous and experimental metastasis in a syngeneic BALB/c host. Dis Model Mech *11*.

Kalluri, R. (2016). The biology and function of fibroblasts in cancer. Nat Rev Cancer *16*, 582-598.

Kalluri, R., and Zeisberg, M. (2006). Fibroblasts in cancer. Nat Rev Cancer *6*, 392-401.

Kaplan, R. N., Rafii, S., and Lyden, D. (2006). Preparing the “Soil”: The Premetastatic Niche.

Katzenellenbogen, B. S., and Katzenellenbogen, J. A. (2000). Estrogen receptor transcription and transactivation: Estrogen receptor alpha and estrogen receptor beta: regulation by selective estrogen receptor modulators and importance in breast cancer. Breast Cancer Res *2*, 335-344.

Kennecke, H., Yerushalmi, R., Woods, R., Cheang, M. C., Voduc, D., Speers, C. H., Nielsen, T. O., and Gelmon, K. (2010). Metastatic behavior of breast cancer subtypes. J Clin Oncol *28*, 3271-3277.

Khalili, J. S., Liu, S., Rodriguez-Cruz, T. G., Whittington, M., Wardell, S., Liu, C., Zhang, M., Cooper, Z. A., Frederick, D. T., Li, Y.*, et al.* (2012). Oncogenic BRAF(V600E) promotes stromal cell-mediated immunosuppression via induction of interleukin-1 in melanoma. Clin Cancer Res *18*, 5329-5340.

Kim, J. H., Oh, S. H., Kim, E. J., Park, S. J., Hong, S. P., Cheon, J. H., Kim, T. I., and Kim, W. H. (2012). The role of myofibroblasts in upregulation of S100A8 and S100A9 and the differentiation of myeloid cells in the colorectal cancer microenvironment. Biochem Biophys Res Commun *423*, 60-66.

Kitamura, T., Qian, B. Z., and Pollard, J. W. (2015). Immune cell promotion of metastasis. Nat Rev Immunol *15*, 73-86.

Klebanoff, C. A., Gattinoni, L., Torabi-Parizi, P., Kerstann, K., Cardones, A. R., Finkelstein, S. E., Palmer, D. C., Antony, P. A., Hwang, S. T., Rosenberg, S. A.*, et al.* (2005). Central memory self/tumor-reactive CD8+ T cells confer superior antitumor immunity compared with effector memory T cells. Proc Natl Acad Sci U S A *102*, 9571-9576.

Knutson, K. L., and Disis, M. L. (2005). Tumor antigen-specific T helper cells in cancer immunity and immunotherapy. Cancer Immunol Immunother *54*, 721-728.

Kojima, Y., Acar, A., Eaton, E. N., Mellody, K. T., Scheel, C., Ben-Porath, I., Onder, T. T., Wang, Z. C., Richardson, A. L., Weinberg, R. A., and Orimo, A. (2010). Autocrine TGF-beta and stromal cell-derived factor-1 (SDF-1) signaling drives the evolution of tumor-promoting mammary stromal myofibroblasts. Proc Natl Acad Sci U S A *107*, 20009-20014.

Kraman, M., Bambrough, P. J., Arnold, J. N., Roberts, E. W., Magiera, L., Jones, J. O., Gopinathan, A., Tuveson, D. A., and Fearon, D. T. (2010). Suppression of antitumor immunity by stromal cells expressing fibroblast activation protein-alpha. Science (New York, NY) *330*, 827-830.

Kroemer, G., Senovilla, L., Galluzzi, L., Andre, F., and Zitvogel, L. (2015). Natural and therapy-induced immunosurveillance in breast cancer. Nat Med *21*, 1128-1138.

Lakins, M. A., Ghorani, E., Munir, H., Martins, C. P., and Shields, J. D. (2018). Cancer-associated fibroblasts induce antigen-specific deletion of CD8 (+) T Cells to protect tumour cells. Nat Commun *9*, 948.

Lanitis, E., Dangaj, D., Irving, M., and Coukos, G. (2017). Mechanisms regulating T-cell infiltration and activity in solid tumors. Ann Oncol *28*, xii18-xii32.

Laoui, D., Movahedi, K., Van Overmeire, E., Van den Bossche, J., Schouppe, E., Mommer, C., Nikolaou, A., Morias, Y., De Baetselier, P., and Van Ginderachter, J. A. (2011). Tumor-associated macrophages in breast cancer: distinct subsets, distinct functions. Int J Dev Biol *55*, 861-867.

Larkin, J., Chiarion-Sileni, V., Gonzalez, R., Grob, J.-J., Rutkowski, P., Lao, C. D., Cowey, C. L., Schadendorf, D., Wagstaff, J., Dummer, R.*, et al.* (2019). Five-Year Survival with Combined Nivolumab and Ipilimumab in Advanced Melanoma. https://doiorg/101056/NEJMoa1910836.

Larouche, J., Sheoran, S., Maruyama, K., and Martino, M. M. (2018). Immune Regulation of Skin Wound Healing: Mechanisms and Novel Therapeutic Targets. In Adv Wound Care (New Rochelle), pp. 209-231.

Le, D. T., Uram, J. N., Wang, H., Bartlett, B. R., Kemberling, H., Eyring, A. D., Skora, A. D., Luber, B. S., Azad, N. S., Laheru, D.*, et al.* (2015). PD-1 Blockade in Tumors with Mismatch-Repair Deficiency. N Engl J Med *372*, 2509-2520.

Li, H., and Durbin, R. (2010). Fast and accurate long-read alignment with Burrows-Wheeler transform. Bioinformatics *26*, 589-595.

Li, H., Handsaker, B., Wysoker, A., Fennell, T., Ruan, J., Homer, N., Marth, G., Abecasis, G., and Durbin, R. (2009). The Sequence Alignment/Map format and SAMtools. Bioinformatics *25*, 2078-2079.

Liao, D., Luo, Y. P., Markowitz, D., Xiang, R., and Reisfeld, R. A. (2009). Cancer Associated Fibroblasts Promote Tumor Growth and Metastasis by Modulating the Tumor Immune Microenvironment in a 4T1 Murine Breast Cancer Model. PLoS One *4*, 10.

Loke, P., and Allison, J. P. (2003). PD-L1 and PD-L2 are differentially regulated by Th1 and Th2 cells. Proceedings of the National Academy of Sciences of the United States of America *100*, 5336-5341.

Long, G. V., Dummer, R., Hamid, O., Gajewski, T. F., Caglevic, C., Dalle, S., Arance, A., Carlino, M. S., Grob, J. J., Kim, T. M.*, et al.* (2019). Epacadostat plus pembrolizumab versus placebo plus pembrolizumab in patients with unresectable or metastatic melanoma (ECHO-301/KEYNOTE-252): a phase 3, randomised, double-blind study. Lancet Oncol *20*, 1083-1097.

Lord, C. J., and Ashworth, A. (2013). Mechanisms of resistance to therapies targeting BRCA-mutant cancers. Nat Med *19*, 1381-1388.

Lu, Y. C., and Robbins, P. F. (2016). Cancer immunotherapy targeting neoantigens. Semin Immunol *28*, 22-27.

Lutz, M. B., and Schuler, G. (2002). Immature, semi-mature and fully mature dendritic cells: which signals induce tolerance or immunity? Trends Immunol *23*, 445-449.

Machiels, J.-P., Salazar, R., Rottey, S., Duran, I., Dirix, L., Geboes, K., Wilkinson-Blanc, C., Pover, G., Alvis, S., Champion, B.*, et al.* (2019). A phase 1 dose escalation study of the oncolytic adenovirus enadenotucirev, administered intravenously to patients with epithelial solid tumors (EVOLVE). Journal for ImmunoTherapy of Cancer *7*, 1-15.

Malhotra, V., and Perry, M. C. (2003). Classical Chemotherapy: Mechanisms, Toxicities and the Therapeutc Window. http://dxdoiorg/104161/cbt199.

Mantovani, A., Sozzani, S., Locati, M., Allavena, P., and Sica, A. (2002). Macrophage polarization: tumor-associated macrophages as a paradigm for polarized M2 mononuclear phagocytes. Trends Immunol *23*, 549-555.

Mao, Y., Keller, E. T., Garfield, D. H., Shen, K., and Wang, J. (2013). Stromal cells in tumor microenvironment and breast cancer. Cancer Metastasis Rev *32*, 303-315.

Mariathasan, S., Turley, S. J., Nickles, D., Castiglioni, A., Yuen, K., and Wang, Y. (2018). TGFbeta attenuates tumour response to PD-L1 blockade by contributing to exclusion of T cells. Nature *554*.

Marshall, M. A., Ribas, A., and Huang, B. (2010). Evaluation of baseline serum C-reactive protein (CRP) and benefit from tremelimumab compared to chemotherapy in first-line melanoma. https://doiorg/101200/jco20102815_suppl2609.

Martinez, F. O., and Gordon, S. (2014). The M1 and M2 paradigm of macrophage activation: time for reassessment. In F1000Prime Rep.

Martinez-Lostao, L., Anel, A., and Pardo, J. (2015). How Do Cytotoxic Lymphocytes Kill Cancer Cells? Clin Cancer Res *21*, 5047-5056.

Masoud, V., and Pagès, G. (2017). Targeted therapies in breast cancer: New challenges to fight against resistance. World J Clin Oncol *8*, 120-134.

Massague, J. (2008). TGFbeta in Cancer. Cell *134*, 215-230.

McCarthy, E. F. (2006). The Toxins of William B. Coley and the Treatment of Bone and Soft-Tissue Sarcomas. Iowa Orthop J *26*, 154-158.

McKenna, A., Hanna, M., Banks, E., Sivachenko, A., Cibulskis, K., Kernytsky, A., Garimella, K., Altshuler, D., Gabriel, S., Daly, M., and DePristo, M. A. (2010). The Genome Analysis Toolkit: a MapReduce framework for analyzing next-generation DNA sequencing data. Genome Res *20*, 1297-1303.

Melaiu, O., Mina, M., Chierici, M., Boldrini, R., Jurman, G., Romania, P., D'Alicandro, V., Benedetti, M. C., Castellano, A., Liu, T.*, et al.* (2017). PD-L1 Is a Therapeutic Target of the Bromodomain Inhibitor JQ1 and, Combined with HLA Class I, a Promising Prognostic Biomarker in Neuroblastoma. Clin Cancer Res *23*, 4462-4472.

Melander, M. C., Jurgensen, H. J., Madsen, D. H., Engelholm, L. H., and Behrendt, N. (2015). The collagen receptor uPARAP/Endo180 in tissue degradation and cancer (Review). Int J Oncol *47*, 1177-1188.

Miliotou, A. N., and Papadopoulou, L. C. (2018). CAR T-cell Therapy: A New Era in Cancer Immunotherapy. Curr Pharm Biotechnol *19*, 5-18.

Miller, L. D., Chou, J. A., Black, M. A., Print, C., Chifman, J., Alistar, A., Putti, T., Zhou, X., Bedognetti, D., Hendrickx, W.*, et al.* (2016). Immunogenic Subtypes of Breast Cancer Delineated by Gene Classifiers of Immune Responsiveness. Cancer immunology research *4*, 600-610.

Mishra, P., Banerjee, D., and Ben-Baruch, A. (2011). Chemokines at the crossroads of tumor-fibroblast interactions that promote malignancy. Journal of leukocyte biology *89*, 31-39.

Mlecnik, B., Tosolini, M., Kirilovsky, A., Berger, A., Bindea, G., Meatchi, T., Bruneval, P., Trajanoski, Z., Fridman, W. H., Pages, F., and Galon, J. (2011). Histopathologic-based prognostic factors of colorectal cancers are associated with the state of the local immune reaction. J Clin Oncol *29*, 610-618.

Monteran, L., and Erez, N. (2019). The Dark Side of Fibroblasts: Cancer-Associated Fibroblasts as Mediators of Immunosuppression in the Tumor Microenvironment. Front Immunol *10*, 1835.

Morris, V. L., Tuck, A. B., Wilson, S. M., Percy, D., and Chambers, A. F. (1993). Tumor progression and metastasis in murine D2 hyperplastic alveolar nodule mammary tumor cell lines. Clin Exp Metastasis *11*, 103-112.

Motz, G. T., and Coukos, G. (2013). Deciphering and reversing tumor immune suppression. Immunity *39*, 61-73.

Muntasell, A., Cabo, M., Servitja, S., Tusquets, I., Martínez-García, M., Rovira, A., Rojo, F., Albanell, J., and López-Botet, M. (2017). Interplay between Natural Killer Cells and Anti-HER2 Antibodies: Perspectives for Breast Cancer Immunotherapy. Front Immunol *8*.

Nanda, A., Karim, B., Peng, Z., Liu, G., Qiu, W., Gan, C., Vogelstein, B., St Croix, B., Kinzler, K. W., and Huso, D. L. (2006). Tumor endothelial marker 1 (Tem1) functions in the growth and progression of abdominal tumors. Proc Natl Acad Sci U S A *103*, 3351-3356.

Newman, A. M., Liu, C. L., Green, M. R., Gentles, A. J., Feng, W., Xu, Y., Hoang, C. D., Diehn, M., and Alizadeh, A. A. (2015). Robust enumeration of cell subsets from tissue expression profiles. Nat Methods *12*, 453-457.

Ni Chonghaile, T., Sarosiek, K. A., Vo, T. T., Ryan, J. A., Tammareddi, A., Moore Vdel, G., Deng, J., Anderson, K. C., Richardson, P., Tai, Y. T.*, et al.* (2011). Pretreatment mitochondrial priming correlates with clinical response to cytotoxic chemotherapy. Science *334*, 1129-1133.

Nolan, E., Savas, P., Policheni, A. N., Darcy, P. K., Vaillant, F., Mintoff, C. P., Dushyanthen, S., Mansour, M., Pang, J. B., Fox, S. B.*, et al.* (2017). Combined immune checkpoint blockade as a therapeutic strategy for BRCA1-mutated breast cancer. Sci Transl Med *9*.

Nowarski, R., Gagliani, N., Huber, S., and Flavell, R. A. (2013). Innate immune cells in inflammation and cancer. Cancer immunology research *1*, 77-84.

Oh, S. A., and Li, M. O. (2013). TGF-β: Guardian of T Cell Function. J Immunol *191*, 3973-3979.

Ohlund, D., Handly-Santana, A., Biffi, G., Elyada, E., Almeida, A. S., Ponz-Sarvise, M., Corbo, V., Oni, T. E., Hearn, S. A., Lee, E. J.*, et al.* (2017). Distinct populations of inflammatory fibroblasts and myofibroblasts in pancreatic cancer. J Exp Med *214*, 579-596.

Orimo, A., Gupta, P. B., Sgroi, D. C., Arenzana-Seisdedos, F., Delaunay, T., Naeem, R., Carey, V. J., Richardson, A. L., and Weinberg, R. A. (2005). Stromal fibroblasts present in invasive human breast carcinomas promote tumor growth and angiogenesis through elevated SDF-1/CXCL12 secretion. Cell *121*, 335-348.

Osborne, C. K., and Schiff, R. (2011). Mechanisms of endocrine resistance in breast cancer. Annu Rev Med *62*, 233-247.

Ozdemir, B. C., Pentcheva-Hoang, T., Carstens, J. L., Zheng, X., Wu, C. C., Simpson, T. R., Laklai, H., Sugimoto, H., Kahlert, C., Novitskiy, S. V.*, et al.* (2014). Depletion of carcinoma-associated fibroblasts and fibrosis induces immunosuppression and accelerates pancreas cancer with reduced survival. Cancer Cell *25*, 719-734.

Paget, S. (1889). THE DISTRIBUTION OF SECONDARY GROWTHS IN CANCER OF THE BREAST. The Lancet *133*, 571-573.

Paoli, P., Giannoni, E., and Chiarugi, P. (2013). Anoikis molecular pathways and its role in cancer progression. Biochim Biophys Acta *1833*, 3481-3498.

Pardoll, D. M. (2012). The blockade of immune checkpoints in cancer immunotherapy. Nature reviews Cancer *12*, 252-264.

Paulin, D., and Li, Z. (2004). Desmin: a major intermediate filament protein essential for the structural integrity and function of muscle. Exp Cell Res *301*, 1-7.

Paulsson, J., Rydén, L., Strell, C., Frings, O., Tobin, N. P., Fornander, T., Bergh, J., Landberg, G., Stål, O., and Östman, A. (2017). High expression of stromal PDGFRβ is associated with reduced benefit of tamoxifen in breast cancer. In J Pathol Clin Res, pp. 38-43.

Pegram, H. J., Andrews, D. M., Smyth, M. J., Darcy, P. K., and Kershaw, M. H. (2011). Activating and inhibitory receptors of natural killer cells. Immunol Cell Biol *89*, 216-224.

Perou, C. M., Sorlie, T., Eisen, M. B., van de Rijn, M., Jeffrey, S. S., Rees, C. A., Pollack, J. R., Ross, D. T., Johnsen, H., Akslen, L. A.*, et al.* (2000). Molecular portraits of human breast tumours. Nature *406*, 747-752.

Pitt, J. M., Vetizou, M., Daillere, R., Roberti, M. P., Yamazaki, T., Routy, B., Lepage, P., Boneca, I. G., Chamaillard, M., Kroemer, G., and Zitvogel, L. (2016). Resistance Mechanisms to Immune-Checkpoint Blockade in Cancer: Tumor-Intrinsic and -Extrinsic Factors. Immunity *44*, 1255-1269.

Pitzalis, C., Jones, G. W., Bombardieri, M., and Jones, S. A. (2014). Ectopic lymphoid-like structures in infection, cancer and autoimmunity. Nature Reviews Immunology *14*, 447-462.

Poruchynsky, M. S., Komlodi-Pasztor, E., Trostel, S., Wilkerson, J., Regairaz, M., Pommier, Y., Zhang, X., Maity, T. K., Robey, R., Burotto, M.*, et al.* (2015). Microtubule-targeting agents augment the toxicity of DNA-damaging agents by disrupting intracellular trafficking of DNA repair proteins.

Psaila, B., and Lyden, D. (2009). The Metastatic Niche: Adapting the Foreign Soil. Nat Rev Cancer *9*, 285-293.

Qian, B. Z., Li, J., Zhang, H., Kitamura, T., Zhang, J., Campion, L. R., Kaiser, E. A., Snyder, L. A., and Pollard, J. W. (2011). CCL2 recruits inflammatory monocytes to facilitate breast-tumour metastasis. Nature *475*, 222-225.

Rabinovich, G. A., Gabrilovich, D., and Sotomayor, E. M. (2007). Immunosuppressive strategies that are mediated by tumor cells. Annu Rev Immunol *25*, 267-296.

Raj-Kumar, P. K., Liu, J., Hooke, J. A., Kovatich, A. J., Kvecher, L., Shriver, C. D., and Hu, H. (2019). PCA-PAM50 improves consistency between breast cancer intrinsic and clinical subtyping reclassifying a subset of luminal A tumors as luminal B. Sci Rep *9*, 7956.

Ravetch, J. V., and Bolland, S. (2001). IgG Fc receptors. Annu Rev Immunol *19*, 275-290.

Reis-Filho, J. S., and Pusztai, L. (2011). Gene expression profiling in breast cancer: classification, prognostication, and prediction. Lancet *378*, 1812-1823.

Rettig, W. J., Garin-Chesa, P., Healey, J. H., Su, S. L., Jaffe, E. A., and Old, L. J. (1992). Identification of endosialin, a cell surface glycoprotein of vascular endothelial cells in human cancer. Proc Natl Acad Sci U S A *89*, 10832-10836.

Reymond, N., d'Agua, B. B., and Ridley, A. J. (2013). Crossing the endothelial barrier during metastasis. Nat Rev Cancer *13*, 858-870.

Ribas, A., Hauschild, A., Kefford, R., Punt, C. J., Haanen, J. B., Marmol, M., Garbe, C., Gomez-Navarro, J., Pavlov, D., and Marshall, M. (2008). Phase III, open-label, randomized, comparative study of tremelimumab (CP-675,206) and chemotherapy (temozolomide [TMZ] or dacarbazine [DTIC]) in patients with advanced melanoma. https://doiorg/101200/jco20082615_suppllba9011.

Ribas, A., and Wolchok, J. D. (2018). Cancer immunotherapy using checkpoint blockade. Science *359*, 1350-1355.

Ritchie, M. E., Phipson, B., Wu, D., Hu, Y., Law, C. W., Shi, W., and Smyth, G. K. (2015). limma powers differential expression analyses for RNA-sequencing and microarray studies. Nucleic Acids Res *43*, e47.

Robertson, D., Savage, K., Reis-Filho, J. S., and Isacke, C. M. (2008). Multiple immunofluorescence labelling of formalin-fixed paraffin-embedded (FFPE) tissue. BMC Cell Biology *9*, 1-10.

Roll, P., Palanichamy, A., Kneitz, C., Dorner, T., and Tony, H. P. (2006). Regeneration of B cell subsets after transient B cell depletion using anti-CD20 antibodies in rheumatoid arthritis. Arthritis Rheum *54*, 2377-2386.

Romagnani, S. (1999). Th1/Th2 cells. Inflamm Bowel Dis *5*, 285-294.

Rosales, C. (2018). Neutrophil: A Cell with Many Roles in Inflammation or Several Cell Types? Front Physiol *9*.

Rosales, C., and Uribe-Querol, E. (2017). Phagocytosis: A Fundamental Process in Immunity. Biomed Res Int *2017*.

Rosenberg, J. E., Hoffman-Censits, J., Powles, T., van der Heijden, M. S., Balar, A. V., Necchi, A., Dawson, N., O'Donnell, P. H., Balmanoukian, A., Loriot, Y.*, et al.* (2016). Atezolizumab in

patients with locally advanced and metastatic urothelial carcinoma who have progressed following treatment with platinum-based chemotherapy: a single arm, phase 2 trial. Lancet *387*, 1909-1920.

Rosenberg, S. A., Yang, J. C., Sherry, R. M., Kammula, U. S., Hughes, M. S., Phan, G. Q., Citrin, D. E., Restifo, N. P., Robbins, P. F., Wunderlich, J. R.*, et al.* (2011). Durable complete responses in heavily pretreated patients with metastatic melanoma using T-cell transfer immunotherapy. Clin Cancer Res *17*, 4550-4557.

Rudolph, A., Chang-Claude, J., and Schmidt, M. K. (2016). Gene-environment interaction and risk of breast cancer. Br J Cancer *114*, 125-133.

Sakaguchi, S., Department of Experimental Pathology, I. f. F. M. S., Kyoto University, 53 Shogoin Kawahara-cho, Sakyo-ku, Kyoto 606-8507, Japan, WPI Immunology Frontier Research Center, O. U., Suita 565-0871, Japan, Wing, K., Department of Experimental Pathology, I. f. F. M. S., Kyoto University, 53 Shogoin Kawahara-cho, Sakyo-ku, Kyoto 606-8507, Japan, Present address: Division of Medical inflammation Research, D. o. M. B. a. B., Karolinska Institute, 171 77 Stockholm, Sweden, Onishi, Y., Department of Experimental Pathology, I. f. F. M. S., Kyoto University, 53 Shogoin Kawahara-cho, Sakyo-ku, Kyoto 606-8507, Japan, Present address: Department of Hematology, T. U. S. o. M., Sendai 980-8574, Japan, Prieto-Martin, P.*, et al.* (2019). Regulatory T cells: how do they suppress immune responses? International Immunology *21*, 1105-1111.

Sakaguchi, T., Yoshino, H., Sugita, S., Miyamoto, K., Yonemori, M., Osako, Y., Meguro-Horike, M., Horike, S. I., Nakagawa, M., and Enokida, H. (2018). Bromodomain protein BRD4 inhibitor JQ1 regulates potential prognostic molecules in advanced renal cell carcinoma. In Oncotarget, pp. 23003-23017.

Salgado, R., Denkert, C., Demaria, S., Sirtaine, N., Klauschen, F., Pruneri, G., Wienert, S., Van den Eynden, G., Baehner, F. L., Penault-Llorca, F.*, et al.* (2015). The evaluation of tumor-infiltrating lymphocytes (TILs) in breast cancer: recommendations by an International TILs Working Group 2014. Ann Oncol *26*, 259-271.

Salmon, H., Franciszkiewicz, K., Damotte, D., Dieu-Nosjean, M. C., Validire, P., Trautmann, A., Mami-Chouaib, F., and Donnadieu, E. (2012). Matrix architecture defines the preferential localization and migration of T cells into the stroma of human lung tumors. J Clin Invest *122*, 899-910.

Samji, T., and Khanna, K. M. (2017). Understanding Memory CD8+ T cells. Immunol Lett *185*, 32-39.

Sanmamed, M. F., Department of Immunobiology, Y. U. S. o. M., New Haven, Chester, C., Department of Medicine, D. o. O., Stanford University School of Medicine, Stanford, USA, Melero, I., Division of Immunology and Immunotherapy, C. f. A. M. R. C., University of Navarra, Pamplona, Spain, Kohrt, H., and Department of Medicine, D. o. O., Stanford University School of Medicine, Stanford, USA (2019). Defining the optimal murine models to investigate immune checkpoint blockers and their combination with other immunotherapies. Annals of Oncology *27*, 1190-1198.

Savas, P., Salgado, R., Denkert, C., Sotiriou, C., Darcy, P. K., Smyth, M. J., and Loi, S. (2016). Clinical relevance of host immunity in breast cancer: from TILs to the clinic. Nat Rev Clin Oncol *13*, 228-241.

Schaefer, B. C., Schaefer, M. L., Kappler, J. W., Marrack, P., and Kedl, R. M. (2001). Observation of antigen-dependent CD8+ T-cell/ dendritic cell interactions in vivo. Cell Immunol *214*, 110-122.

Schmid, P., Adams, S., Rugo, H. S., Schneeweiss, A., Barrios, C. H., Iwata, H., Dieras, V., Hegg, R., Im, S. A., Shaw Wright, G.*, et al.* (2018). Atezolizumab and Nab-Paclitaxel in Advanced Triple-Negative Breast Cancer. N Engl J Med *379*, 2108-2121.

Schnurr, M., Chen, Q., Shin, A., Chen, W., Toy, T., Jenderek, C., Green, S., Miloradovic, L., Drane, D., Davis, I. D.*, et al.* (2005). Tumor antigen processing and presentation depend critically on dendritic cell type and the mode of antigen delivery. Blood *105*, 2465-2472.

Schumann, J., Stanko, K., Schliesser, U., Appelt, C., and Sawitzki, B. (2015). Differences in CD44 Surface Expression Levels and Function Discriminates IL-17 and IFN-γ Producing Helper T Cells. In PLoS One.

Schwartz, R. H. (2003). T cell anergy. Annu Rev Immunol *21*, 305-334.

Scott, A. M., Wolchok, J. D., and Old, L. J. (2012). Antibody therapy of cancer. Nature Reviews Cancer *12*, 278.

Shankaran, V., Ikeda, H., Bruce, A. T., White, J. M., Swanson, P. E., Old, L. J., and Schreiber, R. D. (2001). IFNgamma and lymphocytes prevent primary tumour development and shape tumour immunogenicity. Nature *410*, 1107-1111.

Sharma, A., Subudhi, S. K., Blando, J., Scutti, J., Vence, L., Wargo, J., Allison, J. P., Ribas, A., and Sharma, P. (2019). Anti-CTLA-4 Immunotherapy Does Not Deplete FOXP3(+) Regulatory T Cells (Tregs) in Human Cancers. Clin Cancer Res *25*, 1233-1238.

Sharma, P., Hu-Lieskovan, S., Wargo, J. A., and Ribas, A. (2017). Primary, Adaptive, and Acquired Resistance to Cancer Immunotherapy. Cell *168*, 707-723.

Sharon, Y., Alon, L., Glanz, S., Servais, C., and Erez, N. (2013). Isolation of normal and cancer-associated fibroblasts from fresh tissues by Fluorescence Activated Cell Sorting (FACS). Journal of visualized experiments : JoVE, e4425.

Shultz, L. D., Schweitzer, P. A., Christianson, S. W., Gott, B., Schweitzer, I. B., Tennent, B., McKenna, S., Mobraaten, L., Rajan, T. V., Greiner, D. L., and et al. (1995). Multiple defects in innate and adaptive immunologic function in NOD/LtSz-scid mice. J Immunol *154*, 180-191.

Singh, S., Ross, S. R., Acena, M., Rowley, D. A., and Schreiber, H. (1992). Stroma is critical for preventing or permitting immunological destruction of antigenic cancer cells. J Exp Med *175*, 139-146.

Song, Q., Hawkins, G. A., Wudel, L., Chou, P. C., Forbes, E., Pullikuth, A. K., Liu, L., Jin, G., Craddock, L., Topaloglu, U.*, et al.* (2019). Dissecting intratumoral myeloid cell plasticity by single cell RNA-seq. Cancer Med *8*, 3072-3085.

Soran, A., Ozmen, V., Ozbas, S., Karanlik, H., Muslumanoglu, M., Igci, A., Canturk, Z., Utkan, Z., Ozaslan, C., Evrensel, T.*, et al.* (2018). Randomized Trial Comparing Resection of Primary Tumor with No Surgery in Stage IV Breast Cancer at Presentation: Protocol MF07-01. Ann Surg Oncol *25*, 3141-3149.

Soria, G., and Ben-Baruch, A. (2008). The inflammatory chemokines CCL2 and CCL5 in breast cancer. Cancer Lett *267*, 271-285.

Soto-Perez-de-Celis, E., Chavarri-Guerra, Y., Leon-Rodriguez, E., and Gamboa-Dominguez, A. (2017). Tumor-Associated Neutrophils in Breast Cancer Subtypes. In Asian Pac J Cancer Prev, pp. 2689-2694.

Stanton, S. E., Adams, S., and Disis, M. L. (2016). Variation in the Incidence and Magnitude of Tumor-Infiltrating Lymphocytes in Breast Cancer Subtypes: A Systematic Review. JAMA Oncol *2*, 1354-1360.

Stingl, J., and Caldas, C. (2007). Molecular heterogeneity of breast carcinomas and the cancer stem cell hypothesis. In Nat Rev Cancer, (England), pp. 791-799.

Strilic, B., and Offermanns, S. (2017). Intravascular Survival and Extravasation of Tumor Cells. Cancer Cell *32*, 282-293.

Strutz, F., Okada, H., Lo, C. W., Danoff, T., Carone, R. L., Tomaszewski, J. E., and Neilson, E. G. (1995). Identification and characterization of a fibroblast marker: FSP1. J Cell Biol *130*, 393-405.

Sugimoto, H., Mundel, T. M., Kieran, M. W., and Kalluri, R. (2006). Identification of fibroblast heterogeneity in the tumor microenvironment. Cancer Biol Ther *5*, 1640-1646.

Sznol, M., Powderly, J. D., Smith, D. C., Brahmer, J. R., Drake, C. G., McDermott, D. F., Lawrence, D. P., Wolchok, J. D., Topalian, S. L., and Lowy, I. (2010). Safety and antitumor activity of biweekly MDX-1106 (Anti-PD-1, BMS-936558/ONO-4538) in patients with advanced refractory malignancies. https://doiorg/101200/jco20102815_suppl2506.

Tabib, T., Morse, C., Wang, T., Chen, W., and Lafyatis, R. (2018). SFRP2/DPP4 and FMO1/LSP1 Define Major Fibroblast Populations in Human Skin. J Invest Dermatol *138*, 802-810.

Taga, K., and Tosato, G. (1992). IL-10 inhibits human T cell proliferation and IL-2 production. J Immunol *148*, 1143-1148.

Takai, K., Le, A., Weaver, V. M., and Werb, Z. (2016). Targeting the cancer-associated fibroblasts as a treatment in triple-negative breast cancer. Oncotarget *7*, 82889-82901.

Talevich, E., Shain, A. H., Botton, T., and Bastian, B. C. (2016). CNVkit: Genome-Wide Copy Number Detection and Visualization from Targeted DNA Sequencing. PLoS Comput Biol *12*, e1004873.

Tao, L., Huang, G., Wang, R., Pan, Y., He, Z., Chu, X., Song, H., and Chen, L. (2016). Cancer-associated fibroblasts treated with cisplatin facilitates chemoresistance of lung adenocarcinoma through IL-11/IL-11R/STAT3 signaling pathway. In Sci Rep.

Tarin, D., and Croft, C. B. (1969). Ultrastructural features of wound healing in mouse skin. J Anat *105*, 189-190.

Tauriello, D. V. F., Palomo-Ponce, S., Stork, D., Berenguer-Llergo, A., Badia-Ramentol, J., Iglesias, M., Sevillano, M., Ibiza, S., Canellas, A., Hernando-Momblona, X.*, et al.* (2018). TGFbeta drives immune evasion in genetically reconstituted colon cancer metastasis. Nature *554*, 538-543.

Tesmer, L. A., Lundy, S. K., Sarkar, S., and Fox, D. A. (2008). Th17 cells in human disease. Immunol Rev *223*, 87-113.

Thannickal, V. J., Lee, D. Y., White, E. S., Cui, Z., Larios, J. M., Chacon, R., Horowitz, J. C., Day, R. M., and Thomas, P. E. (2003). Myofibroblast differentiation by transforming growth factor-beta1 is dependent on cell adhesion and integrin signaling via focal adhesion kinase. J Biol Chem *278*, 12384-12389.

Thorsson, V., Gibbs, D. L., Brown, S. D., Wolf, D., Bortone, D. S., Ou Yang, T. H., Porta-Pardo, E., Gao, G. F., Plaisier, C. L., Eddy, J. A.*, et al.* (2018). The Immune Landscape of Cancer. Immunity.

Tommaso, P. D., Chatzou, M., Floden, E. W., Barja, P. P., Palumbo, E., and Notredame, C. (2017). Nextflow enables reproducible computational workflows. Nature Biotechnology *35*, 316-319.

Toullec, A., Gerald, D., Despouy, G., Bourachot, B., Cardon, M., Lefort, S., Richardson, M., Rigaill, G., Parrini, M. C., Lucchesi, C.*, et al.* (2010). Oxidative stress promotes myofibroblast differentiation and tumour spreading. EMBO Mol Med *2*, 211-230.

Trujillo, J. A., Sweis, R. F., Bao, R., and Luke, J. J. (2018). T Cell–Inflamed versus Non-T Cell–Inflamed Tumors: A Conceptual Framework for Cancer Immunotherapy Drug Development and Combination Therapy Selection.

Tsung, K., and Norton, J. A. (2016). In situ vaccine, immunological memory and cancer cure. In Hum Vaccin Immunother, pp. 117-119.

Tumeh, P. C., Harview, C. L., Yearley, J. H., Shintaku, I. P., Taylor, E. J., Robert, L., Chmielowski, B., Spasic, M., Henry, G., Ciobanu, V.*, et al.* (2014). PD-1 blockade induces responses by inhibiting adaptive immune resistance. Nature *515*, 568-571.

Twyman-Saint Victor, C., Rech, A. J., Maity, A., Rengan, R., Pauken, K. E., Stelekati, E., Benci, J. L., Xu, B., Dada, H., Odorizzi, P. M.*, et al.* (2015). Radiation and dual checkpoint blockade activate non-redundant immune mechanisms in cancer. Nature *520*, 373-377.

van Vliet, S. J., Garcia-Vallejo, J. J., and van Kooyk, Y. (2008). Dendritic cells and C-type lectin receptors: coupling innate to adaptive immune responses. Immunol Cell Biol *86*, 580-587.

Vinay, D. S., Ryan, E. P., Pawelec, G., Talib, W. H., Stagg, J., Elkord, E., Lichtor, T., Decker, W. K., Whelan, R. L., Kumara, H.*, et al.* (2015). Immune evasion in cancer: Mechanistic basis and therapeutic strategies. Semin Cancer Biol *35 Suppl*, S185-s198.

Viski, C., Konig, C., Kijewska, M., Mogler, C., Isacke, C. M., and Augustin, H. G. (2016). Endosialin-Expressing Pericytes Promote Metastatic Dissemination. Cancer Res *76*, 5313-5325.

Vonderheide, R. H., Domchek, S. M., and Clark, A. S. (2017a). Immunotherapy for breast cancer: what are we missing? Clin Cancer Res *23*, 2640-2646.

Vonderheide, R. H., Domchek, S. M., and Clark, A. S. (2017b). Immunotherapy for Breast Cancer: What Are We Missing? Clin Cancer Res *23*, 2640-2646.

Wagner, S., Vlachogiannis, G., Brandon, A. D. H., Valenti, M., Box, G., Jenkins, L., Mancusi, C., Self, A., Manodoro, F., Assiotis, I.*, et al.* (2018). Suppression of interferon gene expression overcomes resistance to MEK inhibition in KRAS -mutant colorectal cancer. Oncogene *38*, 1717-1733.

Wang, J., and Zhou, P. (2017). New Approaches in CAR-T Cell Immunotherapy for Breast Cancer. Adv Exp Med Biol *1026*, 371-381.

Wang, K., Li, M., and Hakonarson, H. (2010). ANNOVAR: functional annotation of genetic variants from high-throughput sequencing data. Nucleic Acids Res *38*, e164.

Wang, L. C., Lo, A., Scholler, J., Sun, J., Majumdar, R. S., Kapoor, V., Antzis, M., Cotner, C. E., Johnson, L. A., Durham, A. C.*, et al.* (2014a). Targeting fibroblast activation protein in tumor stroma with chimeric antigen receptor T cells can inhibit tumor growth and augment host immunity without severe toxicity. Cancer Immunol Res *2*, 154-166.

Wang, W., Erbe, A. K., Hank, J. A., Morris, Z. S., and Sondel, P. M. (2015). NK Cell-Mediated Antibody-Dependent Cellular Cytotoxicity in Cancer Immunotherapy. Front Immunol *6*.

Wang, Y., Waters, J., Leung, M. L., Unruh, A., Roh, W., Shi, X., Chen, K., Scheet, P., Vattathil, S., Liang, H.*, et al.* (2014b). Clonal evolution in breast cancer revealed by single nucleus genome sequencing. Nature *512*, 155-160.

Wang, Y. J., Fletcher, R., Yu, J., and Zhang, L. (2018). Immunogenic effects of chemotherapy-induced tumor cell death. In Genes Dis, pp. 194-203.

Watson, H. A., Durairaj, R. R. P., Ohme, J., Alatsatianos, M., Almutairi, H., Mohammed, R. N., Vigar, M., Reed, S. G., Paisey, S. J., Marshall, C.*, et al.* (2019). L-Selectin Enhanced T Cells Improve the Efficacy of Cancer Immunotherapy. Front Immunol *10*, 1321.

Wei, S. C., Duffy, C. R., and Allison, J. P. (2018). Fundamental Mechanisms of Immune Checkpoint Blockade Therapy. Cancer Discov *8*, 1069-1086.

Wei, S. C., Levine, J. H., Cogdill, A. P., Zhao, Y., Anang, N. A. S., Andrews, M. C., Sharma, P., Wang, J., Wargo, J. A., Pe'er, D., and Allison, J. P. (2017). Distinct Cellular Mechanisms Underlie Anti-CTLA-4 and Anti-PD-1 Checkpoint Blockade. Cell *170*, 1120-1133.e1117.

Wilm, A., Aw, P. P., Bertrand, D., Yeo, G. H., Ong, S. H., Wong, C. H., Khor, C. C., Petric, R., Hibberd, M. L., and Nagarajan, N. (2012). LoFreq: a sequence-quality aware, ultra-sensitive variant caller for uncovering cell-population heterogeneity from high-throughput sequencing datasets. Nucleic Acids Res *40*, 11189-11201.

Wolchok, J. D., Chiarion-Sileni, V., Gonzalez, R., Rutkowski, P., Grob, J. J., Cowey, C. L., Lao, C. D., Wagstaff, J., Schadendorf, D., Ferrucci, P. F.*, et al.* (2017). Overall Survival with Combined Nivolumab and Ipilimumab in Advanced Melanoma. N Engl J Med *377*, 1345-1356.

Wolchok, J. D., Hoos, A., O'Day, S., Weber, J. S., Hamid, O., Lebbe, C., Maio, M., Binder, M., Bohnsack, O., Nichol, G.*, et al.* (2009). Guidelines for the evaluation of immune therapy activity in solid tumors: immune-related response criteria. Clin Cancer Res *15*, 7412-7420.

Wolf, K., and Friedl, P. (2011). Extracellular matrix determinants of proteolytic and non-proteolytic cell migration. Trends Cell Biol *21*, 736-744.

Wu, M. H., Hong, H. C., Hong, T. M., Chiang, W. F., Jin, Y. T., and Chen, Y. L. (2011). Targeting galectin-1 in carcinoma-associated fibroblasts inhibits oral squamous cell carcinoma metastasis by downregulating MCP-1/CCL2 expression. Clin Cancer Res *17*, 1306-1316.

Yamamoto, K., Tateishi, K., Kudo, Y., Hoshikawa, M., Tanaka, M., Nakatsuka, T., Fujiwara, H., Miyabayashi, K., Takahashi, R., Tanaka, Y.*, et al.* (2016). Stromal remodeling by the BET bromodomain inhibitor JQ1 suppresses the progression of human pancreatic cancer. In Oncotarget, pp. 61469-61484.

Yamashita, M., Ogawa, T., Zhang, X., Hanamura, N., Kashikura, Y., Takamura, M., Yoneda, M., and Shiraishi, T. (2012). Role of stromal myofibroblasts in invasive breast cancer: stromal expression of alpha-smooth muscle actin correlates with worse clinical outcome. Breast Cancer *19*, 170-176.

Yang, S., Liu, F., Wang, Q. J., Rosenberg, S. A., and Morgan, R. A. (2011). The shedding of CD62L (L-selectin) regulates the acquisition of lytic activity in human tumor reactive T lymphocytes. PLoS One *6*, e22560.

Yang, X., Lin, Y., Shi, Y., Li, B., Liu, W., Yin, W., Dang, Y., Chu, Y., Fan, J., and He, R. (2016). FAP Promotes Immunosuppression by Cancer-Associated Fibroblasts in the Tumor Microenvironment via STAT3-CCL2 Signaling. Cancer Res *76*, 4124-4135.

Yang, Y., Yang, H. H., Hu, Y., Watson, P. H., Liu, H., Geiger, T. R., Anver, M. R., Haines, D. C., Martin, P., Green, J. E.*, et al.* (2017). Immunocompetent mouse allograft models for development of therapies to target breast cancer metastasis. In Oncotarget, pp. 30621-30643.

Yoshimura, T., Howard, O. M., Ito, T., Kuwabara, M., Matsukawa, A., Chen, K., Liu, Y., Liu, M., Oppenheim, J. J., and Wang, J. M. (2013). Monocyte chemoattractant protein-1/CCL2 produced by stromal cells promotes lung metastasis of 4T1 murine breast cancer cells. PLoS One *8*, e58791.

Yu, P. F., Huang, Y., Han, Y. Y., Lin, L. Y., Sun, W. H., Rabson, A. B., Wang, Y., and Shi, Y. F. (2017). TNFalpha-activated mesenchymal stromal cells promote breast cancer metastasis by recruiting CXCR2(+) neutrophils. Oncogene *36*, 482-490.

Zacharakis, N., Chinnasamy, H., Black, M., Xu, H., Lu, Y.-C., Zheng, Z., Pasetto, A., Langhan, M., Shelton, T., Prickett, T.*, et al.* (2018). Immune recognition of somatic mutations leading to complete durable regression in metastatic breast cancer. Nature Medicine *24*, 724-730.

Zamai, L., Ahmad, M., Bennett, I. M., Azzoni, L., Alnemri, E. S., and Perussia, B. (1998). Natural Killer (NK) Cell–mediated Cytotoxicity: Differential Use of TRAIL and Fas Ligand by Immature and Mature Primary Human NK Cells. J Exp Med *188*, 2375-2380.

Zarour, H. M. (2016). Reversing T-cell Dysfunction and Exhaustion in Cancer.

Zhu, H., Bengsch, F., Svoronos, N., Rutkowski, M. R., Bitler, B. G., Allegrezza, M. J., Yokoyama, Y., Kossenkov, A. V., Bradner, J. E., Conejo-Garcia, J. R., and Zhang, R. (2016). BET Bromodomain Inhibition Promotes Anti-tumor Immunity by Suppressing PD-L1 Expression. Cell Rep *16*, 2829-2837.

Ziani, L., Chouaib, S., and Thiery, J. (2018). Alteration of the Antitumor Immune Response by Cancer-Associated Fibroblasts. Front Immunol *9*, 414.

Österreicher, C. H., Penz-Österreicher, M., Grivennikov, S. I., Guma, M., Koltsova, E. K., Datz, C., Sasik, R., Hardiman, G., Karin, M., and Brenner, D. A. (2011). Fibroblast-specific protein 1 identifies an inflammatory subpopulation of macrophages in the liver.